STUDIES OF THE HYDRATION OF TRICALCIUM SILICATE

P. J. Le Sueur

Keble College

Oxford



A thesis submitted for the degree of Doctor of Philosophy in the University of Oxford, Michaelmas 1984

ABSTRACT

STUDIES OF THE HYDRATION OF TRICALCIUM SILICATE

P.J. Le Sueur, Keble College
D.Phil - Michaelmas 1984

The hydration reaction of tricalcium silicate and the various factors which influence it have been investigated using calorimetry, thermogravimetry, quantitative X-ray diffractometry, scanning and transmission electron microscopy and energy dispersive X-ray analysis.

Various factors associated with the synthesis and subsequent storage of tricalcium silicate were found to alter its reactivity and it is thought that these may be responsible for much of the variability in the reported reactivity of tricalcium silicate preparations. The contribution of the individual factors (such as particle size distribution and impurity ion content) to such reactivity changes was investigated.

Use of the Avrami equation to model the rate of heat output curves obtained by calorimetry was found to give good fits to the experimental data. Apparent activation energies of control and calcium chloride accelerated reactions were determined from the rate parameters derived from the fitting procedure. However, it is shown that the amount of mechanistic information which can be obtained from such a fitting procedure is limited.

Observation of the detailed chemical and morphological changes occurring during the hydration of tricalcium silicate and the manner in which they are influenced by incorporation of calcium chloride (as a model accelerator) and sucrose (as a model retarder) show that during the later stages of hydration the chemistry of the reaction is not affected by the presence of the admixtures, but that their incorporation does cause some changes in the microstructure of the gel product.

STATEMENT

The research described in this thesis is

my own except where stated in the text

or acknowledgements.

Signed

P. Le Sueur

ACKNOWLEDGEMENTS

I would like to thank:

At the Department of Metallurgy and Science of Materials, Oxford:

Prof. Sir Peter Hirsch F.R.S. for the provision of laboratory facilities.

Dr. D.D. Double for initiating my interest in cement and for advice and encouragement during the work.

Dr. G.W. Groves for his supervision during the final stages of the project and for advice during the writing of this thesis.

All the members of the Cement group, especially to Dr. W. Sinclair for helpful (and unhelpful) comments throughout the course of the work and for instruction in the use of the TEM and EDXA facilities and to Naleem Salih for technical assistance and practical help with broken machinery.

At the Cement and Concrete Association, Wexham Springs, Slough:

Dr. C.D. Pomeroy for advice and encouragement and for the permission to use the C&CA X-ray analysis, chemical analysis, library, computing and printing facilities.

Walter Gutteridge for his expert assistance with the quantitative X-ray analysis and many helpful comments.

Mike Taylor for instruction and help with the chemical analysis.

Roger Musson for the preparation of many of the QXDA samples.

Brian Best and the staff of the computing and printing divisions for their help with the transfer, formatting and final printing of this thesis.

At the School of Geography, Mansfield Road, Oxford:

Dr Goudie for the use of the Laser granulometer to measure the particle size distributions of the C_3S samples

Mr. Jackson for carrying out the particle size analyses.

In addition the provision of a grant by the SERC, without which this work would not have been possible, is acknowledged together with the financial assistance of the C&CA.

STANDARD CEMENT NOTATION AND ABBREVIATIONS

The following standard cement notation hes been used throughout this text:

$C = CaO$
$S = SiO_2$
$A = Al_2O_3$
$F = Fe_2O_3$
$H = H_2O$

Thus for example: $C_3S = (CaO)_3.SiO_2$ or Ca_3SiO_5

In addition the following abbreviations have been used:

C/S ratio	calcium to silicon ratio
CSH gel	calcium silicate hydrate gel
DTGA	differential thermogravimetric analysis
ESCA	electron spectroscopy for chemical analysis
H/S ratio	water to silicon ratio
HVEM	high voltage electron microscopy
NMR	nuclear magnetic resonance
OPC	ordinary Portland cement
powder XRD	powder X-ray diffractometry
QXDA	quantitative X-ray diffractometry
SEM	scanning electron microscopy
STEM	scanning transmission electron microscopy
TEM	transmission electron microscopy
TGA	thermogravimetric analysis
w/c ratio	water to cement ratio

Note: All temperatures are in degrees centigrade unless otherwise stated in the text.

CONTENTS

STATEMENT i

ACKNOWLEDGEMENTS ii

STANDARD CEMENT NOTATION AND ABBREVIATIONS iii

CHAPTER 1 INTRODUCTION 1

1.1 Cement 1
1.2 Types of cement 2
1.2.a Portland cements 2
1.2.b Lime Cements 2
1.2.c Slag cements 3
1.2.d High alumina cements 3
1.2.e Pozzolanas 3
1.2.f Sorel cement 4
1.2.g Gypsum cements 4
1.3 Ordinary Portland cement 4
1.4 Composition of ordinary Portland cement 5
1.5 The cement minerals 7
1.5.a Tricalcium silicate (C_3S) 7
1.5.b Dicalcium silicate (C_2S) 8
1.5.c Tricalcium aluminate (C_3A) 9
1.5.d Tetracalcium aluminoferrite ('C_4AF') 10
1.6 Hydration of OPC 10
1.7 Observations during the setting of OPC 13
1.8 Theories of the hydration mechanism of Portland cement 16
1.9 Subsequent hydration - setting and hardening 17
1.10 Influences on the hydration mechanism 18
1.10.a Influence of composition 19
1.10.b Influence of burning and cooling 19
1.10.c Influence of fineness and particle size distribution 20
1.10.d Influence of admixtures 20
1.10.e Influence of storage 20
1.11 Reasons and objectives for this work 22

CHAPTER 2 CALORIMETER - CONSTRUCTION AND CALIBRATION 23

2.1 Introduction 23
2.2 Calorimeter construction 27
2.3 Theory of conduction calorimetry 30
2.4 Calorimeter calibration 31
2.4.a Theory 31
2.4.b Method 32
2.4.c Results 34
2.4.d Discussion 36
2.5 Calorimeter operation 38
2.6 Analysis of a calorimetric trace 40
2.7 Calorimeter performance 43
2.7.a Accuracy and reproducibility 43
2.7.b Effect of mixing technique 45
2.8 Conclusions 47

CHAPTER 3 SYNTHESIS OF TRICALCIUM SILICATE 48

3.1 Background 48
3.2 Method 50
3.3 Discussion 52

CHAPTER 4 FACTORS AFFECTING THE REACTIVITY OF C_3S 54

4.1 Introduction 54
4.1.a Intrinsic factors 54
4.1.a.i Lattice defects 55
4.1.a.ii Surface composition 56
4.1.b Extrinsic factors 56
4.2 Previous work 57
4.2.a Impurity ions 57
4.2.a.i Effect of altering the polymorph 59
4.2.a.ii Other effects of impurity ions 59
4.2.b Particle size distribution and grinding 61
4.2.c Aging 63
4.2.d Heat treatment 64
4.2.d.i Cooling rate 65
4.2.d.ii Effect of annealing 66
4.2.e Water/cement ratio 67
4.3 Experimental procedure and results 67
4.3.a Impurity ions 67
4.3.b Particle size distribution and grinding 70
4.3.c Aging 74
4.3.d Heat treatment 76
4.3.e Water/cement ratio 81
4.4 Discussion and conclusions 84
4.4.a Impurity ions 84
4.4.b Particle size distribution and grinding 85
4.4.c Aging 86
4.4.d Heat treatment 87
4.4.e Water/cement ratio 89
4.4.f General comments 91
4.5 Summary 92

CHAPTER 5 KINETIC MODELLING OF CALORIMETRIC DATA 95

5.1 Introduction 95
5.1.a Nucleation and growth models 96
5.1.b Models involving phase boundary reaction and diffusion through hydrate layers 98
5.1.c Models involving poisoning 100
5.1.d Models incorporating particle size distribution 101
5.2 Modelling using the Avrami equation 102
5.3 Experimental details 103
5.3.a Materials 103
5.3.b Calorimetry 103

5.4 Results and Discussion 104
5.4.a Calorimetry 104
5.4.b Fitting the Avrami equation 105
5.4.b.i Determination of the power exponent n 105
5.4.b.ii Determination of K and H 110
5.4.c Effect of temperature and accelerating admixture 114
5.5 Conclusions 117

CHAPTER 6 CHEMICAL STUDIES OF THE HYDRATION OF C_3S 120

6.1 Introduction 120
6.1.a Observations 120
6.1.b Proposed mechanisms 124
6.1.b.i Stage 1 124
6.1.b.ii Stage 2 and the start of stage 3 126
6.1.b.iii Stages 3, 4 and 5 130
6.1.c Effect of admixtures on the hydration of C_3S 131
6.1.d Extent of this study 132
6.2 Experimental 132
6.3 Methods of investigation 133
6.4 Analysis of results 134
6.4.a Thermogravimetric data 134
6.4.b X-ray data 135
6.5 Results 137
6.5.a Calorimetry 137
6.5.b Phase analysis 140
6.6 Discussion and conclusions 143

CHAPTER 7 SCANNING AND TRANSMISSION ELECTRON MICROSCOPE STUDIES OF THE HYDRATION OF C_3S 146

7.1 Introduction 146
7.1.a Morphological observations during the hydration of C_3S 146
7.1.b Difficulties encountered when interpreting morphological data 149
7.1.c Effect of admixtures on the morphological development of C_3S 150
7.2 Experimental 151
7.2.a Scanning electron microscopy 151
7.2.b Transmission electron microscopy and analysis 152
7.3 Results of the scanning studies 153
7.3.a Anhydrous material 153
7.3.b Control 153
7.3.c $CaCl_2$ accelerated 159
7.3.d Sucrose retarded 164
7.4 Results of the transmission studies 170
7.5 Discussion and conclusions 175
7.5.a Morphological development 175
7.5.b Effect of admixtures 180
7.5.c X-ray analysis 182

CHAPTER 8 CONCLUSIONS AND SUGGESTIONS FOR FURTHER WORK 184

8.1 Calorimetry 184
8.2 Factors affecting the reactivity of C_3S 184
8.3 Mathematical modeling of C_3S hydration 186
8.4 Chemical and morphological studies 187
8.5 Suggestions for further work 188

APPENDICES 190

REFERENCES 212

CHAPTER 1

INTRODUCTION

1.1 Cement

'Cement' in its broadest sense can be used to describe any substance capable of acting as an adhesive. In more general use, however, it has come to mean the range of substances used in combination with sand or aggregate to bind bricks, stones etc. in the construction industry. Even when used in this more limited sense it still describes a wide variety of materials, all with the same basic property of hardening after being mixed with a liquid (usually water), but each differing in constituent minerals and, hence, in the chemistry of their hardening processes. Cements of this type have been used for thousands of years for constructional purposes and their position in the construction industry is not likely to be challenged by any other material. Many improvements have been made to these original cements and careful study of the reasons why certain combinations of minerals are cementitious has led to the development of many new types of cement, usually with a view to overcoming a specific problem encountered with existing cements.

The wide applicability of cement, which has led to an annual demand in excess of 800 million tonnes and which makes cement the second largest manufactured commodity in the world today, derives from its cheapness of manufacture, ease of use and its ability to form a solid mass capable of binding other building materials and supporting comparatively high compressive stresses merely by the addition of water at room temperature.

Detailed accounts of the history of cements, their application and the manner in which they hydrate can be found in books such as Taylor (1964),

Lea (1970), Ghosh (1982), Bye (1983) and Barnes (1983). Much of the material contained in this chapter is drawn from these sources.

1.2 Types of cement

1.2.a Portland cements

Portland cements are made by heating a mixture of clay and limestone, or material of similar overall composition, to a temperature at which partial fusion occurs and then intergrinding the product (clinker) with about two weight percent of gypsum. Many phases have been identified in ordinary Portland cement clinker; the four main phases being impure forms of tricalcium silicate (C_3S), dicalcium silicate (C_2S), tricalcium aluminate (C_3A) and a ferrite phase often approximating to tetracalcium aluminoferrite (C_4AF). Portland cements are by far the most important cements, accounting for about 95% of world cement production. By careful control of the manufacturing conditions, numerous different types of Portland cement have been made, each suiting different requirements. The most important variables which can be controlled are the rate of hardening, rate and total extent of heat evolution and resistance of the hardened cement to attack by sulphate solutions.

1.2.b Lime cements

Lime cements are mainly of historical interest as they are one of the earliest types of cements known. Lime mortars have been found in constructions dating as far back as the Romans, Greeks and Cretans. Examples of Roman brickwork are still in existance today. Lime cements are the simplest cements. They are made by calcining calcium hydroxide or calcium carbonate to give calcium oxide (lime). The lime is converted to calcium hydroxide when water is added and this, when dry, reacts with atmospheric carbon dioxide to give calcium carbonate which is hard and

impervious to water. Lime cements are of little use as commercial cements because the hardening process only occurs in the absence of water and is unpredictable and slow.

1.2.c Slag cements

Slag cements are made from a mixture of granulated blastfurnace slag and another constituent such as ordinary Portland cement, lime or gypsum, which increases the latent hydraulicity of the slag. Slag cements are of interest because of the energy savings which can result from using a waste by-product such as slag in combination with a cementitious material instead of the cement on its own.

1.2.d High alumina cements

High alumina cement has proved popular because of its very high early strength development, though it has now been banned from structural use because it can undergo catastrophic strength loss under certain conditions of temperature and humidity. High alumina cements are made by fusing or sintering a mixture of bauxite and limestone, cooling and grinding to a very fine powder. Its main constituents are lime and alumina, the main cementing compound being monocalcium aluminate (CA).

1.2.e Pozzolanas

Pozzolanas are not in themselves cementitious, but they will react with lime (or other lime producing materials) and water at room temperature to give a cementing mixture. Originally they were naturally occurring deposits formed by volcanic activity; the name derives from the Pozzoli region of Italy, an area where a high grade form of the material was found. Such materials can also be produced artificially and the best

known example today is pulverised fuel ash from coal fired power stations.

1.2.f Sorel cement

Sorel cement is different from all those others mentioned so far in that it does not harden by the addition of water. It is formed by the reaction of magnesia with a concentrated solution of magnesium chloride. Its use is limited by the fact that it is attacked by water but it has found wide use as a flooring material (magnesite flooring) where it is usually protected from water by polishing with a mixture of wax in turpentine.

1.2.g Gypsum cements

Gypsum cements consist of partially or fully anhydrous calcium sulphate. Addition of water yields the fully hydrated material by a complex solution and reprecipitation mechanism which results in the mass setting solid in a few hours. Although now used mainly for decorative plaster work, historically they are, together with lime cements, the earliest cements known, being used by the Egyptians in major constructions such as the Great Pyramid.

1.3 Ordinary Portland cement

Ordinary Portland cement (OPC) is by far the most common cement in use today. Its invention is usually attributed to Joseph Aspdin who took out a patent for its production in 1824. His process of mixing clay, calcined limestone and water to form a slurry, calcining the slurry in a kiln and grinding the resultant clinker, forms the basis of the commercial production of OPC today. Since then, all aspects of its formation and subsequent hydration reaction have been studied with the result that many improvements have been made, both to the efficiency of the firing and

grinding processes and to the ultimate quality of the cementitous product.

1.4 Composition of ordinary Portland cement

The end product of the manufacturing process is a mixture of silicates and aluminates, each of which is usually modified to a greater or lesser degree by impurities which are taken up into solid solution. The relative proportions of these compounds within the cement depends both on the specific firing and cooling conditions and on the overall composition of the raw mix. These parameters vary from batch to batch and process to process which introduces a degree of variability into the composition of OPC. The range of compositions which an OPC can have are illustrated in fig 1.1. It is possible to calculate the approximate phase composition which will result from a given starting oxide composition using a set of rules first derived by Bogue (1955). The approximate phase composition calculated using the method of Bogue is usually termed the 'potential phase composition', to distinguish it from the actual phase composition which will not be exactly the same. A breakdown of the oxide composition of a typical OPC is given in table 1.1 together with the potential phase composition calculated from it.

Raw Mix Composition		Potential Phase Composition	
Oxide	%	Phase	%
CaO	67.7	C_3S	65.4
Al_2O_3	5.3	C_2S	12.9
Fe_2O_3	2.6	C_3A	9.6
SiO_2	21.7	C_4AF	7.9
MgO	1.3		
Na_2O	0.2		
K_2O	0.5		
SO_3	1.95		
Free CaO	1.5		

Table 1.1: Raw mix composition and calculated potential phase composition of a typical OPC

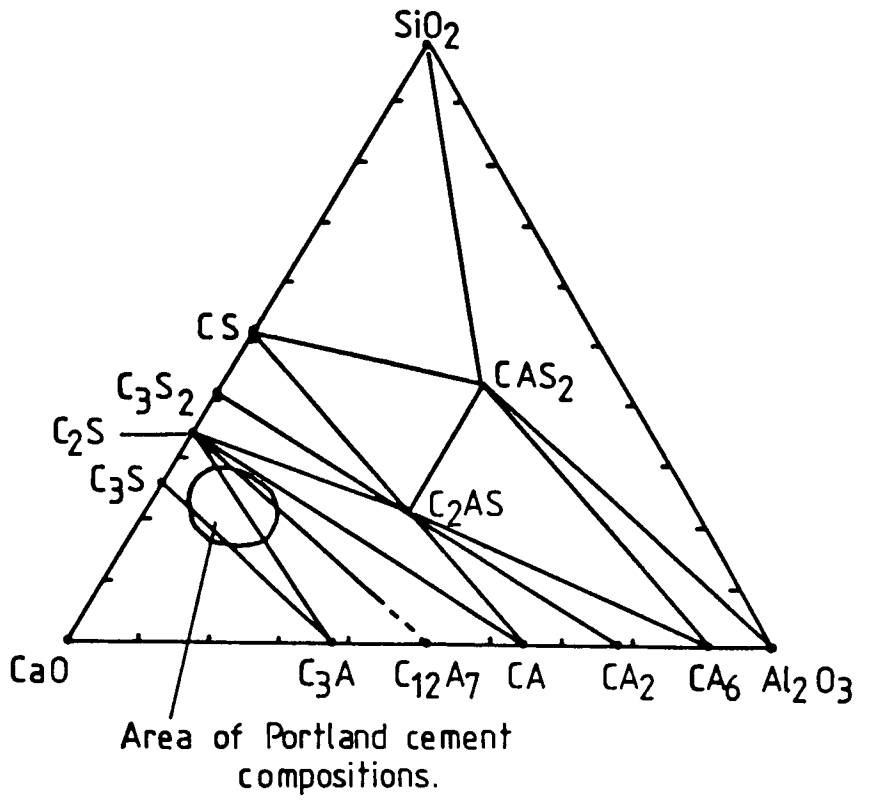

Fig 1.1: $CaO/SiO_2/Al_2O_3$ phase diagram to illustrate possible compositional ranges for OPC

Nowadays several types of Portland cements are usually recognised, in addition to OPC, each having different characteristics. These characteristics are influenced by the relative proportions of the four major phases and by other factors such as fineness of grinding. The classification of Portland cements adopted in the USA is commonly used to distinguish the various types. Table 1.2 gives the names and the average potential phase composition of the five types of cement manufactured in the USA. (Type 1 corresponds to OPC).

Type	Description	Potential phase composition					free lime	$CaSO_4$	Total
		C_3S (%)	C_2S (%)	C_3A (%)	C_4AF (%)	MgO (%)	(%)	(%)	(%)
I	General Use	45	27	11	8	2.9	0.5	3.1	98
II	Moderate Heat	44	31	5	13	2.5	0.4	2.8	99
III	High Early Strength	53	19	11	9	2.0	0.7	4.0	99
IV	Low Heat	28	49	4	12	1.8	0.2	3.2	98
V	Sulphate Resisting	38	43	4	9	1.9	0.5	2.7	99

Table 1.2: Potential phase compositions for cements of different types made in the USA. (Taylor 1964)

The presence of the various phases within OPC was determined independently by Le Chatelier in 1883 (Mack 1905) and by Tornebohm (1897) by microscopic examination of thin sections of clinker which show up to four different phases embedded in a glassy matrix. At the time of the work, it was not known what the various phases consisted of and they were distinguished by their appearance and refractive index. Tornebohm named them alite, belite, celite and felite. Subsequent reexamination of Tornebohm's original slides (Assarsson and Sundius 1929), together with modern analytical techniques has shown that alite is an impure (usually monoclinic) form of C_3S, belite and felite are impure C_2S, usually of the beta form, celite is a ferrite phase and the glassy matrix contains tricalcium aluminate.

1.5 The cement minerals

1.5.a Tricalcium silicate (C_3S)

The C_3S found in cement is impure, containing other oxides in solid solution, and is usually referred to as alite to distinguish it from the pure material. Pure C_3S has a triclinic crystal structure at room temperature (Golovastikov et al 1975) which on heating undergoes a series of phase changes (chapter 3 section 3.1).

The CaO/SiO_2 phase diagram (fig 1.2) shows that C_3S is formed by the solid state reaction between C_2S and lime above 1250°C and that it melts incongruently to lime and liquid above 1900°C. Below 1250°C C_3S is metastable, decomposing into lime and C_2S. This decomposition can be accelerated by the presence of various salts, but under normal conditions (below 700°C) is slow enough to be ignored.

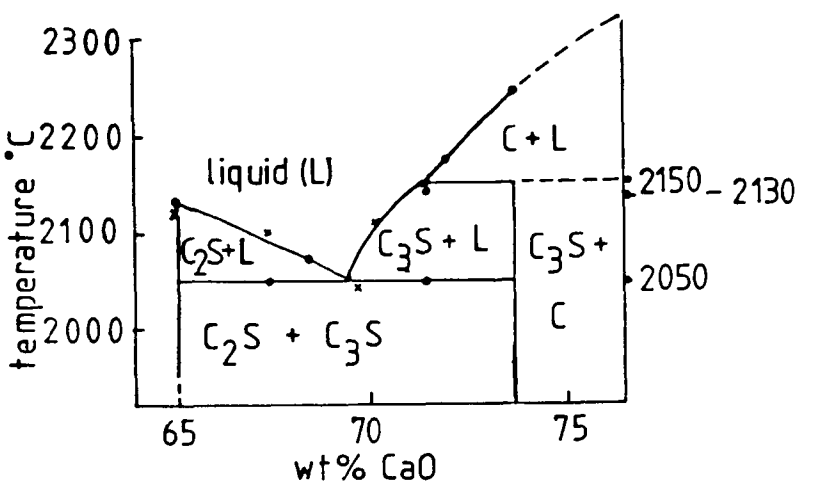

Fig 1.2: Lime rich portion of the CaO/SiO_2 phase diagram

Alite (impure C_3S) is the main component of OPC. It is thought to be responsible for the major portion of the early heat evolution and strength development of OPC.

1.5.b Dicalcium silicate (C_2S)

Five crystalline forms of C_2S exist between room temperature and 1500 degrees. The transition temperatures of these five polymorphs, which depend on whether the sample is being heated or cooled, are summarised in fig 1.3.

All the polymorphs can be stabilised at room temperature by the incorporation of appropriate impurity ions, but in marked contrast to the stabilised polymorphs of C_3S (see section 4.2.a), the polymorphs of C_2S all have very different crystal structures, reactivities and cementing abilities.

The beta form of C_2S is the most important of the polymorphs as in its impure form (belite) it is one of the four main constituents of OPC. Pure beta C_2S is thought to be metastable as it cannot be obtained purely by

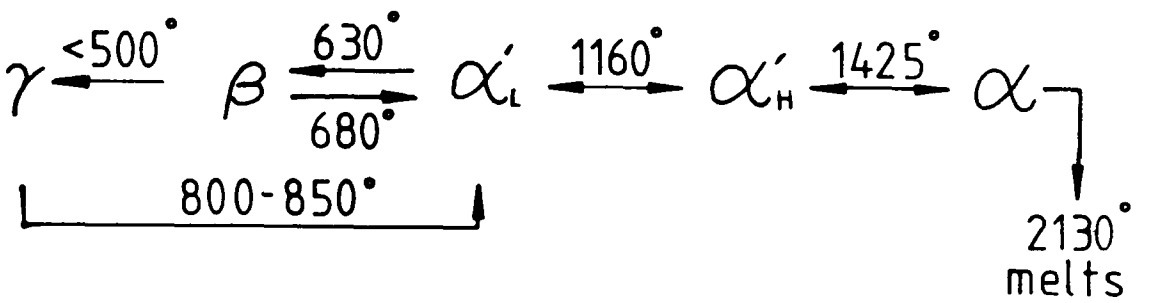

Fig 1.3: Polymorphic transforations of C_2S (Bye 1983).

heating the gamma form. Its stability is influenced markedly by the presence of impurity ions and very small additions of B_2O_3 or Cr_2O_3 are sufficient to stabilise it at room temperature. The reaction of beta C_2S with water is similar to that of C_3S but is much slower, a large proportion of unreacted material remaining after a year of hydration.

1.5.c Tricalcium aluminate (C_3A)

Tricalcium aluminate is unique among the clinker minerals in that, when pure, it is a definite compound, showing no polymorphic transformations. It has a cubic crystal lattice (Mondal & Jeffery 1975). It is formed by the solid state reaction of lime and alumina at 1345°C. It melts incongruently at 1539°C to give lime and liquid hence it cannot be made by melting techniques. It readily forms solid solutions with Fe_2O_3, SiO_2, alkalis and MgO. Increasing additions of alkalis change the symmetry of the structure from cubic through orthorhombic to monoclinic while the other ions have no effect on the structure. It reacts very quickly with water with evolution of a large amount of heat. The initial reaction leads to the mass setting solid almost immediately in what is known as a 'flash set'. If this set material is broken up then a plastic paste can

be obtained which, if kept in a moist environment, will set solid and attain a fair strength. However, if placed in water, the set material will disintegrate and crumble. The 'flash set' is undesirable and is prevented from occuring in OPC by the addition of gypsum during the grinding process. It is possible that gypsum also prevents the expansion and disintegration shown by tricalcium aluminate on its own. It is doubtful whether tricalcium aluminate is a truly hydraulic cement and its value in OPC seems mainly to be limited to rendering burning possible at the temperatures commercially available. Although it may contribute somewhat to the strength of the initial set the long term strength of OPC does not seem to be affected by its presence.

1.5.d Tetracalcium aluminoferrite ('C_4AF')

The iron containing mineral in OPC was long considered to have the definite composition of C_4AF, melting at 1415°C. Numerous investigations have now established the existence of a series of solid solutions between C_2F and a hypothetical C_2A. The material in cement, therefore, has a variable composition, though it often approximates to that of C_4AF. Its reaction with water is similar to that of C_3A though slower and its contribution to strength in OPC still seems uncertain. Though setting occurs in a few minutes, it does not show a flash set like that of tricalcium aluminate.

1.6 Hydration of OPC

On mixing with water, OPC forms an easily workable paste, which after a few hours loses its workability (setting phase) and subsequently develops strength (hardening phase) over a period of weeks, months or even years, eventually reaching an almost rocklike consistency. The reaction of OPC with water is highly complex, many different processes occurring

simultaneously. The products are often very poorly crystallised, making them difficult to characterize, and the various reactions all affect one another. In addition, the composition of OPC varies from batch to batch making comparison of results from different batches difficult, if not impossible.

The general reaction sequence is illustrated diagramatically in fig 1.4. The aluminates react relatively quickly with the dissolved gypsum, forming hydrated sulphoaluminates, while the silicates react more slowly to form hydrated calcium silicates. The reaction products gradually fill in the spaces between the residual grains forming a cohesive matrix which binds the whole structure together. After the cement has set the reaction continues to occur, though at a much reduced rate, and the cement continues to gain in strength, as long as water and clinker material are present.

A considerable amount of research has been carried out to determine the processes which occur when OPC is mixed with water and the mechanisms by which they operate. Unfortunately, the variability in the properties of cement used by different workers as well as its changing properties with age, have led to many inconsistencies in the literature. This makes differentiating the true observations from those that are merely a product of the particular batch of cement being used very difficult and so much confusion still exists as to the actual mechanism of OPC hydration.

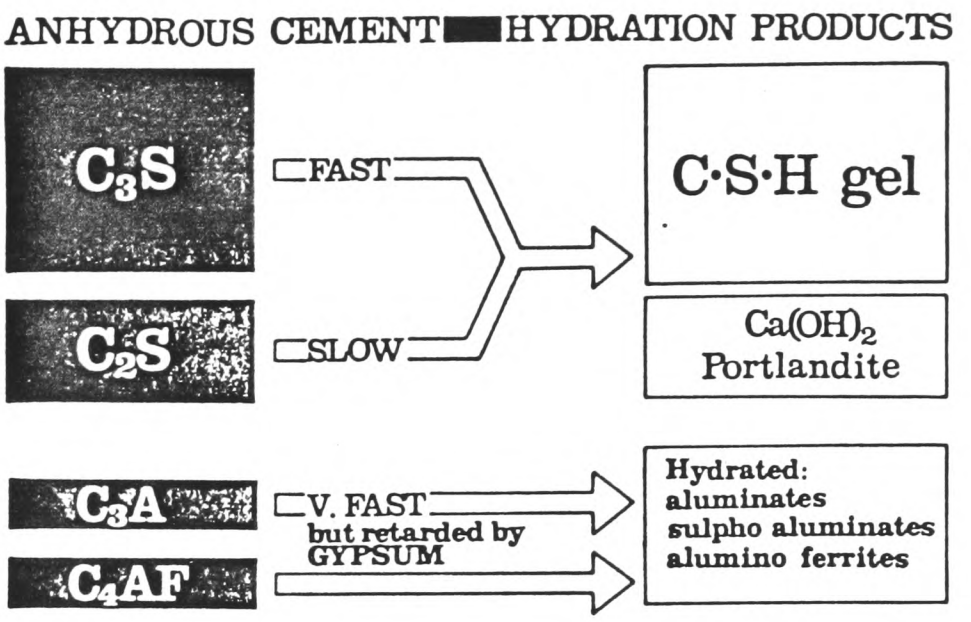

$2(3CaO \cdot SiO_2)$ (Tricalcium Silicate)	$+ 5.5H_2O$	$= 3CaO \cdot 2SiO_2 \cdot 2.5H_2O$ (Calcium Silicate Hydrate)	$+ 3Ca(OH)_2$ (Portlandite)	(1)
$2\beta(2CaO \cdot SiO_2)$ (Dicalcium Silicate)	$+ 3.5H_2O$	$= 3CaO \cdot 2SiO_2 \cdot 2.5H_2O$ (Calcium Silicate Hydrate)	$+ Ca(OH)_2$ (Portlandite)	(2)
$4CaO \cdot Al_2O_3 \cdot Fe_2O_3$ ("Tetracalcium Aluminoferrite")	$+ 10H_2O$	$+ 2Ca(OH)_2$	$= 6CaO \cdot Al_2O_3 \cdot Fe_2O_3 \cdot 12H_2O$ (Calcium Aluminoferrite Hydrate)	(3)
$3CaO \cdot Al_2O_3$ (Tricalcium Aluminate)	$+ 12H_2O$	$+ Ca(OH)_2$	$= 4CaO \cdot Al_2O_3 \cdot 13H_2O$ (Tetracalcium Aluminate Hydrate)	(4)
$3CaO \cdot Al_2O_3$	$+ 10H_2O$	$+ CaSO_4 \cdot 2H_2O$ (Gypsum)	$= 3CaO \cdot Al_2O_3 \cdot CaSO_4 \cdot 12H_2O$ (Calcium Monosulfo-Aluminate)	(5)

Fig 1.4: Cement hydration: general processes and reactions

1.7 Observations during the setting of OPC

The general sequence of events that occur after mixing OPC with water are reasonably well documented (Lea 1970; Ghosh 1982; Barnes 1983). On first contact with water each phase reacts independently and quickly. A relatively large amount of heat is produced which shows up as a sharp peak on a calorimetric curve (fig 1.5) and the concentrations of calcium, sulphate, potassium, sodium and hydroxyl ions all rise rapidly as the calcium sulphate and free lime dissolve and the initial reaction takes place at the surface of the cement grains themselves (fig 1.6). Surprisingly, during this period and indeed throughout the whole reaction sequence the concentrations of silicate, aluminate and iron all remain very low, generally being at least 50 - 100 times less than those of the other species present (Double 1983).

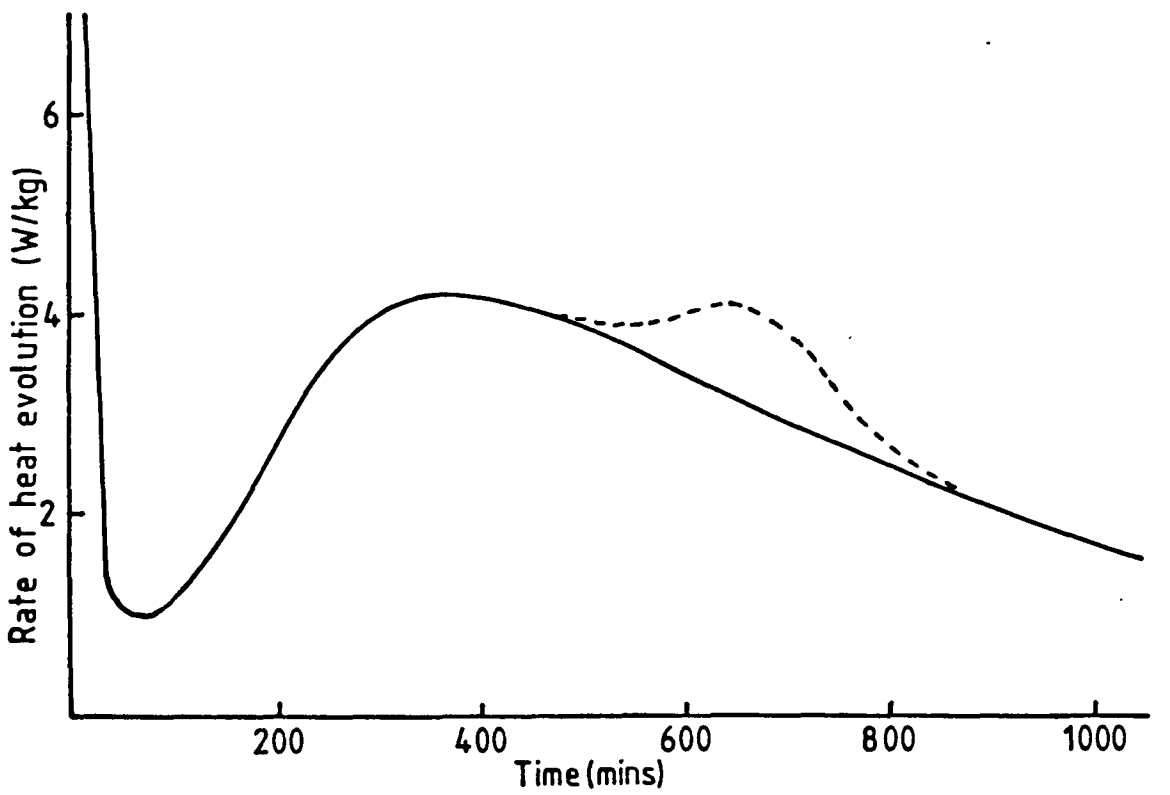

Fig 1.5: Typical calorimetric curve for an OPC

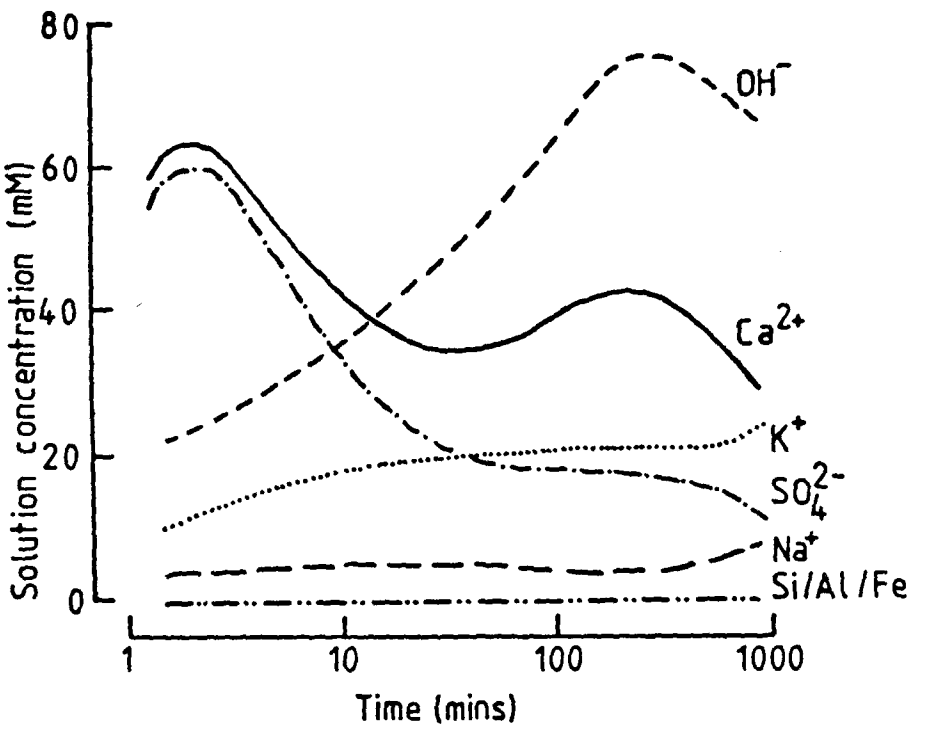

Fig 1.6: Typical solution composition curves for an OPC

After the initial burst of reaction the heat output starts to fall while the concentrations of calcium, sulphate, hydroxyl and alkali ions continue to rise, though more slowly, until, for calcium and sulphate, a high supersaturation is reached.

The subsequent timing of events is highly dependent on the particular cement being studied. Thus, in some cases, it has been reported that the calcium and sulphate concentrations start to fall off after only ten minutes until they reach the saturation level, while in other cases, in particular for cements having a low alkali content, this drop off occurs at a much later stage - up to a day after mixing (Locher & Richartz 1974). This drop is accompanied by the appearance of crystalline calcium hydroxide and sulphoaluminates in the paste. These initial reactions are mainly those of the tricalcium aluminate and the ferrite phases. The calcium silicates produce small amounts of hydration products (hydrated calcium silicates usually referred to as CSH gel) during the first few minutes of reaction after which the reaction all but stops for a few

hours. The detailed course of the reaction of the C_3S and C_2S during these early stages is by no means clear (see Chapter 6 section 6.1 for a more complete discussion of the hydration reaction of C_3S).

After about an hour the heat output has fallen to a minimum where it stays for a half to two hours. During this period very few reaction products are formed and the cement remains in a plastic state. At the end of this so called 'induction period', the reaction starts to speed up once more. The heat output rises (fig 1.5), CSH gel formation increases, calcium hydroxide formation begins and the calcium and hydroxyl ion concentrations in solution decrease. Shells of hydration product form around the original cement grains and these gradually increase in depth as the cement grains dissolve. CSH and calcium hydroxide are precipitated in the interstitial spaces and contacts are gradually built up between the grains as the material starts to set. As the amount of product around the grains builds up and the unreacted cores get smaller, the reaction rate and hence heat output falls off once more. By the time about 15 hours have elapsed (the actual time will depend on the particular batch and type of cement) the heat output has once more fallen to a low value and the calcium and sulphate levels are constant and have been so for some time. In some instances it is possible for a third heat peak to appear on the heat evolution curve (dotted line of fig 1.5). This may occur before or after the main peak, its position and height being very dependent on the particular cement being used. When this occurs the solution shows a marked drop in calcium and sulphate concentrations, there is an increase in the rate of tricalcium aluminate hydration and the alkali ion concentrations rise. Over the next few days the reaction continues, though now at a much reduced rate and the cement gets gradually harder and stronger.

1.8 Theories of the hydration mechanism of Portland cement

Over the years various theories have been formulated to explain these observations. The very first of these was developed by Le Chatelier (1887). He took as a model Lavoisier's ideas on the mechanism of setting of Plaster of Paris and supposed that the cement dissolved in water to give a solution supersaturated relative to the hydration product. From this, crystals precipitated and interlocked in the same manner as calcium sulphate in the setting of Plaster of Paris. An essential feature of the hypothesis is that the material passes through the solution before being precipitated. This theory has therefore become the basis of what is now known as the 'through solution' mechanism. Slightly later, Michaelis (1893) formed an alternative hypothesis in which the hardening of cement was attributed to the formation of a gel. On first mixing the cement with water a gel was supposed to be formed almost immediately which encapsulated the residual grains. This was at first a soft gel, containing a large proportion of water, and easily broken by mechanical agitation. During the hydration process the unreacted cement grains absorbed water from this soft gel which then became hard and impermeable and bound the mass together.

The essential difference between these two theories is that in the former the hardening action is supposed to come from the interlocking of crystals while in the latter it is the formation of a rigid gel which serves to bind the mass together. It is now generally agreed that the more important mechanism is gel formation, with crystal formation and interlocking contributing little to the overall strength development of a cement.

Subsequent theories have been more concerned with attempting to explain the observations described above, in particular the characteristic heat output with its induction period and the variations in concentration of the species in solution with time. To this end a large amount of controversy existed, and still does, about the relative importance of mechanisms involving dissolution and reprecipitation (the 'through solution' mechanism), and those taking place by the conversion of the solids in situ (the 'topochemical' mechanism).

This controversy has led to the existence of two main schools of thought concerning the hydration mechanism; those that treat the reaction in terms of nucleation and growth of calcium hydroxide and CSH gel, and those that treat it in terms of a protective membrane which forms around the cement grain. These two types of mechanism arise largely from observations of the hydration behaviour of C_3S on its own and are discussed in more detail in chapter 6, section 6.1. The reactions going on in a cement system will be more complicated than those in a pure C_3S system but it is thought that the mechanism of hydration of C_3S applies to OPC hydration, at least during the induction and early acceleratory periods, because it is thought that the reaction of C_3S dominates over the reactions of the other components of cement during these stages. Thus C_2S is known to react much more slowly than C_3S while the reaction of C_3A, while potentially fast, is retarded by the presence of the gypsum in the cement.

1.9 Subsequent hydration - setting and hardening

Cement pastes begin to set when the hydrate material from adjacent grains begins to impinge and so form a three dimensional network. As more hydrate is produced a rigid structure is gradually developed which is initially weak and is easily destroyed by mechanical action but, as new

hydrate phases are continuously formed in the spaces between the grains, it grows stronger and stronger, the increase in strength being partly due to a reduction in pore volume (Locher & Richartz 1974) and partly to the increasing number of contact points. It has also been suggested that the interlocking of the fibrillar growths helps to build up the strength (Higgins & Bailey 1976). QXDA, calorimetry and TGA studies have shown that cement continues to hydrate as long as water is available for continued reaction and unreacted clinker is present. According to Brunauer et al (1973), by this stage, the rate of the reaction is solely governed by the rate of diffusion of products and reactants through the intervening hydration products. While the early processes of hydration and setting involve mainly low molecualr mass silicate species it has been shown (Lentz 1966) that the proportion of polymeric material increases with time. Thus the long term reaction of cement is not only one of continuing slow reaction of the clinker, but also one of rearrangement of the hydrate phases. Such changes may involve the migration of calcium from CSH to such 'calcium sinks' as calcium hydroxide crystals and may also involve morphological change in the CSH. This change of the hydrates with time has also been noted by other workers. Thus Butt et al (1969) concluded that during the later stages of hydration a repeated recrystallisation of the CSH and all other hydrate phases occurs and Ciach et al (1971) reported that in the course of time the CSH hydrates change shape.

1.10 Influences on the hydration mechanism

The course of hydration of cement is influenced by a number of variables introduced both during its manufacture and afterwards. Changes arise from differences in the phase composition of the cement, from differences in the reactivity of the cement constituents, from the addition of

admixtures (compounds added with the mixing water to change the rate of reaction and/or change its rheological properties) and from changes in the cement's properties as a result of increasing age and of the storage conditions.

1.10.a Influence of composition

It has long been known that the composition of cement clinker has a marked influence on the overall course of the hydration reaction. The relative proportions of the cement compounds influence the rate of hardening (Celani et al 1968; Alexander et al 1968; Mehta & Williamson 1973). The crystal modification of the alite has been found to have an effect though this has little practical significance as the modification in normal OPC is almost always monoclinic. Minor components within the cement can also have a marked influence on the hydration behaviour (Sakurai et al 1968; Kurdowski 1974; Tashiro 1980). Finally the alkali and sulphate content of a cement has a marked influence on its hydration and hence its setting and strength development (Locher & Richartz 1974).

1.10.b Influence of burning and cooling

Normally cement is burnt under oxidising conditions. In moderately reducing conditions the iron (Fe^{3+}) is reduced to Fe^{2+}. This can cause the decomposition of C_3S into C_2S and lime and because divalent iron cannot form compounds with lime and alumina analogous to 'C_4AF' the relative proportions of C_3A and 'C_4AF' are altered. Clinker cooling influences mainly the formation of C_3A and 'C_4AF' crystallizing from the melt, slower cooling leading to a more rapid set by enhancing the crystallinity of the two phases (Sylla 1972). It has also been suggested that rapid cooling quenches disorder into the crystals thus promoting

faster hydration (Tomita et al. 1969; Maycock et al. 1974; Fierens et al. 1982)

1.10.c Influence of fineness and particle size distribution

In general the finer a cement is ground the faster it will reach its ultimate strength. The actual value of this strength is not usually altered significantly (Ritzman 1968; Kondo et al. 1971). It has also been shown (Knudsen 1980) that the distribution of particle sizes influences the overall kinetics of hydration.

1.10.d Influence of admixtures

Admixtures are substances that are added to the mixing water for cement to either speed up or slow down its setting or hardening or otherwise alter its rheology. Even very small amounts can have a marked effect on the setting speed and they are of great importance in the building trade where they are used to control the setting times and flow properties of concrete. They have been the subject of numerous studies, both to try and categorize their effect and to explain their action (Edwards & Angstadt 1966; Kantro 1975; Wilding et al. 1984). It would appear that this is far from simple with different types of mechanisms being involved for different admixtures.

1.10.e Influence of storage

The properties of cement alter gradually with time. Moisture in the atmosphere reacts with the cement leading to partial hydration at the surface. This partial hydration generally leads to a retardation of the hydration reaction especially during the first hours after mixing. This can give a reduction in early strength, though the final strength may not be affected significantly. It has been found that the strength can be

reduced by as much as 30% after 6 months storage (Maultzsch et al 1980). Although part of the effect is due to surface hydration it is also thought that carbonation and the slow disappearance of defects quenched in during cooling or introduced during grinding may play a significant role (Odler & Schuppstuhl 1981).

The result of this inherent variability in the reactivity of cement has led to a great deal of contradictory evidence being accumulated in the literature. There has been little standardisation in the cements used by different research workers making correlation of the effects observed by one set of workers with those of another set, working with a different cement, difficult. In addition the reaction is complicated by the number of components that are reacting together. Each compound has its individual reaction with water, but when combined with the others the compounds are no longer in isolation. For example it is known that C_3S hydration is retarded when C_3A is involved in uncontrolled initial reaction (Copeland & Kantro 1969). A large amount of work has been carried out to determine the reactions of the individual cement compounds by themselves and in combination with one another. Work has also been carried out on selectively doping the compounds with various impurities and comparing the reactivities of the doped compounds with those of the pure materials. It is hoped that it will be possible to build up a picture of the reaction of cement as a whole from considerations of the perturbations of the reactions of the compounds in combination with one another from those of the pure compounds. Unfortunately even this approach is not without its problems. Preparation of the pure compounds is by no means easy and their reactivity is influenced by their synthesis parameters (e.g. cooling rate and particle size distribution) in much the same way as cement.

1.11 Reasons and objectives for this work

The bulk of OPC consists of C_3S (usually greater than 50%) and because the reaction of C_3S is thought to be the most representative of that of OPC it is considered important to understand its reaction as an aid to understanding that of OPC. Consequently, the bulk of the research work which has been carried out on the cement compounds has been carried out on C_3S. In spite of this, the reaction mechanism of C_3S and the influences of admixtures and its synthesis parameters on its reactivity are still not known in detail.

This work sets out to investigate:

a) The effect of synthesis and storage parameters on the reactivity of C_3S.

b) The mathematical modelling of the hydration of C_3S using the Avrami equation.

c) The detailed chemical and morphological changes taking place during the hydration reaction and the influence of admixtures on those changes.

A sensitive conduction calorimeter was constructed to measure the rate of heat output of the hydrating C_3S and to determine any changes in reactivity resulting from the various experiments.

The calorimeter was used in conjunction with QXDA, TGA and electron microscopy (both SEM and TEM) in the chemical and morphological studies to build up as complete a picture as possible of the chemical and physical changes that take place during the hydration reaction.

CHAPTER 2

CALORIMETER - CONSTRUCTION AND CALIBRATION

2.1 Introduction

The reaction of cement with water is exothermic. Variations in the rate of this heat liberation imply variations in the reaction rate of the hydrating cement. Measurement of this heat output is therefore a useful procedure for investigating the reaction of cement. In addition, because the thermal conductivity of cement and concrete is low, the temperature rise resulting from the heat liberation can be quite significant in structures where large pours of fresh concrete are used. Too large a temperature rise can give rise to stresses within the concrete which may cause cracking as it cools. A knowledge of the heat producing characteristics of a cement is therefore important to prevent such behaviour.

Most ordinary Portland cements produce over 50 percent of their heat of hydration in the first three days after mixing with water. The standard method used for the measurement of the heat of hydration of a cement (B.S. 1370) involves measuring the difference between the heat of solution of anhydrous and hydrated samples of known degree of hydration. It is inconvenient and inaccurate to use during the early stages of the reaction. For this reason, when information about the heat output during these early stages is required, a calorimetric method is often employed. It can not only provide an accurate measurement of the heat output during the first hours, even minutes of reaction, but also has the advantage of providing a continuous record of the heat output as a function of time.

Calorimeters generally come in two types; an adiabatic variety and an isothermal variety. Each has different operating characteristics and each

is useful in different circumstances (Calvet & Prat 1963). In an adiabatic calorimeter the heat produced by the reaction is, as far as is possible, kept within the calorimeter and goes to heat it up together with the sample. In an isothermal calorimeter, on the other hand, the heat liberated is dissipated in such a manner that the temperature of the calorimeter and sample remain constant. Measurement of the heat output of the sample is obtained in the case of the adiabatic calorimeter by following the temperature rise of the calorimeter and sample. Such a method cannot be employed for the isothermal type as by definition no heat rise occurs. Therefore a quantity must be measured which is related to the amount of heat which has been produced. For example in the case of an ice calorimeter the amount of ice which melts is measured and the heat produced calculated from a knowledge of the latent heat of fusion of water.

Calorimetric measurement of the heat given out by a hydrating cement is most often carried out using a calorimeter which is neither adiabatic nor truly isothermal. In this type of calorimeter the heat produced by the sample is conducted away to a heat sink kept at constant temperature, the difference in temperature between the sink and sample being a measure of the heat output of the sample. A calorimeter of this type is called a 'conduction' calorimeter. It is useful for measuring the heat output of a cement because it has the ability to measure very small heat outputs which occur over prolonged periods. The method can never be truly isothermal, since it relies on there being a temperature difference between the sample and the heat sink, but as long as this temperature difference is small, it can be considered so. These conditions are usually satisfied in the case of cements as the heat given out by cement is not large and with small samples the temperature seldom rises more than half a degree above its starting value.

The conduction calorimeter was first studied by Tian (1923 a & b) and was first adapted for cement work by Carlson (1934). Carlson's calorimeter, based largely on that of Tian, consisted of a reaction vessel thermally connected to a heat sink and placed in a five litre water bath. The whole arrangement was insulated with wadding and sunk in the ground. The heat produced was conducted to the heat sink (maintained at constant temperature by the waterbath) so keeping approximately constant temperature in the sample. The heat flow was determined by measuring the (small) temperature difference between the sample and the water bath.

Carlson's design was later adapted by Lerch (1946) who used a 400 gram sample of cement paste in a cylindrical copper cup 2" in diameter and 4" high. The cup was seated on a 6 inch long brass column. The section of the column in contact with the water had eight copper vanes attached to facilitate the conduction of heat to the waterbath. The heat given out by the setting cement was determined by measuring the temperature difference between the two ends of the brass column. Unfortunately the apparatus suffered from quite considerable temperature rises (2 to 15 degrees) which were by no means uniform throughout the sample so making conclusions difficult to draw.

A later development by Stein (1961) overcame this problem to a large extent by using a smaller reaction cell which held only 15 grams of cement and was ten times as wide as it was high. The smaller cell size meant that not only were the temperature rises and temperature variations within the sample kept to a minimum but also that less heat was produced. The sensitivity of the instrument was increased by using a heat flow meter (essentially a thermopile mounted in a plastic disc with alternate junctions on opposite faces), rather than a thermocouple, to measure the temperature difference between the sample and heat sink.

More recently Forrester (1970) described a conduction calorimeter using sensitive, solid state heat flow discs to measure the heat flow from the sample. The cement was mixed in a plastic bag and placed in a small quantity of oil in an aluminium tin. The heat flow disc was sandwiched between the tin and the heat sink. The whole arrangement was then insulated and contained in a large water bath.

These changes in design made significant improvements to the ability of conduction calorimeters to accurately measure the heat liberation of setting cements, but they all suffered from the drawback that the water and cement had to be mixed outside the calorimeter. This resulted in a considerable loss of information during the first few hours of hydration, both while the cement was outside the calorimeter, and while the calorimeter and sample were coming into equilibrium with the waterbath. The alternative arrangement of mixing the cement and water inside the calorimeter produces heat from the stirring which tends to swamp the real heat output during the early stages of the reaction. This problem was overcome by Perry (1974) who designed a calorimeter with a reaction cell which could be evacuated and hence into which water could be drawn by suction. It was found that this spread the water evenly throughout the cement, so doing away with the need for mixing altogether and enabling the heat output to be measured from the moment of addition of the water. This type of calorimeter has since been developed and has become known as a 'Calox' calorimeter

Perry's calorimeter used a reaction cell which could hold up to 18 grams of cement. When using synthetic cements, which can only be made in small quantities, such a large cell would limit the number of experiments which could be carried out. The calorimeters used in this work were therefore constructed with smaller reaction cells, holding up to three grams of

cement. Reducing the sample size in this manner reduces the heat output; in this case by five sixths. To overcome this problem the calorimeter was designed to be more sensitive than the larger model by reducing the amount of copper in the reaction cell and by the use of a more sensitive device for measuring the temperature difference between the cell and heatsink. This was a Melcor solid state cooling module (or Peltier device) working in reverse (suppliers: Thermoelectric Devices, PO Box 10, Reading. Type: CP 1.4-71-06L) and giving an output of approximately 30 mV per degree difference between its faces.

2.2 Calorimeter construction

Two calorimeters were constructed and used in this work. They are illustrated in fig 2.1. A schematic diagram is given in fig 2.2.

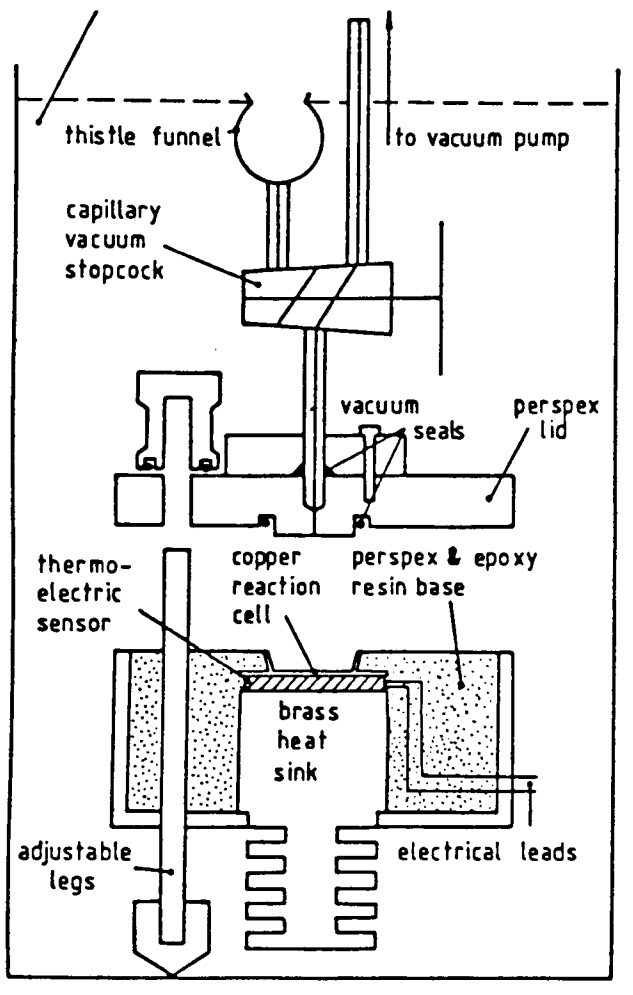

Fig 2.2: Schematic diagram of the conduction calorimeter used in this work

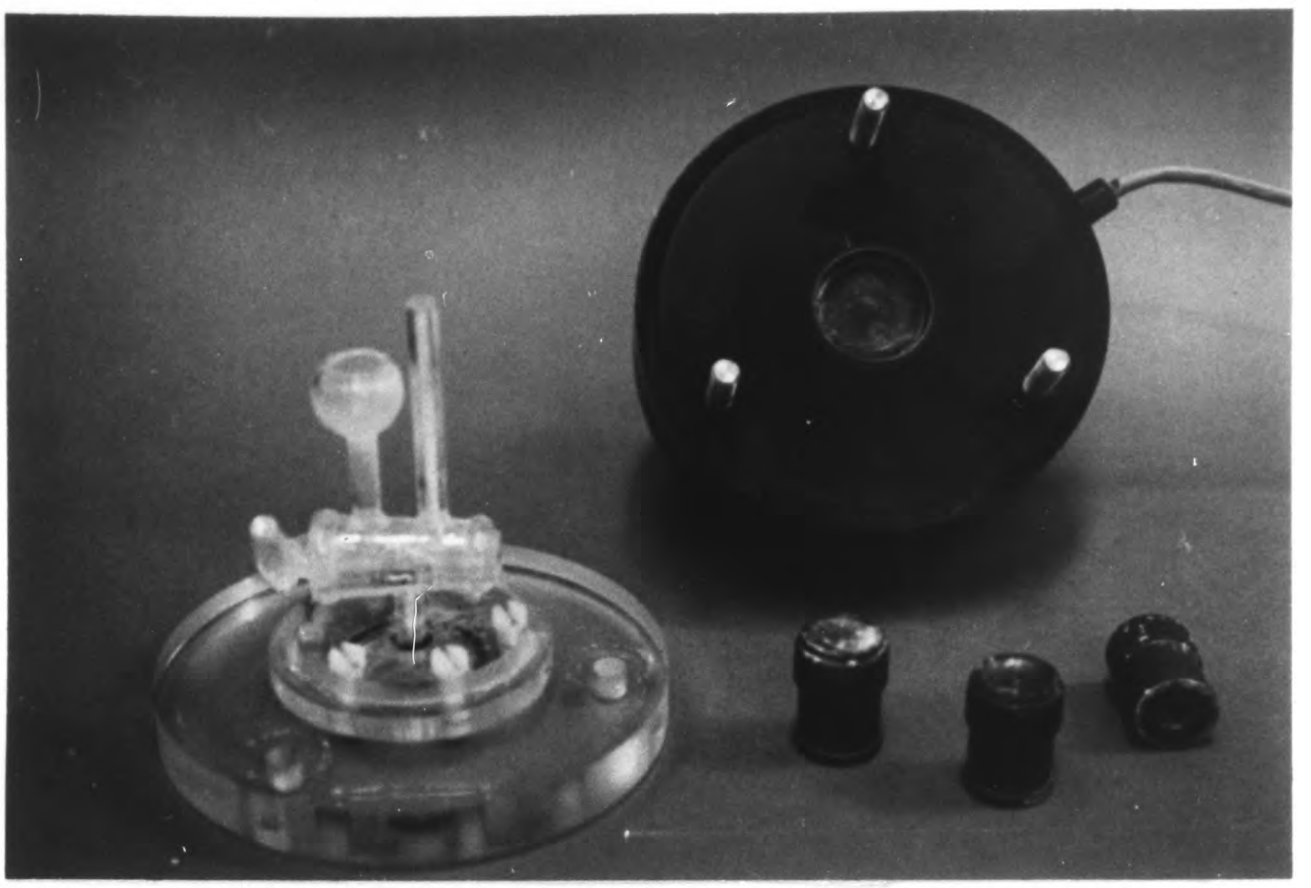

a

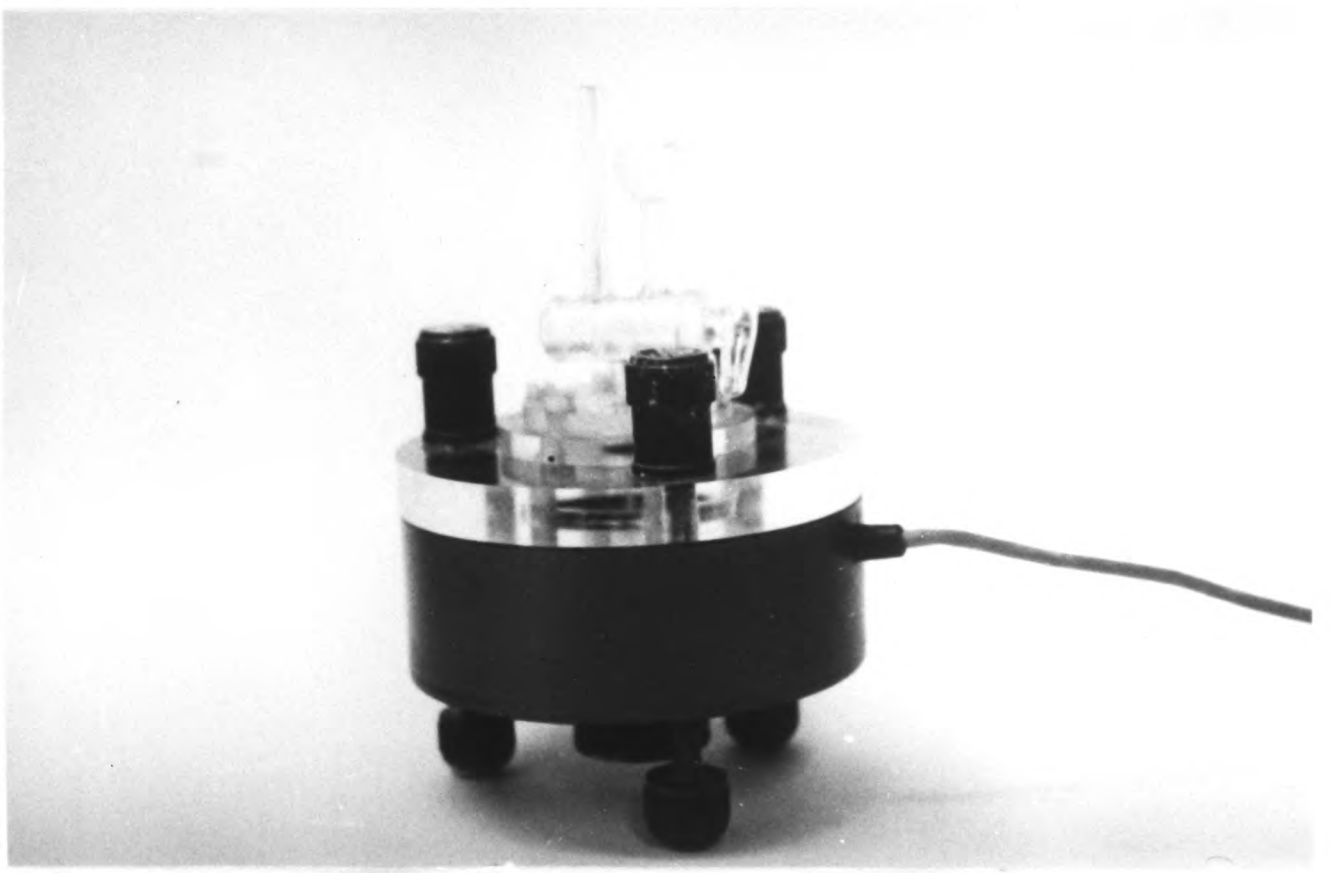

b

Fig 2.1 a) Calorimeter with lid removed to show reaction cell.
b) Assembled calorimeter.

The basic design of the calorimeter is very simple and rugged. The copper reaction cell, which is specially shaped to maximise the heat transfer to the thermoelectric sensor and minimise the amount of copper used, is mounted on one face of the sensor and a large brass heatsink, the bottom half of which has several vanes cut into it, is mounted on the other. This arrangement is encapsulated in epoxy resin (Araldite) with the top of the reaction cell level with the resin surface and the vaned portion of the heat sink protruding from the bottom. The top surface is machined flat to ensure a good seal with the '0' ring on the lid. Three adjustable legs are used to raise the heat sink above the surface of the waterbath and three stainless steel bolts are screwed into the upper surface of the resin to enable the lid to be attached. The lid is constructed from two disks of Perspex held together with six Nylon screws. The bottom disk has a circular raised portion on its undersurface which locates inside the reaction cell and presses on the sample. A groove is let into the Perspex at the perimeter of the raised portion to take an '0' ring which seats on the resin of the body of the calorimeter, just outside the reaction cell. An 8mm hole is drilled all the way through the centre of the top disc and half way through the bottom one, a 1mm hole being drilled through the remainder. A double oblique capillary vacuum stopcock with a thistle funnel attached to one arm (as illustrated) is inserted into the 8mm hole with an '0' ring between the two discs so that when the assembly is screwed together the joint is both air and water tight. The lid is held in place by three large knurled nuts which fit on the bolts of the lower half of the calorimeter. When assembled, the sample cell can be evacuated through the straight arm of the vacuum stopcock and the liquid in the small thistle funnel can be drawn into the reaction cell under vacuum by rotating the tap through half a revolution.

2.3 Theory of conduction calorimetry

To get useful results from a calorimeter it must be possible to calculate the amount of heat being given out by the sample. A knowledge of the theory of its operation is thus essential.

As mentioned earlier, a conduction calorimeter does not operate under truly isothermal conditions. Its operation depends on the measurement of a small temperature difference between the specimen container and the heat sink (the latter being maintained at constant temperature). Provided that this temperature difference is small, in practice less than 1 degree centigrade, Tian's analysis (1923 a) may be applied.

Part of the heat (W) generated by the cement at any time (t) is lost to the heat sink via the thermoelectric sensors (w_1) and the rest is used to raise the temperature of the calorimeter cell and its contents (w_2).

$$W = w_1 + w_2 \qquad \ldots 2.1$$

By Newton's law of cooling, the heat lost from the container to the heat sink is proportional to the temperature difference (Q) across the interface; the constant of proportionality (c_1) being the heat transfer coefficient.

$$w_1 = c_1 \cdot Q \qquad \ldots 2.2$$

Given that the heat capacity of the system is c_2, the heat required to raise the temperature of the cell and its contents is:

$$w_2 = c_2 \cdot \frac{dQ}{dt} \qquad \ldots 2.3$$

The total power output (W) is the sum of these two quantities:

$$W = w_1 + w_2 = c_1 \cdot Q + c_2 \cdot \frac{dQ}{dt} \qquad \ldots 2.4$$

For small temperature differences, the voltage output (V) from the thermoelectric sensors is proportional to the temperature difference (Q):

$$W = k_1 \cdot V + k_2 \cdot \frac{dV}{dt} \text{ (Tian's equation)} \qquad \ldots 2.5$$

where k_1 and k_2 are constants for the calorimeter and sample.

Once k_1 and k_2 have been determined (see section 2.4), Tians equation (eqn. 2.5) allows the power being given out by the sample to be calculated by measuring the voltage being generated by the thermoelectric device.

2.4 Calorimeter calibration

2.4.a Theory

If a constant amount of heat is supplied to the calorimeter for a length of time and then cut off, the voltage measured from the calorimeter rises to a steady state value and then decays exponentially when the heat is cut off (fig 2.3).

During the heating cycle, if the power being supplied is W and the voltage output of the calorimeter is V then applying Tian's analysis (eqn. 2.5) gives:

$$W = k_1 \cdot V + k_2 \cdot \frac{dV}{dt} \qquad \ldots 2.6$$

where t is measured from the start of the heating cycle.

When the steady state condition is reached all heat supplied is being conducted away through the heat sink. At this point dV/dt is zero so if V = V_o then:

$$W = k_1 . V_o \qquad \ldots 2.7$$

W is known, V_o can be measured and hence k_1 can be determined.

The other calibration constant can be determined either from the heating cycle or from the cooling cycle.

For the heating cycle, rearranging eqn. 2.6 and dividing through by k_2 gives:

$$\frac{dV}{dt} = \frac{W}{k_2} - V . \frac{k_1}{k_2} \qquad \ldots 2.8$$

A graphical plot of dV/dt against V should therefore be a straight line of slope $-k_1/k_2$

For the cooling cycle the power W is zero, so:

$$\frac{dV}{dt} = - V . \frac{k_1}{k_2} \qquad \ldots 2.9$$

A graphical plot of dV/dt against V should be a straight line of slope $-k_1/k_2$.

k_1 is already known so k_2 can now be calculated.

2.4.b Method

The evaluation of the calibration constants for a conduction calorimeter requires a known, constant heat to be supplied to the calorimeter reaction cell for a fixed length of time. The simplest method of

supplying this heat is to use an electrical heater. Such a method was used in this work and to ensure the conditions in the reaction cell were as similar to those encountered when using a real cement, the heater was embedded in a hydrated C_3S block.

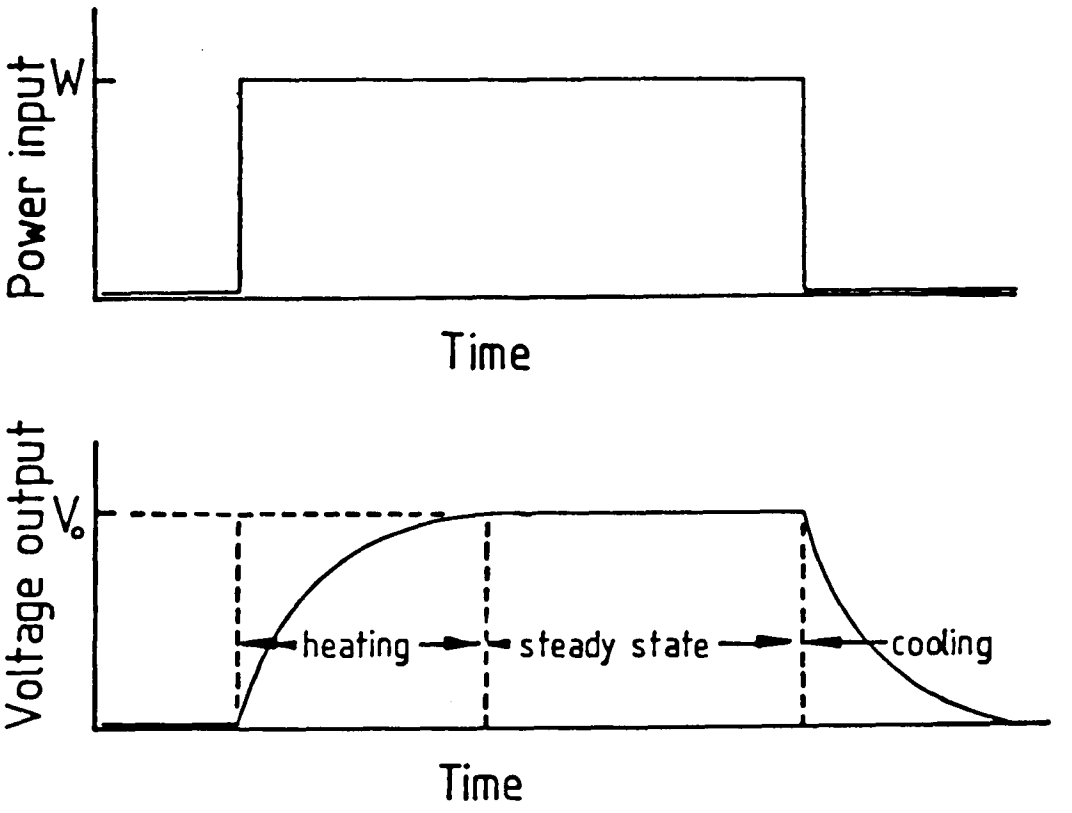

Fig 2.3: (a) Power input and (b) voltage output during a calibration.

The heater consisted of two 120 ohm strain gauges (Tinsley Telcon, part no. 13/120/EC) connected in series and glued to either side of a thin copper disc. In this way the heat was made to dissipate through the whole cement block quickly and evenly. Two thin leads were connected to the two remaining contacts (as thin as practical to minimise heat loss by conduction) and the whole heater was coated in lacquer to prevent shorting.

The block was made by embedding the heater in C_3S powder in the calorimeter (passing the leads through a hole in the filter paper), evacuating and hydrating in the usual way (section 2.5). The block was then left until all measurable heat output had ceased (usually about two weeks).

Immediately before using the block it was soaked in water for ten minutes, excess water was removed with a tissue, the leads were fed up through the capillary tubes of the vacuum stopcock, the calorimeter was assembled, placed in the water bath and allowed to come to thermal equilibrium. A known voltage was applied and the current passing and the voltage output were recorded.

2.4.c Results

Calorimeter No.1

Various calibration curves were obtained using different power inputs. Fig 2.4 is a graph of the power input against the steady state voltage (V_o) for these. As predicted by eqn 2.7, the graph is a straight line through the origin. The slope of this line gives k_1.

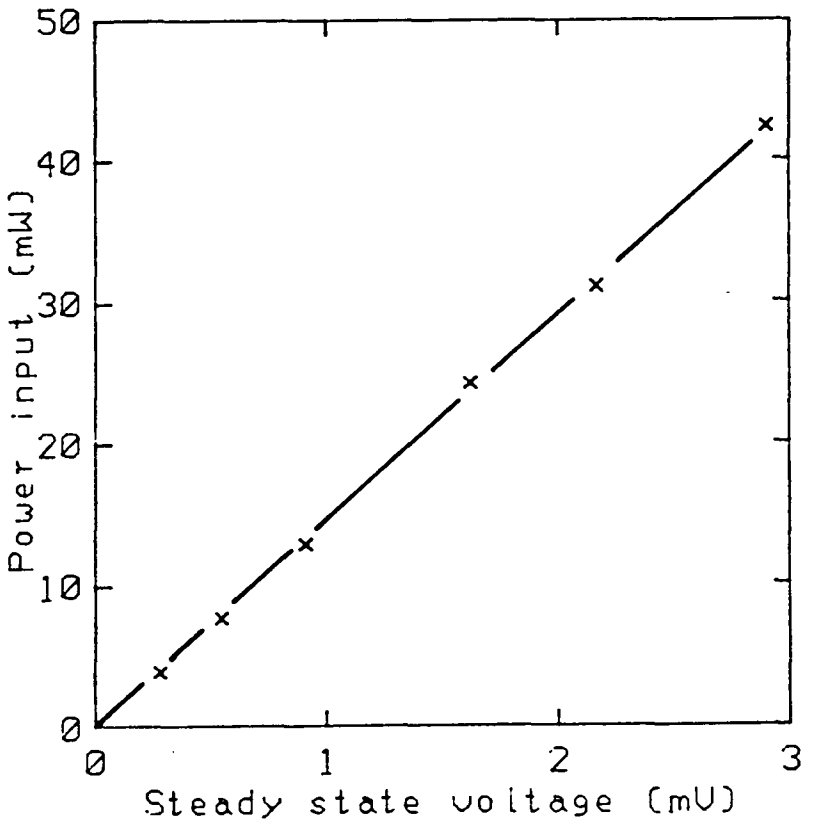

Fig 2.4: Plot of steady state voltage against power input during calibration to determine k_1.

To find the value of k_2, a graph of dV/dt against V for one of the cooling curves was plotted (fig 2.5). Although the analysis (above) predicts that this should be a straight line of gradient $-k_1/k_2$, in

practice, a sigmoidal curve was obtained. k_2 was therefore determined from the gradient of the central section of this curve which approximates to a straight line.

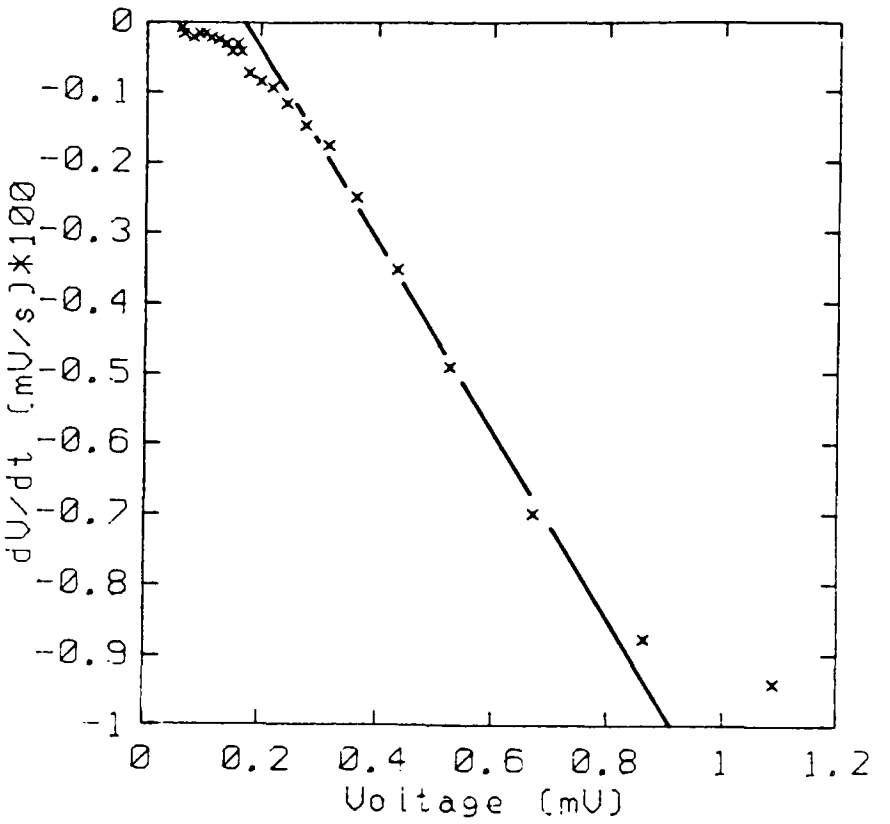

Fig 2.5: Plot of dV/dt against V for the cooling part of a calibration curve. The gradient of the central, approximately linear, portion was used to determine k_2.

The gradients of the lines in figs 2.4 and 2.5 gave the following values for the calibration constants of calorimeter no.1:

k_1 = 0.0149 J/s/mV

k_2 = 1.08 J/mV

Two methods were used to check the accuracy of this calibration:

1) The values of k_1 and k_2 derived above and the calibration curve were used to calculate the power input during the calibration to see how it compared with the actual power input. The results from this calculation are illustrated in fig 2.6

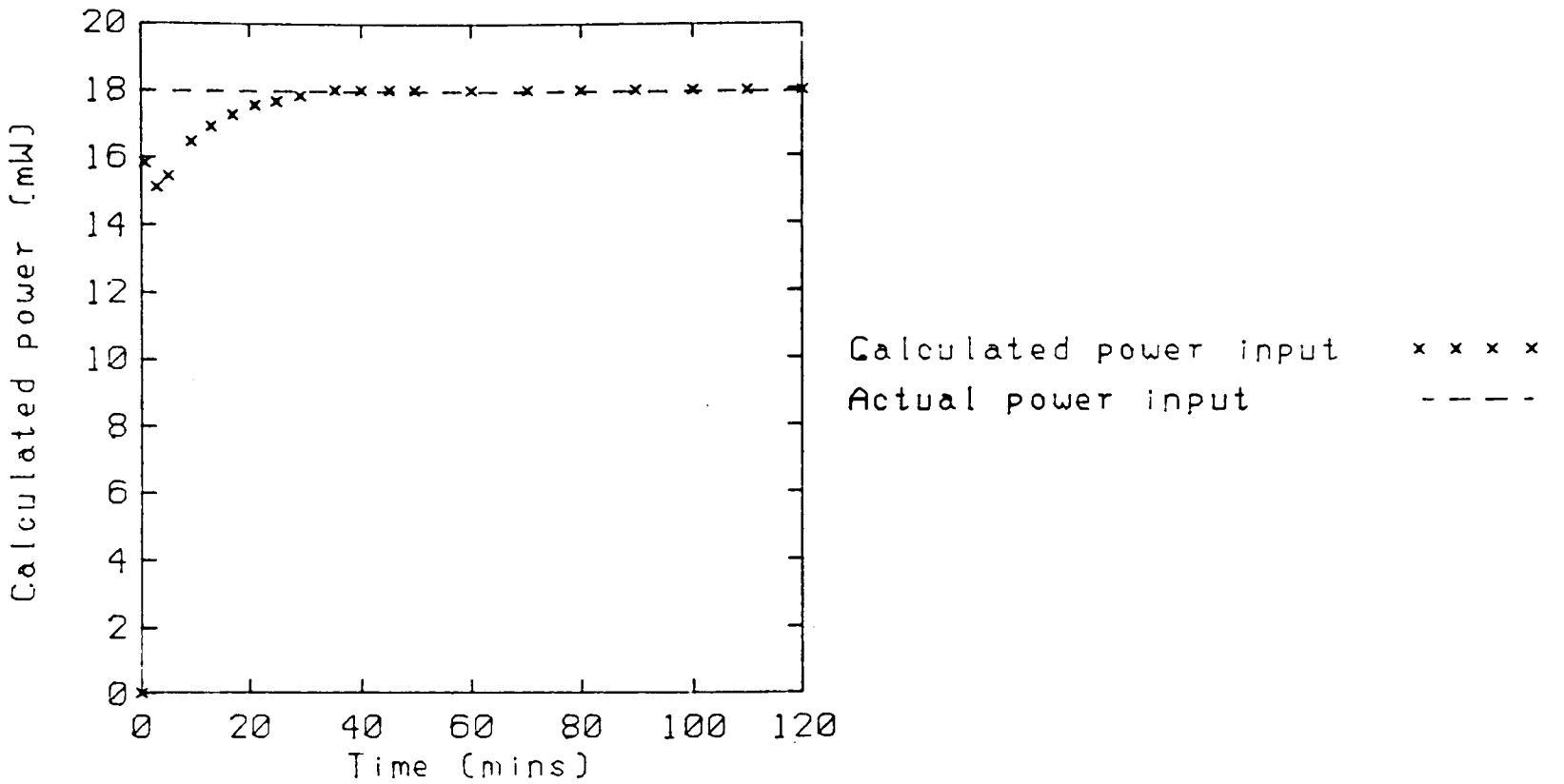

Fig 2.6: Comparison of the calculated power input with the actual power input during a calibration when the power input remains constant.

2) A varying power was supplied to the heater and the voltage response of the calorimeter measured. The values of k_1 and k_2 and this curve were then used to calculate the changing power input which had given rise to the measured voltage response and this was compared to the actual power input. The results are shown in fig 2.7.

Calorimeter No.2

k_1 and k_2 were calculated in the same manner as for calorimeter no.1. The following values were obtained:

k_1 = 0.0132 J/s/mV

k_2 = 1.04 J/mV

2.4.d Discussion

The agreement between the calculated power input and the actual power input (figs 2.6 & 2.7) indicate that the calorimeters can measure heat outputs of only a few milliwatts to a high degree of accuracy. The heat

output of hydrating C_3S seldom rises above 10 mW. The calorimeters should therefore be well suited to recording the heat output of hydrating C_3S.

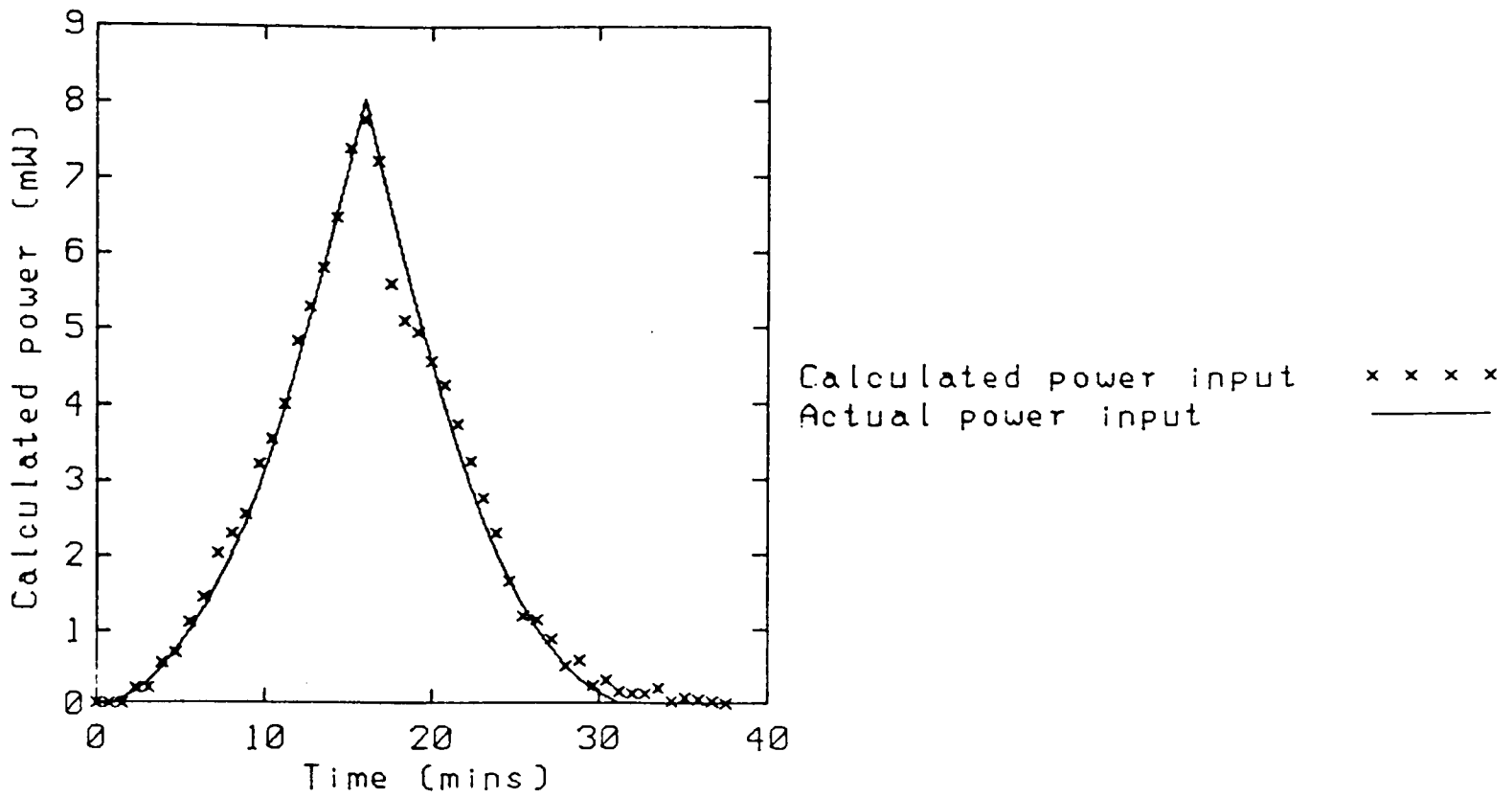

Fig 2.7: Comparison of the calculated power input with the actual power input when the power input is varying.

The small inaccuracy which does exist arises mainly from the k_2 term. The graph of fig 2.5 shows that while Tian's analysis is followed during the central portion of the cooling curve, deviations occur both at the start and towards the end. The cause of the deviation from the predicted behaviour is not certain, but it is likely that the deviation during the later stages arises from inaccuracies in reading the calorimetric curve. The base line tends to fluctuate slightly due to very small random temperature variations in the water bath and the errors introduced by this are largest when the heat output is at its lowest. One other possible source of error comes from the incomplete insulation of the Araldite surrounding the reaction cell and the Perspex lid leading to a small loss of heat from the reaction cell which is not accounted for in Tian's analysis.

However, because the heat output of C_3S changes only very slowly, the gradient of the calorimetric trace of voltage against time for hydrating C_3S is very low; largest values being of the order of 0.00013 mV/s compared with average values of 0.0004 mV/s during the test of the calibration constants (fig 2.7) and considerably higher values during the calibration itself. When the rate of change of voltage with time is so low, the $k_2.dV/dt$ term becomes relatively unimportant and small inaccuracies in the measurement of k_2 have a minimal effect on the accuracy of the rate of heat release calculated from the calorimeter output.

2.5 Calorimeter operation

The following sequence was followed to obtain a calorimetric trace:

1. Clean and dry the reaction cell and surrounding Araldite.
2. Line the reaction cell with 'Clingfilm'. This facilitates later removal of the hydrated sample.
3. Place an accurately weighed amount of cement into the lined cell.
4. Cut a disc of filter paper to fit snugly into the reaction cell. Place it on the cement and press it down using a flat circular disc of the same size, until the cement is slightly compacted.
5. Clean the '0' ring surfaces and grease them with a small amount of vacuum grease. Place a small amount of vacuum grease on the Araldite surrounding the reaction cell where the '0' ring will seat.
6. Clean and dry the lid of the calorimeter and remove any water remaining in the capillary tubes or the thistle funnel.
7. Fit the lid and tighten the knurled knobs to finger tightness.
8. Checking that the tap on the stopcock is closed, measure out the appropriate quantity of water into the thistle funnel and fit a rubber bung to prevent loss by evaporation. (N.B. All experiments in

this work were carried out at a water/cement ratio of 0.5 unless otherwise stated in the text.)

9. Place the assembled calorimeter into a thermostatically controlled water bath set to the required temperature (the water bath should be capable of keeping temperature fluctuations to less than 0.01 degrees). Adjust the legs so that the lip of the thistle funnel just protrudes above the surface of the water. Take care not to allow any water to get into the thistle funnel at this stage. (N.B. All experiments were carried out at a temperature of 25 degrees unless otherwise stated in the text.)

10. Connect a vacuum pump to the arm of the stopcock. Start the pump and open the tap to evacuate the reaction cell. Continue pumping throughout the equilibration period.

11. Connect the electrical output leads to a suitable chart recorder and start the recording.

12. Allow the assembly to come to temperature equilibrium (1-3 hours) signified by a level, nearly zero output on the chart.

13. Set the chart recorder to an appropriate full-scale deflection and the chart speed to less than 1mm/min.

14. Remove the rubber bung from the thistle funnel. Rotate the tap on the stopcock through 180 degrees. The water in the funnel will be rapidly sucked into the reaction cell. Rotate the tap by a further 90 degrees and turn off the vacuum pump. Place a lid on the waterbath.

15. Leave the apparatus to record the exotherm over the next day or so.

2.6 Analysis of a calorimetric trace

The calorimetric trace so obtained (fig 2.8) is of voltage against time and must be converted to rate of heat output against time before it can be used further. This is carried out using Tian's equation (eqn. 2.5) and the two constants found in the calibration (section 2.4).

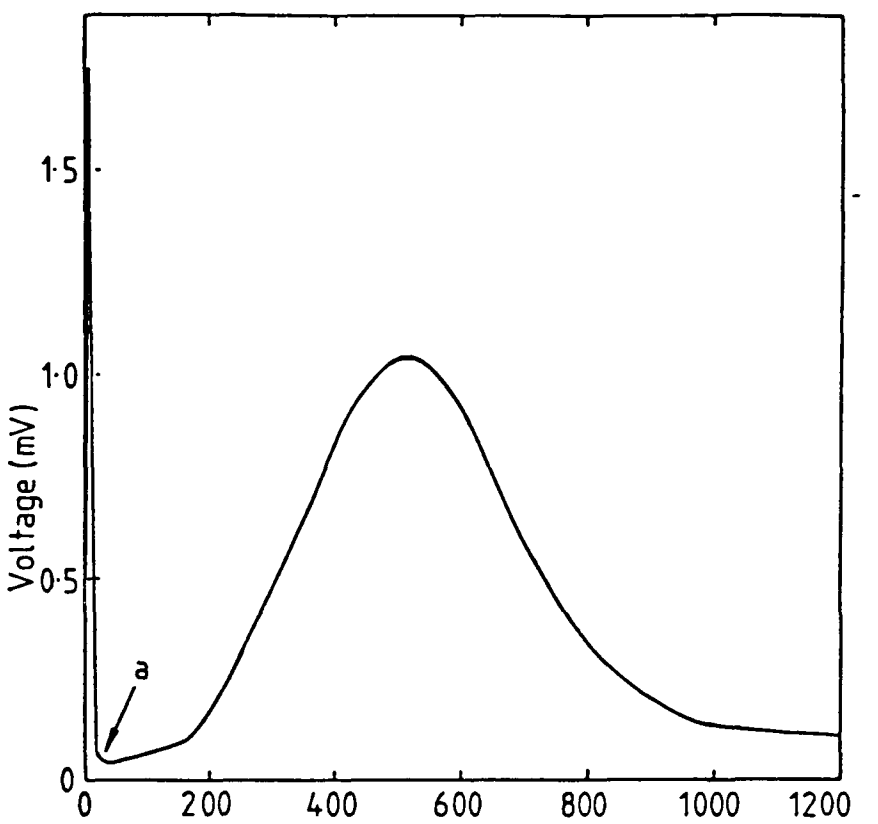

Fig 2.8: A typical calorimetric curve from a sample of C_3S.

The heat output during the first heat peak (fig 2.8) has been found to be very variable and is produced at too fast a rate for Tian's analysis to apply. Hence, for the purposes of this work, the heat produced during the first peak has been ignored and all measurements have been taken from the minimum in the curve following this peak (fig 2.8 point a). The sole use of the calorimetry in this work is for comparison purposes; comparing the time to, and height of, the main heat peak, and the length of the induction period, of different preparations. The first heat peak has no bearing on these comparisons and discounting it does not affect the results.

The rate of heat output of the sample and the total heat which had been produced at any given time were calculated using the following procedure:

1) Measure the voltage recorded on the chart at convenient time intervals from the minimum in the curve. In this work, to standardise the readings obtained, the following time intervals were used:

From 0 to 100 mins - intervals of 10 mins
From 100 to 400 mins - intervals of 20 mins
From 400 to 1000 mins - intervals of 50 mins

In certain circumstances these intervals proved impractical in which case other more suitable ones were chosen.

2) Calculate the gradient of the voltage against time curve at each point (n).This can conveniently be carried out using the following simple routine.

$$Grad_{(n)} = \frac{V_{(n+1)} - V_{(n-1)}}{t_{(n+1)} - t_{(n-1)}}$$

3) Using Tian's equation and the two calibration constants for the calorimeter, calculate the rate of heat output (Q) at each point (n).

$$Q_{(n)} = k_1 . V_{(n)} + k_2 . Grad_{(n)}$$

4) Using the trapezium rule, calculate the area under the curve from the minimum to the point n, this being the total heat output of the sample up to that point (H):

$$H_{(o \text{ to } n)} = H_{(o \text{ to } n-1)} + \frac{1}{2}(Q_{(n)} + Q_{(n-1)})(t_{(n)} - t_{(n-1)})$$

PREPARATION A1 (CONTROL)

CALOX NO.10 EXPERIMENTAL RUN NO.1000
TEMPERATURE = 298K WATER/CEMENT RATIO = 0.5
K1=.0149(J/S/MV), K2=1.079(J/MV)
BASE LINE VOLTAGE CORRECTION: 0 MV
TIME TO MINIMUM IN HEAT CURVE: 100 MINUTES
INTEGRATED AREA UNDER SECOND HEAT PEAK: 254.88 (J/G)

TIME (MINS)	RAW DATA (MV)	CORRECTED DATA (MV)	RATE OF HEAT EVOLUTION (J/S/KG)	INTEGRATED HEAT OUTPUT (J/G)
100	.08	.08	.375	0
110	.08	.08	.4	.23
120	.08	.08	.411	.48
130	.09	.09	.424	.73
140	.09	.09	.437	.98
150	.09	.09	.471	1.26
160	.1	.1	.499	1.55
170	.1	.1	.512	1.85
180	.11	.11	.552	2.17
190	.12	.12	.6	2.52
200	.13	.13	.627	2.88
220	.15	.15	.753	3.71
240	.18	.18	.891	4.7
260	.21	.21	1.054	5.86
280	.25	.25	1.27	7.26
300	.32	.32	1.588	8.97
320	.41	.41	2.046	11.15
340	.5	.5	2.527	13.9
360	.62	.62	3.09	17.27
380	.74	.74	3.727	21.36
400	.88	.88	4.402	26.24
420	1.04	1.04	5.185	31.99
440	1.17	1.17	5.877	38.63
460	1.31	1.31	6.534	46.07
480	1.44	1.44	7.203	54.31
500	1.56	1.56	7.789	63.31
550	1.78	1.78	8.846	88.26
600	1.86	1.86	9.251	115.41
650	1.8	1.8	8.897	142.63
700	1.56	1.56	7.707	167.54
750	1.32	1.32	6.525	188.89
800	1.05	1.05	5.173	206.43
850	.83	.83	4.072	220.3
900	.62	.62	3.072	231.02
950	.49	.49	2.407	239.23
1000	.38	.38	1.877	245.66
1050	.31	.31	1.532	250.77
1100	.25	.25	1.209	254.88

CEMENT GROUP - 21,BANBURY ROAD, OXFORD

FILE NO. ADMIXTURE

1000 PREPARATION A1 (CONTROL)

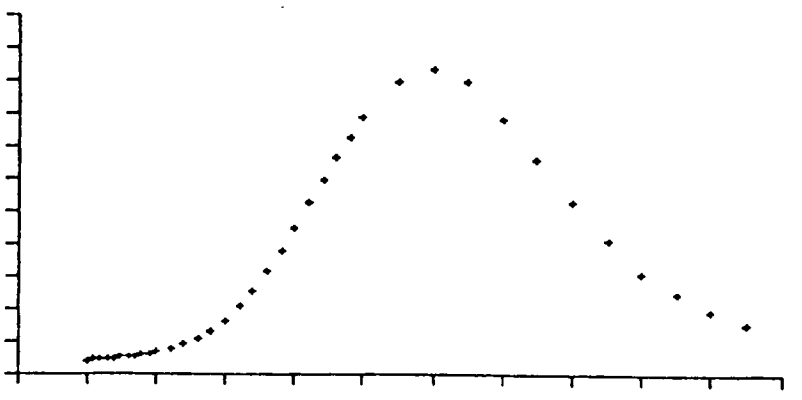

Fig 2.9: Example table of results and graphs from calorimetry data processing program.

To simplify this operation, BASIC computer programs were written for the Apple II to file the raw data, perform the calculations, print out the results and plot graphs of either the rate of heat output as a function of time or the total integrated heat against time. Listings of the programs are included in appendix I. An example printout and graphs are given in fig 2.9.

2.7 Calorimeter performance

2.7.a Accuracy and reproducibility

The tests carried out during the calibration (section 2.4.c) indicate that the calorimeters are sufficiently accurate to measure the heat output of hydrating C_3S.

The manner in which the output from a single calorimeter varied when operating under identical experimental conditions was investigated. Two identical samples were run in calorimeter no. 1. The results are shown in fig 2.10. The two traces are almost identical indicting that, when following the same operating technique for each run (section 2.5), the calorimeter is capable of giving a high degree of reproducibility.

To test the agreement between the two calorimeters, two identical samples were run, one in calorimeter no.1 and one in calorimeter no.2. The results are shown in fig 2.11. The difference between the two calorimeters is no greater than the difference in reproducibility (fig 2.10).

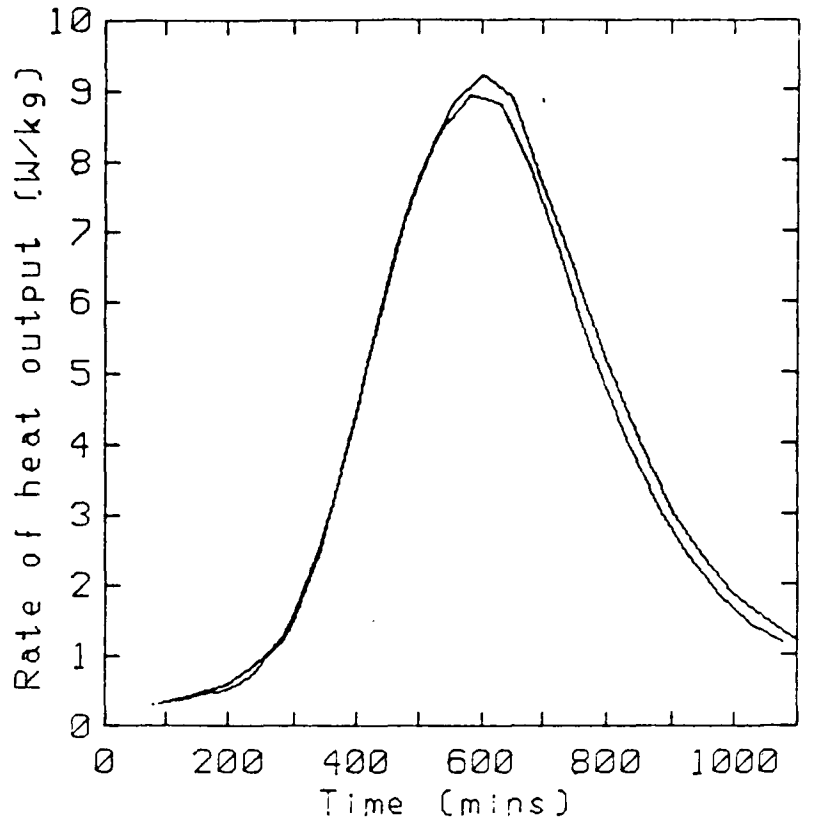

Fig 2.10: Calorimetric curves obtained from calorimeter no. 1 using identical experimental conditions to illustrate the reproducibility of the calorimeters.

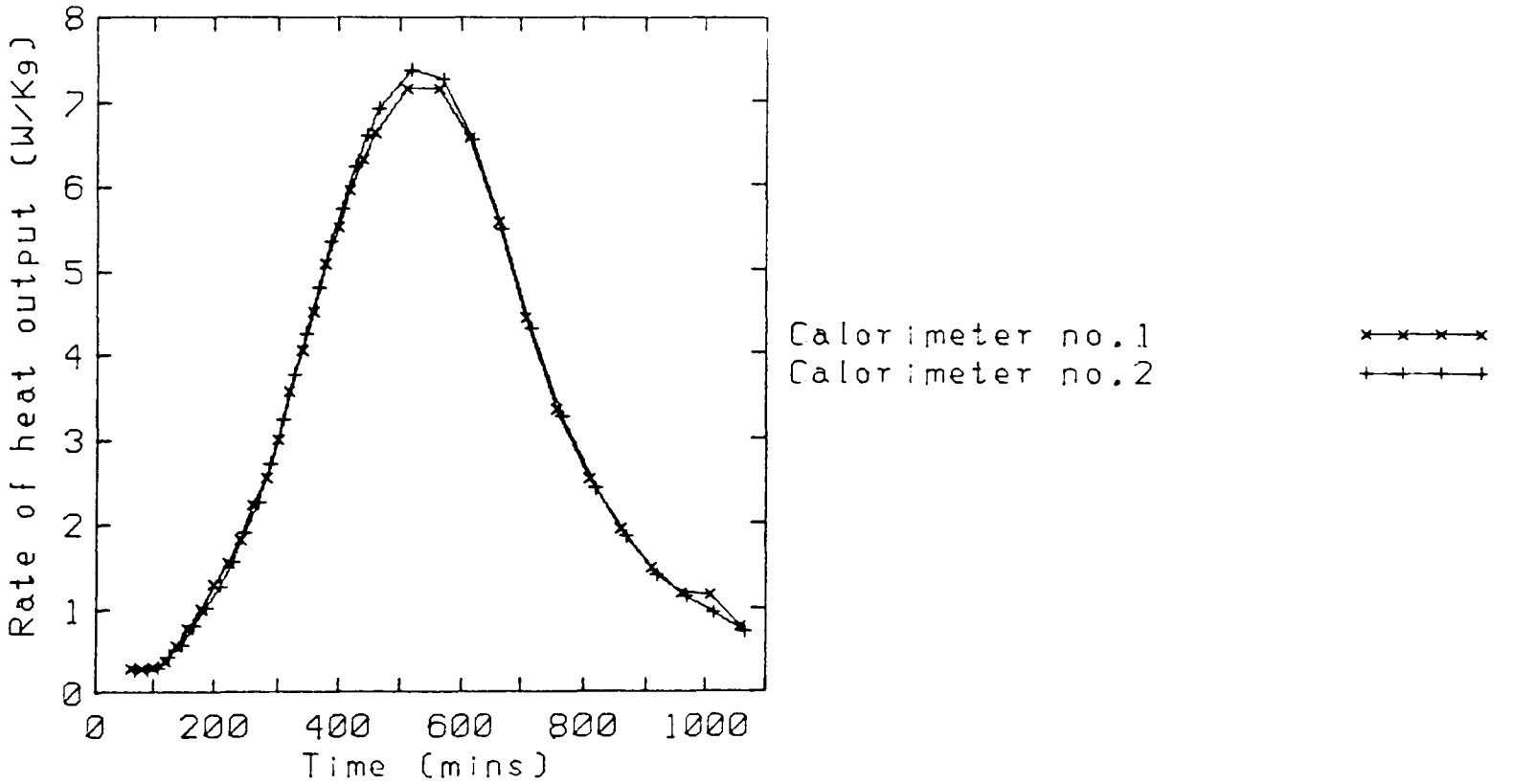

Fig 2.11: Calorimetric curves from the two calorimeters, obtained using identical samples, to illustrate the agreement between the two calorimeters.

Towards the end of the period of study a slight difference between the outputs of the two calorimeters became evident. This is illustrated by the calorimetric curves of fig 2.12. Subsequent comparative experiments were therefore carried out on the same calorimeter as far as was possible. In cases where it was not possible to run all samples on the same calorimeter the fact is indicated in the text and reference should be made to fig 2.12 before taking any differences into account.

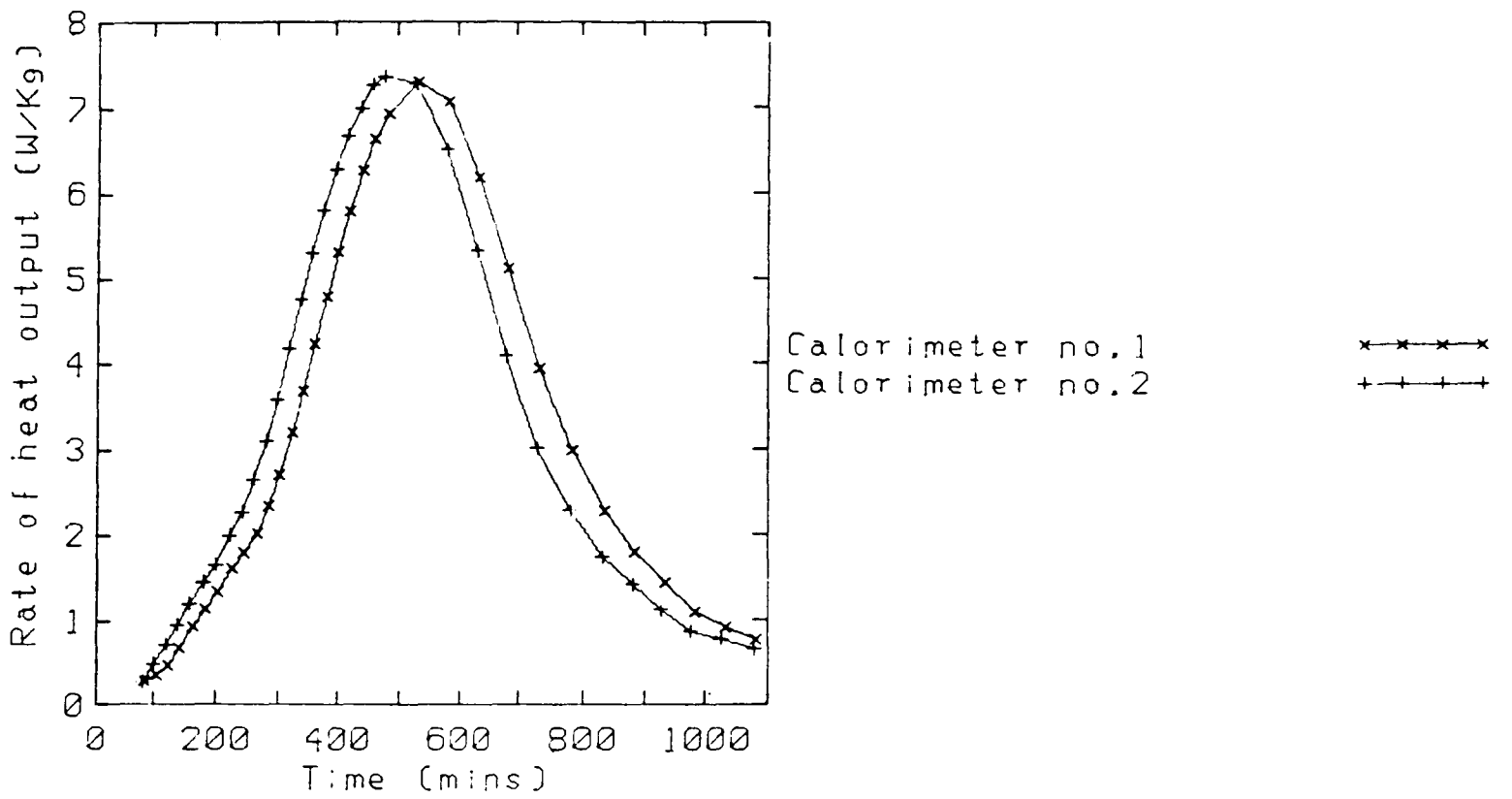

Fig 2.12: Calorimetric curves from the two calorimeters, obtained using identical samples, to illustrate the change which occurred later during the period of study.

2.7.b Effect of mixing technique

It has been noted that the 'Calox' type of calorimeter which was used in this work can, under certain circumstances, give a different response from that given out by conventional conduction calorimeters. In particular, cements with a high C_3A content often show a third heat peak (dotted line on fig 1.5) when hydrated in conventional calorimeters but show none when hydrated in the 'Calox' type. This difference has been attributed to differences in the mixing techniques used. Conventional

calorimeters take samples which have been mixed by hand outside the calorimeter while 'Calox' types take the dry powder and spread the water through the sample by suction. When samples of the cement which produced the third heat peak were mixed by hand outside, and subsequently placed in a 'Calox' calorimeter the heat traces obtained were similar to those obtained by the other methods.

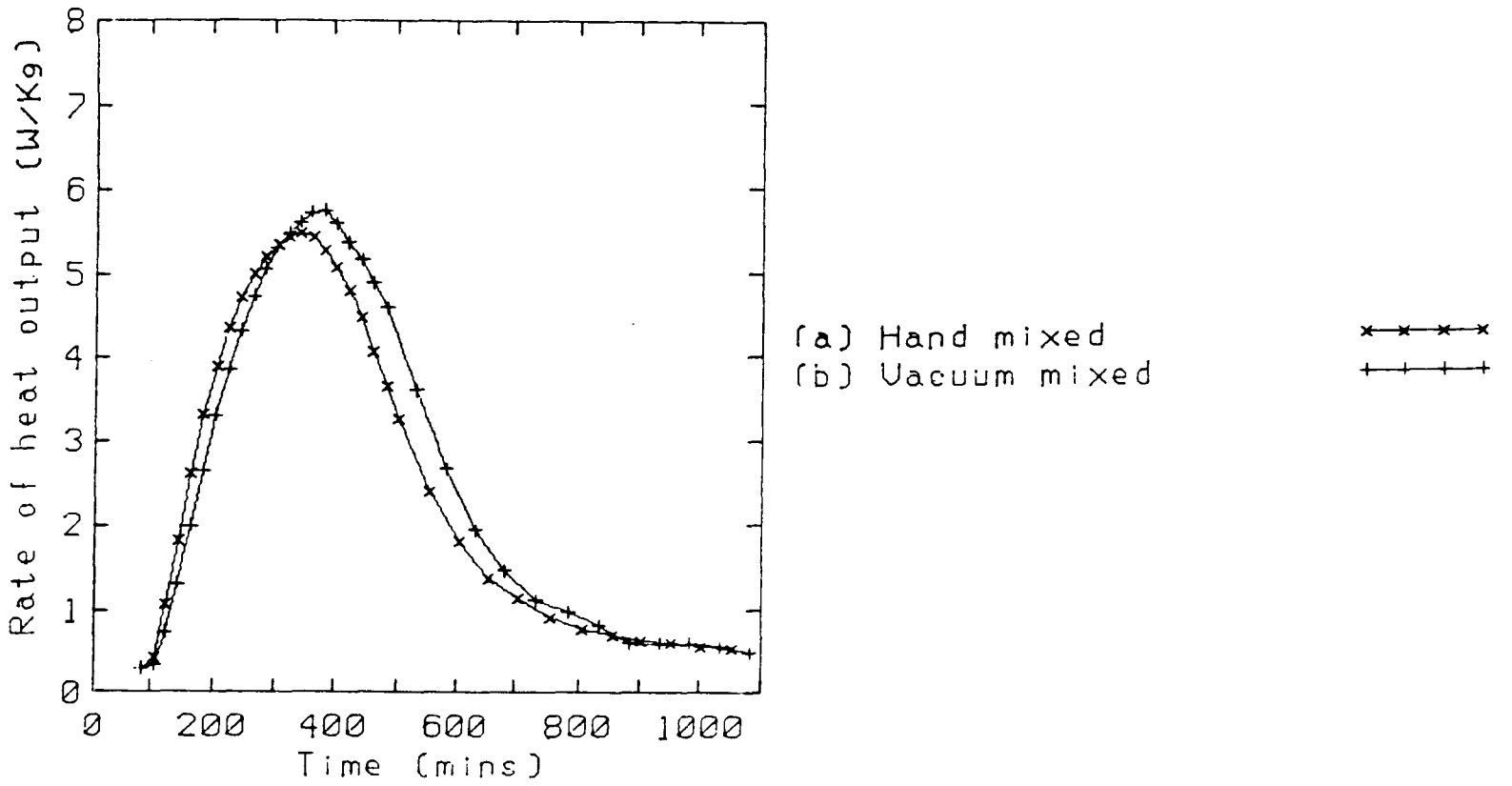

Fig 2.13: Calorimetric curves demonstrating the similarity in rate of heat production from C_3S when it is mixed under vacuum or by hand.

To test whether mixing by hand rather than by vacuum had any effect on the rate of heat evolution of C_3S, two calorimetric runs were carried out. In the first the sample was mixed under vacuum in the usual way while in the second it was mixed by hand outside the calorimeter. The results are shown in fig 2.13. Note that the two traces were obtained from different calorimeters and that they were recorded at the time when the responses of the calorimeters had become slightly different. Comparing fig 2.13 with fig 2.12 shows that while part of the difference between the two traces can be ascribed to the differences between the calorimeters, it can not account for all of it. However, the small

difference between the two is only in the position of the main heat peak, its height and shape have not been affected significantly. Thus it can be concluded that mixing under vacuum rather than in a conventional manner does not alter the reactions which are taking place, but it may slightly influence the rate at which they take place.

2.8 Conclusions

The calorimeters constructed to be used in this work have been shown to be able to accurately and reproducibly measure heat given out by a body in the reaction cell. It can be concluded that the calorimetric curves obtained from them can be compared with similar curves reported in the literature and that differences between curves obtained using the calorimeters are indicative of differences in rate of reaction and not merely due to random errors.

CHAPTER 3

SYNTHESIS OF TRICALCIUM SILICATE

3.1 Background

Using differential thermal analysis and X-ray diffraction at elevated temperatures, it has been shown (Bigare et al 1967) that C_3S can exist in at least six different polymorphic forms between room temperature and its decomposition temperature at 1250 degrees. More recently, microscopical studies of the changes in optical properties and modes of twinning of C_3S as a function of temperature (Maki & Chromy 1978) have indicated the presence of a seventh form. These various forms and their transformation temperatures are summarised in fig 3.1 below.

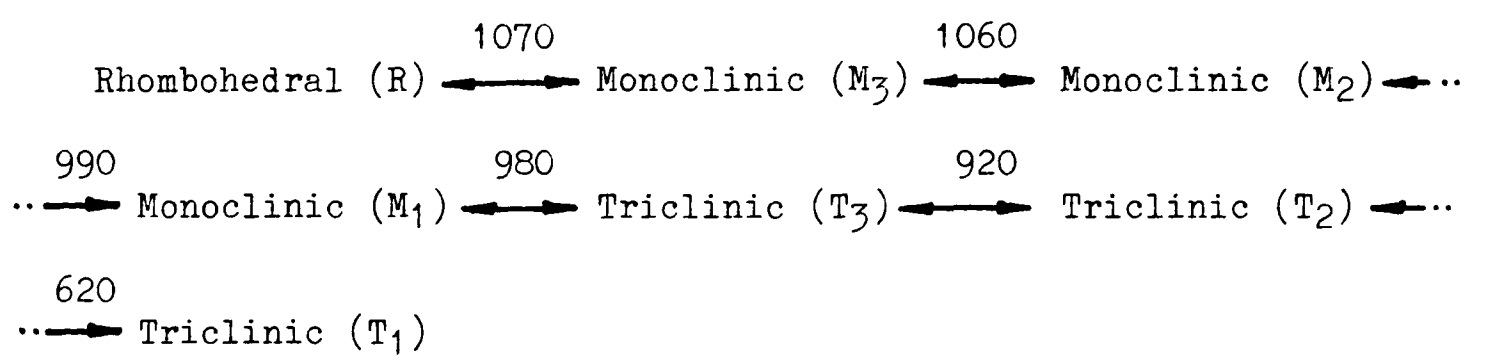

Fig 3.1: Polymorphic forms and transition temperatures of C_3S from room temperature up to its decomposition temperature.

All the transformations are reversible and of the displacive type involving only very small atomic movements. Thus the T_1 form is the only one stable at room temperature and the crystal lattices of the various modifications are all very close to a trigonal lattice.

With reference to the CaO/SiO_2 phase diagram (Chapter 1, fig 1.3) it can be seen that C_3S is formed by the reaction of C_2S and lime above 1250 degrees and that it melts incongruently above 1900 degees to give lime and liquid. Below 1250 degrees C_3S is unstable, decomposing back into lime and C_2S. This decomposition reaction is very slow, its effect being

negligible below 700 degrees, so allowing C_3S to exist at room temperature indefinitely.

A structure for C_3S was first proposed by Jeffery (1952). This was made up of isolated SiO_4 tetrahedra on trigonal axes and had a triclinic crystal structure. Since then a more detailed structure determination has been accomplished (Golovastikov et al 1975) which has shown the structure to consist of layers of calcium and silicon atoms which are shifted slightly with respect to one another and repeat after every seventh layer. The calcium atoms are mostly coordinated to six oxygens lying at the corners of distorted octahedra, though in some cases they are seven coordinated. Silicon is in four-fold coordination with oxygen, forming tetrahedra which lie in various orientations (fig 3.2). The structure indicates the presence of nine distinct sites for silicon. Solid state NMR studies have indicated the presence of at least eight of these (Clayden et al 1984).

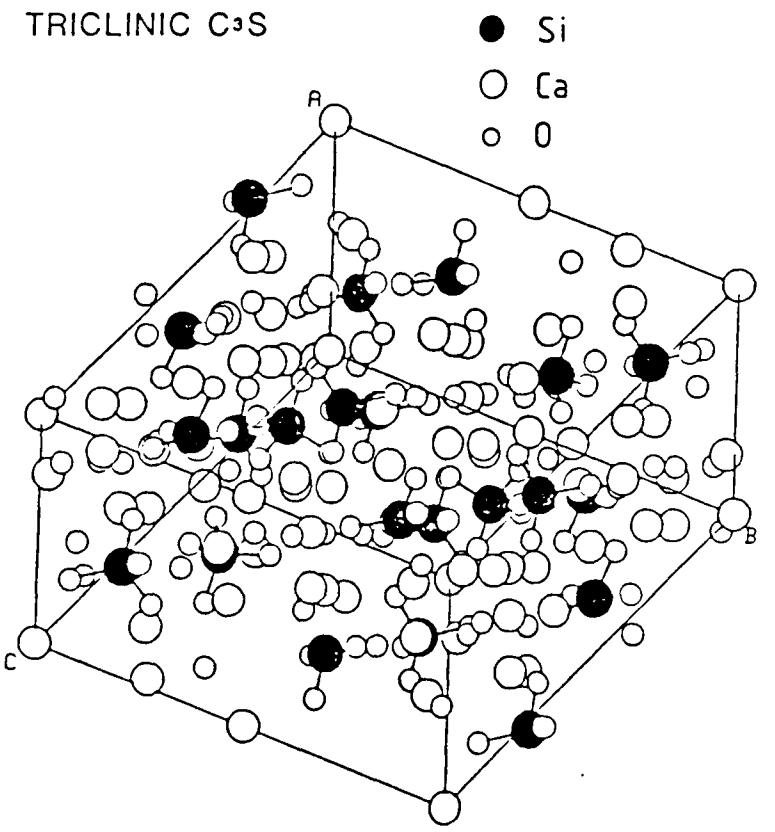

Fig 3.2: Computer drawn structure of C_3S based on the work of Golovastikov et al (1975).

3.2 Method

Various methods have been employed in order to prepare pure C_3S (Lerch & Bogue 1927; Hansen 1928; Polivka et al 1961; Lea 1970; Odler & Dorr 1977; Ghosh 1980; Ludwig & Wolter 1980). Most of these involve intimately mixing together lime and silica (or compounds which yield them on decomposition) and heating them up to a high enough temperature for reaction to occur. In some cases mineralisers and fluxes are added to enable faster reaction at lower temperatures. After one such operation, the reaction is usually incomplete, so the sample is ground, to bring fresh unreacted surfaces into contact, and refired; the process being repeated until satisfactory reaction has been accomplished.

Individual methods differ in the starting materials (usually a compound which will decompose to give very finely divided lime is used), the method of preparing the sample (either as a powder or pressing into pellets), the mineralisers and fluxes used and the temperature of firing.

In this work a stoichiometric mixture of reagent grade calcium carbonate and colloidal silica (low in iron) was ballmilled, pressed into pellets and fired at 1500 degrees for 24 hours in an electric furnace. The product was ground and the firing process repeated while its free lime content, as determined by a modified Franke extraction (appendix II.i), was above 1 wt%. When the free lime content was satisfactory, the sample was analysed to determine its CaO/SiO_2 ratio (C/S ratio) and levels of impurities (appendix II.ii) and stored, unground, ready for use. Powder XRD gave a peak at 51.5 degrees 2-theta split into 3 smaller peaks (fig 3.3). This is characteristic of the triclinic (T_1) phase. This splitting pattern was observed for all preparations made in this study, including the doped samples (section 4.3.a).

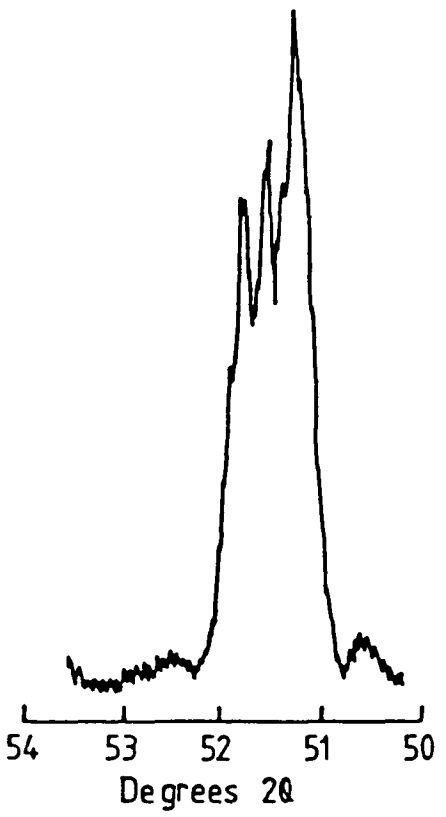

Fig 3.3: The 50.5 to 53.5 degrees 2-theta portion of the powder XRD trace of C_3S preparation A_1 showing a splitting pattern characteristic of the triclinic (T_1) phase.

During the course of this work three preparations of C_3S were made (A,B,C). When a sample of C_3S was required for use, just enough for the experiment was ground and sieved to remove particles greater than 50 microns in diameter. Thus each main preparation gave rise to several subpreparations differing in fineness of grind but not in overall composition. These are indicated by a suffix 1,2,3 etc. Once ground the samples were characterised by measuring their particle size distribution (sample A_1's PSD was determined using a Coulter counter, all other PSDs were measured using a CILAS laser granulometer model 715), specific surface (by the Lea and Nurse method - appendix II.iii) and density. The results for the main three preparations used in this work are summarised in table 3.1. The particle size distributions and specific surfaces of the various subpreparations are given at the appropriate places in the text.

Sample	A_1	B_1	C_1
Composition (wt%)			
Free Lime	0.93	0.20	0.20
CaO	74.32	74.87	74.04
SiO_2	25.69	25.58	25.95
Fe_2O_3 less than	0.01	0.01	0.10
Cr_2O_3 less than	0.01	0.01	0.01
Al_2O_3 less than	0.06	0.01	0.10
Density (g/cm^3)	3.11	3.19	3.17
Specific Surface (cm^2/g)	4000	3700	3100
Particle Size Distributions (Diameter in microns)	(wt% in each fraction)		
0.0- 1.0	0.0	7.4	5.3
1.0- 1.5	0.0	1.1	0.6
1.5- 2.0	1.0	1.2	0.8
2.0- 3.0	1.5	0.7	0.0
3.0- 4.0	1.5	5.0	1.5
4.0- 6.0	4.0	16.6	6.9
6.0- 8.0	4.0	17.7	12.6
8.0- 12.0	5.0	21.0	22.5
12.0- 16.0	8.5	9.0	16.7
16.0- 24.0	25.5	7.5	15.4
24.0- 32.0	33.0	3.5	8.1
32.0- 48.0	14.5	6.3	6.8
48.0- 64.0	1.5	1.9	1.8
64.0- 96.0	0.0	0.3	0.5
96.0-128.0	0.0	0.0	0.0
128.0-190.0	0.0	0.0	0.0

Table 3.1: Chemical compositions and physical characteristics of the main preparations of C_3S used in this work.

3.3 Discussion

When preparing a sample of pure C_3S in the manner described above, the desired reduction in free lime must be balanced against the increase in contamination which arises from each firing and grinding operation and the time available. In practice a free lime content of less than 1% was

found to require three to four firings with the incorporation of minimal levels of impurities.

Powder XRD showed all preparations to consist solely of pure triclinic C_3S.

CHAPTER 4

FACTORS AFFECTING THE REACTIVITY OF C_3S

4.1 Introduction

Fig 4.1 shows the calorimetric heat output curves for the three C_3S preparations described in the previous section. All three traces were obtained under identical conditions (water/cement=0.5, temperature=25 degrees). The diagram shows that, although all the preparations are essentially the same compound, their rates of heat output, and hence reactivities, are not the same. This observation of variability in the reactivity of C_3S is further supported by the wide variability in the reactivity of the numerous other preparations of pure C_3S which have been reported in the literature (e.g. Tenoutasse & De Donder 1970; Maycock et al 1974; Young et al 1977; Odler & Schuppstuhl 1981; Fierens et al 1982a; Stewart & Bailey 1983). It can be concluded that the reactivity of a C_3S preparation is not wholly due to the compound itself, but also depends on other factors, some or all of which are altered by the synthesis procedure. Some of these factors have been identified and these and the mechanisms by which they are thought to operate are discussed below.

Factors affecting the reactivity of C_3S can by divided into two broad groups; those that alter the reactivity of the C_3S by changing the properties of the C_3S itself (intrinsic factors), and those that alter its reactivity by altering the hydration conditions (extrinsic factors).

4.1.a Intrinsic factors

Factors which affect the intrinsic reactivity of C_3S, such as concentration and type of impurity ion, particle size distribution, thermal history, age and storage conditions, are all thought to operate by one or both of two mechanisms: (i) alterations in the nature and

concentration of the defects in the C_3S lattice and (ii) changes in the composition and nature of the surface of the C_3S grains.

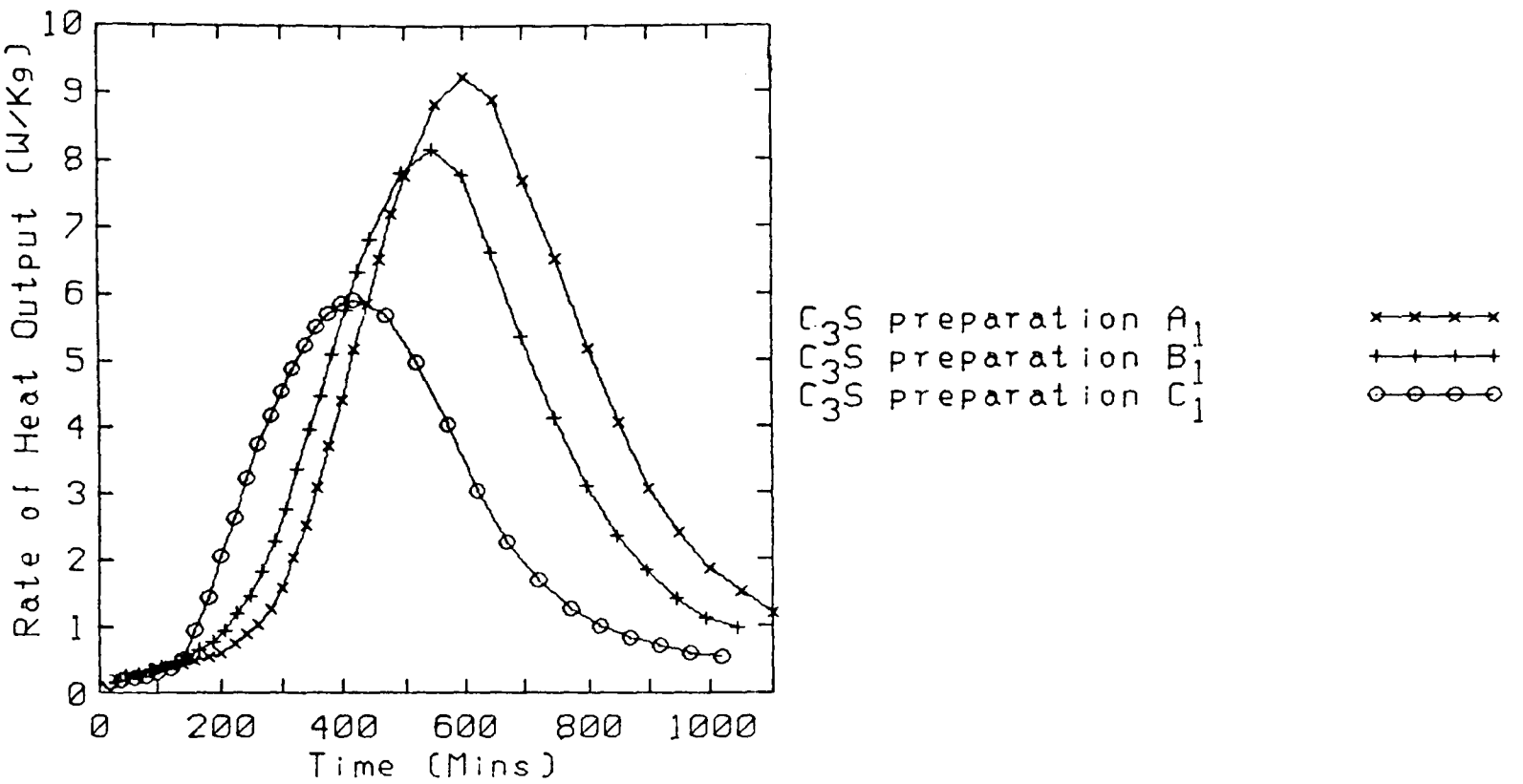

Fig 4.1: Calorimetric heat output curves for the three main preparations (A_1, B_1, C_1) used in this work.

4.1.a.i Lattice defects

Various defects, such as point defects (Schottky and Frenkel defects), line defects, boundary dislocations/stacking faults and lattice distortions, are present in crystal lattices. A defect is associated with a higher energy than the perfect array it replaces, hence defects are thermodynamically unstable. The removal of a defect requires an energy input as there is generally a high activation barrier to be overcome. The existence of defects in a lattice thus arises partly from the thermal energy in the lattice, which supports a certain equilibrium concentration of defects, and partly from the high activation barrier which must be overcome and which prevents their removal. Defects are usually associated with stress concentrations in the lattice. Attack on the lattice is thought to be promoted by such stress concentration so it is generally accepted that the presence of defects in C_3S increases its hydraulic reactivity.

Studies carried out to determine the effect of defects on the reactivity of C_3S have in only a few cases made any attempt to determine their concentration (Sakurai et al 1968; Fierens & Verhaegen 1972; Fierens et al 1982 a & b). In most studies it has simply been assumed that the concentration of defects will be increased by increasing the cooling rate, increasing the grinding and by the introduction of certain types of impurity ions. Conversely it has been assumed that decreases in the concentration of defects could be brought about by holding samples at high temperatures, storing them for long periods and the incorporation of impurity ions which introduce less strain into the crystal structure (Butt et al 1968; Maycock et al 1974).

4.1.a.ii Surface composition

Cement powders have very large surface areas. It is not surprising to find therefore that factors affecting the nature or composition of the surface of the C_3S also affect its reactivity. The extent to which the surface is hydrated or carbonated and the state of decomposition of the surface are thought to be the major factors involved.

4.1.b Extrinsic factors

The main factors altering the reactivity of C_3S by changes in the hydration conditions are (i) changes in the temperature, (ii) the presence of admixtures and (iii) changes in the water/cement (w/c) ratio. Unlike the intrinsic factors mentioned above which are thought to change the reactivity of the C_3S by one of two means, each of these extrinsic factors is thought to operate by an entirely different mechanism (and in the case of admixtures possibly by a variety of mechanisms).

Of the three factors mentioned, only the effect of w/c ratio will be covered in this section. A complete treatment of the effect of admixtures is beyond the scope of this work, but the effects of $CaCl_2$ (as a model accelerator) and sucrose (as a model retarder) are discussed in chapters 6 & 7. The effect of temperature is discussed in relation to mathematical modelling in chapter 5.

4.2 Previous work

4.2.a Impurity ions

The introduction of impurity ions into the C_3S crystal lattice has been extensively studied for a number of different purposes. Firstly, the impurity ions allow most of the various polymorphic forms of C_3S to be stabilised at room temperature, hence allowing the polymorphs to be more completely characterised (Locher 1960; Fletcher 1965; Bigare et al 1967; Woermann et al 1963, 1967; Hahn et al 1968; Roed 1974; Mascolo et al 1974). Secondly, the alite found in OPC is C_3S with varying amounts of impurity ions incorporated in the structure. The study of the effect of these ions is therefore important as an aid to understanding the differences and similarities between C_3S and the alite in cement. Thirdly, the incorporation of the impurity ions can alter the reactivity of the C_3S, in some cases quite markedly. Thus understanding the underlying causes behind these changes in reactivity aids the understanding of the differences in reactivity between cements with different levels of impurities and is potentially important in allowing the reactivity of the alite in cement to be controlled.

Increasing amounts of impurity ions stabilise the modifications of C_3S in the same order as increasing temperature (Woermann et al 1963, 1967; Bigare 1965), different elements stabilising different numbers of

elements. ZnO is unique in stabilising all except the M_3 and T_3 modifications (Bigare et al 1967). Table 3.2 from Bigare et al (1967) shows which polymorphic forms may be stabilised by the various elements, together with the solubility limits of the impurity ions (note the absence of the M_3 phase which was undetected at the time of the work and on which no similar study has been carried out). Much of the evidence for the presence of the various polymorphs is taken from changes in splitting patterns of certain reflections in the X-ray traces of the doped samples. Recent work by Sinclair & Groves (1984) has shown that these splitting patterns can not always be relied upon to give the true lattice. This can only be determined by the combination of both X-ray and electron diffraction studies.

Oxide	Composition ranges (wt% oxide)					Limit of solid solution at 1500 (wt% oxide)
	T(I)	T(II)	M(I)	M(II)	R	
Cr_2O_3	0-1.4					1.4
Fe_2O_3	0-0.9	0.9 -1.1				1.1
Ge_2O_3	0-0.09	0.9 -1.9				1.9
Al_2O_3	0-0.45	0.45-1.0				1.0
MgO	0-0.55	1.55-1.45	1.45-2.0			2.0
ZnO	0-0.8	0.8 -1.8	1.8 -2.2	2.2-4.5	4.5-5.5	5.0 (1400)

Table 4.1: Stabilisation of high-temperature polymorphs by various oxides (Bigare et al 1967).

An understanding of the effect of impurity ions on the reactivity of C_3S is complicated by an additional contributing process, namely that impurity ions can stabilise various high temperature polymorphs at room temperature. These polymorphic forms may vary in reactivity, making it possible for a given change in reactivity to be due to a combination of a change in polymorph and the inherent reactivity change due to that ion. Studies have been carried out on both types of process.

4.2.a.i Effect of altering the polymorph

Regourd & Guinier (1974) and Stevula & Petrovic (1981) found all the crystal forms of alite to have comparable reactivities, Nurse et al (1966) found the effect of polymorphic change to be small apart from the monoclinic to trigonal change, Yamaguchi et al (1966) found the monoclinic polymorph to hydrate more rapidly than the triclinic, Thompson et al (1975) found the reactivity of MgO doped C_3S to be increased around the concentration required for the structure to change from triclinic to monoclinic, Odler & Abdul-Maula (1983) found increasing ZnO doping to lead to an increase in reactivity which they took to be due both to the presence of the dopant ions and the changes in polymorph which the samples underwent and Aldous (1983) found that doping with Al_2O_3 and F led to increased reactivity only when their concentrations were high enough to stabilise the rhombohedral polymorph over the triclinic form.

It seems clear from the work that has been carried out, that changing the polymorph does have some effect on the reactivity of C_3S. The magnitude of this effect does not seem to be large, but at present, its absolute value has not been determined in any particular case because the effect of changes in polymorph has not been fully separated from other factors.

4.2.a.ii Other effects

Many other studies have been carried out to determine the effect of the impurity ions on the reactivity of C_3S either ignoring the effect of any change in polymorph or in the absence of any such change. The results of such studies are often contradictory. Valenti et al (1978), in a study of the hydration characteristics of Fe, Al and Mg doped C_3S, found a lower degree of hydration for the doped samples compared with pure C_3S; the Fe and Al doped samples exhibiting the greatest reduction in reactivity.

Sersale (1974) in a similar study found the same three dopants to increase the reactivity of C_3S, Fe having a larger effect than Al which in turn had a larger effect than Mg. Mascolo & Ramachandran (1978) also used the same dopants but found that at 50% hydration and compared with the strength of prepartions of pure C_3S, doping with Fe led to an increase in strength, Al gave about the same strength, while Mg gave poorer strengths. Sakurai et al (1968) and Fierens & Verhaegan (1972) studied the effect of Cr on the hydration properties of C_3S. They both found the Cr to increase the reactivity of the C_3S but attributed the acceleration to different mechanisms.

The reasons for the variability in the results of the various workers is not clear but it is possible that it partly arises from lack of control of the other factors affecting the reactivity of the preparations. A consequence of this variability is that it has been impossible to decide the manner in which impurity ions affect the reactivity of C_3S. However some suggestions have been made:

Boikova (1968) has found that incorporation of certain impurity ions into the C_3S lattice can lead to large increases in the structural disorder of the sample as measured by X-ray diffraction. He did not attempt to find whether there was any correlation between the increase in disorder and changes in reactivity of the samples.

Butt et al (1968) reports that ions substituting in interstitial positions reduce the reactivity of the preparation by increasing the stability of the structure while ions that substitute for Ca or Si change the reactivity according to whether they increase or decrease the strain energy of the lattice.

Sakurai et al (1968), in their study on the effect of Cr on the reactivity of C_3S, attributed the increase in reactivity to changes in the semiconductivity of the doped sample and an increase in the concentration of screw dislocations which were associated with high concentrations of Cr.

Fierens & Verhaegan (1972), who also found an increase in reactivity for Cr doped samples, attributed this increase to differences in the degree of disorder in the crystal lattice introduced by the Cr replacing the Ca. They measured the increase in disorder using thermostimulated exoelectron emmission.

As well as changing the concentration of defects in the lattice of C_3S it is possible that the incorporation of impurity ions alters the reactivity of C_3S by altering the composition of the liquid phase. It is a well established fact that the presence of foreign ions in the liquid phase alters the rate at which hydration proceeds when those ions are added with the mixing water (i.e. as admixtures - Kantro 1975). Ions originally present in the C_3S lattice should therefore have a similar effect once they have dissolved. However, the effects of ions in solution on the rate of hydration of C_3S are not always the same as the effects of impurity ions. It can be concluded that, while dissolved impurity ions from the lattice must play a part in determining the changes in reactivity which take place when C_3S is doped with different ions, other, more important, factors, such as those mentioned above, must also contribute to the changes in reactivity which take place.

4.2.b Particle size distribution and grinding

It has long been known that the fineness to which a cement is ground influences its hydration properties. The finer a cement is ground, the

greater is its strength, in particular its early strength (Lea 1970). As the fineness is increased, and when the amount of very fine particles in the paste is more than 15-20% of the weight of the cement, the ultimate strength of the paste can be reduced (Vivian 1966). The increase in strength due to increasing fineness is usually accompanied by an increase in shrinkage and heat output and this can be undesirable.

Unfortunately, little attention has been paid to investigating the effect of the fineness of grind on the hydraulic activity of C_3S. Consideration of this effect is of particular importance when comparing the reactivity of doped samples because the incorporation of impurity ions affects the sintering properties of the raw mix and hence the grindability of the product. Thus while various preparations may all be ground in the same manner, if one is harder than another, then the ground sample will contain a higher proportion of larger particles and any observed change in the reactivity will be due both to differences in the particles size distribution and to the incorporation of the impurity ions. A number of workers have recognised the importance of particle size and have attempted to prepare all their specimens with the same distribution, or at least ground to the same specific surface (Ueda et al 1969; Odler & Schuppstuhl 1981). Kondo & Ueda (1969) report that the finer C_3S is ground, the faster is its rate of hydration. However, Ueda et al (1968) have found that the rate of heat liberation of C_3S can be retarded by excessive grinding. Maycock et al (1974), in an investigation of the role of lattice defects on the rate of hydration of C_3S, found that heavy grinding increased the free lime content of the C_3S, decreased the induction period and produced an enlarged double peak in the rate of heat output in place of the single main peak usually observed for C_3S. More recently Odler & Schuppstuhl (1981) studied the effect of changing the specific surface on the reactivity of C_3S, in particular on the length of

the induction period. Increasing the specific surface from 3000 cm^2/g to 4500 cm^2/g did not change the length of the induction period but did enhance the rate of hydration as measured by calorimetry. Increasing the specific surface still further to 7000 cm^2/g resulted in the complete absence of the induction period. The heat output was still further enhanced and a small shoulder appeared on the acceleratory portion of the main heat curve.

Changes in reactivity as a result of altering the particle size distribution or specific surface are thought to come about because of the influence of the surface area on the reaction kinetics (Taplin 1969 a & b; Knudsen 1980). Other contributing factors which are thought to result from heavy grinding are an increase in defects (Maycock 1974) and the formation of an amorphous layer on the surface of the C_3S (Kondo & Ueda 1968). The former is assumed to increase the reactivity of heavily ground samples while the latter is assumed to decrease it.

4.2.c Aging

The properties of all cements gradually change with storage. It is thought that this is a result of the partial hydration/carbonation of the surface layers due to water vapour in the atmosphere (Lea 1970; Maultzsch et al 1980) and of the annealing out of crystal defects (Odler & Schuppstuhl 1981). The relative importance of these two effects is not clear. Maycock et al (1974) found a general decrease in reactivity (lowering of rate of heat output and maximum in rate of heat output occuring at slightly longer time) for stored samples which they attributed to the removal of excess reactive centers (lattice defects) by an annealing process. Odler & Schuppstuhl (1981) investigated the effect of aging for a year on the 3000 cm^2/g and 7000 cm^2/g samples mentioned above. The 3000 cm^2/g sample showed a two hour increase in its induction

period while for the 7000 cm^2/g sample a short induction period was found where before there had been none. In contrast with the work of Maycock et al, however, they found the calorimetric heat peak to be increased and shifted to later times. No explaination was given.

It has been reported that the reactivity of OPC is altered by storage in air, due to hydration and subsequent carbonation from moisture and carbon dioxide in the atmosphere, and that the change in reactivity can be highly erratic, depending on the relative amounts of hydration and carbonation and the thickness of the hydrate layers that are built up (Lea 1970). It is likely that a similar situation exists for C_3S. Certainly, exposure to the atmosphere will lead to some hydration occurring at the surface of the particles and, as the CSH gel product is susceptible to carbonation, it is probable that after a time any hydrates that do form will be converted to the corresponding carbonates. Relatively short term exposure to the atmosphere would therefore be expected to result in the C_3S particles becoming coated in a layer of hydrate, while longer exposure would result in those layers becoming carbonated. In the case of OPC it was found that such partial hydration led to an increase in the reactivity of the cement while subsequent carbonation of the hydrate layer at first led to a decrease in reactivity, but this was followed by an increase when the carbonated layer spalled off. No such study has been carried out on C_3S but it is likely that hydration/carbonation as a result of storage will give similar changes in the reactivity to those observed for OPC.

4.2.d Heat treatment

The effect of heat treatment on C_3S can be further divided into two categories. The effect of cooling rate, and the effect of annealing at different temperatures.

4.2.d.i Cooling rate

The effect of cooling samples of C_3S at different rates has been studied by Fierens et al (1982 a), Odler & Schuppstuhl (1981) and Maycock et al (1975). Fierens et al studied the effect of cooling C_3S in liquid nitrogen against cooling in air and found that the rate of hydration was increased markedly by the fast cooling process. Odler and Schuppstuhl studied three samples; a control, a rapid cooled sample and a slow cooled sample. They found that, although there was a difference between the reactivities of the samples, it did not correlate with the cooling rate. Cooling in liquid nitrogen reduced the length of the induction period but hardly changed the overall rate of heat output apart from during the initial stages where it was higher than normal. Slow cooling had little effect on the length of the induction period and led to an increased rate of reaction and slightly delayed maximum in the heat evolution. Maycock et al, in an experiment similar to that of Fierens et al, found that rapid cooling led to a large increase in the initial heat peak and an acceleration in the main heat peak. The increase in the initial peak could not be ascribed to the increase in free lime produced by the rapid cooling.

These results are in agreement with the theory that defects are causing the observed changes in reactivity. Heating the samples to high temperatures would be expected to allow the formation of a relatively high concentration of defects within the C_3S structure. Fast cooling would quench in those defects leading to a more reactive preparation than one which had been slowly cooled and hence contained fewer defects. This analysis is supported by the work of Boikova (1968) who determined that the degree of disorder in lanthanum doped specimens which had been cooled

quickly was higher than in similar specimens which had been cooled slowly.

The alternative theory, that the changes in reactivity as a result of differences in the rate of cooling arise from changes in the surface properties of the C_3S grains, has not been investigated. It is known, however, that slow cooling increases the extent of decomposition of C_3S to C_2S and lime and it has been reported that increasing concentrations of C_2S on the surface of C_3S lead to a decrease in its reactivity (Kondo et al 1968). It is therefore possible that the reported lower reactivity of slow cooled samples over fast cooled ones is caused by incorporation of C_2S into the surface of the grains as well as a reduction in their defect concentration.

4.2.d.ii Annealing

The effect of annealing C_3S once it has been prepared has the added complication that C_3S decomposes at high temperatures (1000 - 1250 degrees). This decomposition increases the free lime content of the sample so this must be taken into account when considering any changes in reactivity which occur.

Kondo and Ueda (1969) found the reactivity of C_3S to decrease in samples annealed at 800, 1000 and 1200 degrees respectively but a sample heated to 1500 degrees had a higher reactivity than the sample reheated to 800 degrees. They attributed this effect to the progressive decomposition of C_3S on the surface as the temperature was raised. This decomposition only occurs below 1250 degees after which the temperature becomes high enough for recombination to take place so increasing the reactivity again. Fierens et al (1982 b) also studied the influence of annealing temperature on the calorimetric output of samples of C_3S. They found

similar results to Kondo & Ueda but proposed that defects as well as decomposition played an important role in determining the final reactivity of the sample.

One factor which appears to have been missed in these studies of the effect of annealing on the reactivity of C_3S is the possibility of a change in the particle size distribution resulting from the heat treatment. The higher the temperature to which the sample is reheated, the more the particles will tend to sinter together, and the coarser the particle size distribution will become. This would lead to a decrease in the reactivity of the samples heated at higher temperatures.

4.2.e Water/cement ratio.

Different results have been reported by various researchers on the dependence of the rate of hydration of C_3S on the w/c ratio. Kantro et al (1966) and Kondo et al (1967) found that at early ages the degree of hydration of C_3S was independent of w/c ratio while later on it was increased by increasing w/c ratios. In contrast Locher (1966) found that increasing the w/c ratio led to a decrease in the rate of hydration up to a w/c ratio of 0.8; values higher than this giving an increase in the rate of hydration.

4.3 Experimental procedure and results

4.3.a Impurity ions

50 gram portions of C_3S preparation A were doped with 1 mole% of iron, zinc and chromium (as Fe_2O_3, ZnO and Cr_2O_3) respectively. They were ball milled to mix the components, pressed into pellets, fired at 1500 degrees for 24 hours and ground using a centrifugal ball mill operating at

maximum speed for half an hour. X-ray diffraction confirmed all the preparations to be of the triclinic polymorph.

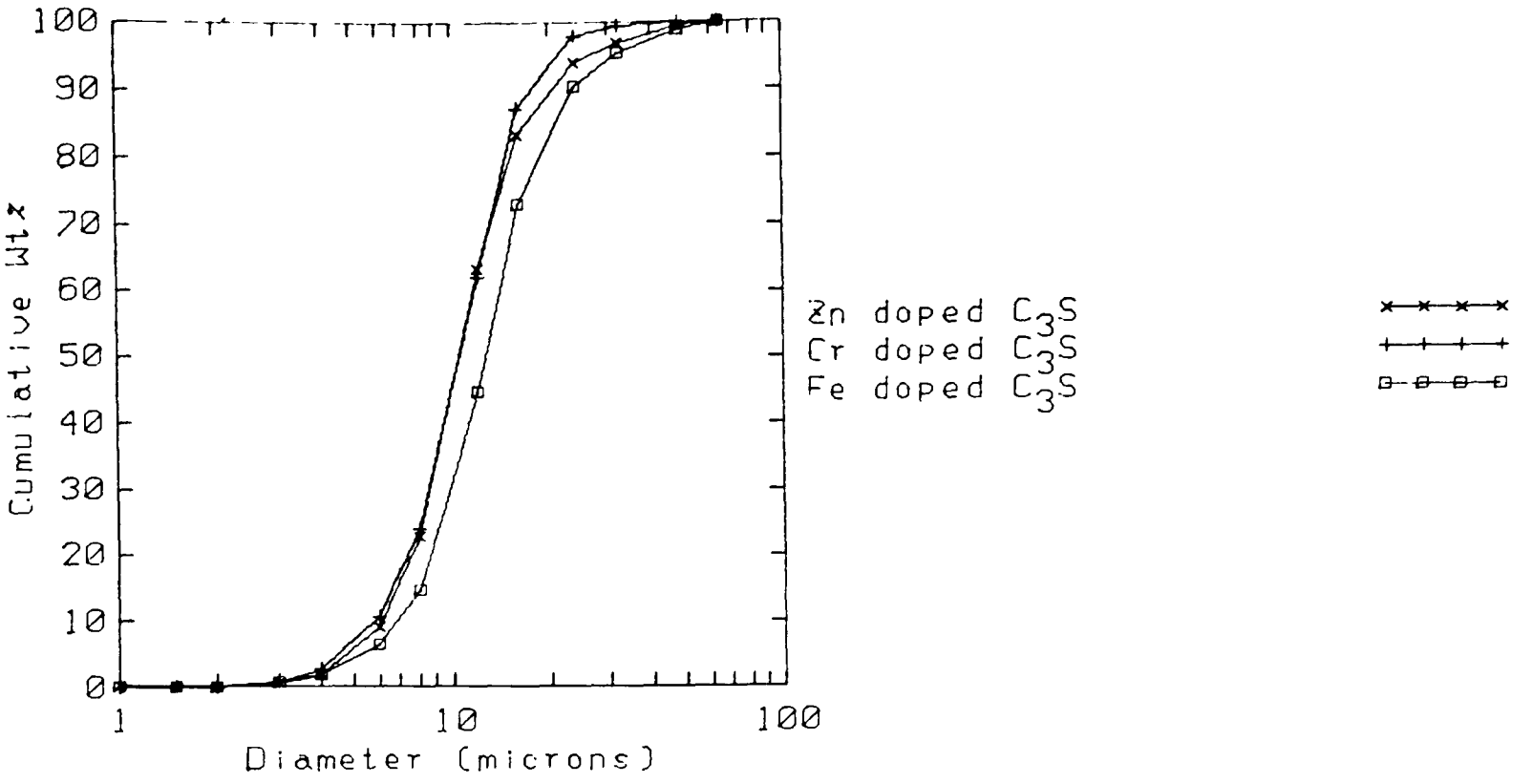

Fig 4.2: Particle size distributions of samples of C_3S doped with 1 mole% of Fe, Zn and Cr, after grinding under identical conditions

In spite of having been ground under identical conditions, the particle size distributions of the three samples (fig 4.2) are all different. In order to carry out meaningful comparisons between the different samples it is important that they have as far as is possible the same distributions. As this was not possible purely by grinding, it was decided to sieve out a particular size fraction (20-32 microns in this case) and obtain the calorimetric curve of that portion alone.

To obtain a larger sample than was currently in the 20-32 micron size range the samples were repelletised, refired and reground. The grinding was carried out at a slower speed than that used previously and the product removed from the grinder at intervals and sieved so that the required fraction could be collected before being ground too fine. Only in this manner was it possible to obtain enough sample for a single calorimetric run.

Calorimetric traces were obtained for the chromium and iron doped samples. Due to an equipment fault, a trace was not obtained from the zinc doped sample. Fig 4.3 shows the two traces together with the control trace obtained from the 20-32 micron size range of preparation A for comparison. In both cases the maximum rate of heat output and the total heat output during the main heat peak were less than those of the control, with the iron doped sample also showing a very marked retardation of the main heat peak. The induction period of the chromium doped sample was almost identical to that of the control, in spite of the difference in the main heat peak, while that of the iron doped sample was extended by over ten hours.

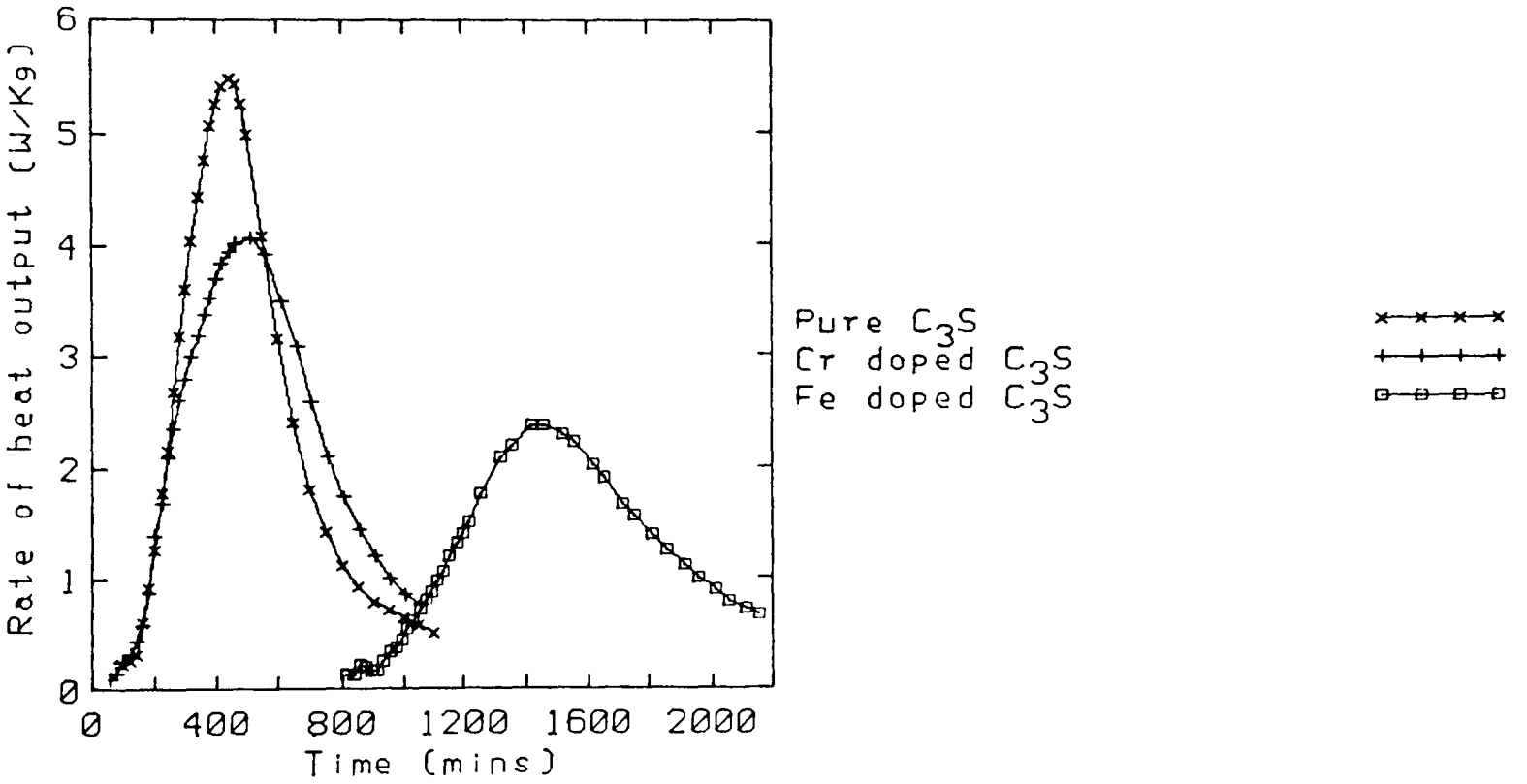

Fig 4.3: Effect of doping C_3S with Fe and Cr on the rate of heat output of the 20-32 micron particle size range.

This study was not carried further because of the difficulties involved in preparing the samples with a given particle size fraction and because it became clear that the grinding and sieving operations necessary to obtain the samples in such a fashion were altering the reactivity of the samples in an unpredictable manner.

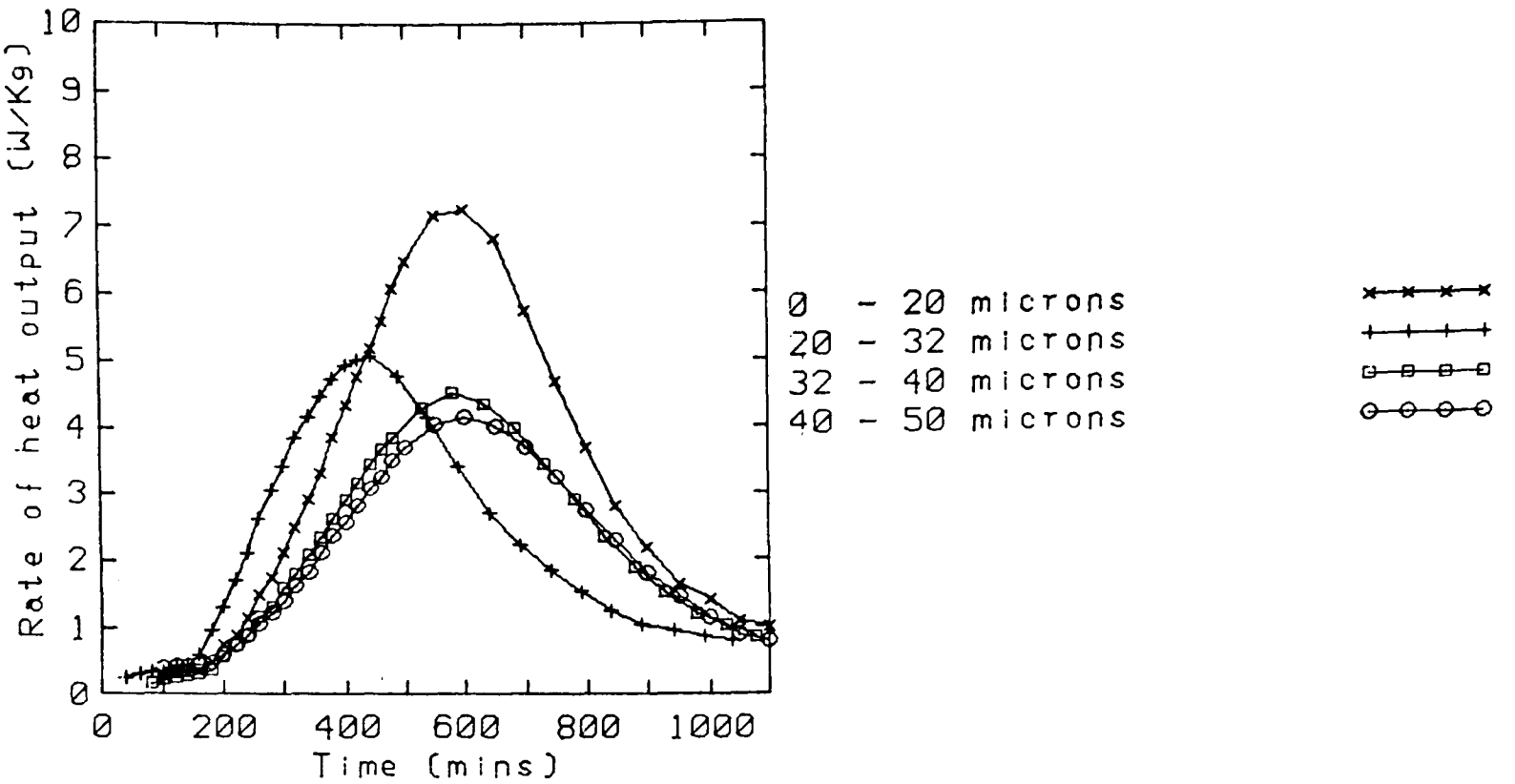

Fig 4.4: Calorimetric traces obtained from the various size fractions of preparation B_1.

4.3.b Particle size distribution and grinding

Preparations B_1 and B_2 were sieved into their various size fractions and calorimetric traces obtained for each fraction. Fig 4.4 shows representative traces for preparation B_1 while fig 4.5 shows traces for B_2. The main peaks in the rate of heat evolution for the smaller particle sizes are generally higher and moved to shorter times than those of the larger particles. The main peak of the 20-32 micron range of preparation B_1 appears to be anomalous, being of about the right height but shifted to an earlier time than expected. Repeat traces obtained from the 20-32 micron range showed no significant differences from the first. The reason for this is not clear.

Preparations C_2 to C_8 were ground under different conditions to obtain a variety of different particle size distributions and specific surfaces. Table 4.2 lists the specific surfaces of the various preparations. Calorimetric traces and particle size distributions were obtained for each of these. The series C_2, C_3, C_4, C_4 and C_8 illustrate how

increasing the specific surface increases the reactivity of the preparation (fig 4.6 a and b).

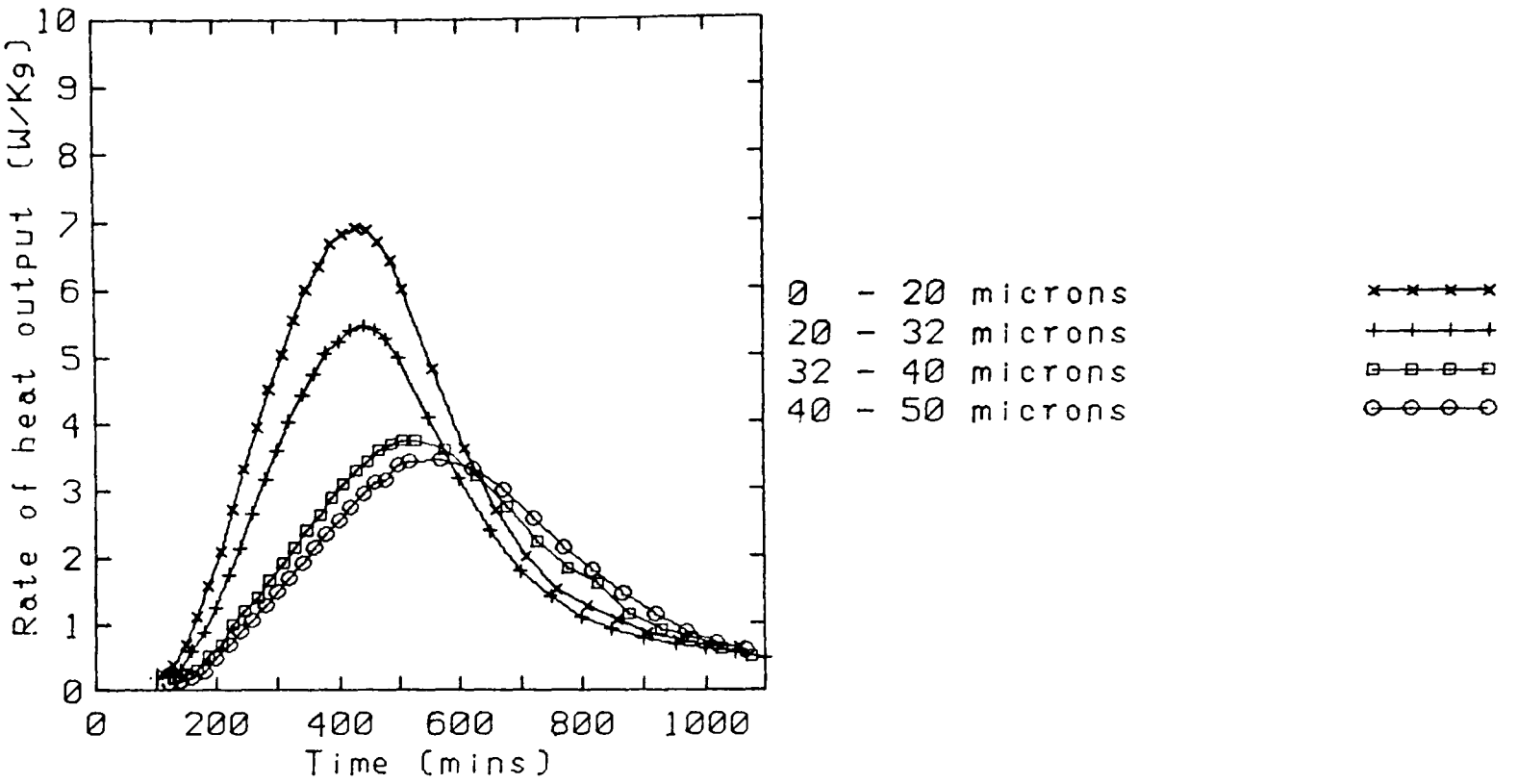

Fig 4.5: Calorimetric traces obtained from the various size fractions of preparation B_2.

Preparation	Specific Surface (m^2/Kg)
C_2	500
C_3	530
C_4	540
C_5	570
C_6	620
C_7	640
C_8	650

Table 4.2: Specific surfaces of preparations C_2 to C_8

The increase in reactivity shows up as an increase in height and larger overall area of the main heat peak, the position of which is not significantly affected.

An increase in reactivity with increase in specific surface was not observed in all cases. Sample C_6 has a lower specific surface than that of C_7 but as their calorimetric curves show (fig 4.7) C_6 has a shorter induction period and larger main heat peak.

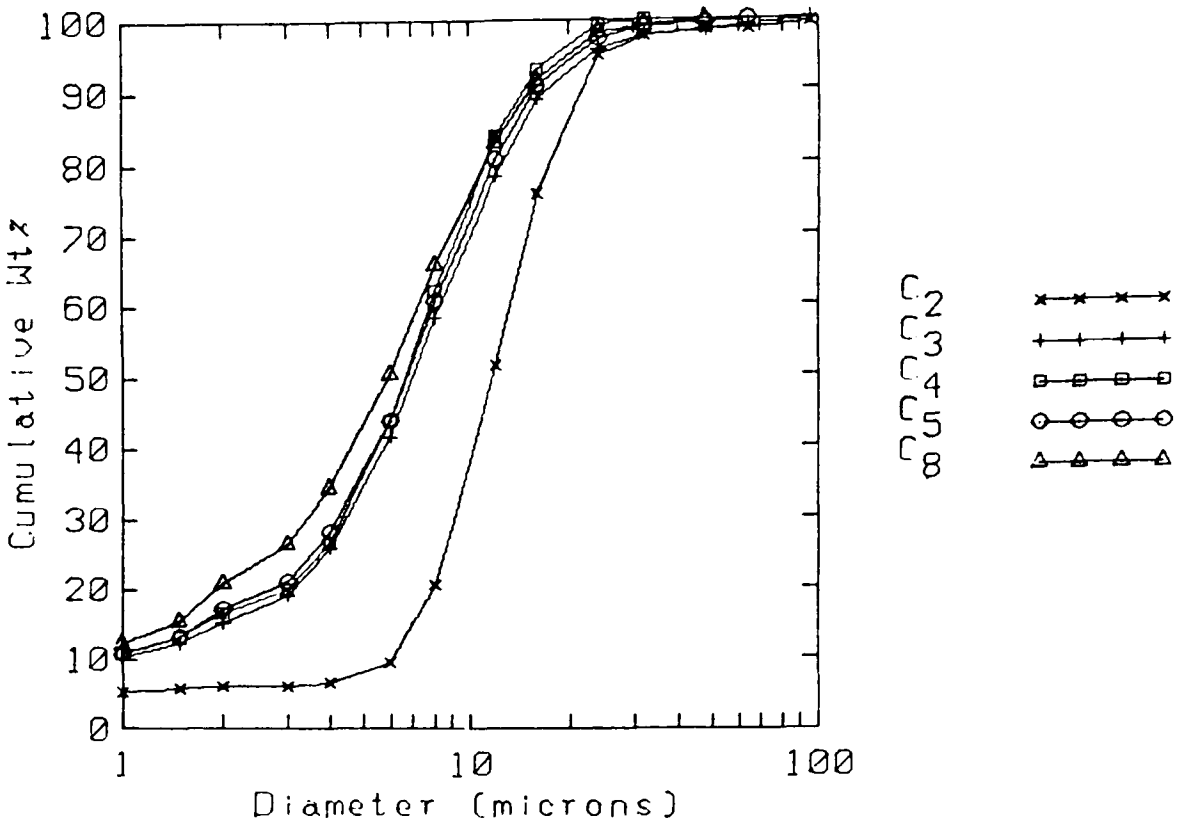

(a)

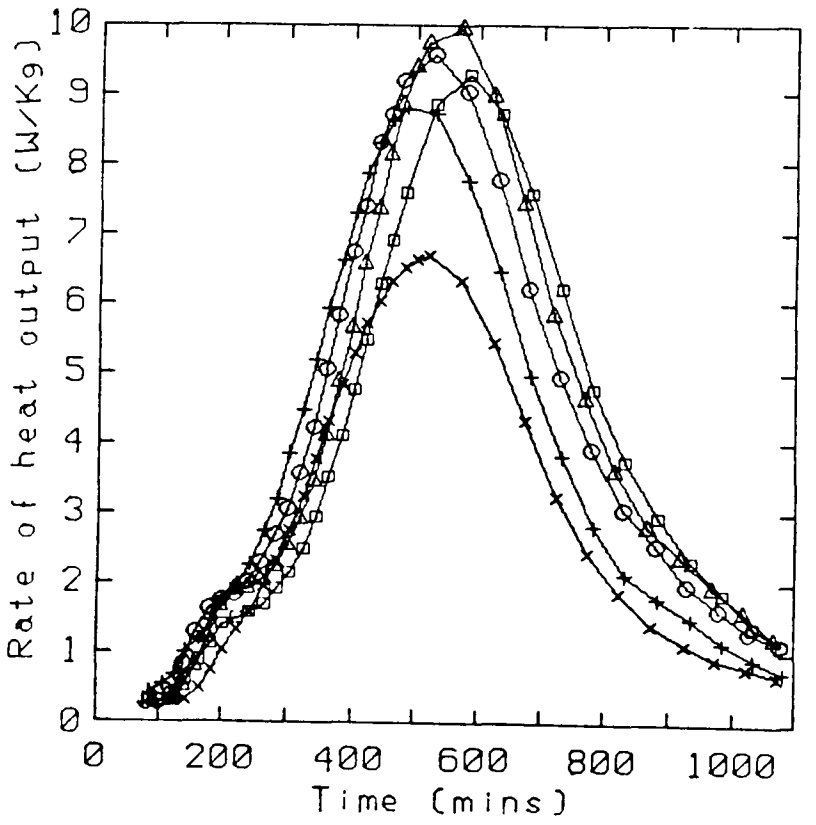

(b)

Fig 4.6: Effect of increasing specific surface on
(a) Particle size distributions
(b) Rate of heat output

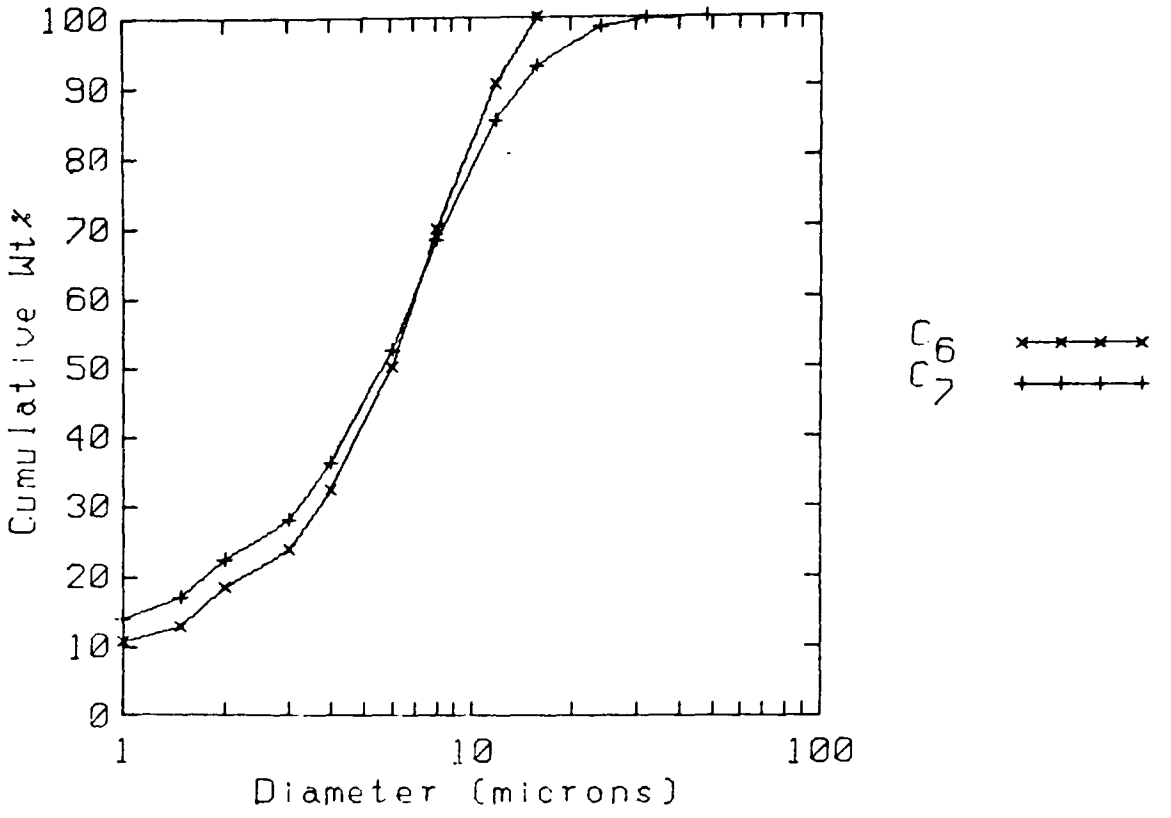

(a)

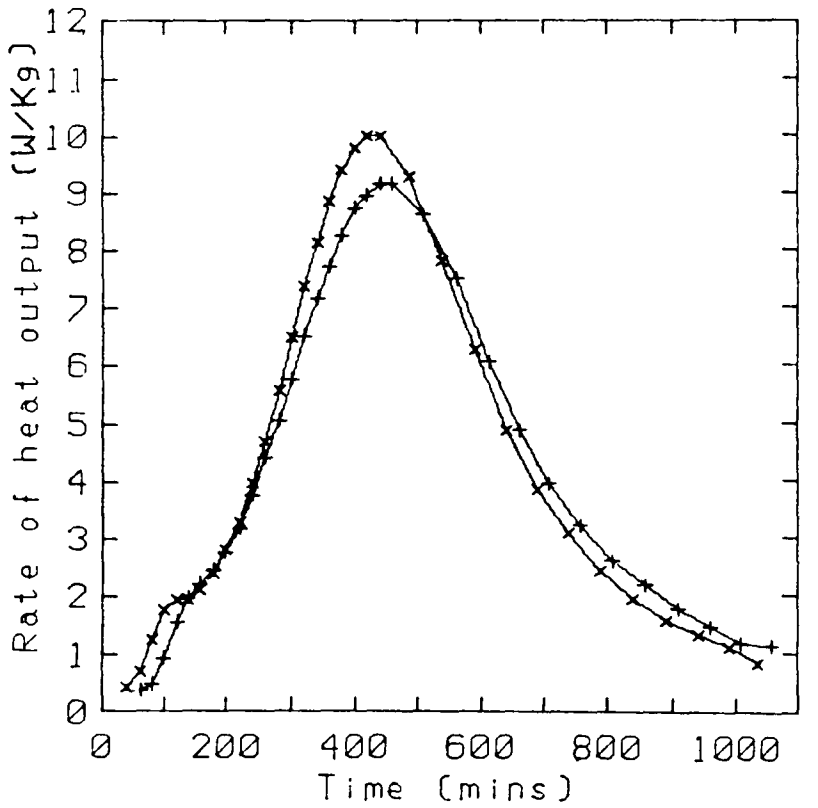

(b)

Fig 4.7: (a) Particle size distributions and (b) calorimetric traces for preparations C_6, C_7 showing a decrease in reactivity with increase in specific surface

Another interesting feature of the calorimetric traces of those samples which have been heavily ground is the appearance of a shoulder on the acceleratory portion of the main heat peak (fig 4.8).

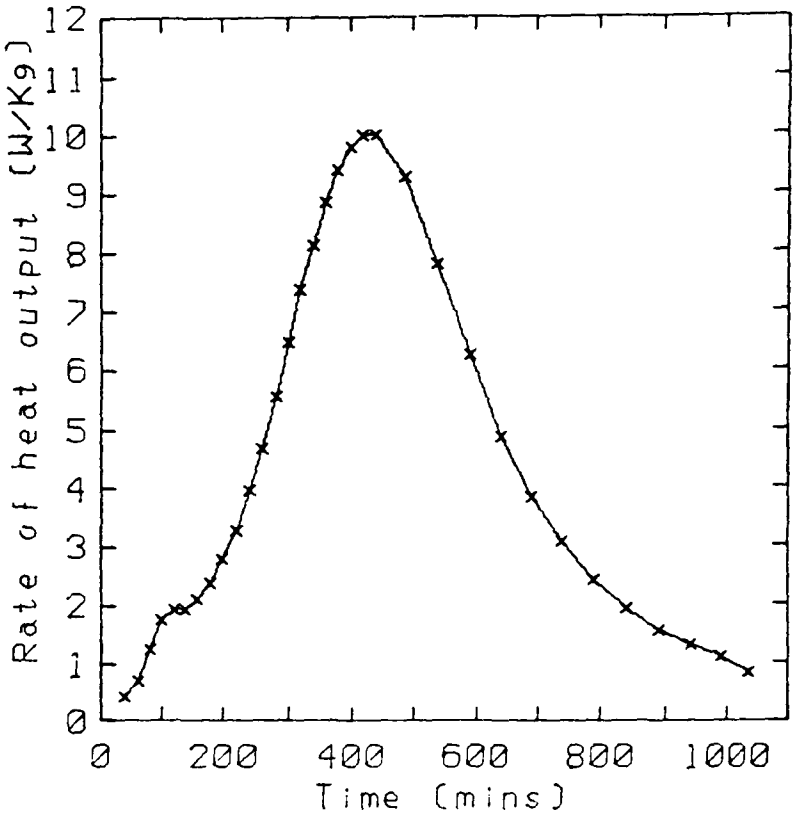

Fig 4.8: Illustration of the shoulder which appears on the side of the acceleratory portion of the main heat peak when the samples have been heavily ground

4.3.c Aging

Figs 4.9 and 4.10 illustrate the effect of storage in a closed polythene bottle on the reactivity of preparations A_1 and C_1 respectively. The induction period is progressively reduced, while the peak maximum is also reduced and shifted to shorter times. The greater part of the shift of the peak maximum is due to the change in the induction period.

In an attempt to accelerate the effect of storage a 100 gram batch of preparation C_1 was placed in a polythene bottle and rolled continuously for over 800 hours. During this time the cap was removed periodically to allow fresh air to enter. Calorimetric traces were obtained at various intervals from samples withdrawn from the bottle. Fig 4.11 shows the results of this series of experiments. Surprisingly the effect of the

C_3S being continually rolled in air is to shift the peak maximum in the opposite direction to the shift with increasing age and slightly reduce its height. Also in contrast with the aged sample the length of the induction period is hardly affected by the rolling process.

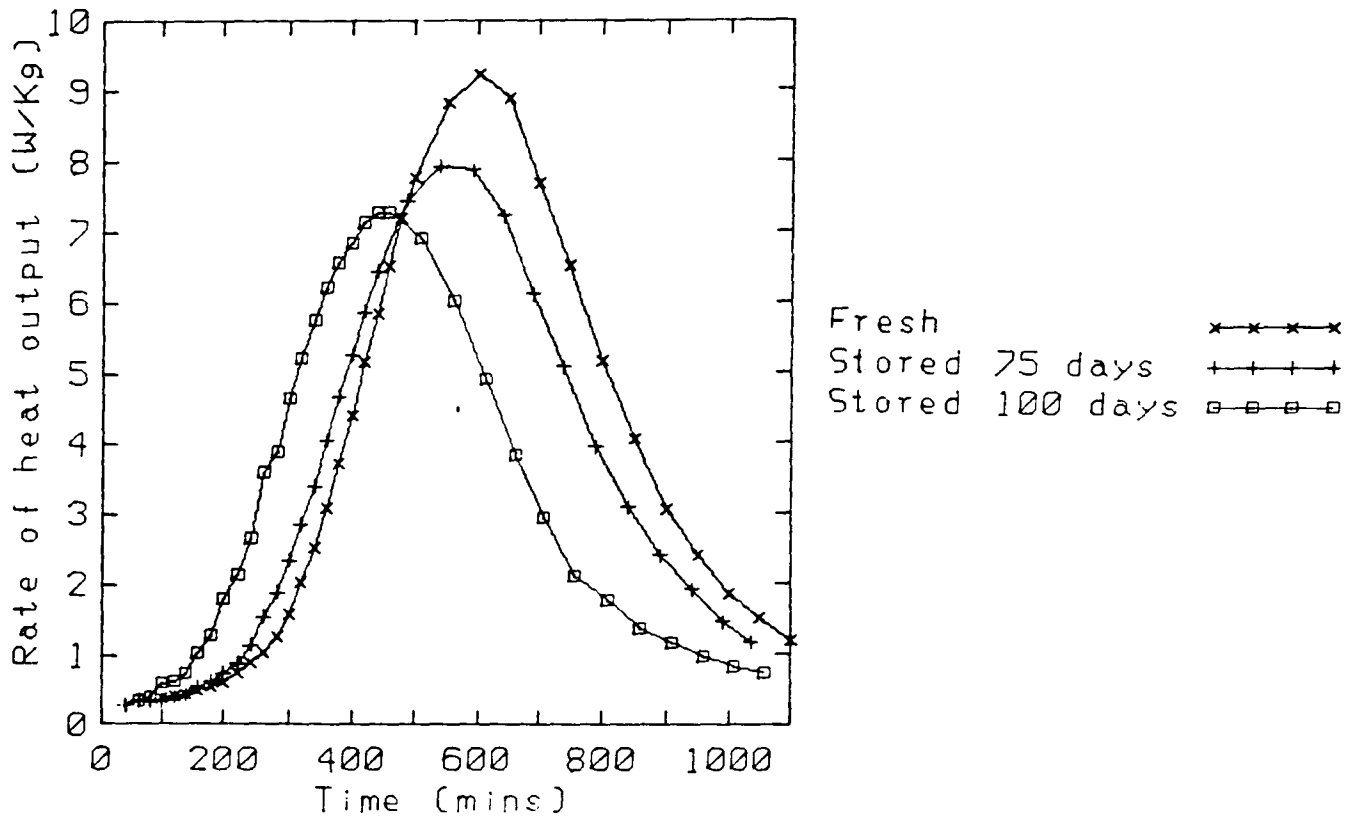

Fig 4.9: Effect of storage on the rate of heat output of preparation A_1.

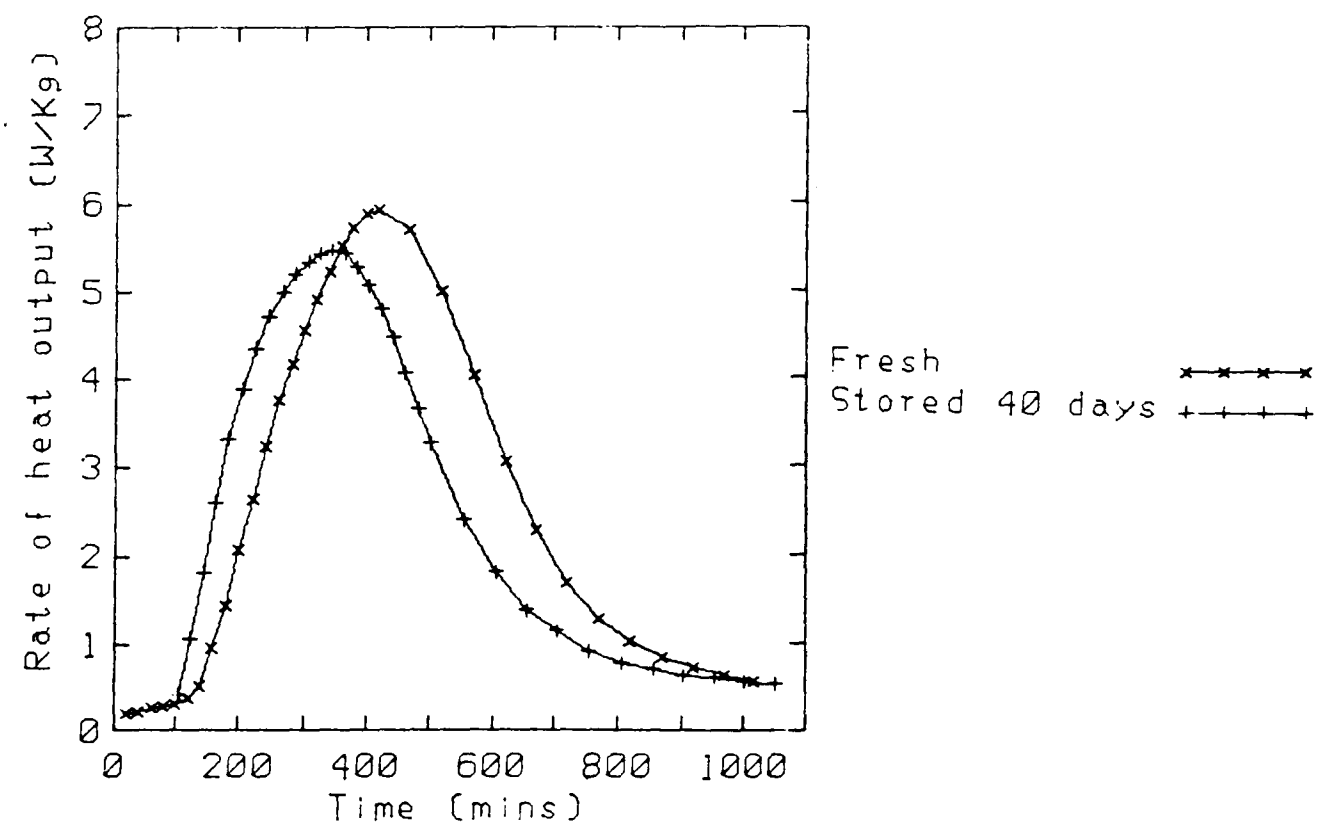

Fig 4.10: Effect of storage on the rate of heat output of preparation C_1.

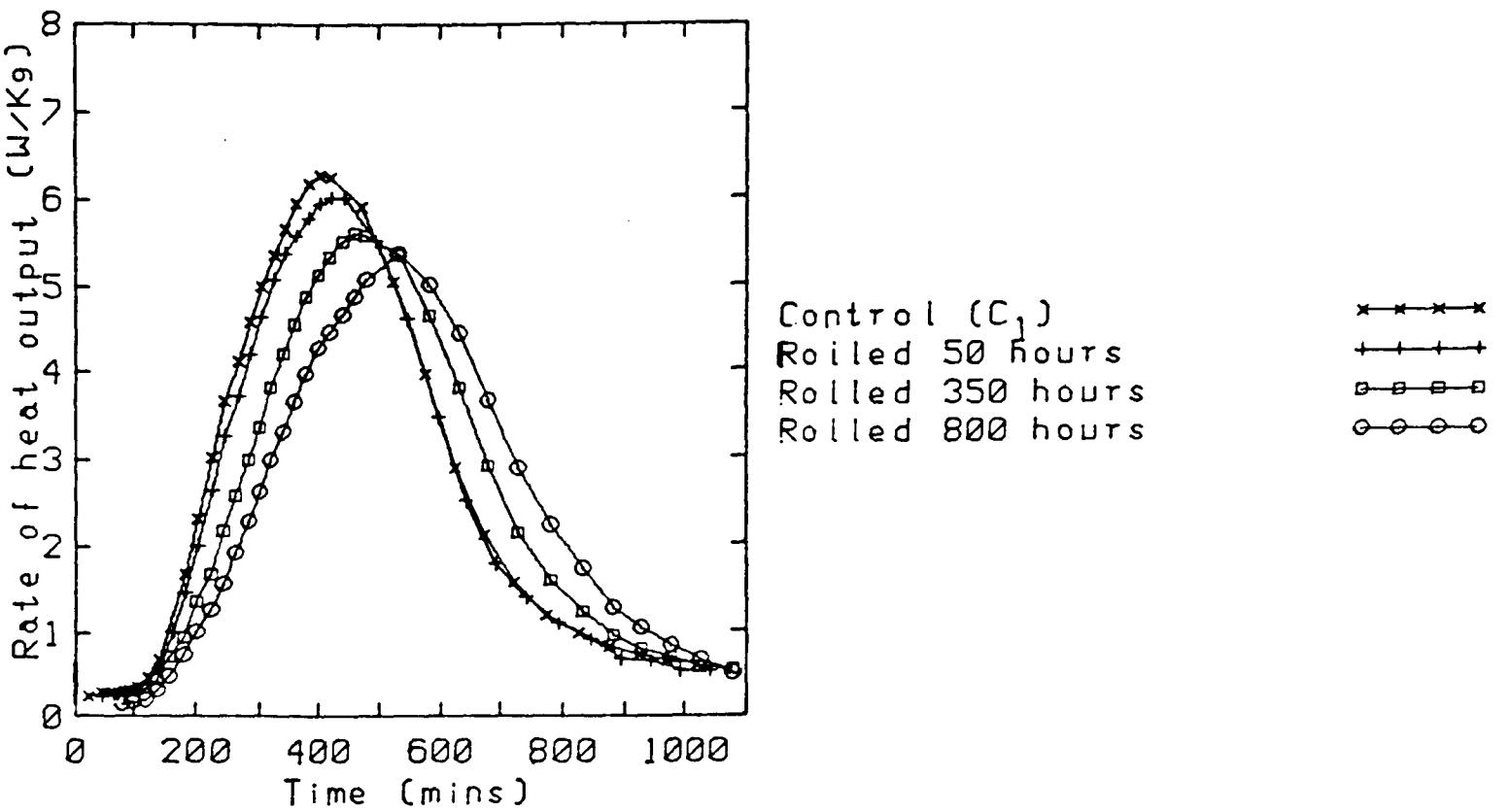

Fig 4.11: Effect of continuously rolling a sample of C_3S in air over a period of 800 hours on its rate of heat output.

In addition to the rolled batch, a batch of the B_1 preparation was stored, open, in a desiccator. Samples were withdrawn from this at intervals to determine how the reactivity of C_3S varies when stored in a dry atmosphere. Fig 4.12 shows the calorimetric traces obtained from these samples. Although there is some variation in the peak height there is no significant variation in the position of the peak maximum and the length of the induction period remains unchanged.

4.3.d Heat treatment

Samples of preparation C were reheated to 1500 degrees for 24 hours and then cooled at different rates. Table 4.3 lists the various samples together with their method of quenching, approximate quenching rate, free lime contents and specific surfaces. Fig 4.13 shows their particle size distributions and fig 4.14 their calorimetric traces. The samples were all ground in the same manner so that their particle size distributions and specific surfaces would be roughly the same.

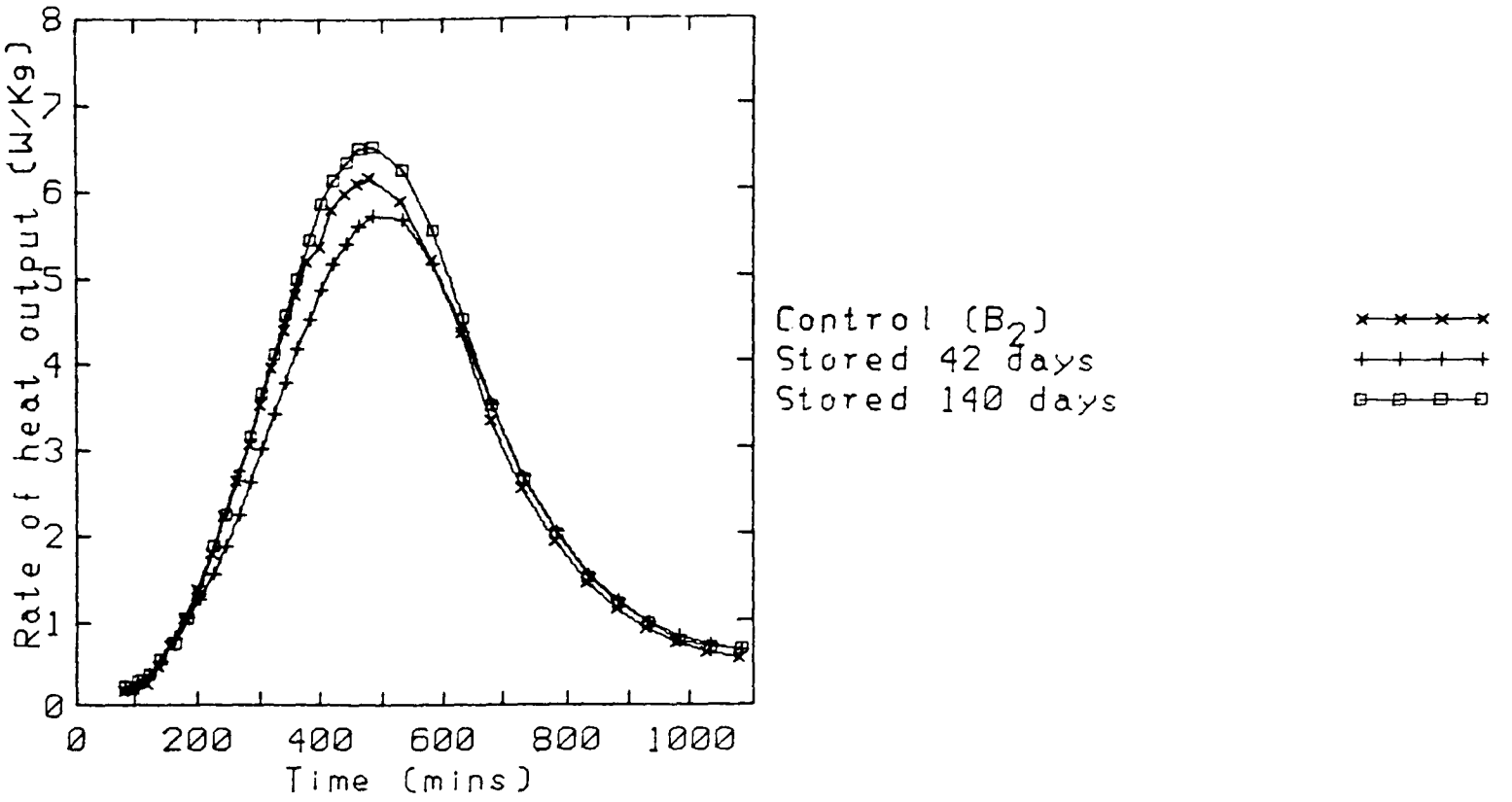

Fig 4.12: Effect of storing C_3S in a desiccator for 140 days on its rate of heat output.

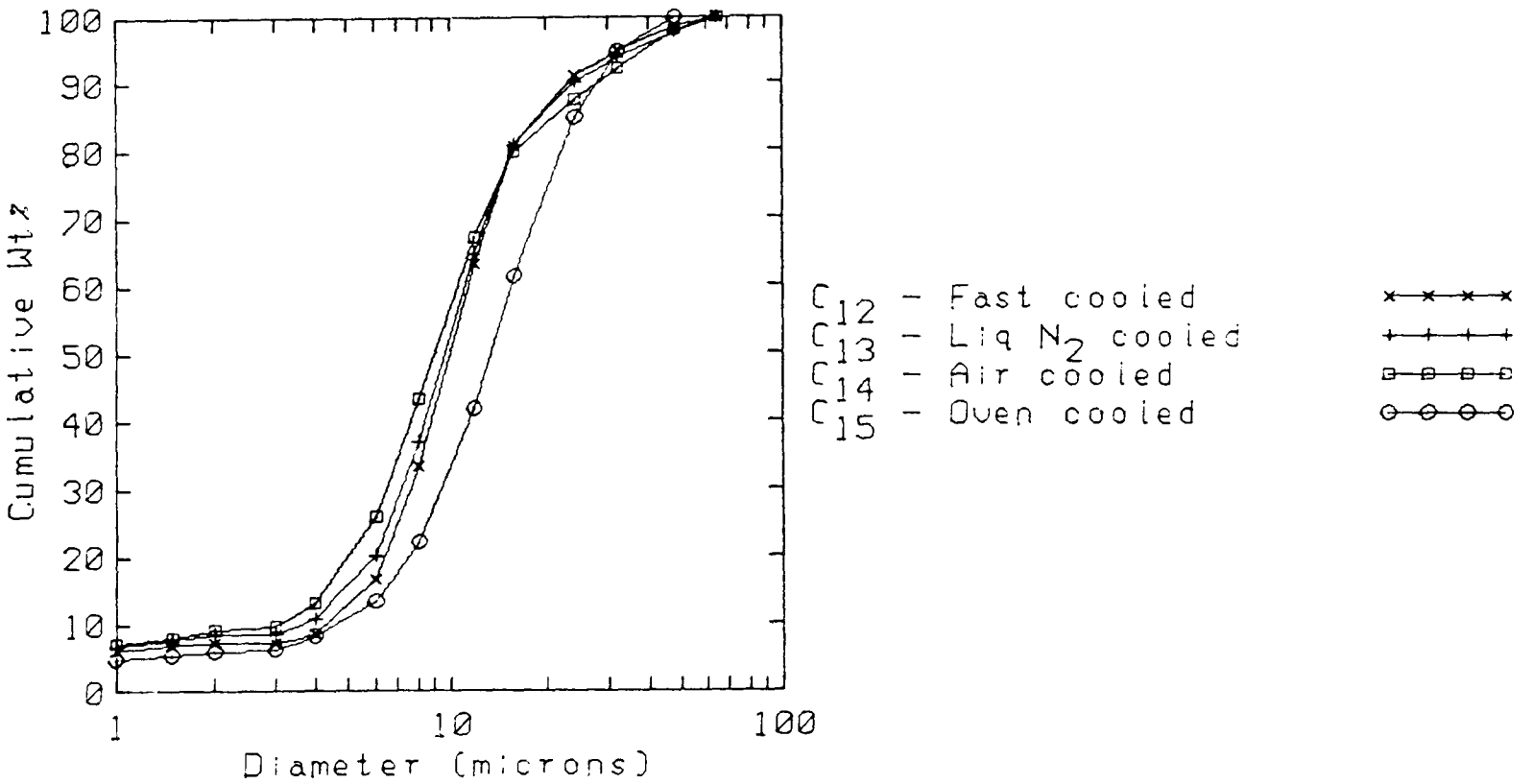

Fig 4.13: Particle size distributions of samples of C_1 cooled at widely different rates.

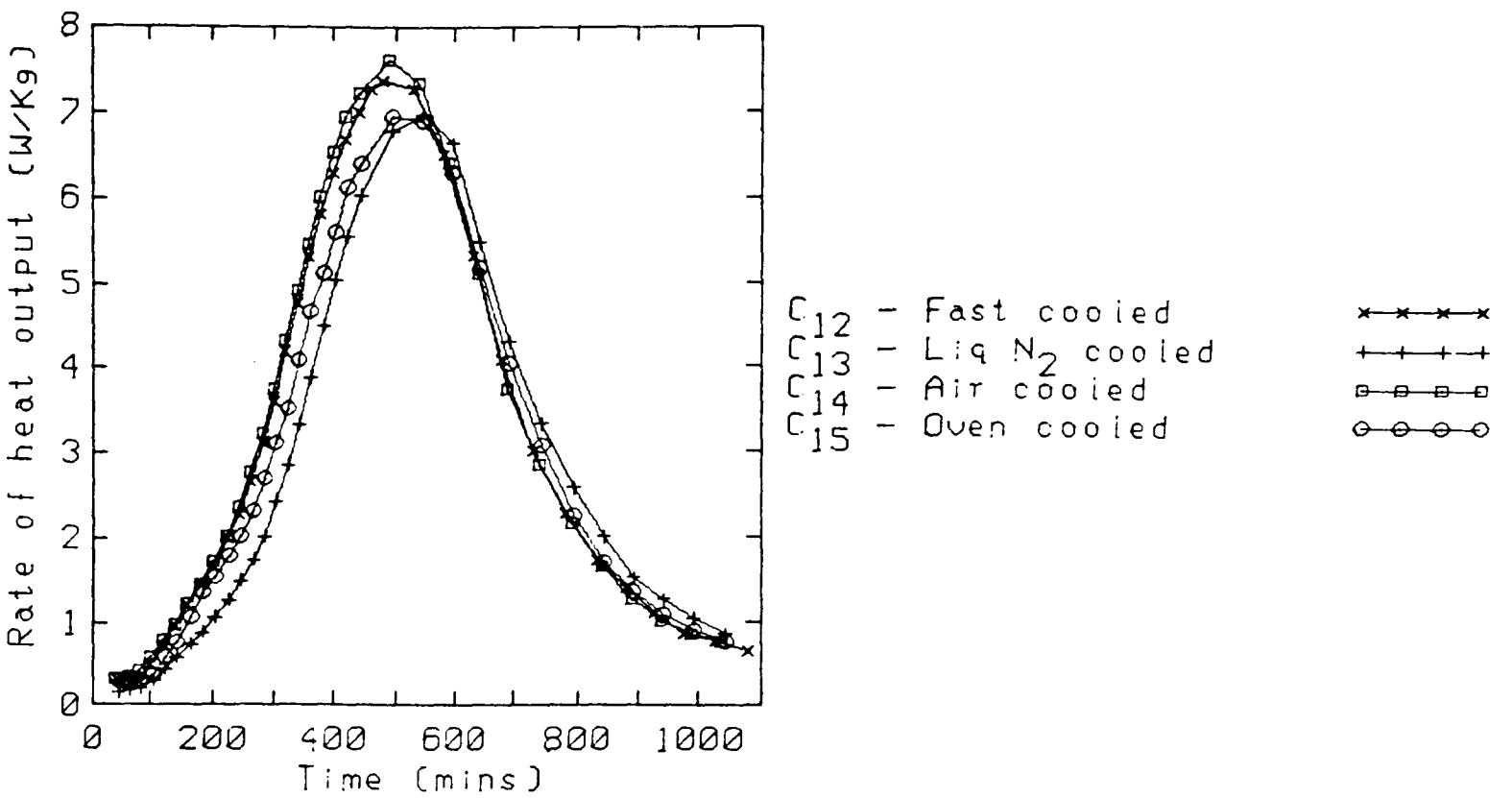

Fig 4.14: Calorimetric traces for the samples of C_1 cooled at widely different rates.

Fig 4.13 shows that preparations C_{12} to C_{14} have similar distributions while C_{15} is slightly different having a greater proportion of larger particles. This is confirmed by the lower specific surface of this preparation. The free lime content of all preparations was the same indicating that no measurable decomposition had occurred. The calorimetric traces obtained from the various preparations are illustrated in fig 4.14. Note that the curves for samples C_{12} & C_{14} were obtined using calorimeter no.2 while the others were obtained using calorimeter no.1 at the time when the responses of the calorimeters had begun to vary slightly (section 2.7.a). Referring to fig 2.12 shows that much of the difference between the two sets of curves can be attributed to the difference in response of the calorimeters and therefore that the curves are all very similar. Thus in this study no systematic variation in the reactivity of the preparations with the rate of cooling was found.

Sample	Quenching Method	Average Cooling rate (Deg/min)	Free Lime (wt%)	Specific Surface (m^2/Kg)
C_{12}	Breaking into pieces while hot	300	0.17	440
C_{13}	Liquid Nitrogen	150	0.16	440
C_{14}	Air cooled	50	0.17	460
C_{15}	Oven cooled	2	0.17	410

Table 4.3: Preparation methods and properties of C_{12} - C_{15}

Samples of preparation B_1 were reheated to 1500 degrees for 5 minutes and to 1500 degrees for 5 minutes followed by mild grinding with a mortar and pestle. The effect of these two treatments is shown in fig 4.15. Compared with the control, reheating has led to a reduction in the reactivity but the reactivity is restored by the mild grinding.

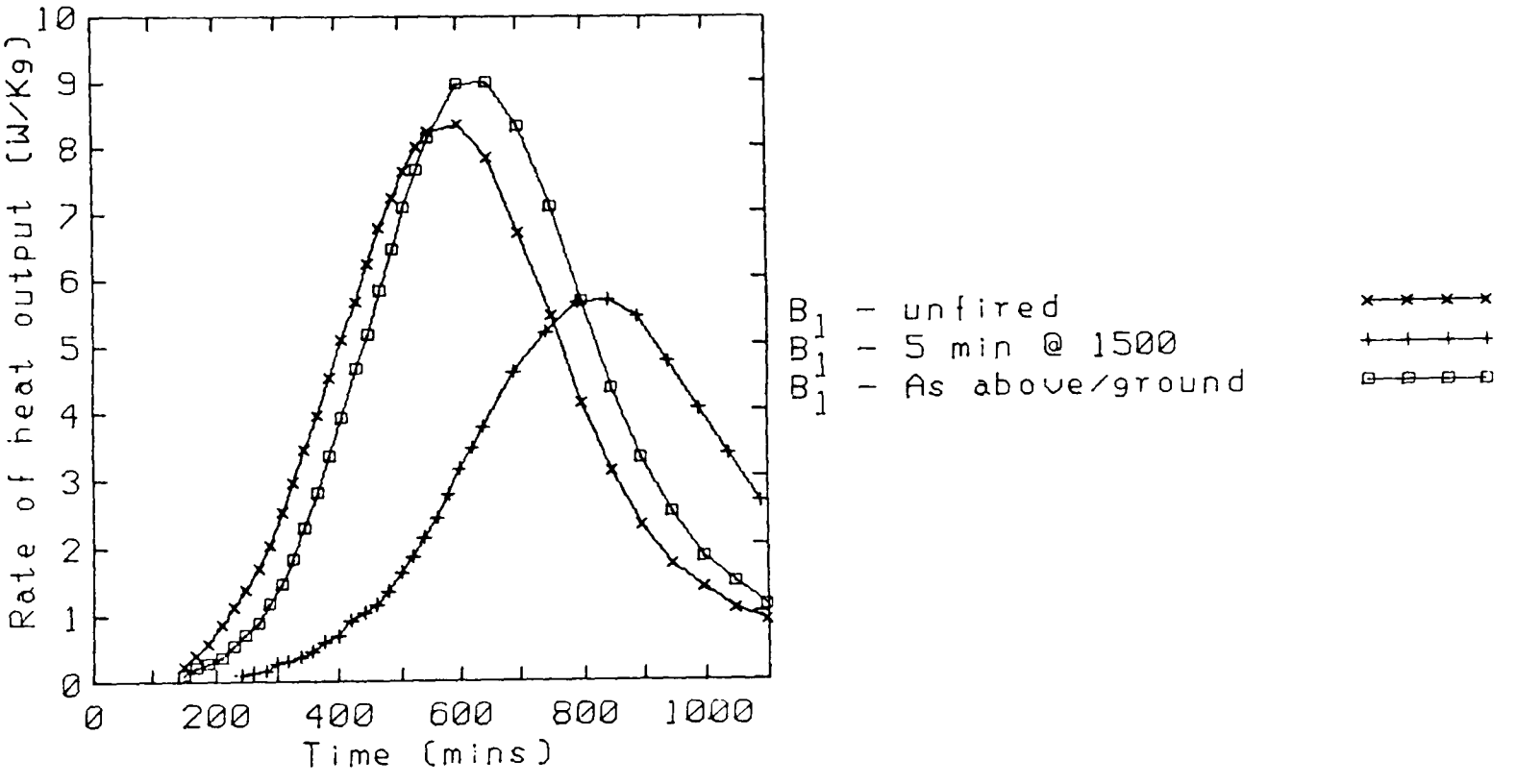

Fig 4.15: Effect of various heat treatments on the rate of heat output of preparation B_1.

Samples of preparation C_1 were annealed at different temperatures for varying lengths of time. The effect of this heat treatment on the reactivity of the samples did not seem to follow any particular pattern. Fig 4.16 shows the effect of annealing samples for increasing periods of

time, keeping the temperature constant at 1000 degrees while fig 4.17 shows the effect of increasing the temperature, keeping the time constant. The only trend which can be seen is for the reactivity of the C_3S to decrease (in terms of the height of the main peak) with increasing time at 1000 degrees.

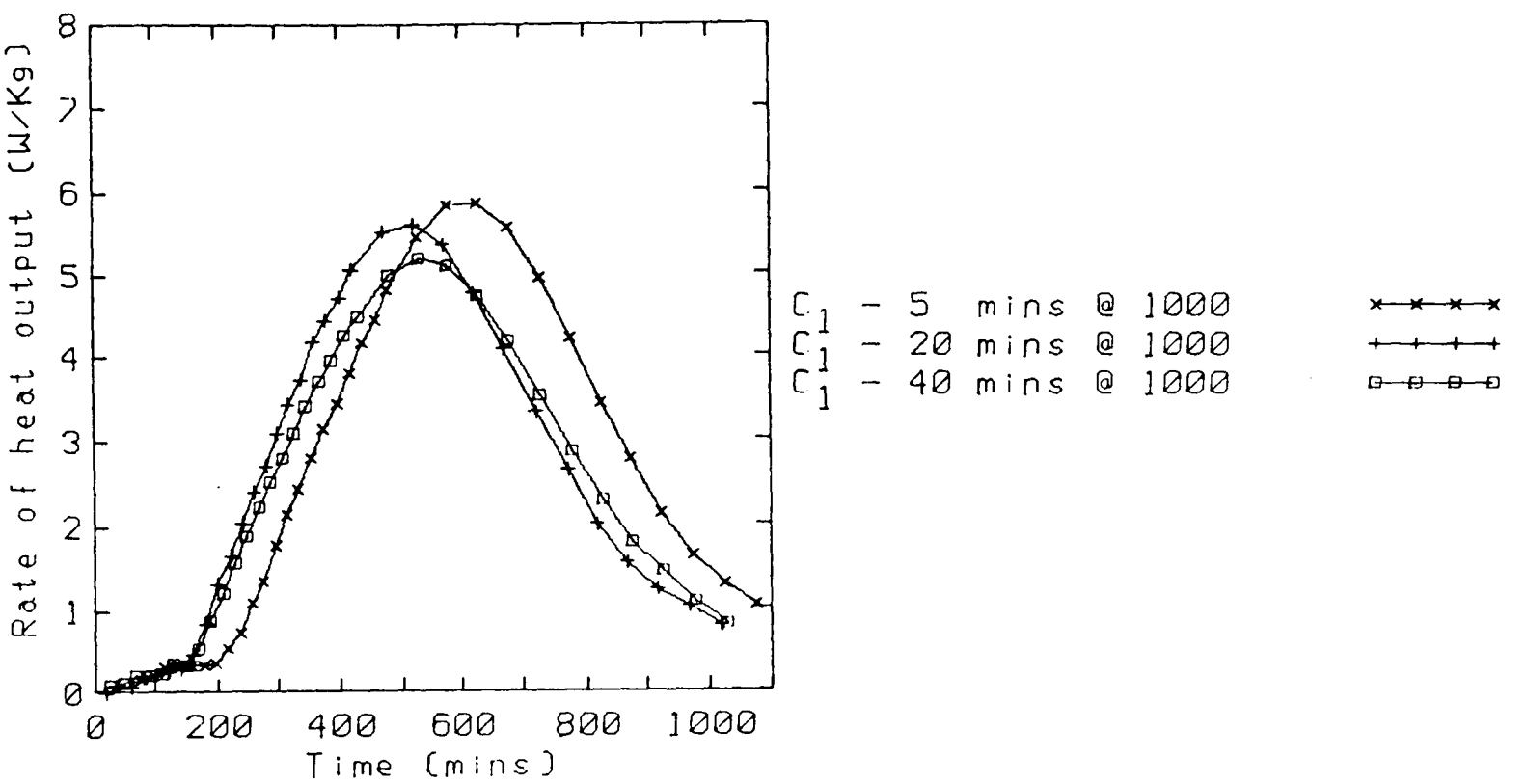

Fig 4.16: Effect of annealing samples of preparation C_1 for increasing periods of time at 1000 degrees

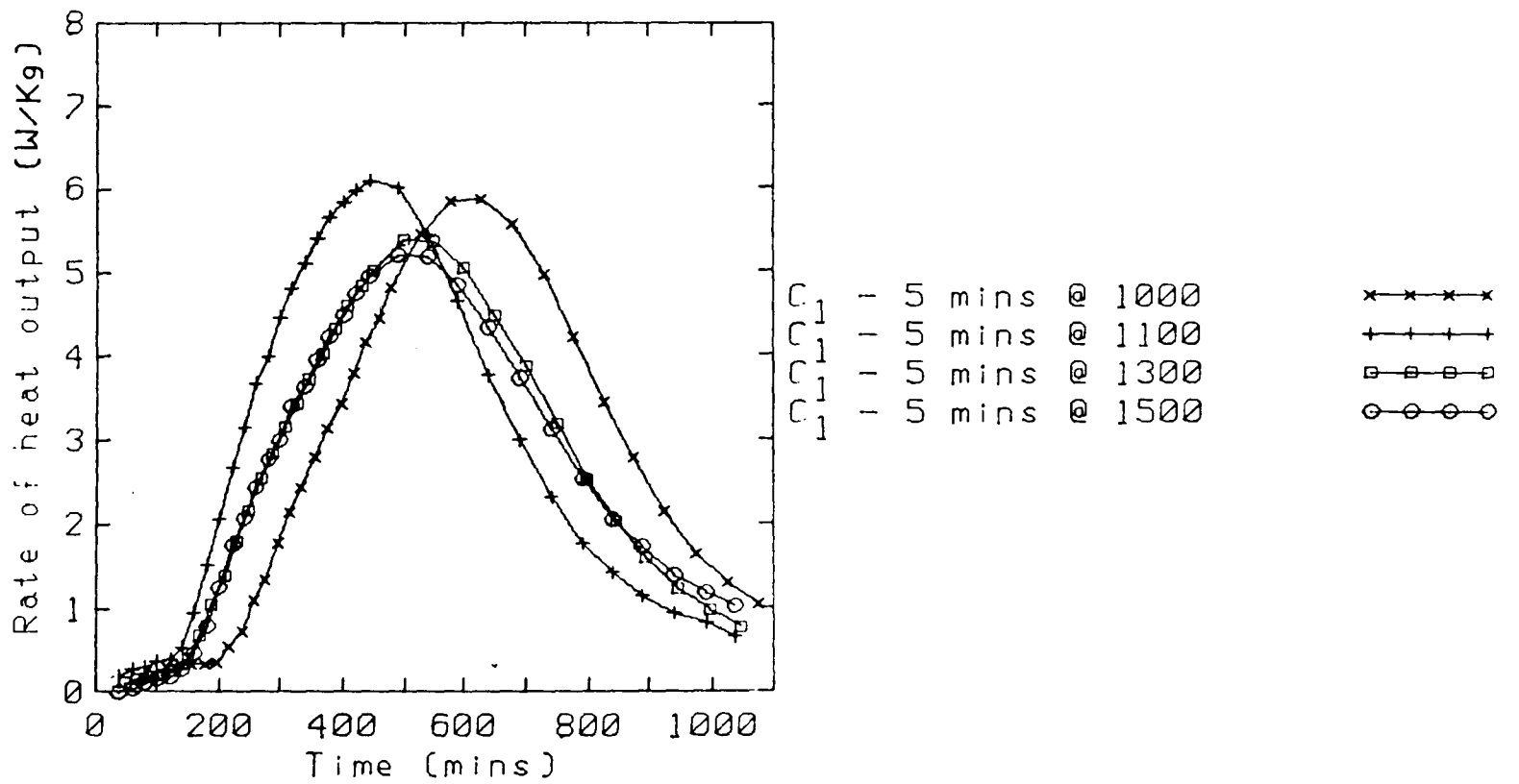

Fig 4.17: Effect of annealing samples of preparation C_1 for the same periods of time at different temperatures

The particle size distributions of the above samples were obtained to see how they were affected by the various heat treatments. Fig 4.18 shows the distributions for the samples annealed at 1000 degrees. All three curves are very similar implying that the heating to 1000 has little effect on the distribution. Fig 4.19 shows the distributions for the samples heated to different temperatures. The higher the temperature the greater the proportion of the larger particles.

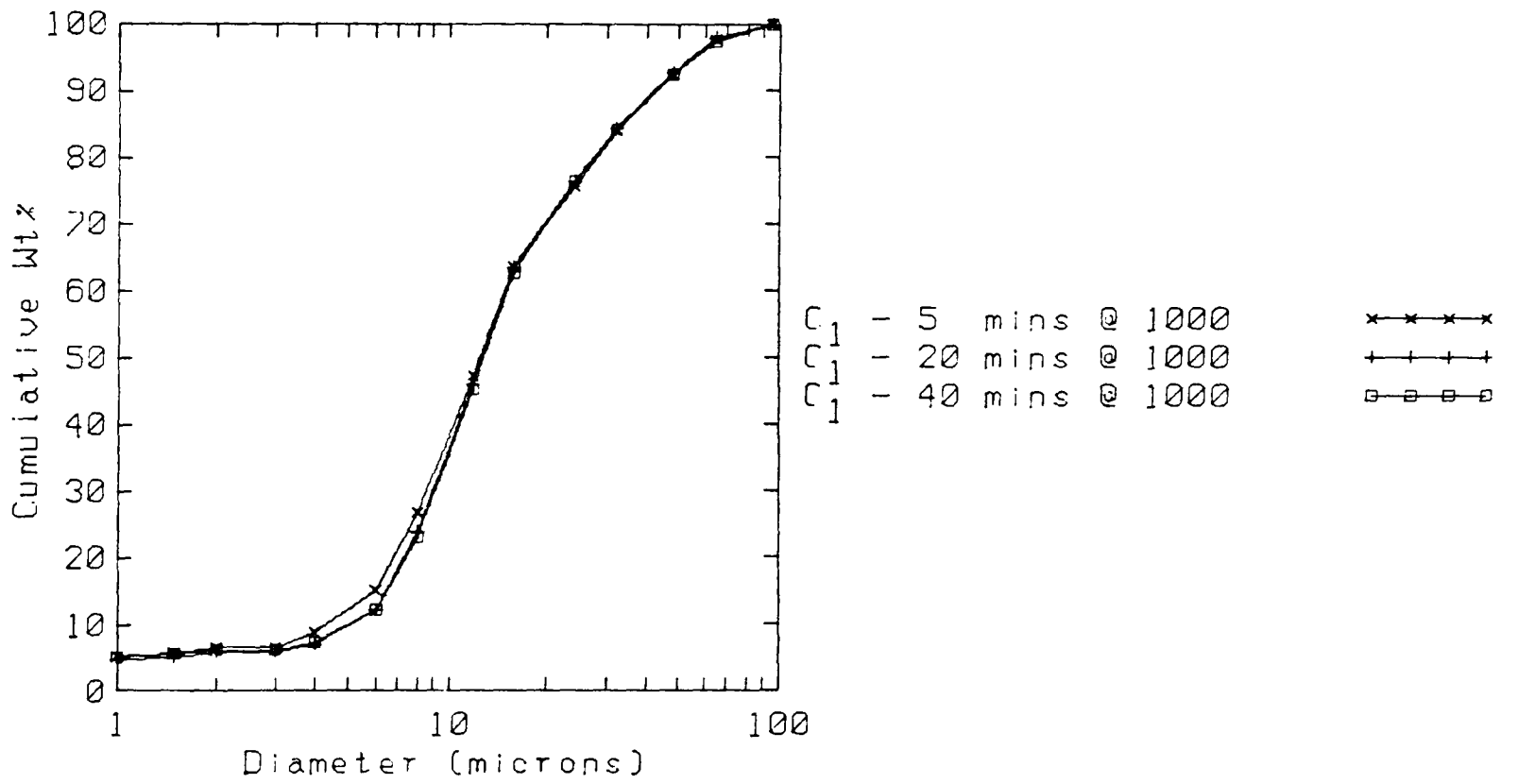

Fig 4.18: Particle size distributions of the samples of preparation C_1 annealed at 1000 degrees for varying amounts of time.

4.3.e Water/cement ratio

Calorimetric traces were obtained for C_3S preparation C_1 hydrated using different w/c ratios. There is a general increase in reactivity on increasing the w/c ratio in this manner showing up as a higher peak maximum occurring at earlier times and a greater overall heat output after 1000 minutes (fig 4.20).

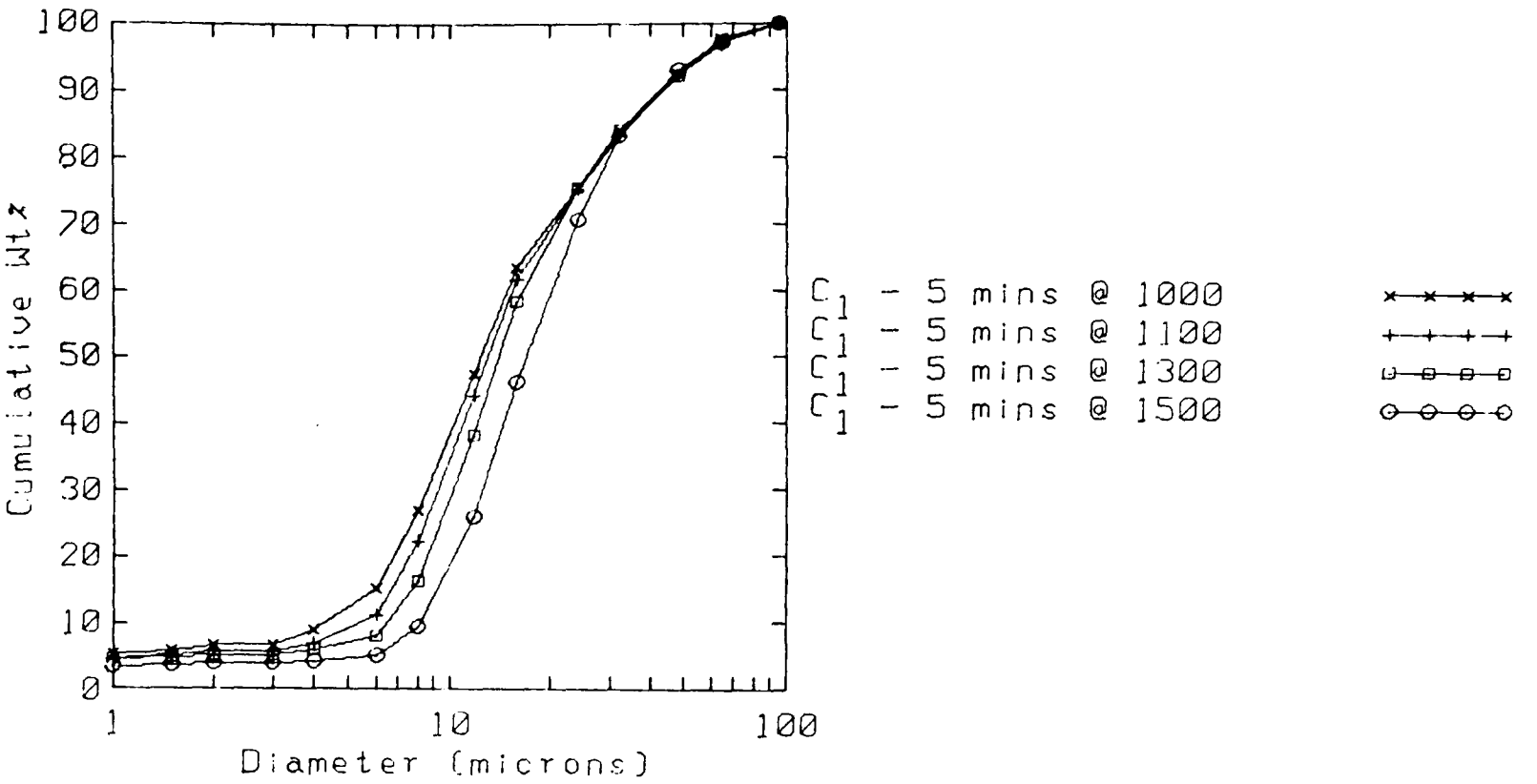

Fig 4.19: Particle size distributions of the samples of preparation C_1 annealed at different temperatures for the same amount of time

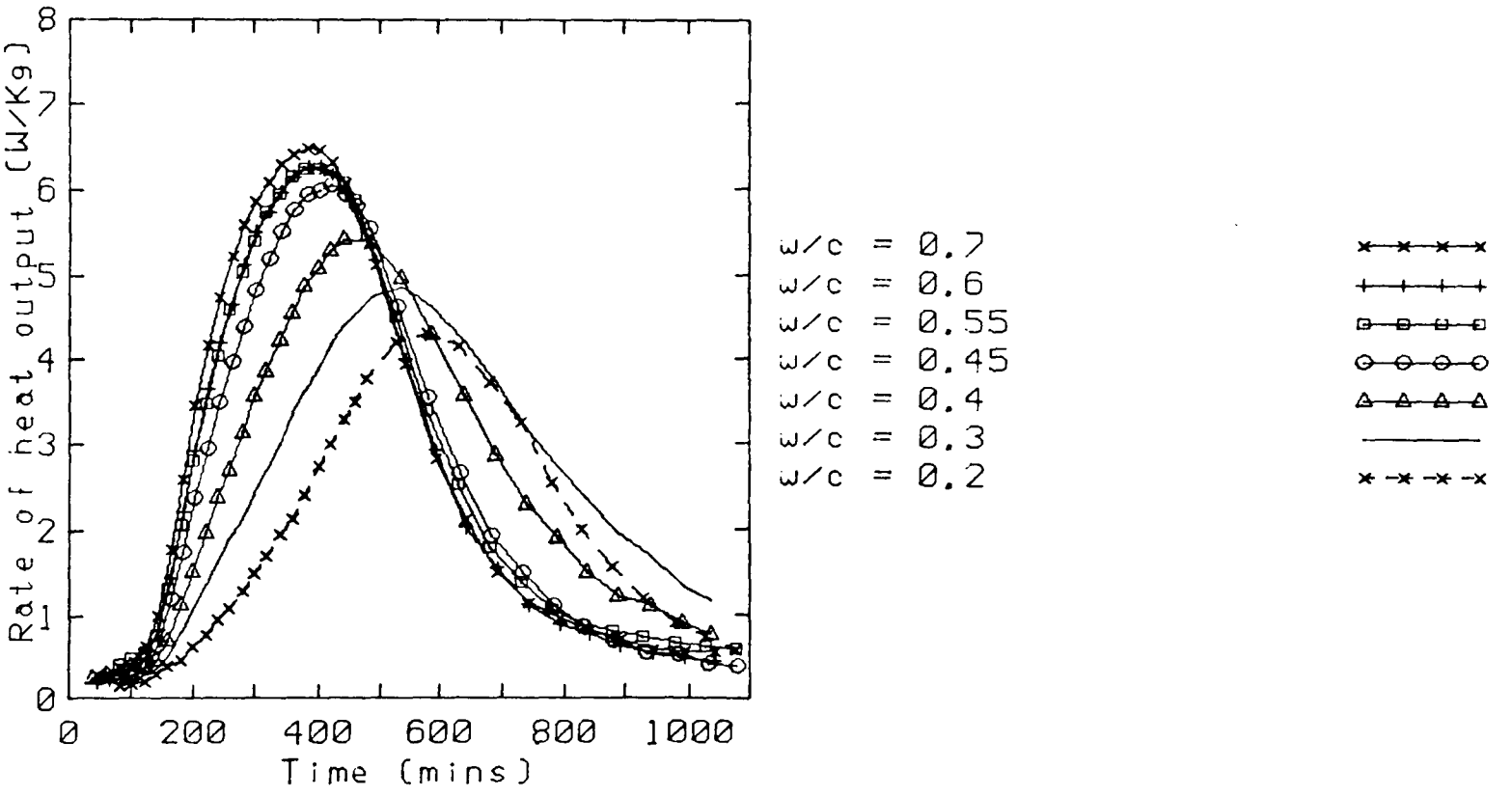

Fig 4.20: Effect of increasing the w/c ratio on the rate of heat output of preparation C_1

A closer study of the curves of fig 4.20 shows that the effect is most marked as the ratio is increased from 0.2 to 0.55, further increases having a much smaller effect. This is illustrated by the expanded diagram of fig 4.21.

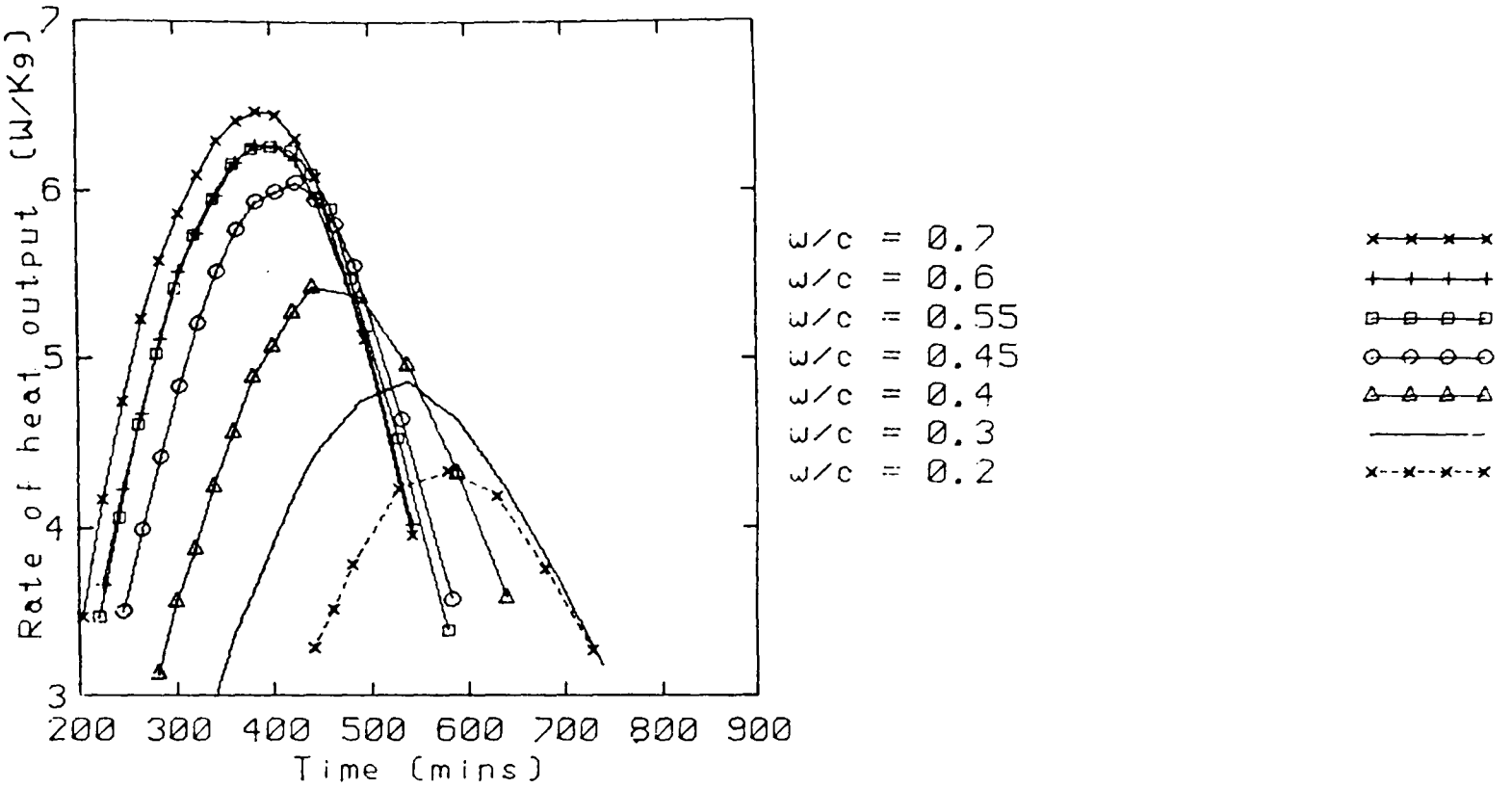

Fig 4.21: Detail of the effect of changing the w/c ratio on the position and height of the peaks in fig 4.20.

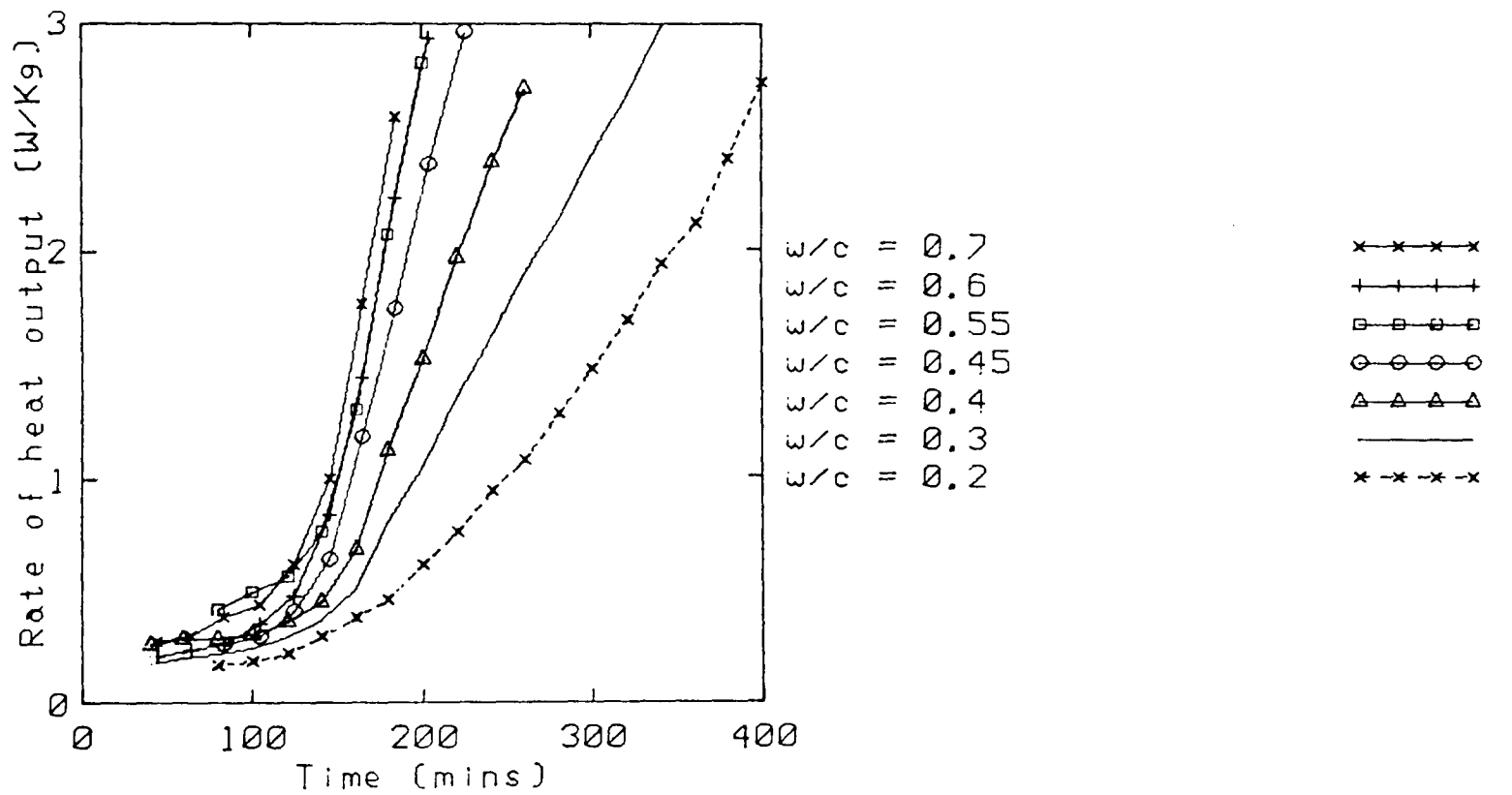

Fig 4.22: Detail of the effect of changing the w/c ratio on the length of the induction period of the curves of fig 4.20

Expanding the early portion of the curve in a similar manner (fig 4.22) shows that the induction period is affected in the same way, initial increases in the w/c ratio (up to a w/c of about 0.6) leading to relatively large decreases in the length of the induction period while further increases lead to much smaller changes.

4.4 Discussion and conclusions

4.4.a Impurity ions

The results of this study and those of the other workers mentioned above (4.2.a.ii) illustrate the wide variability in reactivity which can be exhibited by doped samples of C_3S. This variability brings into question the validity of attempting to draw conclusions regarding the way in which impurity ions affect the reactivity of C_3S. It becomes uncertain which results are true effects of the impurity ions and which are merely the result of differences in the C_3S preparation technique. It is therefore only really possible to postulate the cause of that wide variability in reactivity. The results of this study indicate that variations in the particle size distributions and degree of hydration/carbonation (as a result of sieving) will alter the reactivity of C_3S, but not to the degree which has been observed for impurities such as iron which is reported to retard in some cases and accelerate in others. The reported effect of changing concentration of impurity ions is also not sufficient to account for the variation in reactivity observed by different workers (Thompson et al 1975; Odler & Abdul-Maula 1983). The increases in reactivity caused by impurity ions are usually ascribed to higher concentrations of defects. The work of Boikova (1968) has shown that the degree of disorder (or concentration of defects) in doped samples, and hence by implication their reactivity, is markedly affected by the manner in which they are cooled. It is possible, therefore, that the wide variability in reactivity of samples of C_3S doped with the same element arises from variations in the degree of disorder in the lattice as a result of cooling differences. However, the measurement of the degree of disorder in the C_3S lattice and its correlation with reactivity has not

yet been achieved and more work is required in this area before such a hypothesis can be substantiated.

4.4.b Particle size distribution and grinding

Figs 4.4 & 4.5 indicate that the greater the proportion of small particles in a sample of C_3S the greater its reactivity. The increase in reactivity must mean that small particles of C_3S react faster than an equivalent weight of large ones. This conclusion is supported by the appearance of the shoulder on the acceleratory portion of certain heat output curves (fig 4.8). This has been observed before in heavily ground samples (Odler & Schuppstuhl 1981). The particle size distributions of the samples which exhibit this feature all have two ranges containing relatively large proportions of material (the sub-micron and 8 - 24 micron ranges), and an intermediate range (1 - 8 microns) containing substantially less material. It is likely therefore that the shoulder arises from the exhaustion of the smaller particles after their initial rapid reaction. By the time the smaller particles are fully reacted the contribution of the larger particles to the total heat output will not be very great and so the total rate of heat output will stop increasing or may even fall slightly. This dependence of the heat output, and hence the rate of hydration, on the distribution of particle sizes rather than simply on the overall specific surface has been reported before (Knudsen 1980) but it has only been thought to act during the later stages of the reaction.

As long as the particle size distributions of samples are of the same overall shape then the effect of increasing the specific surface should be to lead to higher reactivity. Fig 4.6 & 4.7 show that this is generally the case but that at very high specific surfaces the effect of increasing the specific surface becomes less predictable and may lead to

a decrease in reactivity. This behaviour at high specific surfaces has been observed by Kondo & Ueda (1968) who suggest that with very heavy grinding an amorphous layer is built up on the surface of the C_3S which inhibits the hydration reaction and hence accounts for the reduction in reactivity.

4.4.c Aging

Exposure of C_3S to the atmosphere leads to reaction with the atmospheric water vapour and, if the exposure is long enough, to carbonation. This changes the reactivity of the C_3S and it is this changing of properties with time which is one of the most difficult factors to contend with in any comparison of the reactivities of different samples of C_3S. In this study storage of C_3S in a bottle which was opened periodically resulted in a decrease in the induction period and a decrease in the time to, and the height of, the maximum of the heat peak of the calorimetric curve (figs 4.9 & 4.10). On the other hand continuous rolling of C_3S in air which was replenished periodically, led to no change in the induction period, a decrease in the height of, and increase in the time to, the maximum in the heat peak. It was not possible to ascertain the degree of hydration/carbonation resulting from the two types of storage. However, given that the rolled samples must have had the greater contact with the atmosphere it is reasonable to suggest that they would also exhibit the greater degree of carbonation. If that were so then these results agree with those reported for OPC and mentioned in section 4.2.c. that prehydration leads to a small acceleration in the rate of hydration and that carbonation leads to a retardation. On the basis of the above conclusions, storage in a desiccator would be expected to preserve the original reactivity of the C_3S. The small variation in the height of the main heat peak of those samples stored in a desiccator and the lack of

changes both in the position of the peak and in the length of the induction period indicate that the variation in reactivity of the desiccator stored samples is much less than the variation in reactivity of the samples stored by the other methods. This is also, therefore, consistent with the theory that hydration/carbonation is causing at least part of the change in reactivity.

It has been suggested that the change in reactivity with storage of C_3S arises from a reduction in the concentration of crystal defects. Crystal defects that have been quenched in to the C_3S crystal lattice are thermodynamically unstable and hence their removal is thermodynamically favourable. However, the very high melting temperature of C_3S indicates that at room temperature the activation barrier for this process is likely to be very high, making it unlikely to occur. The lack of any significant change in the reactivity of the samples stored in the desiccator seems to bear this conclusion out.

4.4.d Heat treatment

In this study the rate of cooling was not found to significantly affect the reactivity of C_3S preparations. This result is in direct disagreement with the results of other workers who have carried out similar experiments (Maycock 1974; Odler & Schuppsthul 1981; Fierens 1982 a). However it should be noted that even the results of these three studies do not entirely agree with each other. When fast cooling has been found to increase the rate of reaction (Maycock 1974; Fierens et al 1982), it has been concluded that the increase in reactivity arises from an increase in the concentration of defects quenched in by the rapid cooling. As mentioned earlier (section 4.4.a) Boikova (1968) has found that the amount of disorder (or defects) which can be quenched in by rapid cooling depends on the disorder which is present at the firing

temperature which in turn is highly dependent on the impurity ions present. It is possible therefore that traces of impurity ions (such as the Cr reported to be present in the samples of Maycock) could lead to a large difference in reactivity between slow and fast cooled samples while the reactivity of pure C_3S samples would exhibit little or no dependence on the rate of cooling. Otherwise it is difficult to see how such a large variation in results could be obtained for experiments which are so similar.

Two factors may be responsible for changes in reactivity as a result of heating C_3S to temperatures in the region of 1000-1500 degrees; changes in defect concentration and changes in surface composition. If changes in the defect concentration are responsible for the changes in reactivity then heat treatment should result in a decrease in the reactivity as a result of a reduction in the concentration of defects. If, on the other hand, changes in the surface composition are the cause, then heat treatment should lead to a decomposition of the hydrate/carbonate on the surface of the grains and so result in either a decrease in the reactivity (if the decomposition of the hydrates is to C_2S) or a reattainment of the original reactivity (if the temperature is high enough for recombination of the decomposed hydrates to give C_3S).

The effects of heating on the reactivity of C_3S can be further complicated by an increase in particle size as a result of sintering effects and by decomposition of C_3S to C_2S and lime at temperatures below 1250 degrees.

Reheating a sample of C_3S to 1500 degrees for 5 minutes led to a marked reduction in reactivity while mild grinding of that sample restored its original reactivity (fig 4.15). This implies that the major cause of the reduction in reactivity in this case was an increase in particle size.

This is supported by the particle size distributions of samples heated for 5 minutes at 1000, 1100, 1300 and 1500 degrees respectively (fig 4.19). The higher the firing temperature the greater the increase in average particle size. The change in particle size distribution with increasing temperature means that the true effect of heating to different temperatures cannot be ascertained from the results of this study as a quantitative knowledge of the effect of particle size distribution on the reactivity of C_3S is not known.

Samples reheated to 1000 degrees for varying lengths of time showed no such variation in particle size distribution (fig 4.18). However neither did they show any systematic variation in reactivity with time of reheating (fig 4.16) so no conclusions could be drawn from that part of the experiment.

The hydration reaction of C_3S has already been shown to be highly dependent on the nature and composition of the surface of the unreacted C_3S grains. It is not surprising therefore to find that the effects of heating are unpredictable because of the many variables which are affected by heating which could also affect the state of the surface. Factors such as the atmosphere in the furnace, the presence of impurity ions, the exact temperature of firing, the nature of the air in contact with the samples as they cool and the length of time from firing to hydration in the calorimeter could all affect the final observed rate of heat output. In this study only a preliminary look at the effect of heating was possible and a large amount of work still remains to be done.

4.4.e Water/cement ratio

The results of this study on the effect of changes in the w/c ratio on the reactivity of C_3S, while not agreeing with those of similar studies

(Kantro et al 1966; Locher 1966; Kondo et al 1967), do follow a definite trend. Increasing the w/c ratio was found to lead to an increase in reactivity, the increase tailing off at higher w/c ratios (fig 4.20). The change in reactivity is not simply a result of there being insufficient water for complete reaction at low w/c ratios and excess water at the higher ratios. If this were so, the induction and early acceleratory periods of the calorimetric curves for each sample would be expected to follow the same line. Similarly if the additional water merely provided more space within which reaction products could form the reaction would still be expected to proceed at the same rate initially, regardless of w/c ratio, deviations only becoming apparant at later ages.

Under normal circumstances (normal particle size distribution and normal w/c ratios) the solution surrounding the C_3S becomes saturated/supersaturated with respect to $Ca(OH)_2$ and CSH within a matter of minutes (Brown et al 1984) no matter what the w/c ratio. Once saturation is reached it is difficult to see how increases in the w/c ratio could increase the subsequent rate of reaction. It seems likely therefore that it is the processes which occur during the very initial stages, before saturation is reached, that influence the subsequent hydration behaviour. It has been postulated that during these early stages a protective layer is formed around the C_3S grains which inhibits further reaction (see chapters 6 and 7). If that is so then the possibility exists for changes in the w/c ratio to alter the manner in which this layer is formed and hence its composition and/or physical nature. This in turn could affect the subsequent rate of reaction. However, whether a membrane is formed and if so, the manner in which it might be altered by changes in the w/c ratio still remains to be elucidated.

4.4.f General comments

It is clear from the work of past researchers and the results in this study, that the rate of hydration of C_3S is affected in a highly complex manner by a variety of factors. The relative importance of these factors in determining the reactivity of a preparation of C_3S is very difficult, if not impossible, to determine. In certain cases, most notably when trying to determine the effect of impurity ions on the reactivity, it was found that changes in the reactivity due to other factors could not be eliminated. In these cases it was not possible to separate the factors responsible for the changes in reactivity and so no conclusions could be drawn. It has not been possible to account for all of the observations made in this study and it is quite possible that one or more of the factors studied operates in a more complex manner than anticipated or even that there are other factors operating which have not been taken into account. In spite of these limitations, the observations made in this study do throw some light on the way in which the various factors influence the reactivity of C_3S. However they also indicate that there remains a great deal of work to be done in this area. Until all the various factors influencing the reactivity of C_3S have been determined and the manner in which they operate, understood, considerable care must be taken when drawing ones conclusions. Altering one factor can lead to alterations in other factors (eg changing the impurity ion and reheating to temperatures in the region of 1200 - 1500 degrees can both lead to changes in the particle size distribution) and unless these are recognised and accounted for, the wrong conclusions may be drawn.

4.5 Summary

The results of previous work on the effect of impurity ions on the reactivity of C_3S are often inconsistent. In this work, attempts to prepare samples of C_3S doped with various impurity ions, but keeping all other variables constant, failed. It is suggested that part of the reason for the inconsistency of results reported in the literature stems from a lack of control of the other factors affecting the reactivity of C_3S.

The effect of the particle size distribution and grinding on the reactivity of C_3S has not been well researched. It is known that fine grinding increases the rate of reaction and the possibility that heavy grinding introduces defects which increase the reactivity has been suggested (Maycock et al). The increase in reactivity on increasing the specific surface has been demonstrated in this work as well as a dependence of the form of the calorimetric heat output curve on the particle size distribution. Both results point to the size of the reacting particle playing a part in the rate at which it hydrates. While this has been recognised for the later stages of hydration, it is not usually considered to affect the reaction until after its acceleratory stage.

Changes in reactivity as a result of storage are thought to come about either by surface hydration and/or carbonation from water vapour and carbon dioxide in the atmosphere or by a reduction in the concentration of crystal defects by an annealing process. Results from this study show that the effect of storage depends very much on the conditions under which the C_3S is stored and favor the theory that the changes in reactivity arise from hydration and/or carbonation of the surface layer.

Fast cooling of C_3S has been found to increase its reactivity, the explanation usually given being that the faster the rate of cooling the greater the concentration of defects which are quenched in and hence the greater the reactivity. Results from this study showed no such increase in reactivity with increasing rate of cooling. The only possible explanation would seem to be that some preparations of C_3S (perhaps because of trace amounts of impurity ions) can stabilise greater concentrations of defects at high temperatures which can then be quenched in by rapid cooling. Others such as the preparation used for this study can not stabilise such high concentrations at high temperatures and hence the difference in reactivity between slow and fast cooled samples is minimal.

Annealing samples of C_3S at high temperatures has been found to decrease the reactivity up to the temperature at which C_3S is formed from C_2S and lime, after which an increase in reactivity has been observed. It is thought that the changes in reactivity arise from decomposition of the surface layer of C_3S to C_2S and lime at the lower temperatures and recombination of that C_2S with the lime at higher temperatures. Defects are also thought to play a part in determining the final reactivity. No obvious correlation between the reactivity and either the reheating temperature or the time of reheating was found in this study. An increase in average particle size with increasing temperature was noted. The possibility therefore exists for part of the change in reactivity to be due to the change in particle size distribution as a result of the heating.

The effect of the w/c ratio on the reactivity of C_3S, while being different from those other factors considered in that it is not dependent on the properties of the C_3S itself, is nevertheless of interest in such

a study. Previous studies have found conflicting effects. The results of this study indicate an increase in reactivity as the w/c ratio is increased, the increase being greatest in the range 0.2 to 0.55. It is thought that the increase in reactivity, which involves both an increase in the height of the main heat output peak and a decrease in the length of the induction period, could be due to changes in a protective layer whose properties are dependent on the solution composition during the very early stages of the reaction and hence on the w/c ratio. These changes in the protective layer could then influence the formation of subsequent products in such a manner that the later reactivity of the system was also affected.

In conclusion the marked dependence of the hydration of a compound such as C_3S on its surface properties was noted. This has the implication that great care must be taken when comparing results from different studies until a greater understanding of (a) the manner in which the various factors influence the reactivity of C_3S and (b) the manner in which they may be controlled, has been attained.

CHAPTER 5

KINETIC MODELLING OF CALORIMETRIC DATA

5.1 Introduction

The hydration reaction of C_3S is, as has already been described, a highly complex one and is by no means completely understood. Developing a mathematical model to predict the course of the reaction and the effect of various conditions upon it therefore seems, at first sight, to be rather premature.

However, useful information can be obtained from such an exercise. Even if the model developed is purely empirical and the equations being used do not have any conceptual relationship to what is thought to occur; if it can predict the behaviour of the C_3S under a variety of conditions then it should not be dismissed. It is always possible that later developments may indicate a physical significance. Conversely, if the model arises from the consideration of a hypothetical reaction mechanism, then whether or not the calculated behaviour fits the experimental data is an indication of whether or not the postulated mechanism can be considered as contributing to the overall mechanism. Unfortunately, a good fit does not necessarily indicate that the model is correct; it merely indicates that it cannot be discounted.

Mathematical modelling of hydration processes therefore allows the elimination of unsatisfactory models, gives an insight into the mechanisms which may be involved and, by considerations of deviations of the calculated data from the experimental, can lead to improved understanding of the processes which may be occurring.

A large amount of work has already been carried out on deriving equations to model the hydration of C_3S (Pommersheim & Clifton 1979 b; Gylling 1982; Jelenic & Bezjak 1982). The more common models are described below.

5.1.a Nucleation and growth models

Nucleation and growth of CSH gel is often considered to be the rate determining process for the initial stages of hydration and it is possible to get good correlation between calculated and experimental data during the acceleratory and early deceleratory periods when using equations based on nucleation and growth.

The most common kinetic equation in use to model the nucleation and growth reaction is based on that of Avrami (1939; 1940; 1941) and Erofeev (1946). This equation (5.1) can be applied to a variety of heterogeneous transformations taking place by a nucleation and growth mechanism and in which the transformation is ultimately limited by impingement of the products. It was first used to model C_3S hydration by Tenoutasse & De Donder (1970) and has since been used by Fierens et al (1982 a & b) and Urzhenko & Usherov-Marshak (1974) to model the hydration of C_3S and by Double et al (1978) to model the hydration of OPC.

$$X = 1 - \exp(-K.t^n) \qquad \ldots 5.1$$

X = fraction transformed after time t.

K = transformation rate parameter.

t = time.

n = power exponent.

As it stands the Avrami equation predicts that at the maximum in rate of hydration the degree of hydration should be from 45 to 53% (for n = 2.5 to 4). However calorimetric and X-ray data show that the value is more

usually about 20%. This apparent inconsistency can be taken into account by considering only a certain fraction of the solid to be able to react by the nucleation and growth mechanism. The fraction transformed (X in eqn. 5.1) is then only the fraction of that fraction which can react by the nucleation and growth mechanism.

There has been some controversy over the value of the power exponent n. Differences in the value of n arise from variations in the relative speed of the nucleation and growth processes and in the way the nucleation takes place (whether it is linear, planer or three dimensional). For surface nucleation in which there is very rapid exhaustion of nucleation sites and planar growth, the n exponent should be 2, while continuous nucleation and slow exhaustion of sites leads to a value of 3 (Double et al 1978). Tenoutasse and Fierens both used an empirical value of 3 in their calculations and achieved very good fits to experimental data. Urzhenko and Double calculated the value of n which gave the best fit to their data, the former arriving at a value of 2.5 and the latter finding values in the range 2.0-2.5. This use of values other than three for the exponent has been questioned by Bezjak & Jelenic (1980).

Other equations for modelling nucleation and growth of CSH gel have also been derived. For example, Frohnsdorff et al (1969) applied classical nucleation-rate and ion-product equations to crystal growth from saturated solution to give expressions relating heat evolution and amount of gel produced to strength and other physical properties, while Fujii and Kondo (1974) derived a single expression describing both the induction and the acceleration/decay periods from a model involving a propagative surface nucleation and growth reaction.

5.1.b Models involving phase boundary reaction and diffusion through hydrate layers.

The Avrami equation predicts that the rate of reaction falls off much faster than it actually does. The later stages of the hydration of C_3S are therefore usually considered to be controlled by either the reaction at the boundary between the hydrate and the C_3S core, or the diffusion of water through the layers of hydrate coating the unreacted cores. The phase boundary reaction is usually supposed to be rate determining initially, but as hydration proceeds and the layers of hydrate grow in depth, so diffusion of water through the layers becomes more and more difficult, eventually taking over as the rate determining step.

The kinetic equations which have been derived to describe these processes (Taplin 1962 a; Kondo & Ueda 1969; Pommersheim & Clifton 1979 a, 1980) are based on what has become known as the 'shrinking core model' (fig 5.1). Each particle is considered a homogeneous sphere of original radius R. The radius of the unreacted core is r_i while the radius of the core plus the various layers surrounding it is r_o. Water is considered to diffuse through three layers; an outer layer consisting of fibrils and precipitated gel, a thin barrier layer corresponding to the original particle surface and an inner layer occupying the space left by the reacting grain. Each of these is given a diffusion coefficient and the following assumptions are made:

1) The concentration profile of reacting fluid is linear through the inner and outer product.

2) The coefficients of diffusion in the three layers are independent of concentration and time.

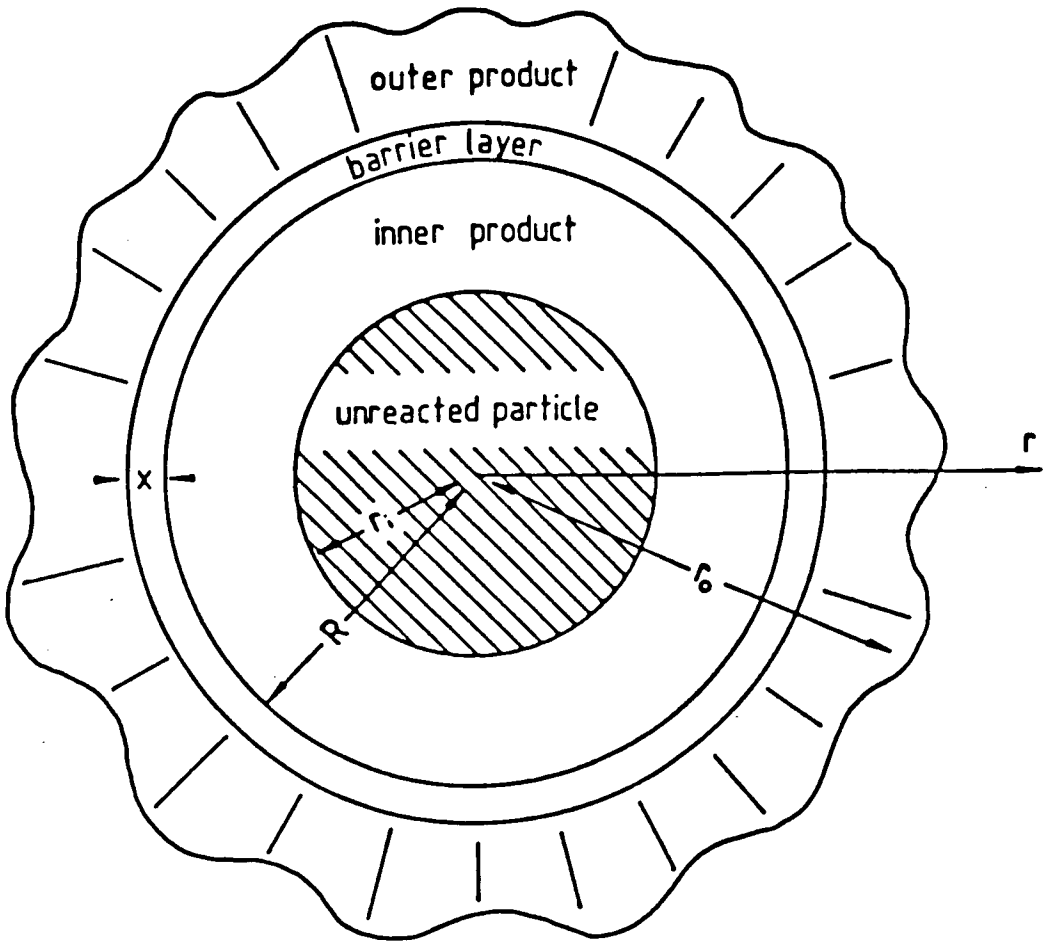

Fig 5.1: Schematic diagram of a reacting C_3S grain according to the 'shrinking core model'.

Analysis yields a complex differential equation, each expression of which is usually solved separately to yield four kinetic equations; each becoming rate determining under different conditions.

1) Phase boundary reaction.

$$1 - (1-X)^{\frac{1}{3}} = k_1 \cdot \frac{t}{R} \qquad \ldots 5.2$$

X = fraction transformed after time t.

k_n = rate constants.

t = time.

R = radius of particle.

2) Reaction controlled by inner product diffusion.

$$1 - (1-X)^{\frac{2}{3}} - \frac{2}{3}.X = k_2.\frac{t}{R^2} \qquad \ldots 5.3$$

3) Reaction controlled by barrier layer diffusion (assuming thickness of barrier layer remains constant)

$$X = k_3.\frac{t}{R} \qquad \ldots 5.4$$

4) Reaction controlled by outer product diffusion.

$$1 + \frac{2}{3}.v.X - (1-v.X)^{\frac{2}{3}} = k_4.\frac{t}{R^2} \qquad \ldots 5.5$$

(v = ratio of inner to outer product)

This argument is not valid when two or more of the terms of the original differential equation are of equal magnitude. However the errors introduced by this and by i) assuming that the particles are spherical, and ii) assuming a linear concentration profile through the inner and outer products together with diffusion coefficients independent of time and distance to the surface, are largely outweighed by the effects of particle size distribution (5.1.d).

5.1.c Models involving poisoning

It was pointed out by Taplin (1969 b) that, while in the above description (5.1.b) the rate determining step is modelled as diffusion of small molecules of water through the hydrate layers to the core surface, a considerably slower process should be the outwards diffusion of the much larger hydration products which go to make up the outer hydrate

layer. This factor can be taken into account by considering the reaction to be slowed down or 'poisoned' by the increased difficulty of diffusion through increasingly thick layers. A modified rate constant is introduced, dependent on the degree of hydration, which yields four modified equations for the four stages considered above; the main difference being that the reactions no longer go to completion in finite time.

5.1.d Models incorporating particle size distribution

An important deficiency in the equations derived from the 'shrinking core model', is that they all apply only to a single particle or a mono-disperse system, while all real cements are poly-disperse. This was first pointed out by Taplin (1969 a & b) who showed that the kinetic equations of an ensemble of particles failed to match the kinetic equations of the individual particles. The blurring effect of the particle size distribution on a kinetic equation was further emphasised by Knudsen (1980).

Only very few attempts have been made to incorporate the particle size distribution into kinetic expressions. One of the earliest attempts was by Sasaki (1964) for modelling the solid state reaction between lead dioxide and zirconium oxide to produce lead zirconate. He divided the sample up into a set of size fractions with a constant factor between each size and, by finding the reacted fraction of each size group and summing over the whole sample, he derived an expression to predict the overall reacted fraction as a function of time and obtained good agreement with experimental results. For cement, however, more than one kinetic equation is usually thought to be involved, in which case the method of Bezjak & Jelenic (1980 a) is perhaps more applicable. In this the degree of hydration at any time is calculated by summing the

individual contributions of each particle size fraction. The degree of hydration of any particular sized particle is obtained from one of three rate equations depending on which is rate determining at the time. Good correlation between experimental and calculated data was obtained for a wide variety of cements (Bezjak & Jelenic 1980; Bezjak et al 1980; Bezjak & Alujavic 1981; Jelenic & Bezjak 1981). A rather different approach was adopted by Taplin (1980) and Knudsen (1980) in which an expression for the particle size distribution was incorporated into the differential rate equation in place of the single radius of a particle. The equation, when solved, then took the effect of the distribution into account implicitly.

5.2 Modelling using the Avrami equation

In this work, calorimetric data was collected during the first 1000 minutes of reaction. During this time it has been shown (Tenoutasse & De Donder 1970; Urzhenko & Usherov-Marshak 1974; Double et al 1978; Fierens et al 1982 a & b) that the Avrami equation (5.1) can yield a relatively simple and effective fit to hydration rate data obtained both by QXDA and by calorimetry. Using the Avrami equation in this manner has several advantages over other methods in that firstly it is simple, secondly it has few variables which have to be determined and thirdly it is independant of particle size distribution.

In this work the Avrami equation was fitted to a range of calorimetric curves obtained from hydrating C_3S at various temperatures both on its own (controls) and in the presence of 0.2M $CaCl_2$ solution (accelerated). The results allowed a value for the thermal conversion constant to be determined, while the temperature variation of the rate parameter allowed the calculation of the apparent activation energies for both control and accelerated samples.

As a result of the work, it became clear that, while the Avrami equation can provide an effective and simple fit to calorimetric data, it does have certain limitations and these are discussed in the final section.

5.3 Experimental details

5.3.a Materials

C_3S preparation A_1 was used in this work. The method of preparation and the chemical and physical analysis of the material are given in chapter 3.

5.3.b Calorimetry

Calorimetric curves were obtained for the hydration of C_3S at various temperatures both with and without $CaCl_2$ accelerator. The experiments were carried out using a w/c ratio of 0.5 at the temperatures given in table 5.1. The voltage output of the calorimeter was converted to rate of heat output using the method described in chapter 2, only those points after the minimum in the voltage curve being used in the calculations.

Experiment	Temperature(°C)						
	25	30	35	40	45	50	55
Control	**	**	**	**	**	**	**
$CaCl_2$ accelerated	**		**		**		**

(** = experiment carried out at this temperature)

Table 5.1: Temperatures at which calorimetric runs were obtained.

5.4 Results and Discussion

5.4.a Calorimetry

A set of typical calorimetric curves are illustrated in fig 5.2. The control curve at 25 degrees illustrates the characteristic form of the heat evolution curve after the initial heat peak (not shown) with a period during which the heat output is relatively low (induction period), a period during which the heat rises to a maximum (acceleration period) and eventually a period during which the heat output falls to a low value (deceleration period). The various stages are described in more detail in chapter 6.

The accelerating effect of the $CaCl_2$ is clearly visible in the larger maximum heat output which occurs after a shorter time.

The effect of increasing the temperature has a similar accelerating effect.

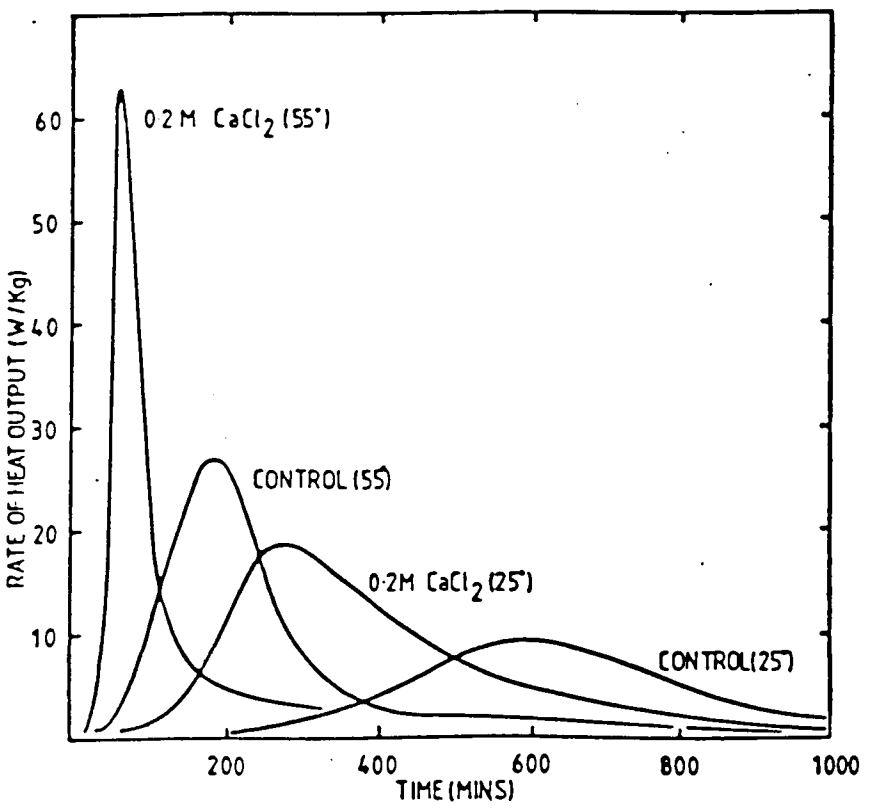

Fig 5.2: Examples of calorimetric curves from C_3S at various temperatures illustrating the accelerating effect of $CaCl_2$ admixture.

5.4.b Fitting the Avrami equation

5.4.b.i Determination of the power exponent, n

The usual method for the determination of n involves plotting $\ln(\ln(1/(1-X)))$ against $\ln(t)$ the slope of which gives n (eqn 5.6).

$$\ln\left(\ln\left(\frac{1}{1-X}\right)\right) = n.\ln(t) + \ln(K) \qquad \ldots 5.6$$

The degree of hydration (X) can be calculated from the heat curve by making the assumption that the heat output (Q) is proportional to the rate of hydration (eqn. 5.7). This assumption is based on the assumption that all heat producing reactions occur at the same relative rate during the period of study and is reasonable given that QXDA and TGA both indicate that all products are produced in approximately the same proportions throughout the reaction (see chapter 6).

$$Q = h.\frac{dX}{dt} \qquad \ldots 5.7$$

H = thermal conversion constant

The degree of hydration at time t is then the ratio of the integrated heat at time t (J) to the total heat given out after 100% hydration (eqn. 5.8).

$$X = J/500 \qquad \ldots 5.8$$

(total heat at 100% hydration ~ 500 J/g (Lea 1970))

Equation 5.6 therefore becomes:

$$\ln\left(\ln\left(\frac{1}{1-\frac{J}{500}}\right)\right) = n.\ln(t) + \ln(K) \qquad \ldots 5.9$$

Fig 5.3 shows the curve obtained by plotting the left hand side of equation 5.9 against ln(t) for the various values of J obtained from a calorimetric curve using a control sample of C_3S, hydrated at 25 degrees. While the curve deviates from linearity both at early times and at late times the central portion is appromimately linear and gives a value of n of about 4.

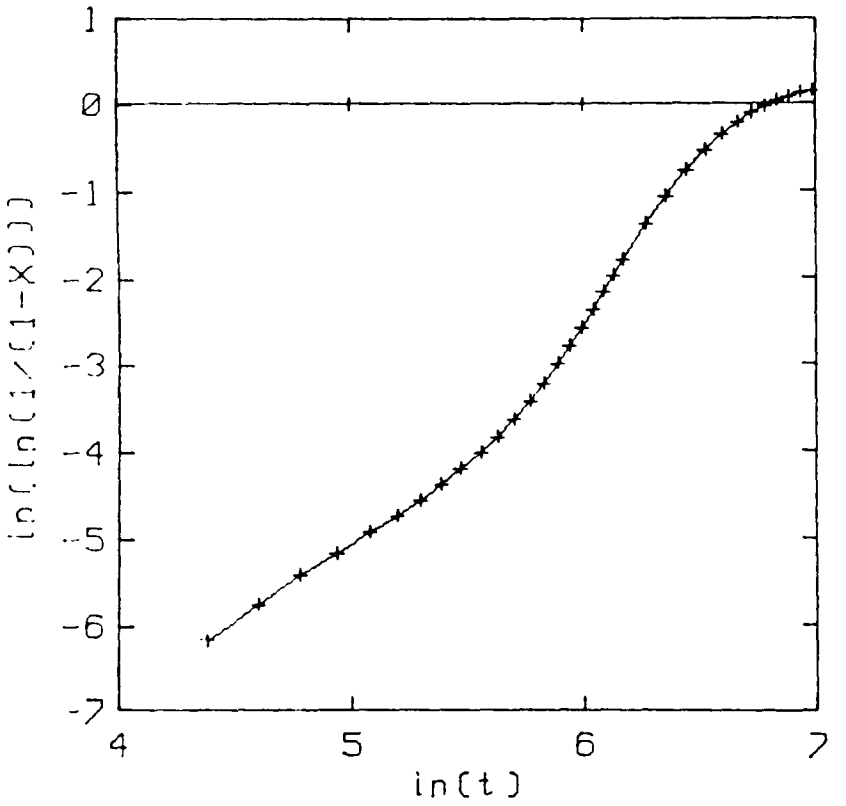

Fig 5.3: Plot of ln(ln(1/(1-X))) against ln(t) for a calorimetric curve. The slope of the linear portion gives the value of n as about 4.

Plotting the differential of the Avrami equation (eqn. 5.10) with this value of n of 4 on the same coordinates as the original heat output curve and choosing values of K and H to make the maxima of the two curves coincide (fig. 5.4) shows that the Avrami equation can not completely account for the induction period.

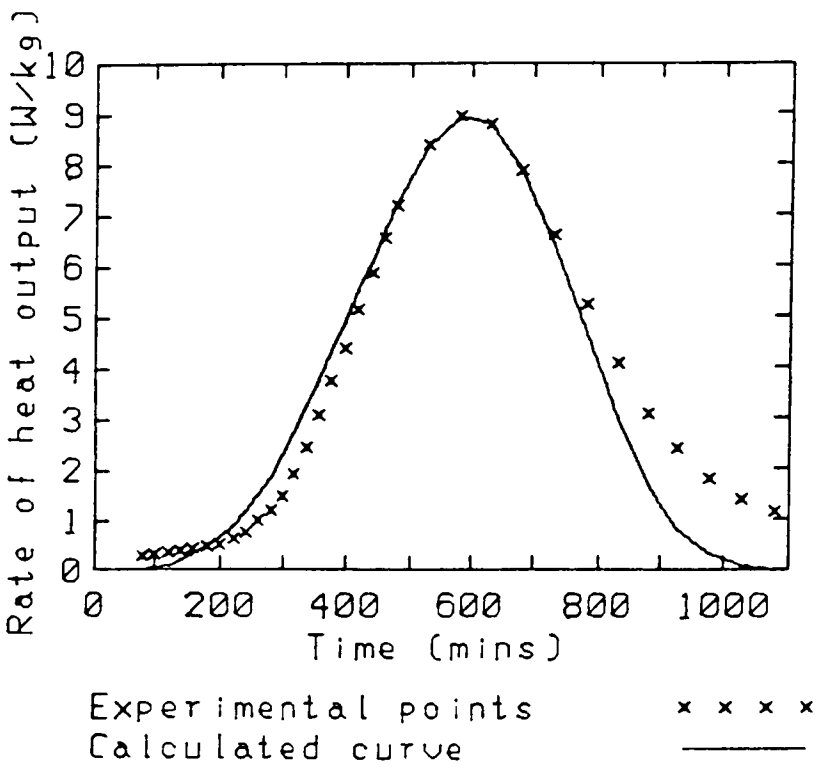

Fig 5.4: Comparison of calculated and experimental heat output curves taking n = 4 and adjusting the height of the calculated curve so that the maxima coincide.

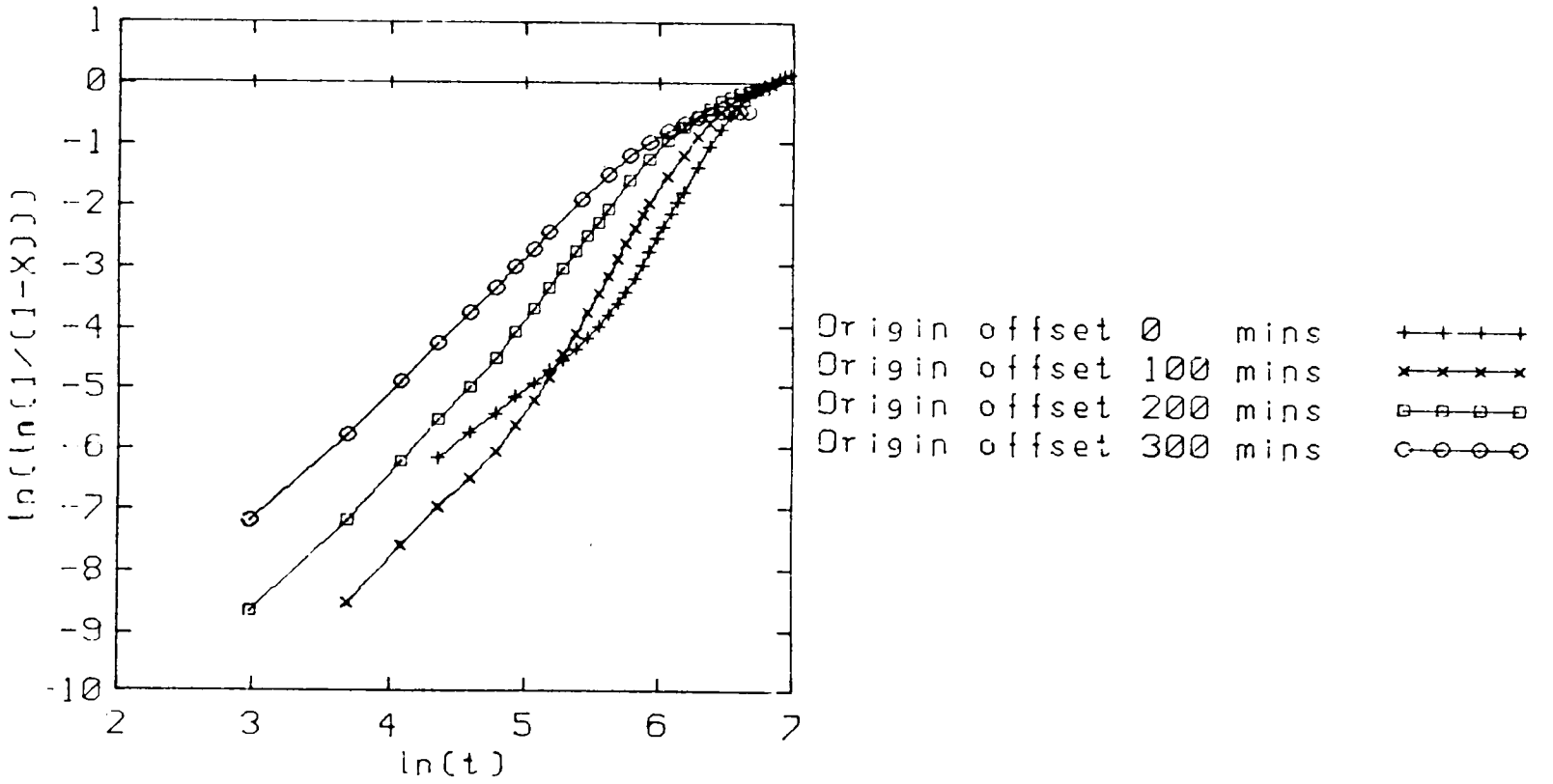

Fig 5.5: Illustration of the effect of altering the origin of the Avrami equation on the ln(ln(1/(1-X))) v ln(t) plot. Moving the origin to greater times extends the linear portion and decreases its gradient.

To get a better fit it is necessary to offset the origin of the Avrami (X=0, t=0) to some point along the heat curve. Changing the origin in this manner also has the effect of altering the ln(ln(1/(1-X))) v ln(t)

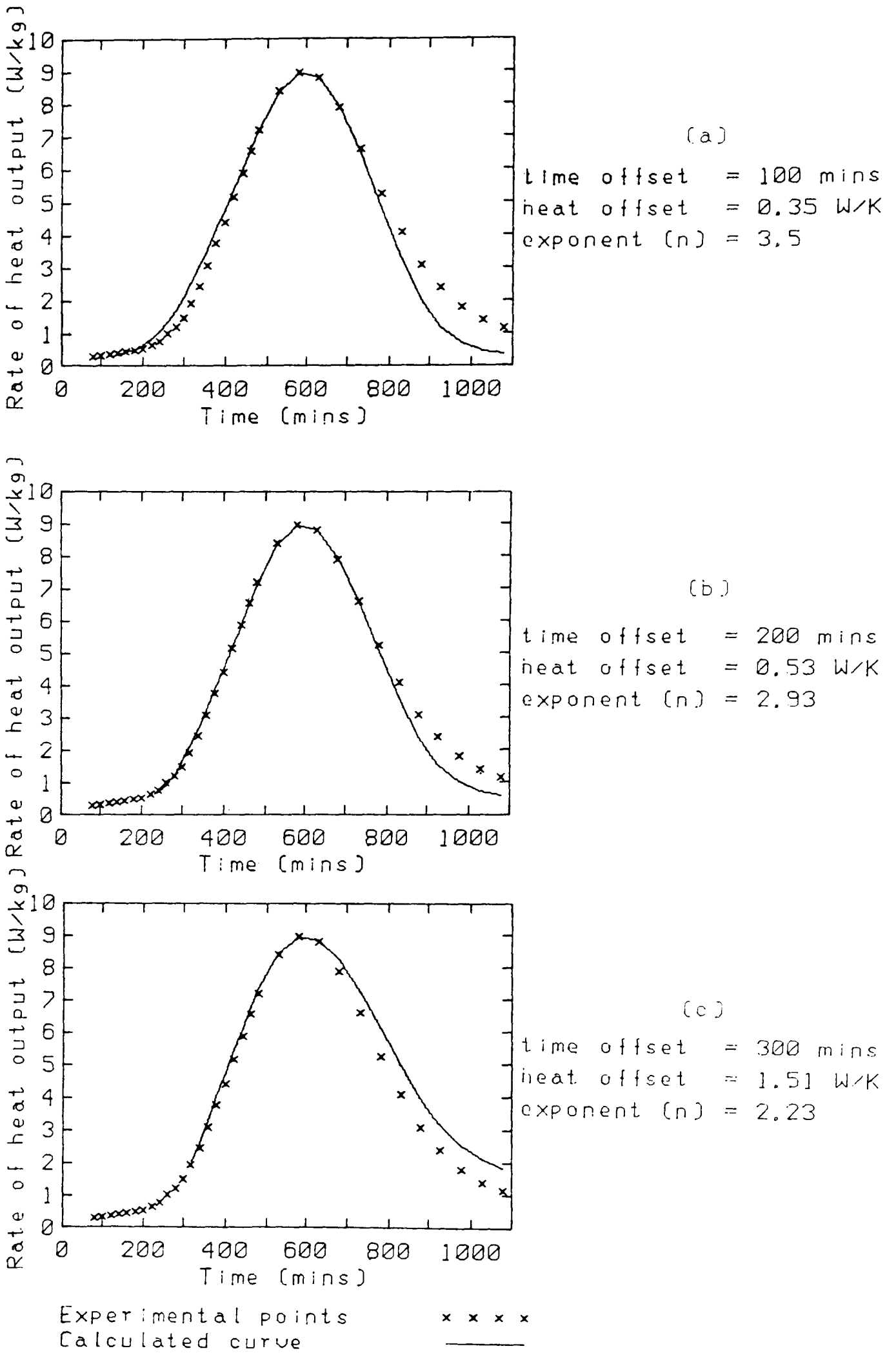

Fig 5.6: Comparison of calculated and experimental heat output curves using different origins. Values of n are calculated from the slopes of the linear portions of the respective curves in fig 5.5. Offsets used were a) 100 mins, b) 200 mins and c) 300 mins.

plot and hence the value of n obtained from the linear portion of the graph. Fig 5.5 shows the effect of altering the origin in this manner on the ln(ln(1/(1-X))) v ln(t) plot while fig 5.6 illustrates the effect this has on the fit of the calculated data to the experimental data.

The fitting procedure therefore consists of finding the value of n appropriate to a particular offset from the ln(ln(1/(1-X))) v ln(t) plot and calculating the predicted heat output according to that value of n to see how it matches up with the experimental values. From fig 5.6 it is clear that a good fit to the early part of the graph is possible for a wide range of values of n (2.5 to 4); the higher values of n giving better fits to the early part of the graph and requiring only small offsets and the lower values giving better fits to the later portions but requiring larger offsets. Generally, the lower values of n give fits for the longest periods of time, a value of 2.5 giving about the best overall fit. The value of 2.5 was therefore chosen for use in this work.

The fact that a wide range of values of n can give satisfactory fits of calculated to experimental data has not been reported before. Urzhenko & Usherov-Marshak do not seem to have taken the induction period into account in their calculations, while Tenoutasse & De Donder and Fierens et al did not attempt to use any value other than three.

The value of the power exponent n can be an indication of both the relative speeds of the nucleation and growth processes and the mode of development of the product (Christian 1975). However, because of the difficulty in determining a single value for n, no conclusions concerning these factors can be drawn in this case.

5.4.b.ii Determination of K and H

To relate the calorimetric curves (rate of heat evolution) to the Avrami equation (change in degree of hydration), it is necessary to have the Avrami equation (eqn. 5.1) in differential form (eqn. 5.10)

$$\frac{dX}{dt} = n.K.t.^{(n-1)} \exp(-K.t^n) \qquad \ldots 5.10$$

Using the assumption that the rate of transformation of the C_3S is proportional to its heat output (eqn. 5.7), allows the prediction of the rate of heat output (Q) as a function of time (eqn. 5.11); time and heat output now being measured from the (offset) origin of the Avrami curve (fig 5.7).

$$Q = n.K.H.t.^{(n-1)} \exp(-K.t^n) \qquad \ldots 5.11$$

Differentiating equation 5.11 gives a relationship (eqn. 5.12) which allows the calculation of K and H from the position (t_{max}) and height (Q_{max}) of the maximum in the heat curve (eqns. 5.13, 5.14)

$$\frac{dQ}{dt} = H.n.K.t.^{(n-2)} \exp(-K.t^n).(n-1-n.Kt^n) \qquad \ldots 5.12$$

At the maximum ($t = t_{max}$, $Q = Q_{max}$) $dQ/dt = 0$. Hence:

$$t_{max}^n = \frac{n-1}{n.k} \qquad \ldots 5.13$$

and

$$Q_{max} = H.(n.K).^{(\frac{1}{n})} (n-1).^{(1 - \frac{1}{n})} \exp(\frac{1-n}{n}) \qquad ...5.14$$

Having chosen the value of n to be 2.5, it is now possible to choose the origin of the Avrami (and hence H and K by equations 5.13 & 5.14) such that the best fit to the experimental data is obtained. This is achieved using the interactive computer program listed in appendix III, which allows the user to enter the position of the Avrami origin in terms of heat and time offsets from the start of the experimental curve. The program then uses values of K and H derived from the values of t_{max} and Q_{max}, based on this new origin, to calculate the heat output according to the Avrami equation and plots these together with the experimental points so that a comparison may be made. The procedure is repeated using different values of time and heat offsets until the best observable fit is obtained. Using this method it is possible to get a very good fit over a wide time range as illustrated in fig 5.7.

By combining equations 5.13 and 5.14 to give equation 5.15 it can be seen that for a given value of n and assuming a constant value for H, the product $Q_{max}.t_{max}$ should also be constant.

$$Q_{max}.t_{max} = H.(n-1).\exp(\frac{n-1}{n}) \qquad ...5.15$$

A plot of Q_{max} against $1/t_{max}$ for a range of calorimetric curves should therefore be a straight line passing through the origin with a slope given by the right hand side of equation 5.15. Fig 5.8 shows such a plot for the calorimetric runs carried out in this study. The plot confirms

the general validity of the relationship predicted in eqn 5.15 and gives an average value of H as 200 J/g.

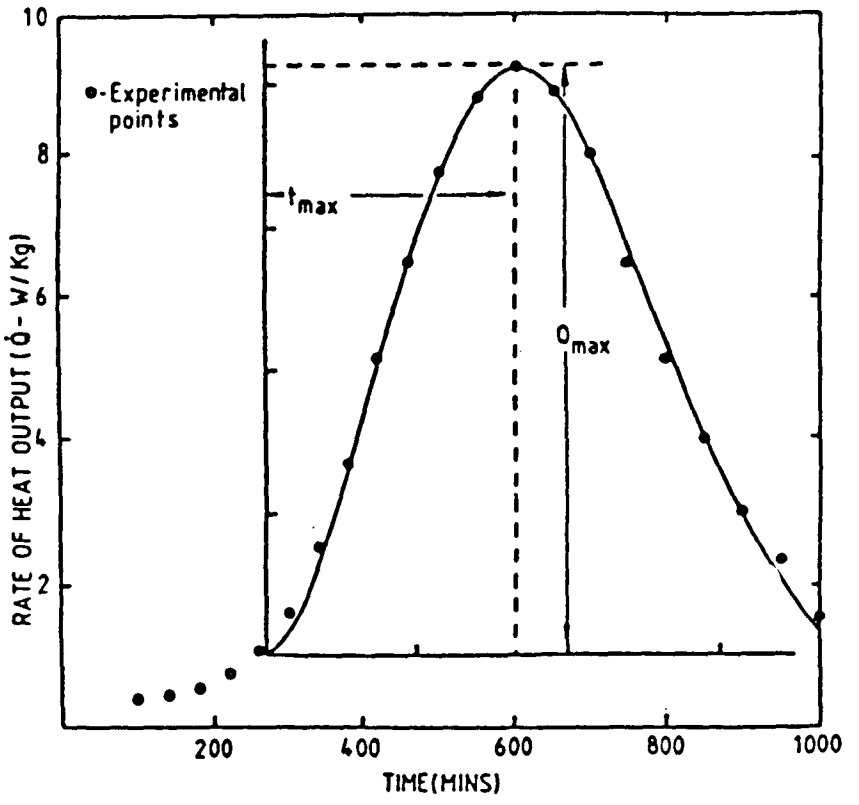

Fig 5.7: An example of the good degree of fit possible of the Avrami equation to a calorimetric curve also showing the offsetting of the origin necessary to obtain the best fit.

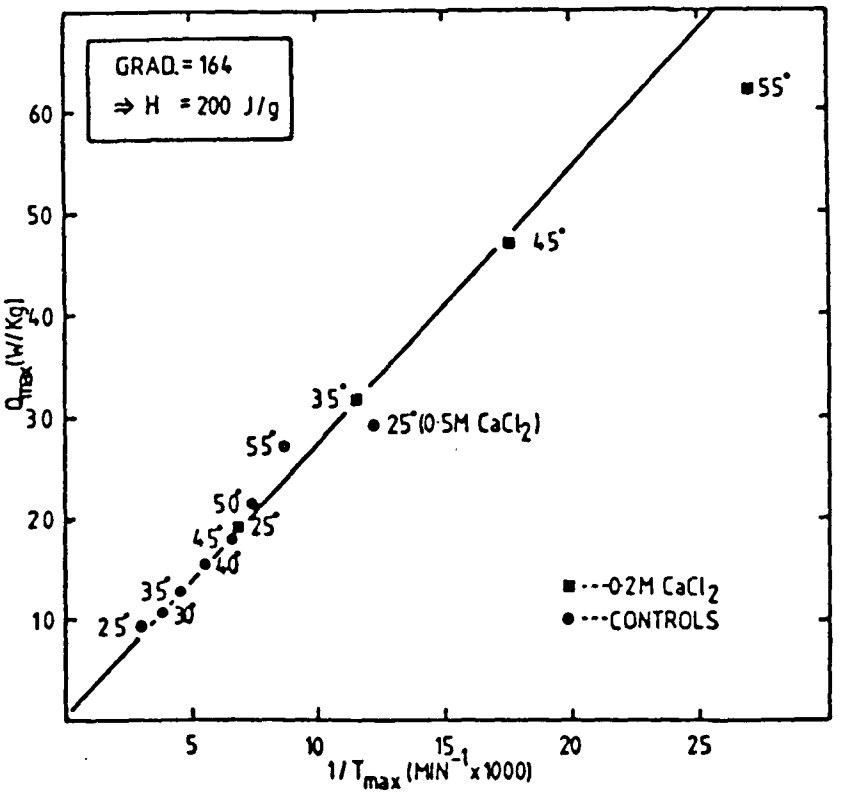

Fig 5.8: Plot of Q_{max} against $1/t_{max}$. The slope of the line gives H as 200 J/g.

The difference in the value of H from that of the total heat of hydration as measured by a heat of solution method (500 J/g - Lea 1970) arises both from the offsetting of the Avrami equation and from the use of the Avrami to describe only a fraction of the total hydration rather than all of it. In effect the fitting procedure uses the Avrami equation to describe that part of the reaction which occurs during the main heat evolution peak after the end of the induction period. The total heat liberated during that time is usually of the order of 250 J/g, which is much closer to the derived value of H, the discrepancy now being due to the heat offset of the origin of the Avrami equation.

When fitting the Avrami equation to the heat output curves of the $CaCl_2$ accelerated samples, the fit obtained is not as good as for the controls. As fig 5.9 shows, the fit is good as far as the peak maximum but deviates progressively at longer time intervals. This effect is also seen on the runs carried out on the $CaCl_2$ accelerated samples at higher temperatures.

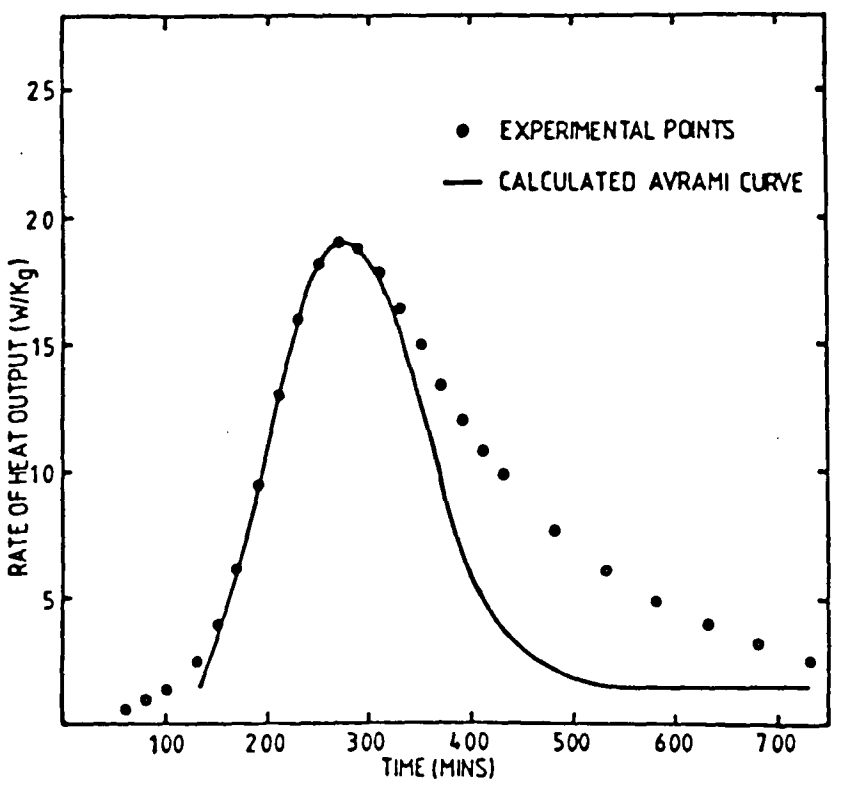

Fig 5.9: Best fit of the Avrami equation to a $CaCl_2$ accelerated curve. Note the deviation at later times.

This deviation at later times has been noted before and is more pronounced the larger the particles that are being used (Tenoutasse & De Donder 1970). The currently accepted explaination is that as the layers of hydrate coating the C_3S grains get thicker, so the reaction takes place by a different process and hence the Avrami equation can no longer be used to account for the measured heat output. For very small particles, the reaction is complete before the layers of hydrate are thick enough for the different reaction to take over. Thus, the larger the proportion of small particles within the sample, the better will be the fit of the Avrami equation to the calorimetric data.

A fit from the Avrami origin to after the maximum in the heat evolution curve can still be obtained in all cases. Hence the plot of Q_{max} against $1/t_{max}$ still holds and the determination of the rate parameter for the various conditions (dependent only on the position and height of the maximum) is still valid.

5.4.c Effect of temperature and accelerating admixture.

The effect of increasing the temperature of hydration is to produce an increase in the rate of heat evolution by variations in the value of K. This type of behaviour is indicative of an activation controlled reaction. For such a reaction the rate constant (k) follows the classical Arrhenius relationship (eqn. 5.16) relating the variations in k to the temperature (in degrees absolute).

$$k = A.\exp\left(\frac{-Ea}{RT}\right) \qquad \ldots 5.16$$

A = Pre-exponential factor

Ea = Activation energy

R = Gas constant

T = Temperture (degrees absolute)

The Arrhenius expression implies that a graphical plot of ln(K) against 1/T should be a straight line of slope -Ea/R. Fig 5.10 shows such a plot for values of the rate parameter K obtained from both the control and the accelerated samples. Good linearity is obtained over the temperature range studied for both control and accelerated samples, the line for the accelerated samples lying rather higher than that for the control. Measurement of the slope of the lines gives the apparent activation energies for hydration as:

Ea (control) = 72 kJ/mol

Ea ($CaCl_2$) = 90 kJ/mol

In order to compare this value with those obtained by other workers it must be recognised that, when applying the Avrami to the hydration of C_3S, previous workers have used a slightly different form of the Avrami equation for the determination of the rate parameter (eqn. 5.17 - c.f. eqn. 5.1).

$$X = 1 - \exp\left(-(K'.t)^n\right) \qquad \ldots 5.17$$

The rate parameter K' in this alternative form of the Avrami equation is therefore related to K, the rate parameter used in this work, through equation 5.18.

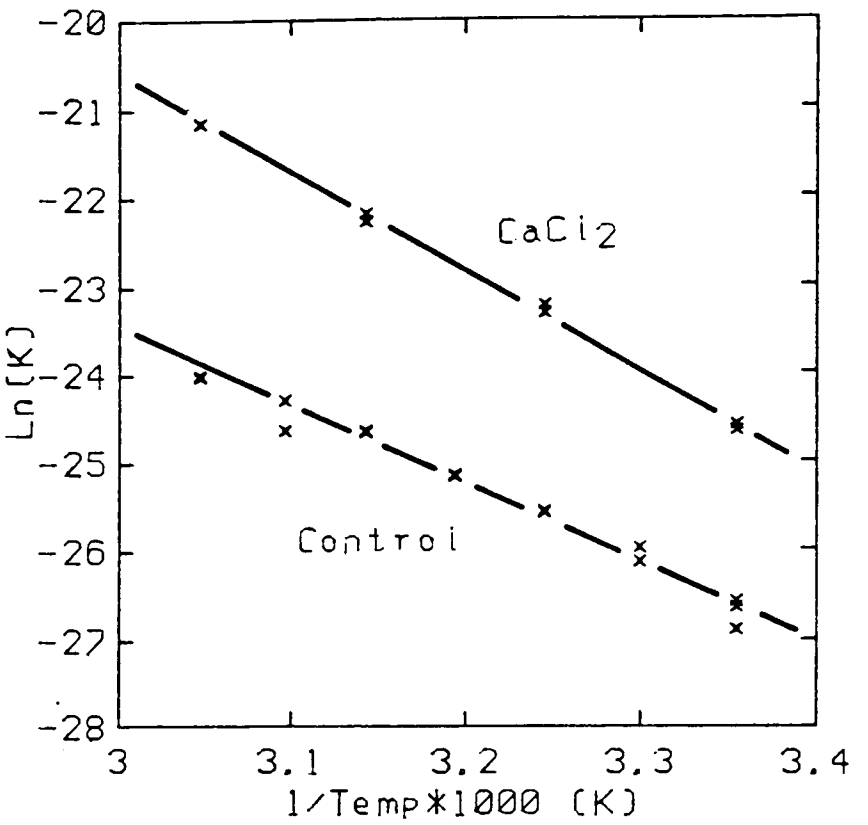

Fig 5.10: Plot of ln(K) against 1/T to illustrate the applicability of the Arrhenius equation and to obtain apparent activation energies for the control and $CaCl_2$ accelerated reactions

$$(K')^n = K \qquad \ldots 5.18$$

The gradient of an Arrhenius plot obtained using values of K', and the value of Ea derived from it, will therefore be n times less than that obtained using K. So, to compare apparent activation energies obtained using the alternative form of the Avrami equation with the apparent activation energies obtained in this work, the former must first be multiplied by 2.5. When this is done reasonable agreement is obtained. For example, calorimetric work by Tenoutasse and De Donder (1970) gave 85 kJ/mol, that of Fierens (1982) gave 115 - 125 kJ/mol, and that of Urzhenko and Usherov-Marshak (1974) gave 81 kJ/mol, all for the apparent activation energy of the hydration of C_3S.

An interesting feature is the slightly higher value of the apparent activation energy for the accelerated samples. A similar result was found

by Tenoutasse and De Donder who obtained an apparent activation energy of 115 kJ/mol for the hydration of C_3S in the presence of $CaCl_2$ at a concentration of 0.3M.

The values of the activation energies determined in this manner have, in the past, been used to argue the case for nucleation being the rate controlling process during the early stages of hydration rather than diffusion. While this may well be so, the rate parameters which the apparent activation energies are derived from are composite constants comprising both nucleation and growth rate terms. Separation of the two would be very difficult, if not impossible, without a very detailed knowledge of the mode of development of the hydration products. In principle this mode of development can be derived from the value of n, but as we have seen, the value of n can not be determined with any accuracy. It is therefore not strictly valid to compare the energies obtained using the Avrami equation with those determined for normal chemical reactions. It is still valid, however, to compare the values for the activation energies obtained for the control samples with those obtained from the accelerated samples; the former being slightly lower. Given the accelerating effect of $CaCl_2$, we can therefore conclude that the increase in rate must arise from increases in the molecular transport and mobility terms which go to make up the pre-exponential factor (A).

5.5 Conclusions

By using the fitting procedure described in this chapter, it has been possible to obtain very reasonable agreement between experimental and calculated data and, using the Arrhenius relationship, to derive an expression predicting the temperature variation in the rate parameter K.

This is useful from a purely empirical point of view in that it allows the prediction of the heat output of the sample of C_3S used in this work at virtually any temperature and also when accelerated with $CaCl_2$ admixture. Using concepts based on this approach, it has been possible to devise a system for the classification of the effect of admixtures on the rate of hydration of OPC (Wilding et al 1984).

In addition, the fact that the Avrami equation fits both accelerated and control data up to the maximum in the rate of heat evolution indicates the possibility that similar processes are occurring in both types of sample, while differences in the temperature variation of the rate parameter between the two types of sample, points to an acceleration by means of increases in the transport terms of the process rather than by a decrease in its activation energy.

However, obtaining a good fit between experimental and calculated data does not necessarily indicate that the process the calculated data derives from actually occurs and, in the case of fitting the Avrami to C_3S hydration data as in this work, even if it was shown to occur, the mechanistic information which could be obtained from the fitting exercise is relatively small. This is because of i) the indeterminacy of the power exponent n which means that conclusions can not be drawn as to the relative rates of nucleation and growth processes and the geometry of growth of the hydrates, ii) the necessity of offsetting the origin of the Avrami equation to obtain a good fit which means that, as the origin can not be calculated, the absolute heat output obtained from the calorimeter can not be calculated directly and iii) the necessity of the assumption that the Avrami equation only accounts for a fraction of the total reaction to obtain a good fit which suggests that the actual process is more complex than has been suggested.

A more realistic approach to the problem of modelling the hydration of C_3S would have been to have used the method of Bezjak et al (eg 1980 a) as described previously (5.1.d) which considers the overall hydration reaction to be a result of several parallel processes rather than as the result of a series of process as has been assumed above. However the method of Bezjak uses the Avrami equation to describe the early part of the reaction and so incorporates most of the above limitations. So, although a better fit may be obtained using their method, as it accounts for most of the deviations at later times (after 1000 minutes), the same restrictions on the derivation of mechanistic information have to be imposed at least during the time when the Avrami equation is supposed to operate. The Avrami equation was therefore chosen for this work as it is much simpler to use than the method of Bezjak et al and, over the time interval of study, gives the same information.

One serous drawback of applying the Avrami equation to describe the hydration of C_3S is that although the effect of surface area on the rate of reaction is incorporated in the rate parameter (K), the effect of changes in the distribution of particle sizes cannot be taken into account. This does not become evident unless the particle size distribution of the sample is deliberately altered in such a way as to make it obvious. Thus if the particle size distribution contains a larger than usual amount of fine material then a shoulder is observed on the acceleratory portion of the heat output curve (Chapter 4, fig 4.8). This therefore brings into doubt the validity of assuming that nucleation and growth processes, as described by the Avrami equation, are the sole contributors to the acceleratory stages of hydration and indicates the need for the development of a new model which takes into account the dependence of the early stages of reaction on particle size as well as the later stages.

CHAPTER 6

CHEMICAL STUDIES OF THE HYDRATION OF C_3S

6.1 Introduction

The hydration of C_3S has often been studied as a model for that of OPC. A large amount of data has been collected concerning the chemical changes which take place during its reaction and various mechanisms have been put forward to explain the observations which have been made. These observations and the mechanisms which have been proposed to explain them are discussed below. Note that much of the background material is taken from Pratt & Jennings (1981), Bensted (1982) and Jennings (1982).

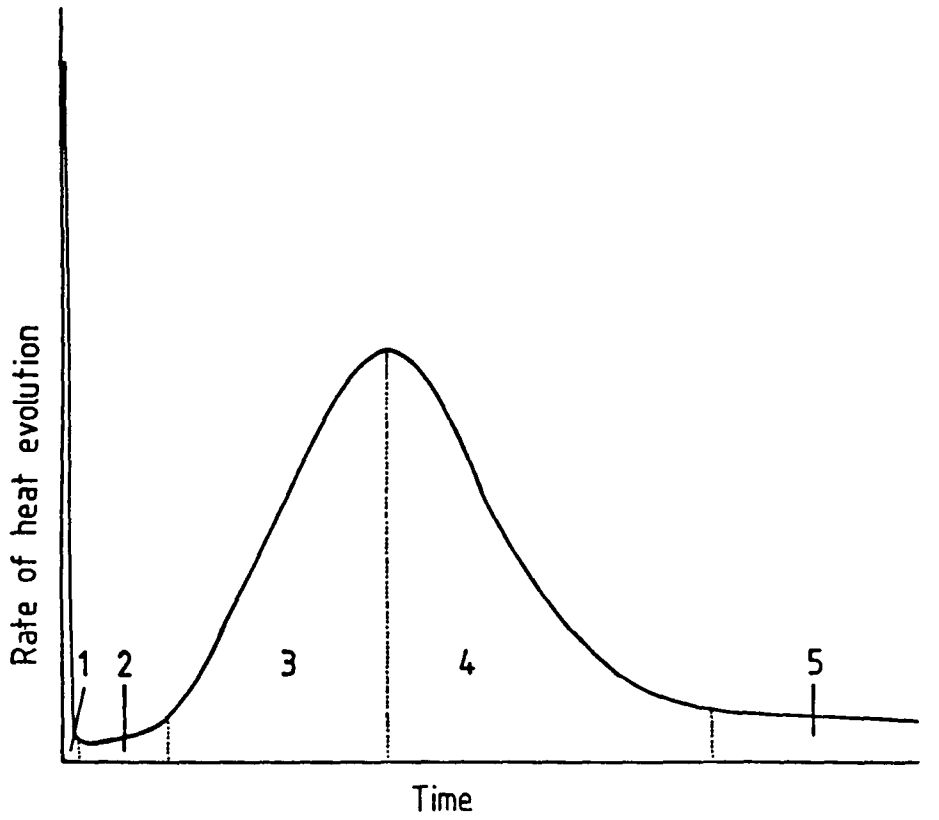

Fig 6.1: Schematic representation of the different stages of hydration of C_3S.

6.1.a Observations

In order to simplify the large amount of data which has been collected over the years, the reaction sequence of C_3S is usually divided up into the five stages indicated in fig 6.1 (Kondo et al 1967). These five stages will be considered in turn.

Stage 1 Addition of water to C_3S wets the surfaces of the particles. This wetting process is exothermic and accounts for much of the heat associated with the first calorimetric peak. Other lesser contributing factors are the dissolution of free lime and the initial reaction of the C_3S. The concentrations of calcium and hydroxyl ions in solution rise rapidly in the first few minutes after mixing. The concentration of silicate in solution during these first minutes also rises rapidly, but only to very small values, and then decreases again (Brown et al 1984). Increasing the w/c ratio is found to increase the maximum level to which the silicate ion concentration rises and decrease the rate at which the calcium ion concentration rises and the final value it attains (Brown et al 1984).

Crystalline calcium hydroxide has been detected during this and the following stages (Menetrier et al 1980) but never in any significant quantities. It is likely that any that is formed is an artifact of drying.

Quantitative X-ray analysis of the residual C_3S and measurement of the non-evaporable water and calcium hydroxide contents (Odler & Dorr 1979 a) have indicated that 1 - 2% hydration occurs during the first heat peak to give a product with a low C/S ratio and high H/S ratio. No direct analysis of this early CSH has been made but recent studies using ESCA (Menetrier et al 1979; Regourd et al 1980) have supported this view. They have shown that the C/S ratio of the C_3S surface falls from 3 to about 2.5 in the first few seconds, increases to nearly three in the next ten or so seconds and then gradually decreases over the next 30 minutes to a value of about 1.5. The initial decrease has been taken to

indicate the formation of CSH with a C/S ratio well below 3 and possibly around 1. More recent evidence (Ball et al 1984) has brought the interpretation of the initial drop in C/S ratio into question by showing that the C/S ratio of the surface of C_3S may not be 3 as had been assumed in the ESCA studies, but might be closer to 2. The ESCA results could then be reinterpreted in terms of dissolution of the surface layer revealing the underlying C_3S, followed by precipitation of CSH of C/S ratio ~1.5.

Stage 2 After a few minutes of fast reaction, a period of very slow activity begins (the dormant or induction period) during which the heat output is very low. Throughout this period the calcium and hydroxyl ion concentrations continue to rise, though at a much slower rate than in stage 1, until (usually) a high supersaturation is reached. Silicate ion concentrations remain very low (of the order of a few parts per million). The length of this stage is highly dependent on a variety of factors. Thus, the extent to which the C_3S has been ground, the presence of impurity ions in its lattice, the manner in which it has been cooled, the extent to which its surface has been hydrated or carbonated by exposure to the atmosphere, the water/cement ratio, the temperature and the presence of admixtures can all affect the length of this period.

Stage 3 The end of the induction period is characterised by (i) the beginning of the second (main) heat evolution peak, (ii) a rapid increase in the rate of the formation of CSH together with changes in its morphology, (iii) attainment of a maximum in the concentration of calcium ions in solution and (iv)

crystallisation of $Ca(OH)_2$ in large amounts to give relatively large crystals. These events do not all occur simultaneously, but the order in which they do occur is not generally agreed. Throughout this stage and the following two, the C_3S grain gradually diminishes in size and CSH is precipitated in the space left by the receding grain (giving 'inner' product) as well as in the pore spaces (giving 'outer' product). QXDA, EMPA, EDXA, chemical extraction and TGA studies to determine the C/S ratio of the CSH show a wide variation in results (Locher 1966; Odler & Skalny 1973; Diamond 1976; Goto et al 1976; Dent Glasser et al 1978; Odler & Dorr 1979 b; Taylor & Newbury 1984). A value of about 1.7 seems to be about the average. There is also evidence that the C/S ratio of the CSH changes during hydration. Trimethylsilylation and magic-angle NMR (Mohan & Taylor 1982; Lippmaa et al 1982; Hirljac et al 1983; Clayden et al 1984) have indicated that the hydrated silicate species in CSH during this stage consist solely of dimeric (Si_2O_7) units.

Stage 4 Eventually the rate of reaction falls off once more as a result both of the increased difficulty of transportation of reactants and products to and from the reaction interface, and of the filling of the available space for the hydration products.

Stage 5 The reaction continues at a much reduced rate for a period of weeks or months during which time the process becomes purely diffusion controlled. The process of infilling of the pore spaces continues and the paste gets harder and stronger. The CSH produced appears to have the same C/S ratio as that produced during stages 3 and 4 but its silicate structure gradually alters as it gets older. For periods up to 3 days only dimers (Si_2O_7

units) have been detected, while longer periods allow the formation of polymeric species. This process continues long after the reaction of the C_3S is virtually complete. The change is slow and even after several years, 40% of the silicate is still present as dimer.

6.1.b Proposed mechanisms

Several mechanisms for the hydration of C_3S have been proposed to account for the observations described above. In most cases these mechanisms only apply to a limited portion of the reaction sequence, particular attention having been paid to attempting to explain the low reactivity during the induction period and the sudden rise in reactivity at its end.

6.1.b.i Stage 1

Analysis of the liquid phase during stage 1, and at high w/c ratios, has suggested that ions dissolve congruently from the surface (Fierens & Verhaegen 1976 b; Tadros et al 1976; Barret & Menetrier 1980; Barret et al 1980, 1983; Brown et al 1984). Barret et al have proposed the following sequence of events to occur on initial contact of C_3S with water.

i) Protonation of the oxide and orthosilicate ions on the C_3S surface to give OH^- and $H_3SiO_4^-$ ions respectively. This process is very rapid and causes the surface to become superficially hydroxylated. An equivalent quantity of OH^- remains in the solution.

ii) Passage of Ca^{2+} ions from the C_3S surface into solution until charge balance is reached.

iii) Passage of the remaining Ca^{2+} ions and the hydroxyl and hydrosilicate ions into solution. This is the most difficult of the three processes as the cations and anions cannot move independently. A new surface is now exposed and the sequence repeats itself.

When the concentrations in solution exceed the solubility limit of CSH, it precipitates. The C/S ratio of this product is lower than 3 which accounts for the build up in the calcium ion concentration in solution.

These observations fit in with an analysis of the situation in terms of the CaO-SiO_2-H_2O ternary phase diagram (fig 6.2). This indicates that, if congruent dissolution does occur, then both calcium and silicate ion concentrations will rise until point A is reached. The solution concentration will then follow the path indicated by the arrows, the calcium ion concentration rising and the silicate ion concentration falling, and CSH with a C/S ratio dependent on the solution composition will precipitate out. When the invariant point (B) is reached, $Ca(OH)_2$ should begin to precipitate out together with CSH of a fixed composition and the solution composition should remain steady. In practice, solution compositions in C_3S pastes do generally lie along the line AB but the calcium ion concentration continues to rise after point B is reached taking the solution into the supersaturated region C.

At lower, more realistic w/c ratios, only very low concentrations of silicate ions are detected (Fujii & Kondo 1975; Young et al 1977; Skalny & Young 1980; Thomas & Double 1983; Brown et al 1984) together with much higher calcium ion concentrations. Under these conditions it is suggested that congruent dissolution can not occur and that instead the formation of CSH occurs directly at the C_3S-water interface without the need for dissolution followed by reprecipitation.

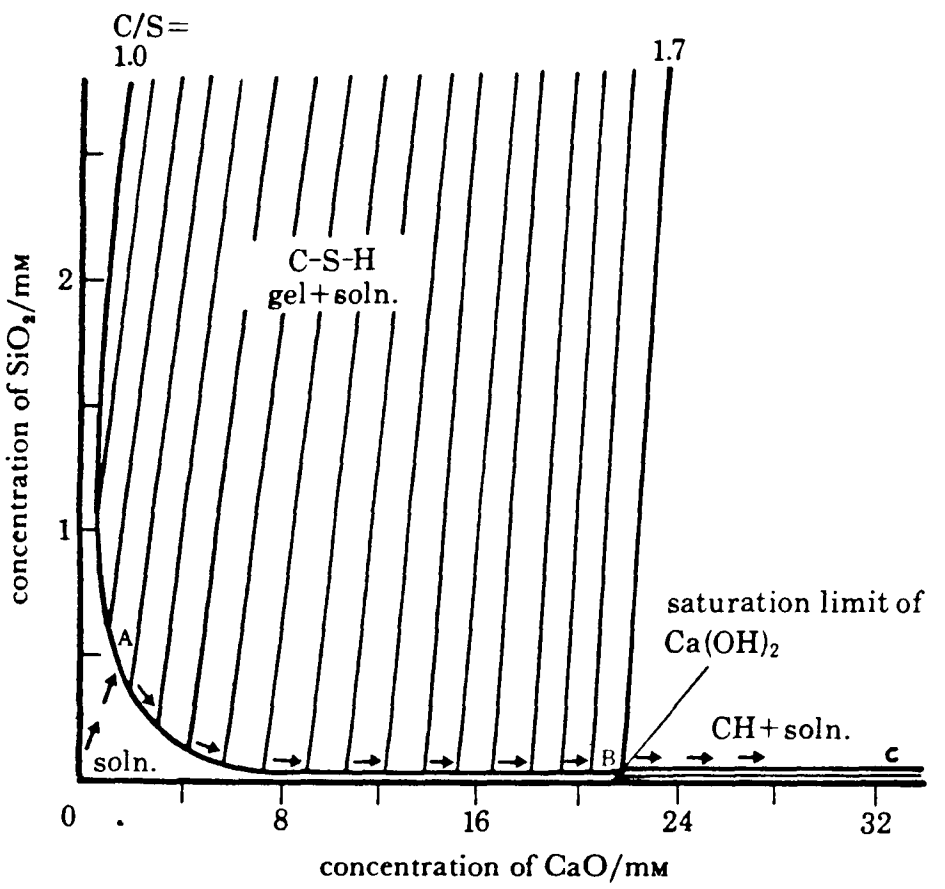

Fig 6.2: General form of the solubility diagram for the ternary $CaO-SiO_2-H_2O$ system at room temperature (based on Flint & Wells 1934).

6.1.b.ii Stage 2 and the start of stage 3

The mechanisms which have been formulated to explain the presence of the induction period and the reasons for it ending may be classified into two broad groups: (i) those that consider the induction period to be brought about by the formation of some kind of protective layer on the surface of the C_3S and (ii) those that consider it to be caused by the delayed nucleation of $Ca(OH)_2$ and/or CSH.

Protective layer theories

Stein & Stevals (1964) and Stein (1977) proposed the successive formation of three different hydrates. The first of these has a C/S ratio of 3 and forms within minutes as a somewhat impervious coating. This retards further reaction of the C_3S and causes the diminished heat evolution and the decreased rate of release of calcium ions. The first hydrate is converted into a second of lower

C/S ratio (~0.8-1.5) with a thin film morphology of greater permeability than the first. The greater permeability of this second hydrate allows the diffusion of ionic species to and from the C_3S surface initiating renewed reactivity and hence ending the induction period. The second hydrate is subsequently transformed into a fibrous third hydrate with a C/S ratio of ~1.5-2.0. The convertion of the first hydrate into the second is a nucleation and growth process and is accelerated under conditions where calcium and hydroxyl ion concentrations are kept low. The observed decrease in calcium ion concentration and increase in crystalline $Ca(OH)_2$ is therefore assumed to be a result of the changes taking place at the end of the induction period rather than the cause of them.

Similarly, Kantro et al (1962) and Brunauer & Kantro (1964) suggest that a protective membrane with a low surface area and high C/S ratio forms during stage 1 and that this converts, with the removal of calcium ions, to a second product of higher surface area and lower C/S ratio. This second product exfoliates and so is no longer protective.

Magnan et al (1974) have considered how the transformation from a first to a second hydrate might occur. They suggest that as calcium ions continue to dissolve from the first hydrate, isolated silica tetrahedra are left which subsequently polymerize into a gel to form a second hydrate. Further reaction with lime stabilises the product.

In a reformulation of the theory first suggested by Powers (1961), Double et al (1978, 1980) and Birchall et al (1978, 1980) independently proposed that the induction period was caused by the formation of a semipermeable membrane around the cement grains which

prevented the diffusion of silicate species into the bulk of the solution but allowed calcium ions and water to pass freely through. Osmotic pressures are presumed to build up inside the membrane which eventually ruptures forming tubular growths by analogy with those formed in silicate gardens (Coatman et al 1980). The renewed reaction following the rupture signals the end of the induction period. The evidence for the mechanism is taken from 'in situ' high voltage electron microscopic studies of wet Portland cement grains contained in an environmental cell which enabled direct observation of a membrane around the grains and formation of tubular growths. As these observations were obtained from studies of Portland cement and subsequent studies have indicated that tubular growths are only formed when substantial amounts of aluminium and sulphate ions are present (Barnes et al 1980), there is some doubt as to whether the osmotic mechanism applies to the hydration of C_3S alone, though Double (1981) points out that tubules are only one of a variety of different growth morphologies which might be expected from an osmotic mechanism and that the absence of tubular growths in the case of C_3S does not necessarily imply that an osmotic mechanism is not operating. A similar study by Jennings & Pratt (1979) on C_3S indicated the formation of a membrane, but suggested that the end of the induction period arose from the disruption of the membrane by nucleation of $Ca(OH)_2$ on its surface rather than as a result of osmotic effects.

Fujii & Kondo (1974, 1975) suggested that in stage 1, two types of reaction occur: (i) congruent dissolution and precipitation and (ii) the formation of a skin, involving 3-4 molecular layers of water, on the surface of the grain. The skin forms a protective layer and is

disrupted when supersaturation of the aqueous phase is high enough for CSH to nucleate on the surface of the C_3S grains.

Delayed nucleation theories

Young (1972) has assumed the induction period to be simply a period of slow dissolution of C_3S. Initial hydration releases calcium and hydroxyl ions into solution giving a C_3S surface deficient in Ca^{2+}. Calcium ions chemisorb on this to make it positively charged. Further hydration is retarded by the high calcium ion concentration in the interfacial region, which results in a solution rich in calcium and hydroxyl ions until sufficient supersaturation accumulates to give stable calcium hydroxide nucleii. The presence of silicate ions in solution retards the nucleation and growth of $Ca(OH)_2$, hence the high supersaturation which is reached. Once $Ca(OH)_2$ nucleates, the end of the induction period is reached as the ions precipitating from the aqueous phase act as sinks for other ions in solution which in turn encourages further dissolution and reaction of C_3S. Since the $Ca(OH)_2$ crystals incorporate silicate ions, they may also act as nuclei for CSH formation.

Odler and Dorr (1979 a & b) also argue that the calcium ion concentration is important in determining the length and eventual end of the induction period. They agree with the formation of first (low C/S ratio) and second (higher C/S ratio) hydrates but propose that the second cannot form in any appreciable amounts without a sink for calcium ions being present. Once it has started to form it produces both solid and amorphous $Ca(OH)_2$ which acts as a seed for further $Ca(OH)_2$ formation.

Tadros et al (1976) suggest that chemisorption of calcium ions forms a surface barrier rather than a precipitated product. The formation of $Ca(OH)_2$ and CSH nuclei act as sinks for calcium and silicate ions which disrupts the barrier and allows the ions to rapidly dissolve and precipitate as product.

Fierens and co-workers (Fierens 1976; Fierens & Verhaegen 1974, 1976 a & b), from considerations of the defect structure of C_3S, have deduced that the induction period is the result of a potential barrier corresponding to the critical size of CSH nuclei on the surface of C_3S. When the CSH nuclei achieve their critical size the induction period ends and the nuclei begin to grow according to the laws of nucleation kinetics. Lattice defects, introduced by heating, quenching or grinding reduced the induction period by providing a greater number of highly nucleophilic sites for nuclei to grow on. The concept of a protective layer was considered not to fit in with this observation. It was assumed that a protective layer would not be influenced by the concentration of defects and hence, any protective layer theory could not account for the observed changes in reactivity as a result of changes in the defect structure of the C_3S.

6.1.b.iii Stages 3, 4 and 5

Rather less work has been carried out on determining the chemical processes which occur after the end of the induction period. During these final stages CSH is being precipitated at the C_3S/CSH and CSH/pore-space interfaces simultaneously. It is therefore possible that (i) reaction is occurring at both interfaces, (ii) reaction is occurring at only one and material is somehow transported to the other site and (iii) the reaction occurs somewhere in mid-region as the reactants come

into contact. The first of these is the generally accepted view (Taylor 1979) but the second, with the reaction occurring at the C_3S/CSH interface, has been proposed by Jennings et al (1981).

6.1.c Effect of admixtures on the hydration of C_3S.

The effect of admixtures on the reactivity of C_3S and OPC has been extensively studied (Stein 1961; Taplin 1962 a; Edwards & Angstadt 1966; Previte 1971; Kantro 1975; Wilding et al 1984). The mechanism of their action is not known and it is possible that different types of admixture alter the mechanism of the hydration in different ways.

In this study the effect of $CaCl_2$ and sucrose on the rate and stoichiometry of the hydration of C_3S was investigated.

The mechanism of acceleration by $CaCl_2$ is not known though it has been suggested that (i) it is due to the formation of a complex oxychloride, (ii) $CaCl_2$ acts as a catalyst altering the pH of the solution phase, (iii) Chloride ions form a surface complex which gets incorporated into the gel in the later stages of the reaction. Studies on the effect of $CaCl_2$ on the hydration of C_3S have found that increasing concentrations of $CaCl_2$ increase the C/S ratio of the CSH produced (Ramachandran 1971 a, b). Investigation of the pore size distribution and microstructure of the hydrate (Skalny et al 1971, Young et al 1973) have indicated that both are altered by the presence of $CaCl_2$.

Very little work has been carried out concerning the influence of sucrose on the rate and chemistry of the hydration of C_3S though rather more has been reported for its effect on the reactivity of OPC. Most explanations for the way in which sucrose retards the hydration involve either adsorption and poisoning of hydrate surfaces (Young 1972) or precipitation of an insoluble saccharate which coats the grains and

prevents further reaction (Suzuki & Nisha 1959; Forsen 1938). A recent study (Thomas & Birchall 1983) has shown that an adsorption and poisoning effect is responsible for the abnormally high concentrations of soluble species which builds up in the presence of saccharides.

6.1.d Extent of this study.

This chapter studies the chemical changes which take place during the hydration reaction and investigates the effect of acceleration by $CaCl_2$ and retardation by sucrose on those chemical processes. Quantitative X-ray diffraction analysis (QXDA) and thermogravimetric analysis (TGA) were used to provide two independent methods of measuring the formation of products and disappearance of reactant during the hydration reaction and the results of these methods are compared with each other and with those obtained by other workers.

6.2 Experimental

100 gram samples of preparations B_1, B_3 and C_2 were used in this work. The compositions of these preparations have already been given (chapter 3). Table 6.2 lists their respective particle size distributions.

Diameter (microns)	Cumulative wt% undersize		
	B_1	B_3	C_2
1.0	8.2	4.5	5.3
1.5	9.3	4.7	5.9
2.0	10.5	4.7	6.7
3.0	11.2	4.7	6.7
4.0	16.2	5.0	8.2
6.0	32.8	6.1	15.1
8.0	50.5	12.1	27.7
12.0	71.5	33.8	50.2
16.0	80.5	56.7	66.9
24.0	88.0	81.4	82.3
32.0	91.5	90.7	90.4
48.0	97.8	97.4	97.2
64.0	99.3	99.7	99.0

Table 6.2: Particle size distributions of B_1, B_3, C_2

Three experiments were carried out:

i) Sample B_1 hydrated with distilled water (control)

ii) Sample B_3 hydrated with 0.2 M $CaCl_2$ ($CaCl_2$ accelerated)

iii) Sample C_2 hydrated with 0.005 M sucrose (sucrose retarded)

Each 100 gram sample was made into a paste at a w/c ratio of 0.5 using the solutions indicated above and divided equally among about 25 glass containers. These were immediately sealed and stored in a constant temperature waterbath at 25 degrees. During this procedure care was taken to minimise the contamination by atmospheric carbon dioxide by flushing the surroundings, sample containers and reaction vessel with dry nitrogen.

At intervals one of the glass containers was withdrawn from the waterbath and the reaction quenched by injecting isopropanol through the cap. The sample was then dried by evacuation in a dessicator and stored over freshly dried silica gel. Material was withdrawn from this as needed for the TGA and QXDA studies. (Note the same samples were used for the SEM study described in chapter 7.)

6.3 Methods of investigation

A trace of the rate of heat output as a function of time was obtained for each sample prior to its being hydrated as described above. This provided an indication of the times at which the important stages of the reaction were occurring and was used to decide when to quench each specimen.

TGA was carried out on 10 mg samples using a Stanton Redcroft thermobalance programmed to heat the sample at a rate of 5 degrees a minute from room temperature to 1000 degrees in an atmosphere of dry nitrogen flowing at a rate of 25 ml/min.

QXDA samples were prepared by milling 2g of sample with exactly 20% of the sample weight of rutile to a particle size of less than 5 microns. X-ray data were obtained by step counting from 24 to 39 degrees 2-theta for 20 secs at intervals of 0.05 degrees using monochromatic copper K-alpha radiation.

6.4 Analysis of results

6.4.a Thermogravimetric data

Fig 6.3 shows a typical trace of weight loss as a function of temperature for a sample of C_3S hydrated for 144 hours under the conditions stated. The three weight losses of interest in this study (w_1, w_2, w_3) are indicated and are:

w_1) The total loss in weight from room temperature to 1000 degrees.

w_2) The loss in weight associated with the decomposition of $Ca(OH)_2$

w_3) The loss in weight associated with the decomposition of $CaCO_3$

The average of three runs was taken for the control and $CaCl_2$ accelerated samples while the average of two was taken for the sucrose retarded sample. Any weight loss due to $CaCO_3$ decomposition was converted to the equivalent weight due to $Ca(OH)_2$ decomposition and added to that already measured.

$$w_2' = w_2 + 0.409.w_3 \qquad \ldots 6.1$$

If the weight of the sample after heating to 1000 degrees is W then the wt% of combined water (W_h - defined as the water which can be removed by heating from room temperature to 1000 degrees) is given by:

$$W_h = 100.w_1/W \qquad \ldots 6.2$$

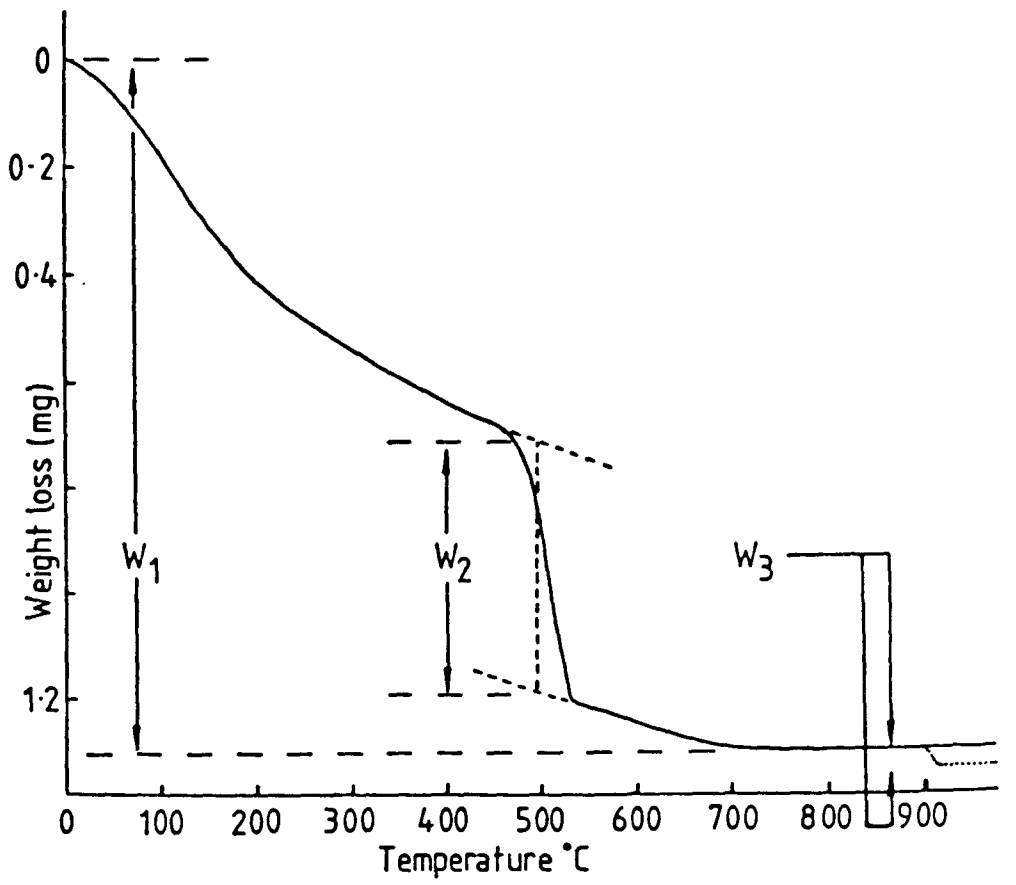

Fig 6.3: Typical TGA trace of weight loss as a function of temperature for a hydrated sample of C_3S. Note that no weight loss due to Ca(CO)3 decomposition was detected in this sample.

and the wt% of $Ca(OH)_2$ (W_c) is given by:

$$W_c = 100.w'_2 / W \qquad ...6.3$$

6.4.b X-ray data

The X-ray data were analysed to find the proportions of C_3S, $Ca(OH)_2$ and $CaCO_3$ contained in each sample. This was achieved using a computer program developed by Gutteridge & Flower at the Cement & Concrete Association, Slough. The method (Gutteridge 1984) involves:

1) Collection of primary standard data for each of the constituent compounds (including each separate preparation of C_3S) and rutile. Primary standard data are collected in two parts. First using the material itself (PS) and second using a mixture obtained by grinding the material with 20% rutile (PSG). Background data are removed and the PSG data are aligned by determining the position of the (110)

rutile peak and interpolating the entire data set until the (110) peak position is at 27.461 (+/- 0.0005) degrees 2-theta. The data are then multiplied by a factor chosen to enable plotting on a suitable scale. The data set from the rutile standard material is aligned and scaled in the same way. Alignment of the PS data then consists of matching the PS and rutile data to that of the PSG data. The data are normalised using the (110) diffraction of the rutile internal standard material.

2) Collection of sample data (as described in section 6.3)

3) Alignment and normalisation of sample data in the same manner as for the PSG material.

4) Assumption that the intensity measured at each data point for the sample material is the sum of the intensities of the constituent compounds at that point multiplied by their weight fraction plus a background term.

5) Description of the background in terms of a polynomial of degree chosen by the operator (3 or 4 was found to work best in this work) and calculation of the background contribution at each point.

6) The setting up and solving of linear equations involving the background term and the sum of the intensities of the constituent compounds multiplied by their respective weight fractions for each point using a least squares method to give the weight fractions of the constituent compounds.

A reliability factor giving a measure of the degree of fit of the calculated to the experimental data is calculated. For hydrated Portland cement analyses a value of less than 0.01 usually constitutes a reliable

fit. For hydrated C_3S analyses the number of constituents is fewer and a better fit is expected.

In this work values of the reliability factor from 0.0005 to 0.0030 were found which were considered to be quite adequate. Overall, the method should be capable of providing analyses of the constituent compounds in a sample of C_3S to better than 1 wt%.

The above method of analysis gave the weight of C_3S remaining, and $Ca(OH)_2$ formed, as a percentage of the weight of the sample. In this case the weight of the sample includes the weight of combined water. Thus these wt% values are not equivalent to those calculated from the TGA data which are a ratio of the weight of the sample at 1000 degrees when all combined water has been driven off. To make the wt% values equivalent those measured by QXDA were multiplied by the ratio of the weight of material at room temperature to that at 1000 degrees (calculated from the TGA data).

6.5 Results

6.5.a Calorimetry

All three samples gave characteristic heat evolution curves, showing an initial fast reaction followed by the usual induction, acceleratory and deceleratory stages. The curves for the three samples are given in fig 6.4 while fig 6.5 shows their respective integrated heat output curves.

Figs 6.4 and 6.5 illustrate the classic acceleration effect of the $CaCl_2$ and retarding effect of the sucrose. Acceleration leads to a shorter induction period, higher peak maximum occurring at a shorter time and larger overall degree of hydration reflected in the larger total heat output after 1000 minutes, while retardation leads to a longer induction

period, lower peak maximum occurring after a longer time and a lower total heat output.

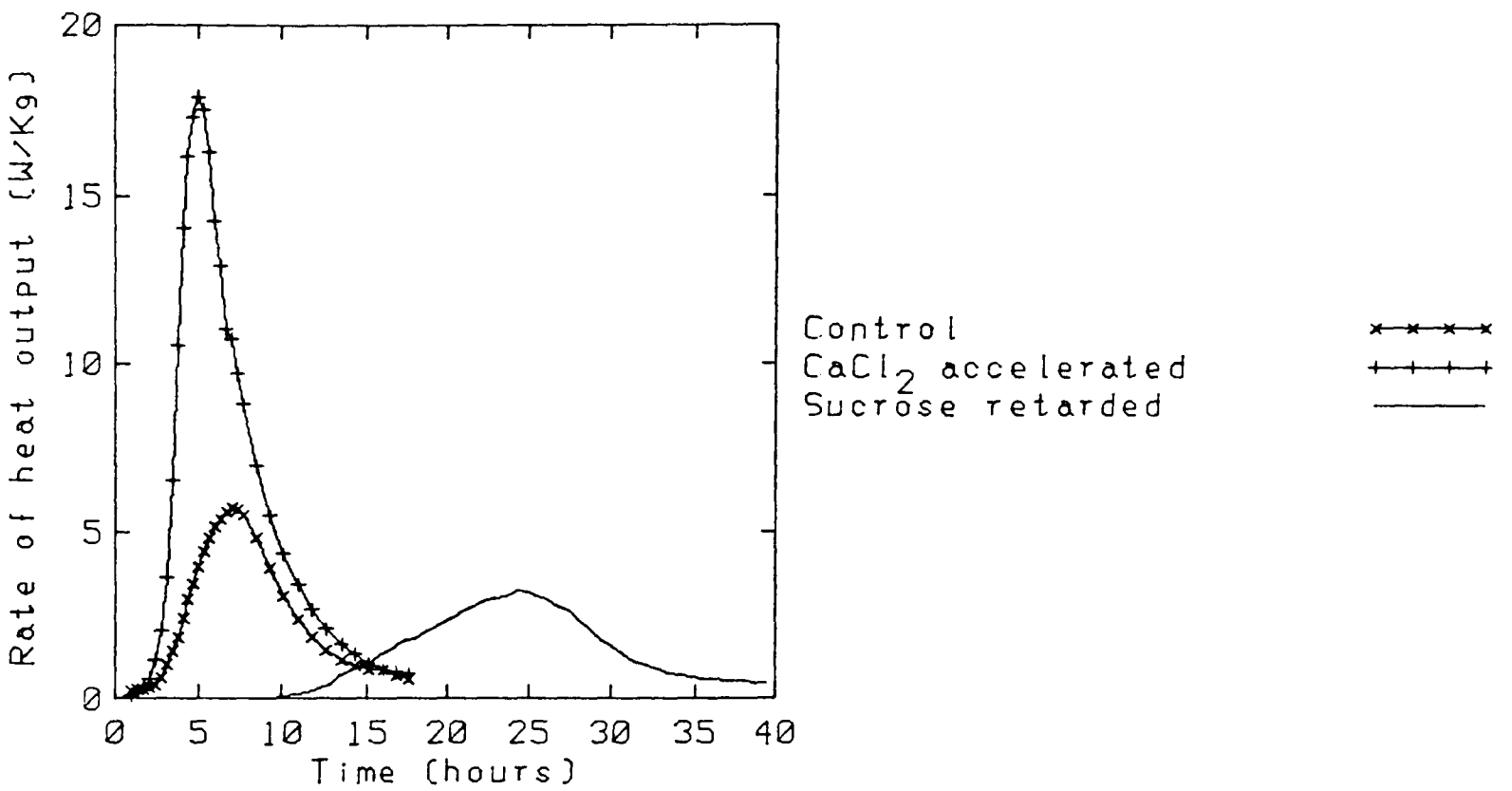

Fig 6.4: Rate of heat output curves for the control, accelerated and retarded samples obtained by calorimetry.

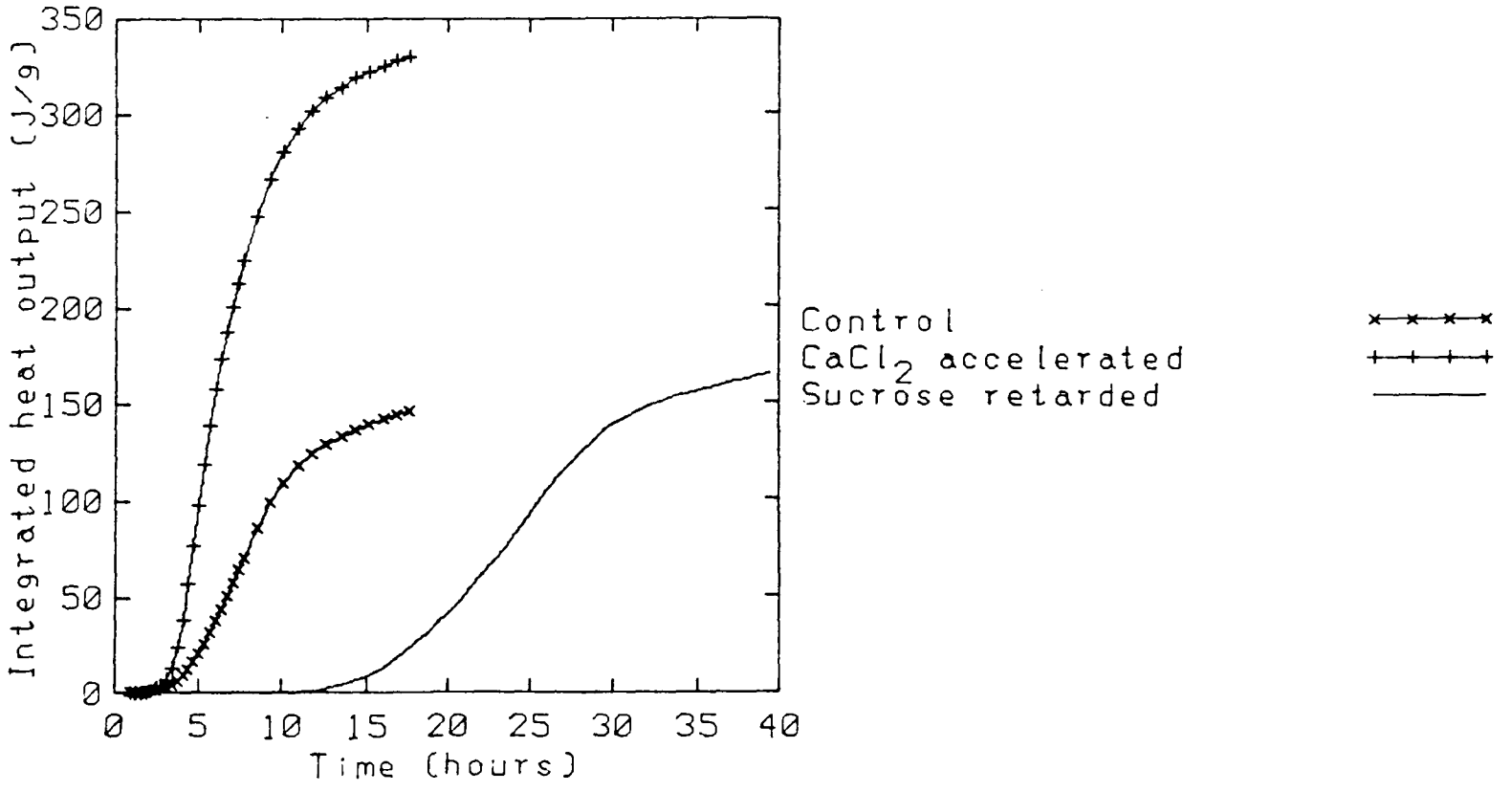

Fig 6.5: Integrated heat output curves for the control, accelerated and retarded samples.

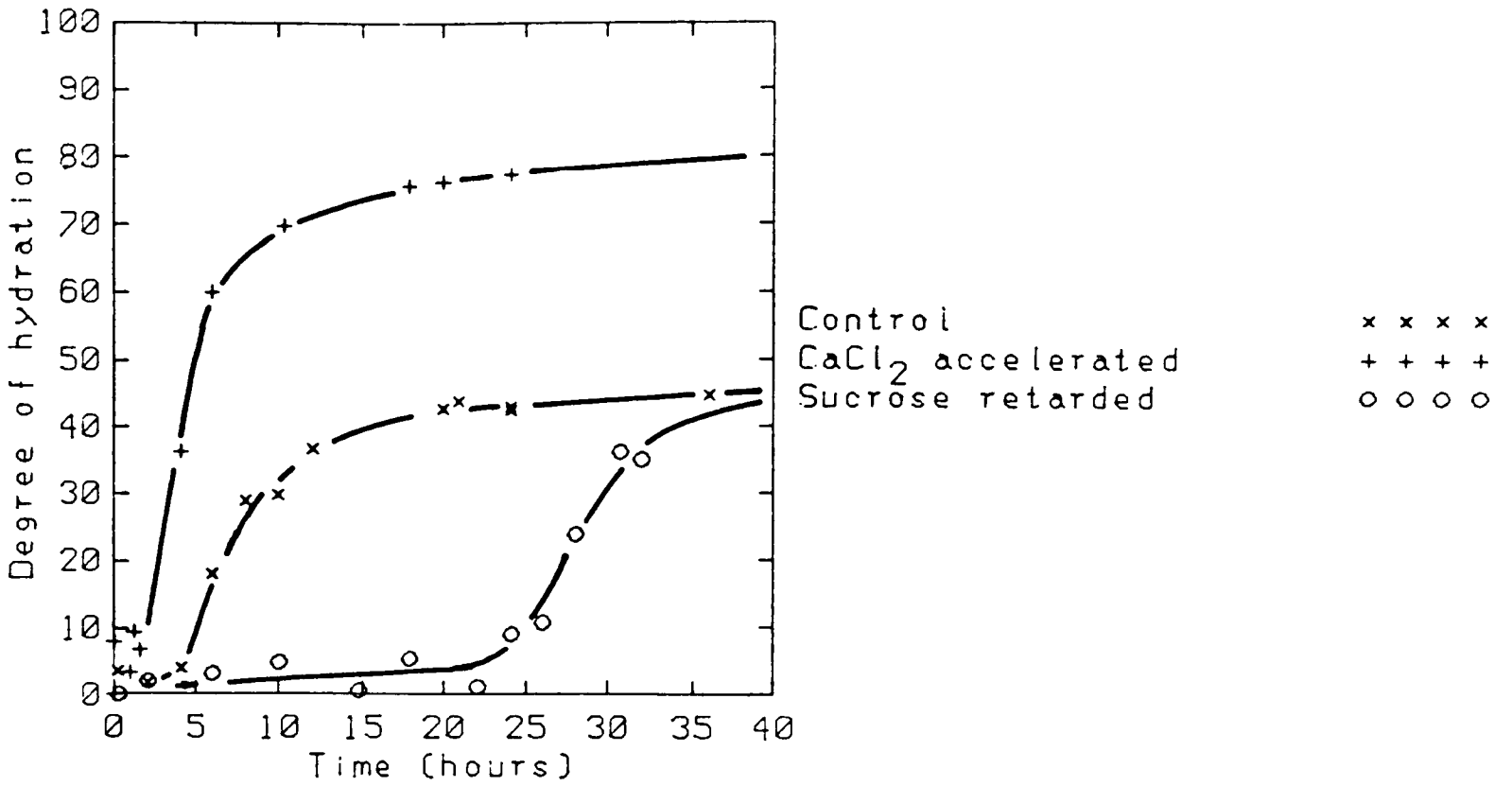

(a)

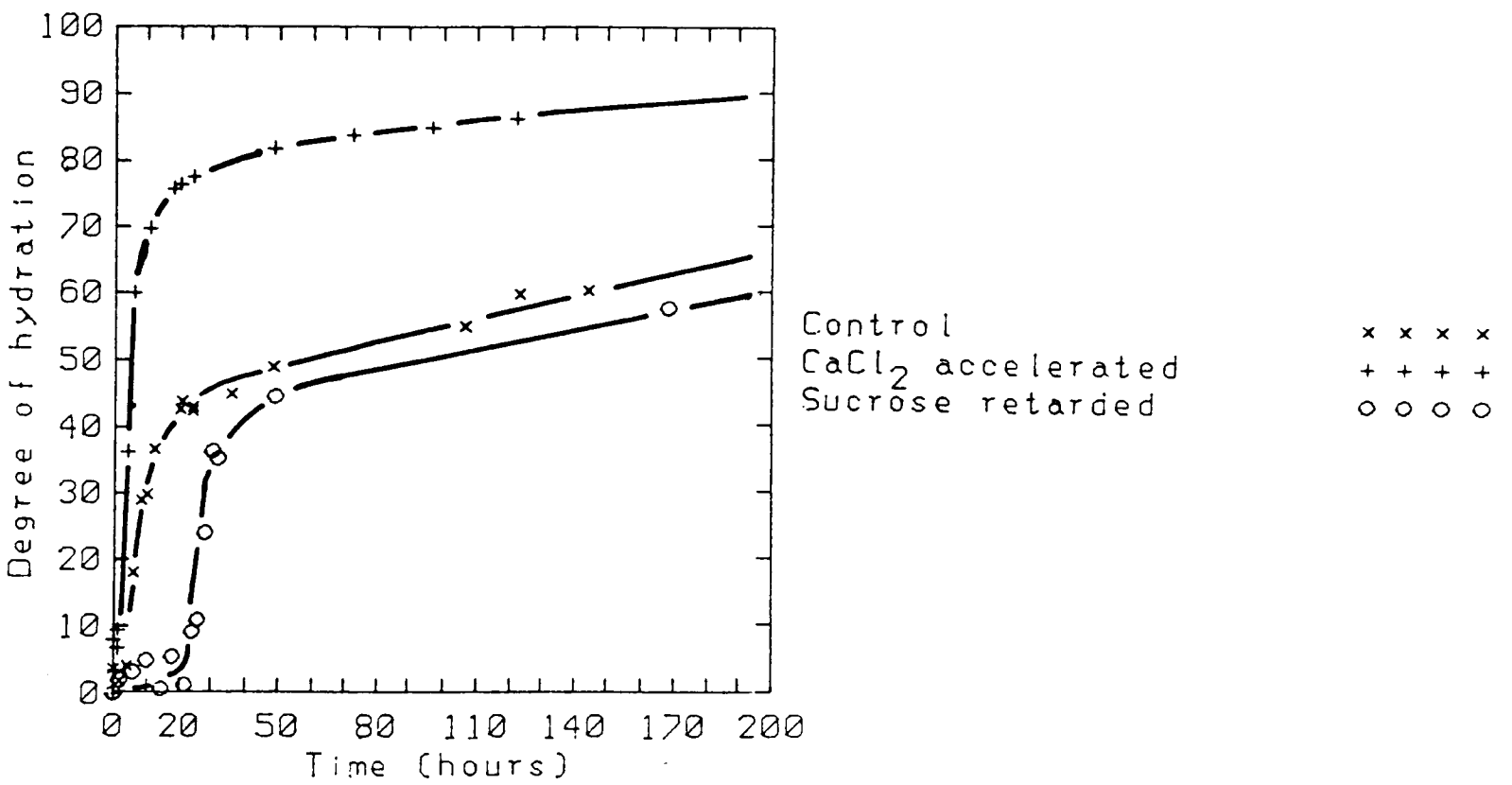

(b)

Fig 6.6: Comparison of the effects of $CaCl_2$ and sucrose on the change in the degree of hydration of C_3S with time. (a) The first 40 hours, (b) the first 200 hours.

6.5.b Phase Analysis

The increase in degree of hydration (measured by QXDA and adjusted for the water content of the samples) with time for the three samples is illustrated in fig 6.6. The degree of hydration, while being difficult to measure accurately during the initial stages of reaction (fig 6.6 a), does show a sigmoidal rise of a very similar shape to the integrated area under the calorimetric curve (fig 6.5).

The independent measurements of the $Ca(OH)_2$ contents of the various samples by QXDA and TGA are compared in fig 6.7. For all three samples the $Ca(OH)_2$ measured by the two methods is very nearly equivalent.

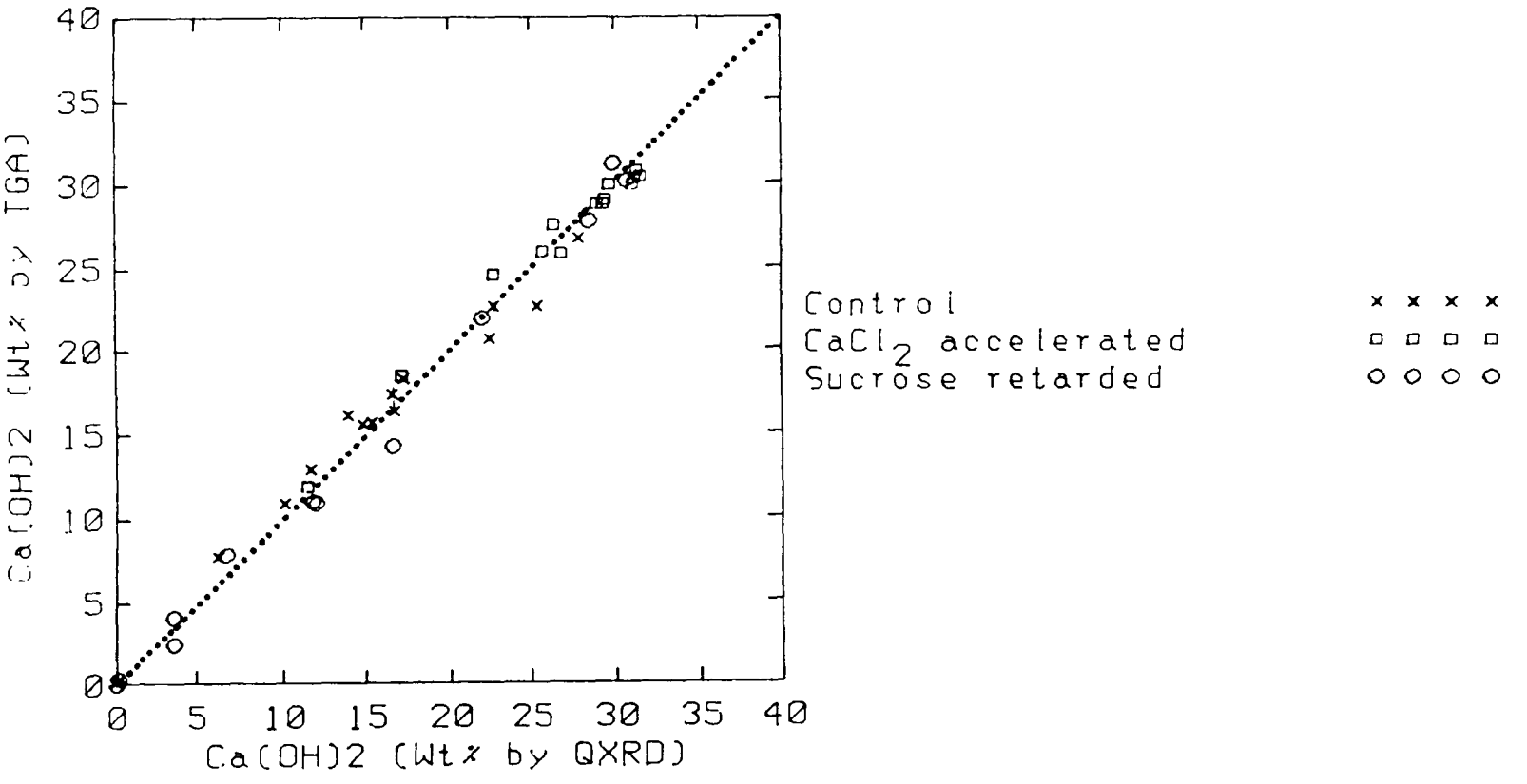

Fig 6.7: Correlation between the measurement of $Ca(OH)_2$ by QXDA and that by TGA. The dotted line indicates the line of 1:1 correlation.

The way in which the $Ca(OH)_2$ and combined water contents of a sample vary with its degree of hydration is important in understanding the hydration mechanism and determining the stoichiometry of the hydration reaction. In this study linear relationships were obtained for both the $Ca(OH)_2$

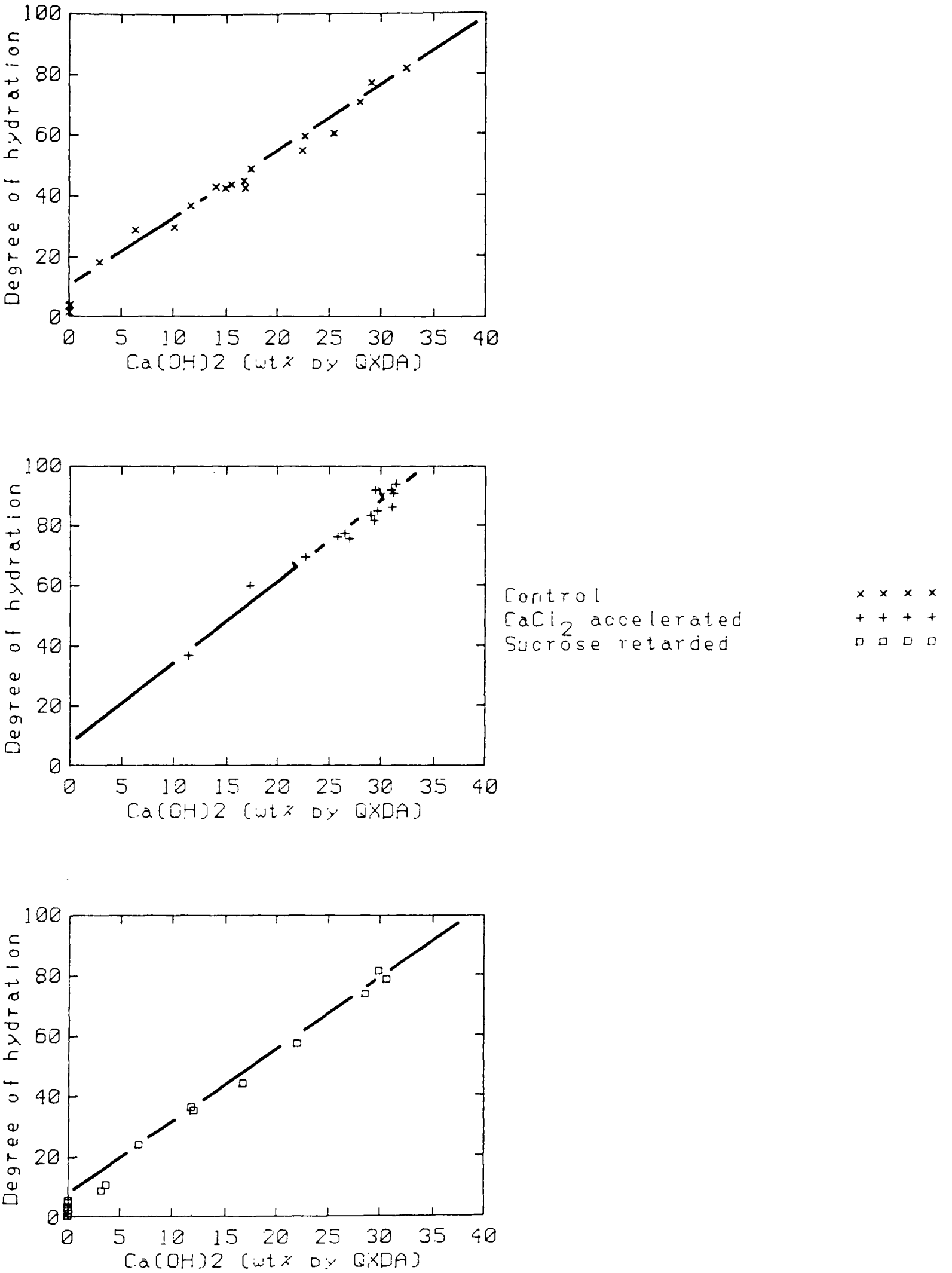

Fig 6.8: Variation of the $Ca(OH)_2$ content of the three samples with their degree of hydration.

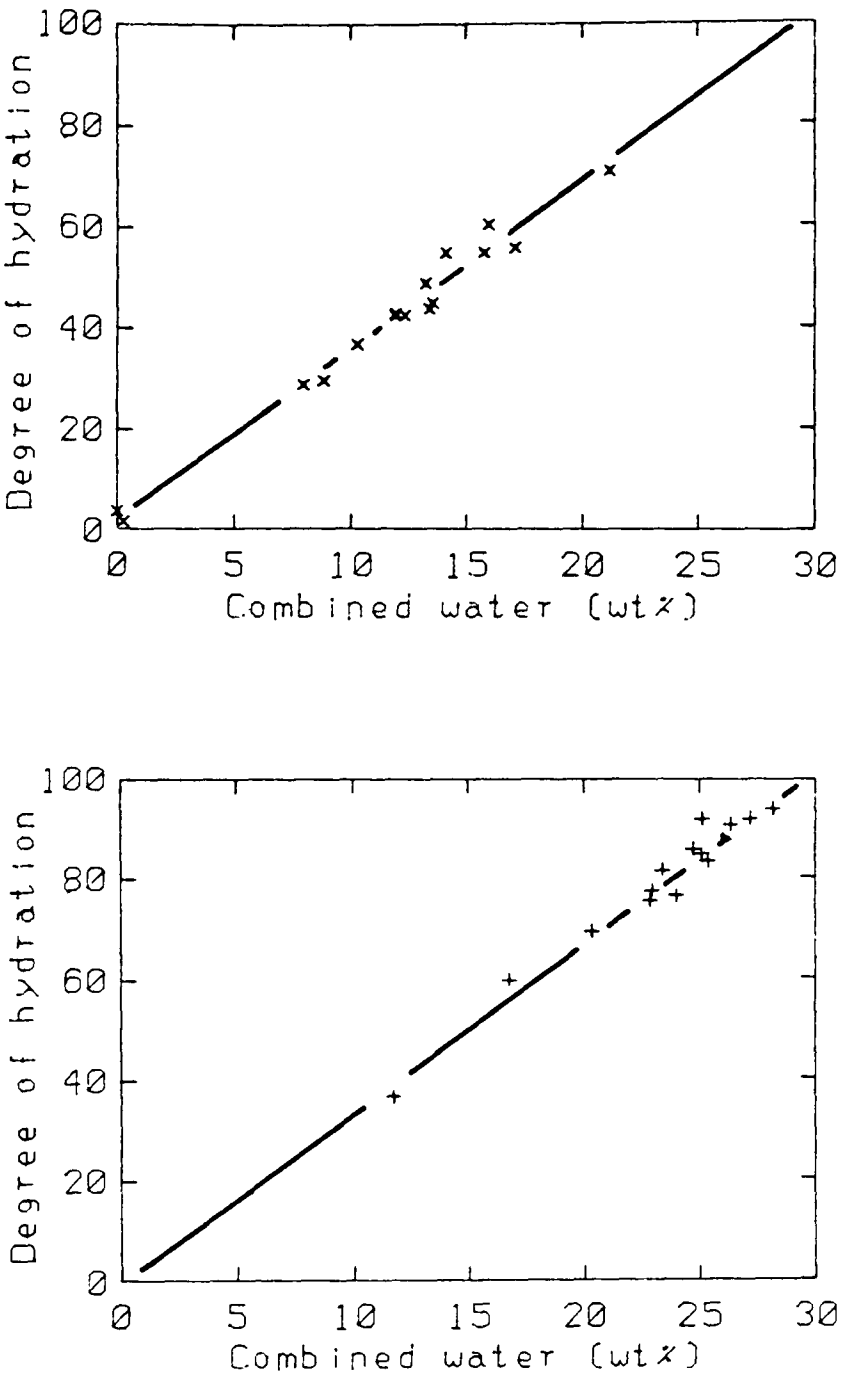

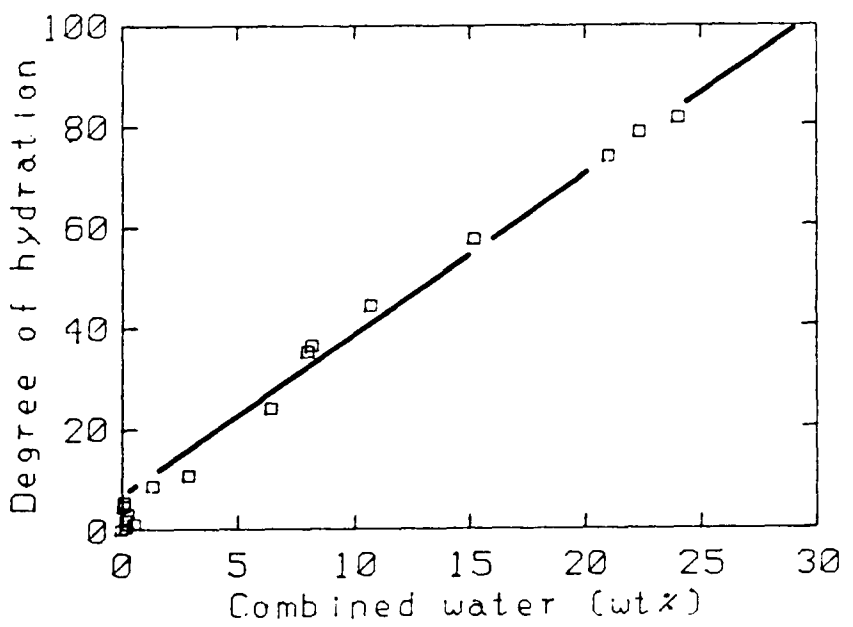

Fig 6.9: Variation of the combined water content of the three samples with their degree of hydration.

content against the degree of hydration (fig 6.8) and the combined water content against the degree of hydration (fig 6.9) for all three samples.

6.6 Discussion and Conclusions

A 1:1 correlation between the $Ca(OH)_2$ measured by QXDA and that measured by TGA has previously been questioned (Odler & Dorr 1979 b). It has been reported that amorphous $Ca(OH)_2$, undetectable by QXDA, forms during the early hydration period of C_3S (Brunauer & Kantro 1964) in particular during the time when C_3S is hydrating and no crystalline $Ca(OH)_2$ is being formed. This time, when C_3S is hydrating and no $Ca(OH)_2$ is detectable, can be seen on the graphs of fig 6.8, the best fit lines of which do not go through the origin. The intersection with the degree of hydration axis indicates a degree of hydration in the region of 5 - 10% before $Ca(OH)_2$ is detected.

In this study a close 1:1 correlation was obtained for the $Ca(OH)_2$ measured by QXDA with that measured by TGA for all three samples. This implies either that amorphous $Ca(OH)_2$ is not formed or that it is undetectable by both techniques.

If amorphous $Ca(OH)_2$ is formed during these early stages then a graph of the crystalline $Ca(OH)_2$ (measured by QXRD) against the combined water content will not pass through the origin. Instead it will show water to be combined without any formation of (crystalline) $Ca(OH)_2$. Fig 6.10 shows such a graph for all three samples. Although there is a fair degree of scatter in the results they clearly show that the amount of combined water formed before the formation of crystalline $Ca(OH)_2$ is at the most very small (less than 2%). Given that part of this combined water must be taken up in CSH gel (some crystalline C_3S has disappeared so CSH gel will have been formed with a C/S ratio of 3 if no $Ca(OH)_2$ has been formed and

with a C/S ratio of less than 3 if $Ca(OH)_2$ has been formed) the amount of amorphous $Ca(OH)_2$ formed, if any, must also be very small.

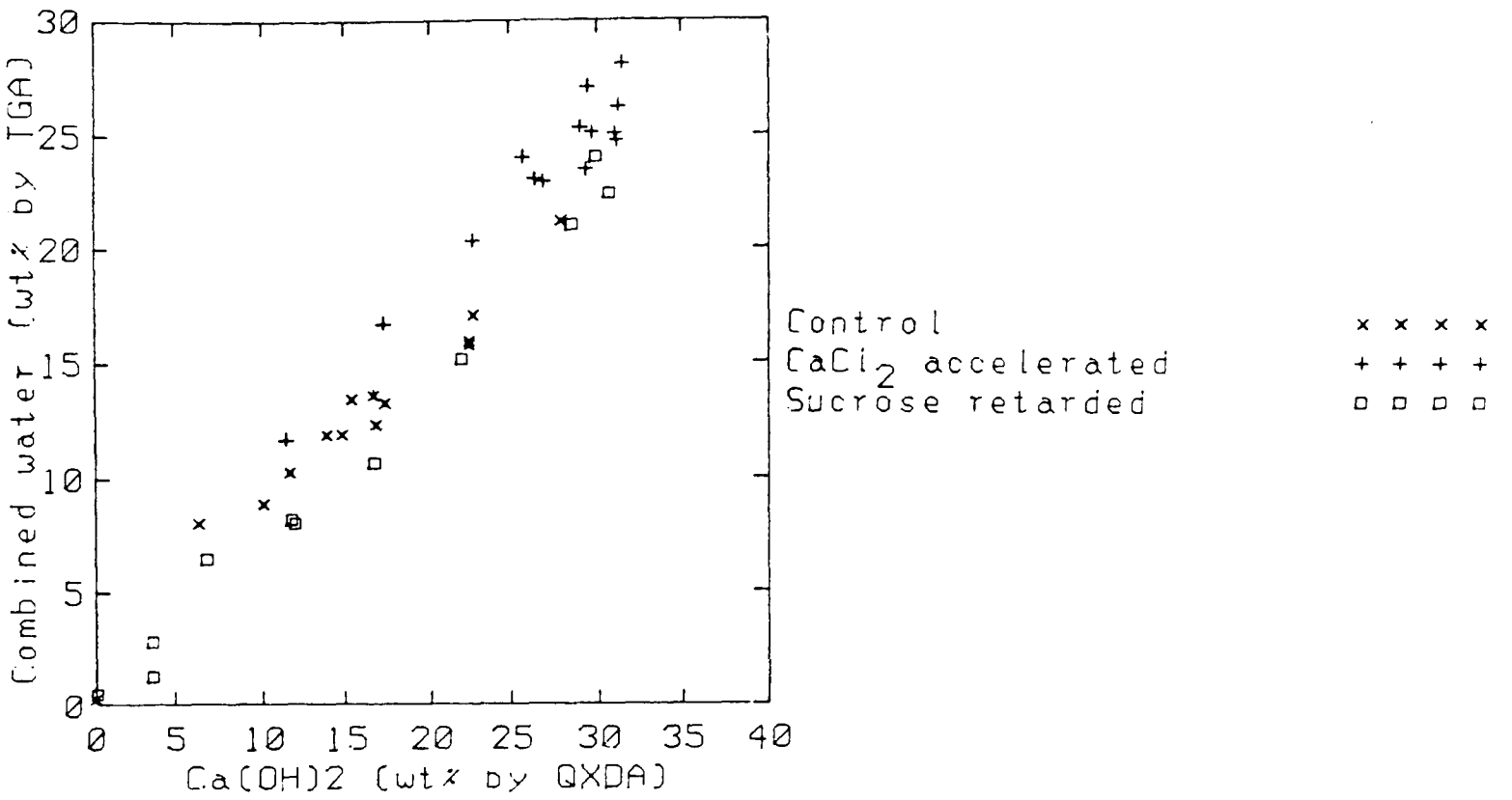

Fig 6.10: Graph of the combined water content of C_3S gel against its $Ca(OH)_2$ content (as measured by QXDA) at different degrees of hydration.

While these results indicate the formation of very little, if any, amorphous $Ca(OH)_2$, and hence CSH gel of C/S ratio close to 3, during the early stages of the reaction it should be recognised that this can not be regarded as conclusive. Both TGA and QXDA suffer from being relatively insensitive when the degree of hydration is low and hence more data needs to be collected to establish the relationships between the combined water content, the $Ca(OH)_2$ content and the degree of hydration more exactly.

A linear relationship between the degree of hydration and the combined water content of the samples was found in all three experiments in this study (fig 6.8). The slope of this line gives the weight of water combined per unit weight of C_3S. The values obtained in this study of 0.30 (+/-0.03) gH_2O/gC_3S for the controls, 0.26 (+/-0.04) gH_2O/gC_3S for the $CaCl_2$ accelerated samples and 0.28 (+/-0.04) gH_2O/gC_3S for the sucrose retarded samples are higher than those obtained by other workers

(0.215 by Odler and Dorr (1979 b), 0.204 by Brunauer and Kantro (1964), 0.21 by Locher (1966) and 0.22 by Odler and Skalny (1973)). This is almost certainly due to the difference in sample drying procedure between this work and that of the others and emphasises the point that the water content of the gel is not a definite quantity but depends on the technique used to bring the samples to a standard situation before measurement begins. The close agreement between the combined water per gram of C_3S in all three cases is taken to indicate that, in spite of the presence of the admixtures and the variation in speed of the different reactions, there is a high degree of similarity in the nature of the reactions taking place. This similarity is also shown by the graph of fig 6.7. The control, the accelerated and the retarded samples all exhibit approximately linear relationships, the slopes of which allow the C/S ratio for the hydrate being produced during the linear portion of the graph to be calculated. This gives values of 1.7 (+/-0.1) for the control, 1.8 (+/-0.2) for the accelerated and 1.8 (+/-0.1) for the retarded samples. The values for the control agree well with those obtained by other workers (1.99 by Odler and Dorr (1979 b), 1.8 to 2.0 by Goto et al (1976), ~1.6 by Dent Glasser et al (1978), 1.4 to 1.9 by Locher (1966), 1.88 by Diamond (1976) and 1.8 by Clayden et al (1984)) and it is interesting to note that the values for the accelerated and retarded samples are not significantly different from this.

It can be concluded that neither the presence of $CaCl_2$ nor that of sucrose has any significant effect on the stoichiometry of the hydration process. This is remarkable given the marked effects that these two admixtures have on the hydration kinetics. These admixtures must therefore act by altering the physical characteristics of the gel. This aspect is discussed in chapter 7.

CHAPTER 7

SCANNING AND TRANSMISSION ELECTRON MICROSCOPE STUDIES OF THE HYDRATION OF C_3S

7.1 Introduction

7.1.a Morphological observations during the hydration of C_3S

Adding water to C_3S powder converts the discrete C_3S particles into a solid mass. The chemical changes which occur during this process (chapter 6) are accompanied by marked changes in the microstructure. A description of the hydration reaction is therefore incomplete without a description of these morphological changes and any mechanism explaining the hydration reaction should also be able to account for the microstructural changes which are occurring. The developing microstructure of hydrating C_3S has been studied by a number of workers.

The nature and composition of the product formed during stage 1 of the hydration reaction is not clear. Menetrier et al (1979) report a very uneven attack with parts of the surface becoming corroded while other parts remained unattacked. In contrast, transmission electron microscopic studies of hydrated ion-beam thinned C_3S specimens by Groves (Double 1983) indicate a much more even attack with the development of a colloidal gel-like reaction product after as little as 5 minutes hydration which was found to completely envelop the grains. Jennings et al (1981) could not differentiate between product formed during this stage and that formed during the next.

Several investigators have reported the formation of a foil or honey-comb like product (early or type E CSH) after about 15 minutes hydration; i.e. by the start of stage 2 (Fujii & Kondo 1974; Menetrier et al 1979; Jawed et al 1980; Jennings et al 1981). Jennings et al (1981) report that this

can roll up on drying to give the cigar shaped folded foils which are often observed radiating at all angles from the surfaces of C_3S grains hydrated for short periods.

When the induction period ends and the acceleratory period or stage 3 begins, the outer morphology of the C_3S changes somewhat. Most workers report the appearance of needle shaped fibers radiating out from the grain (Ciach et al 1971; Daimon et al 1971; Young et al 1973; Jennings et al 1981), though work by Stewart & Bailey (1983) indicates that the morphology of the product formed during this stage can depend on the crystal form and/or the impurity ion content of the C_3S being used. They found triclinic and trigonal C_3S to give the normal needle like growths while a monoclinic sample gave a product with a thin crumpled sheet/foil morphology. Jennings et al (1981) found the first product during stage 3 to be a viscous gelatinous form of CSH which formed around the C_3S grains and underneath the foils of the previously formed type E product. They called it type O and found that it transformed into a product with a needle shaped morphology if large enough open spaces existed between the particles (>1 micron). If no such spaces were available then the type O remained reasonably undisturbed.

During stages 4 and 5 the C_3S grains gradually diminish in size and CSH is precipitated in the space left by the receding grain (giving 'inner product') as well as in the pore spaces (giving 'outer product'). Fracture surface studies only reveal changes in the outer product and these indicate the gradual infilling of the pore spaces leading to a loss in detail of the outer product morphology and a change in mode of fracture from inter- to trans-particle (Young et al 1973). During these stages Stewart & Bailey (1983) found that all three of their samples (triclinic, trigonal and monoclinic) took on approximately the same

morphology and Jennings et al (1981) found that there is a gradual conversion of type 0 CSH to a more fibrous interleaved and interlocked foil structure which they called type 3.

These morphological developments have been the subject of a detailed study by Jennings et al (1981) using SEM, STEM and HVEM. Based on their observations, they proposed a classification of the various morphologies (table 7.1). This has been used in the description above.

Classification		Period formed	Morphology and habits
Early	Type E	First few hours Stages 1 and 2	Thin flakes or foils which, when dried become cigar-shaped tubes, 1/4 microns long radiating from C_3S grains at all angles.
Middle	Type 0	Between 2-24 hr Stages 3 and 4	Amorphous gel approximately 0.5 microns thick surrounding the grains. Behaves as wet plastic material for first several days. Changes into other morphologies depending on space available.
	Type I	Forms from type 0 during first few hours	Slightly tapered needles, 0.75-1.0 microns long, radiating perpendicularly to the grains, with aspect ratio of about 10. Formed from type 0 in open areas > 1 micron. Encouraged by drying and/or age.
	Type I'	Can be formed from type 0 during first few days	Tapered fibres, 0.25-0.5 microns long, often branching. Formed from type 0 by pulling apart particles. Only seen on young fracture surfaces.
Late	Type 3	Forms from type 0 after several days	Partly crumpled foils which are interlocked. Formed as type 0 ages and/or dries in regions where original interparticle spacing < 1 micron.
	Type 4	After first 24 hours	Dense gelatinous inner product.

Table 7.1: Classification of the microstructure of the products of the hydration of C_3S.

Explanations of how the various morphological features develop are fairly sparse. The origin of the fibrous outer morphology has been explained on the basis of the 'osmotic model' described in the previous chapter. Formation of a protective film, which subsequently bursts as a result of osmotic pressures which build up underneath, could, by analogy with the growths which are found in silicate gardens (Coatman et al 1980), give rise to the needle shaped growths. However it has also been suggested that they may be formed by exfoliation or crumpling of type E CSH (Jennings et al 1981) or by the formation of a compressed film of CSH which peels and spalls off to relieve the pressure which builds up because the CSH occupies a larger volume than the C_3S it is formed from (Ball 1983).

7.1.b Difficulties encountered when interpreting morphological data

Study of the changes in morphology which take place during the hydration of C_3S requires a resolution which can only be attained with an electron microscope. Specimens for observation must therefore normally be subjected to a vacuum and are usually fracture surfaces (for scanning microscopy) or thin sections (for transmission microscopy). The preparation procedures necessary to produce such specimens limit the information which can be obtained from them and care must therefore be exercised when interpreting such information.

Cement is a wet material and so under normal circumstances has to be dried out before being placed in an electron microscope. While it is clear that this drying affects the microstructure, the extent to which it can be altered is not known. Thus Jennings et al (1981) have reported that the thin foils of type E CSH roll up to form needles on drying while Bailey & Stewart (1984) found drying to have little effect on the microstructure. Fracture surfaces represent the points of weakest bonding

between grains and are likely to be unrepresentative of the bulk of the material. Observations by Berger et al (1973) and Daimon et al (1971) support this view. They found significantly less $Ca(OH)_2$ on the fracture surface than that calculated to be on a random surface given the total amount of $Ca(OH)_2$ in the sample.

The preparation of thin specimens for TEM involves, either very fine crushing of the material and dispersion onto a grid, or mechanical grinding followed by ion-beam thinning. The crushing/dispersion method is unsatisfactory as it does not preserve spatial relationships while the grinding/ion-beam thinning method can only be carried out on well hydrated specimens which can survive the rough treatment of the preparation procedure without falling apart. The latter problem can be overcome to a certain extent by resin impregnation (Dalgleish & Ibe 1981) but this has not yet been attempted for very young samples.

The advent of high voltage electron microscopes has allowed the use of environmental cells in which wet samples can be maintained at near atmospheric pressure in a moist environment (Double 1973; Jennings & Pratt 1980). Observations of hydrating C_3S under such conditions has provided useful information concerning the early microstructural development of C_3S but only poor resolution can be attained and this has limited the wider use of the technique.

7.1.c Effect of admixtures on the morphological development of C_3S

The presence of some admixtures, such as calcium salts, have been found to modify the morphology of the CSH gel (Odler & Skalny 1971; Young et al 1973; Treatteberg et al 1974; Singh & Ojha 1981), changing it from its normal acicular or needle like appearance to what has been described as a more lacey or 'honeycomb' appearance. The presence of certain admixtures

also resulted in an increase in the concentration of 'pull outs' (i.e. places where the central anhydrous core of a particle has separated from the outer, hydrated rim during fracture - Young et al 1973). Berger et al (1973) also report changes in the pore size distribution of C_3S pastes as a result of addition of $CaCl_2$ as an admixture.

The effect of sucrose on the morphology of C_3S has not been investigated.

7.2 Experimental

In this study the morphological development of the three C_3S samples described in chapter 6 (control, $CaCl_2$ accelerated and sucrose retarded) was studied by SEM and samples of (a) 1 year old C_3S paste and (b) 1.5 year old $CaCl_2$ accelerated C_3S paste, were observed by TEM. Chemical analyses of the areas of gel in the thin sections observed by TEM were carried out using EDXA.

7.2.a Scanning electron microscopy

SEM specimens of the well hydrated samples which had set were fracture surfaces mounted on copper boats and coated with Au/Pd in the usual way. Others, which were still powders, often made unsatisfactory specimens when treated in this manner, either breaking or charging up badly in the microscope. The early specimens for the $CaCl_2$ and sucrose experiments were therefore made by distributing a small amount of the powder on a short length of double sided adhesive tape attached to the specimen holder. These were then coated in the usual manner. For the microscopy a JEOL 100C scanning/transmission electron microscope with chemical analysis facilities was used in the scanning mode.

7.2.b Transmission electron microscopy and analysis

Specimens for TEM were made by sectioning the paste, manually grinding to about 40 microns followed by ion-beam thinning using a 4 KeV argon beam at an angle of 15 degrees to the surface. The thinned specimens were coated with a thin layer of carbon and viewed in the JEOL 100C in transmission mode.

Chemical analysis of the thinned specimens were obtained using the energy dispersive X-ray detector fitted to the JEOL 100C microscope. The microscope was operated in STEM mode at 100 KeV. The specimens were clamped in a graphite holder tilted at 35° towards a lithium drifted silicon detector. A thinned sample of pure wollastonite (CS) was used as a standard.

C/S ratios were obtained from the X-ray spectra by following the technique of Cliff & Lorimer (1975). By assuming that the specimens are thin enough for absorption to have a negligible effect, the calcium to silicon ratio of the material can be obtained merely by comparing the ratio of the areas under the respective peaks with those of a standard (in this case wollastonite with C/S ratio = 1). The areas under the peaks were obtained by setting windows on either side of the peaks and summing the counts detected in each energy interval between the windows.

Counting was carried out for 100 seconds, keeping the average dead time below 30%. Typical count rates were of the order of 250 - 500 counts per second.

7.3 Results of the scanning studies

7.3.a Anhydrous material

Fig 7.1 is a micrograph of a freshly crushed sample of C_3S. It shows the anhydrous material to consist of large grains of C_3S with smooth angular surfaces which are covered with much smaller debris particles.

7.3.b Control

Figs 7.3 to 7.16 illustrate the morphological development of the control sample during its first 24 hours of hydration. The degree of hydration of each sample and its position along the calorimetric heat output curve is given in fig 7.2.

After half an hour's hydration (fig 7.3) the surface is still smooth, broken only by the debris particles, but the outlines appear less sharp than those of the anhydrous specimen.

During the rest of the induction period (figs 7.4 to 7.7) the surface remains relatively smooth but small outgrowths can be seen protruding from it. The size and number of these varies from grain to grain within the same specimen but there does appear to be a gradual increase in numbers with increasing time. Close inspection of the micrographs reveals that the growths appear very thin and foil-like when viewed edge on (e.g. edge of grain in fig 7.9), but when viewed from the top the foil-like appearance is lost.

During the acceleration period (figs 7.8 to 7.11) the original smooth outlines of the surface are lost under a covering of small growths. These increase rapidly in both numbers and size. After 5.5 hours (fig 7.9) the growths appear flakey and very thin while later on, at about the time of the maximum in the rate of heat evolution (6.5 hours, fig 7.10)

the growths are still thin enough to be electron transparent, but are considerably larger (~0.4 microns in length). In many cases they taper to a point. At higher magnification (fig 7.11), the surface is seen to consist of smooth gel apart from the tapered growths and one or two shallow holes.

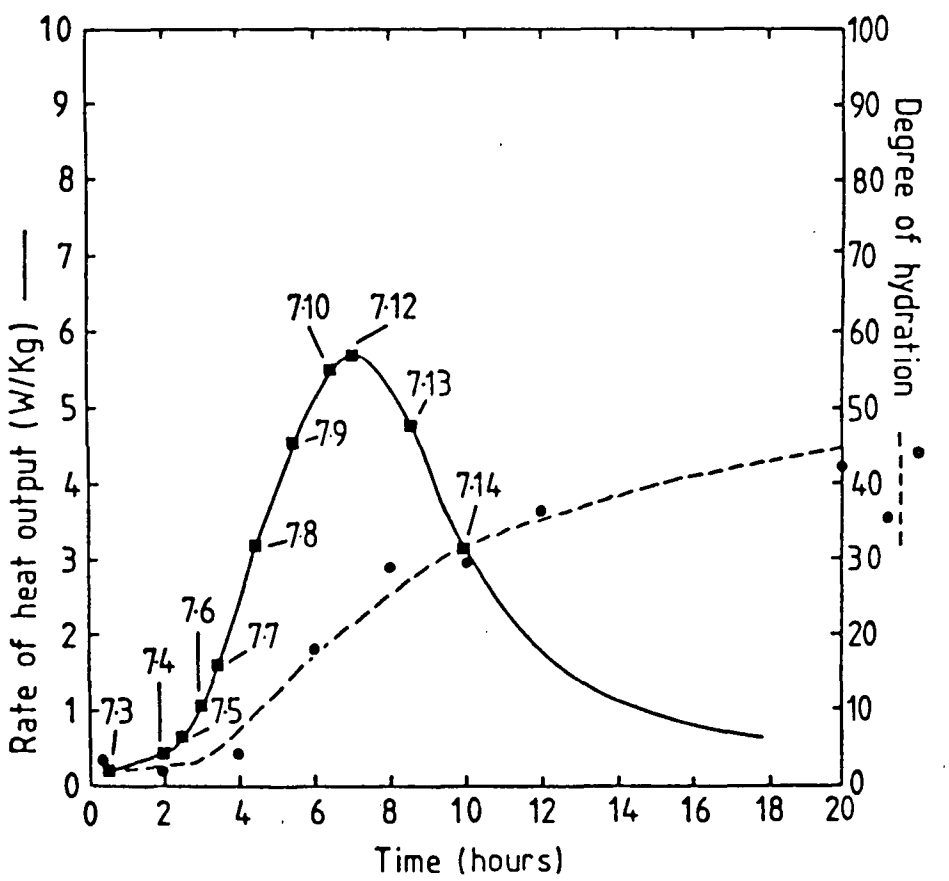

Fig 7.2: The degree of hydration and position along the calorimetric curve of the control C_3S samples used for SEM.

During the deceleratory period (figs 7.12 to 7.15) what was originally a flat surface with isolated growths emerging from it (fig 7.10) becomes a profusion of growths in several interpenetrating layers (fig 7.12). The growths themselves are still mostly tapered but have grown longer (~0.6 microns after 9 hours) and appear to be flatter and thicker and often lie along the surface rather than protruding up from it. An interesting feature of the growths is that they often appear in star shaped groups; the individual tapered growths in each group radiating in different directions from a common base (e.g. fig 7.13).

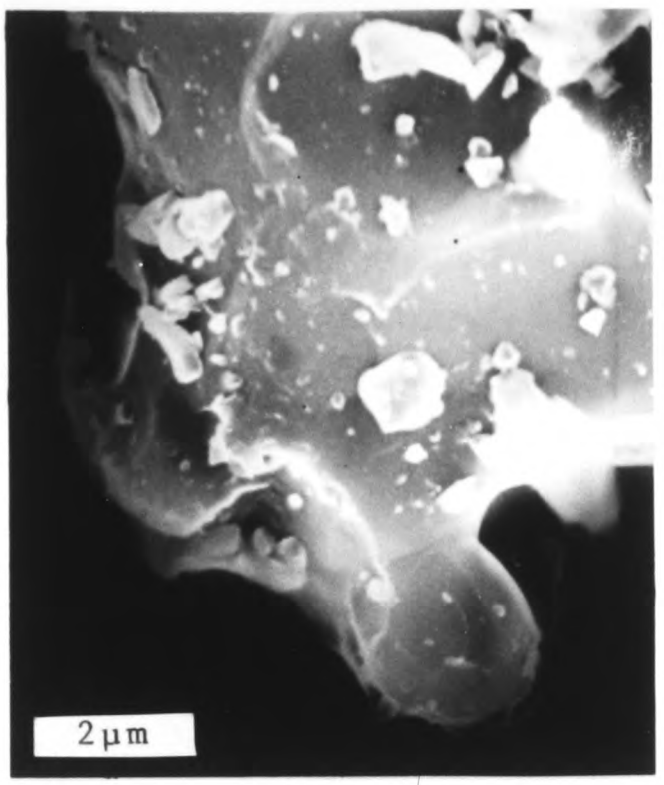

Fig 7.1 Anhydrous C_3S

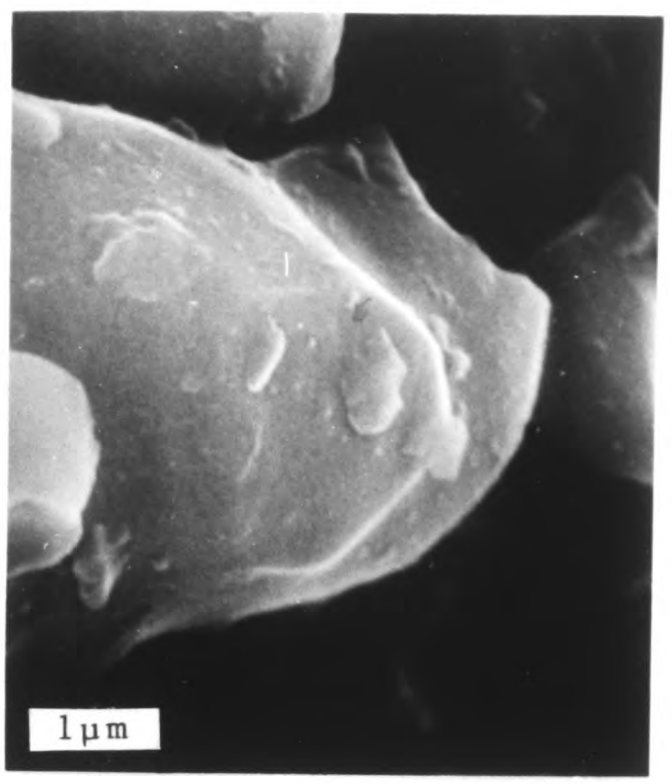

Fig 7.3 Control:
C_3S hydrated 0.5 hours

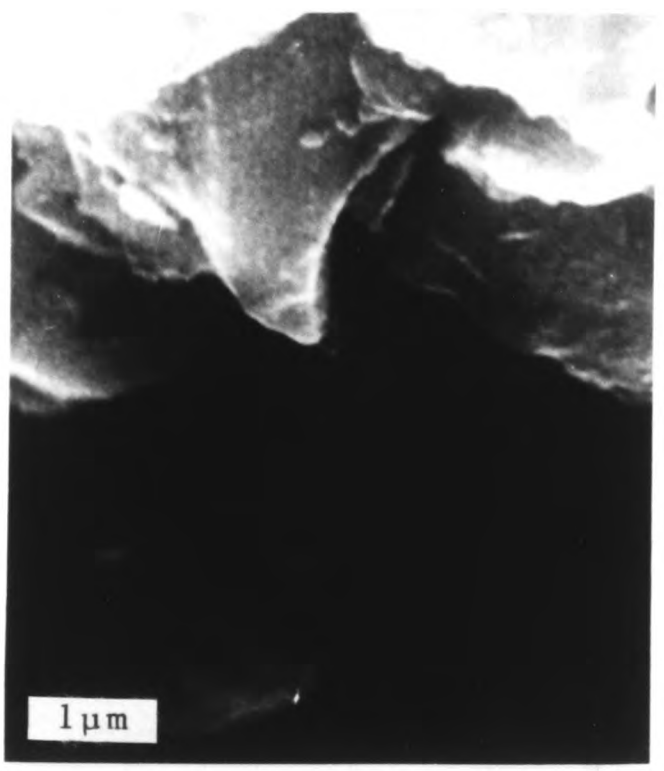

Fig 7.4 Control:
C_3S hydrated 2 hours

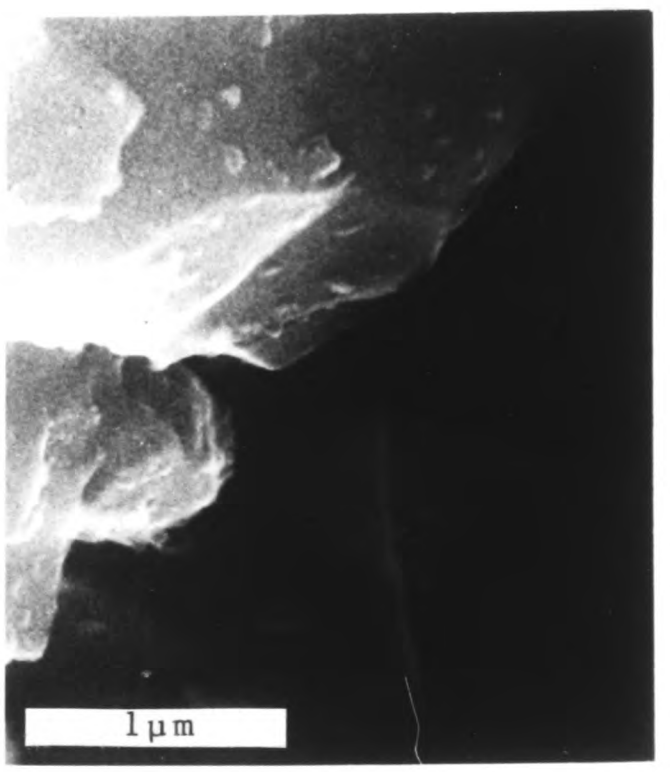

Fig 7.5 Control:
C_3S hydrated 2.5 hours

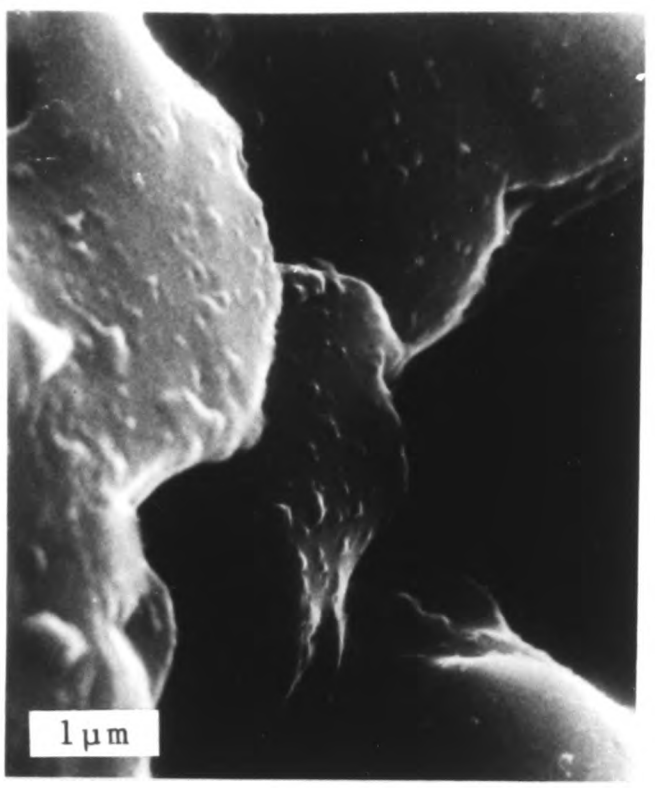

Fig 7.6 Control:
C_3S hydrated 3 hours

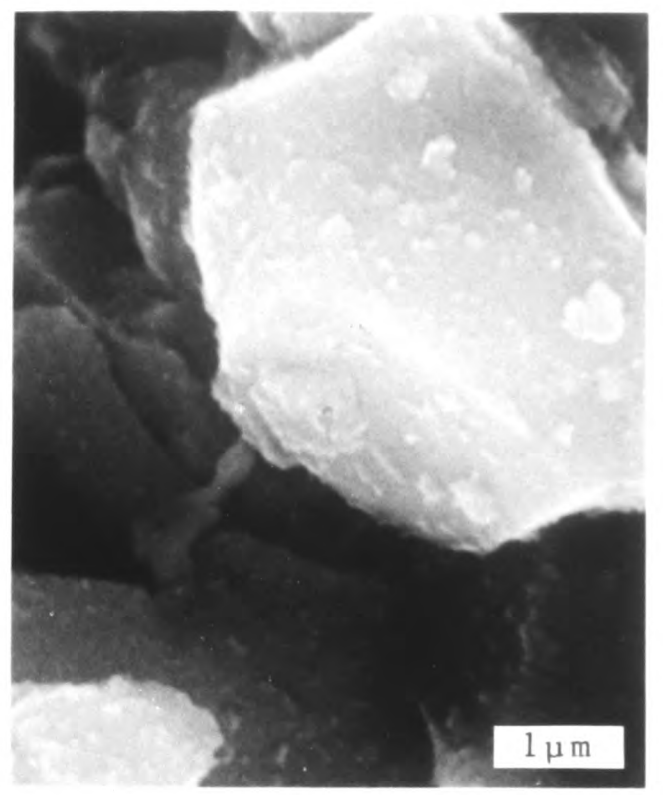

Fig 7.7 Control:
C_3S hydrated 3.5 hours

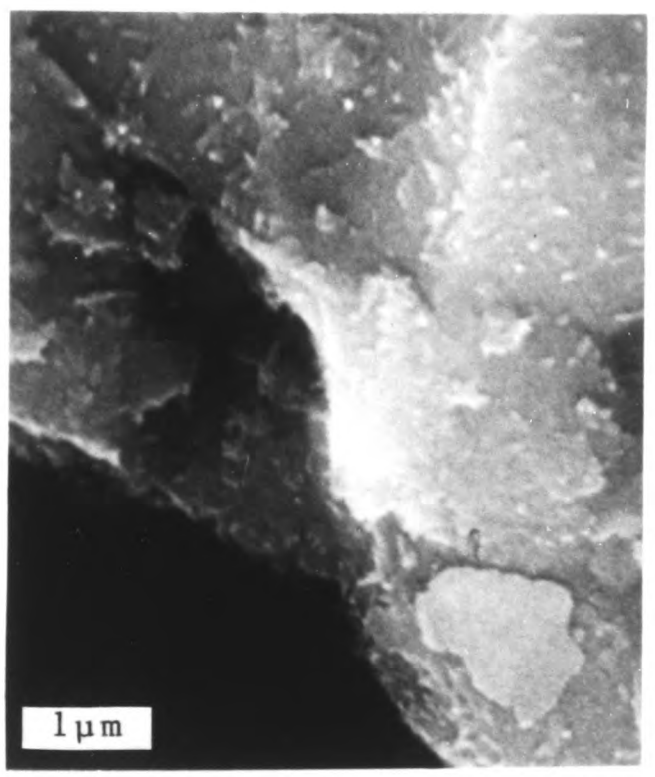

Fig 7.8 Control:
C_3S hydrated 4.5 hours

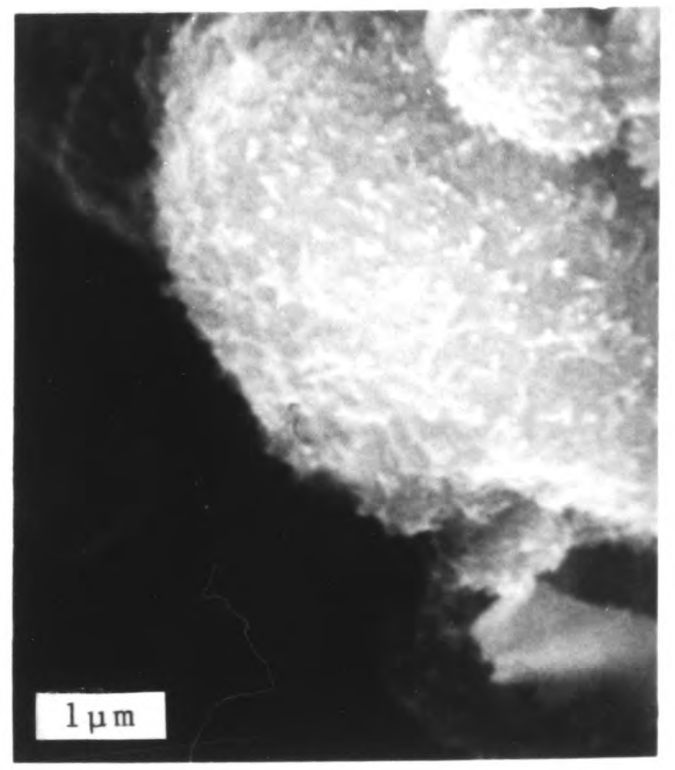

Fig 7.9 Control:
C_3S hydrated 5.5 hours

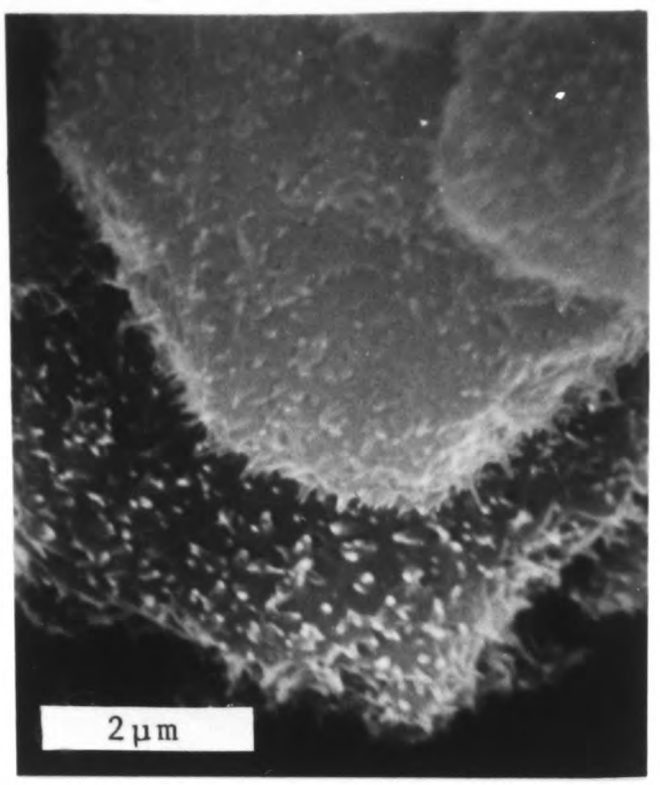

Fig 7.10 Control:
C_3S hydrated 6.5 hours



Fig 7.11 Control:
C_3S hydrated 6.5 hours

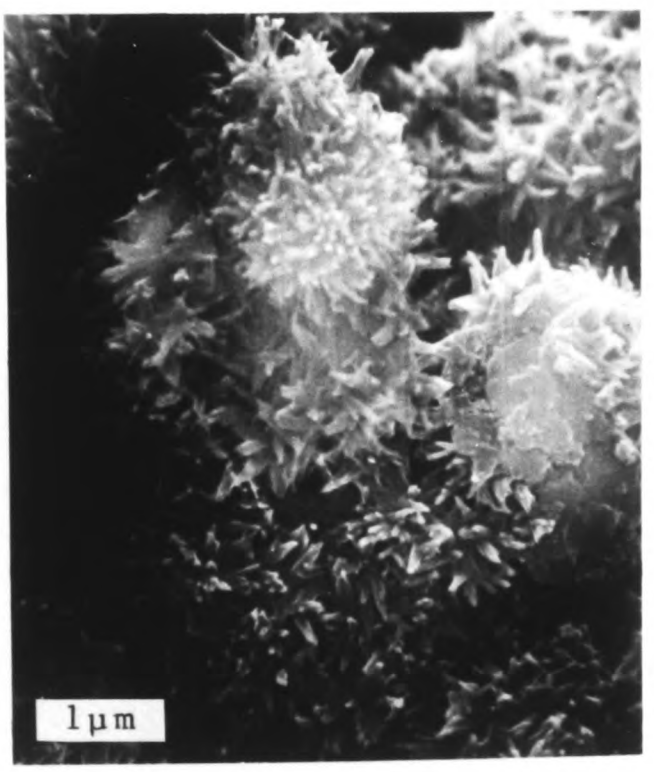

Fig 7.12 Control:
C_3S hydrated 7 hours

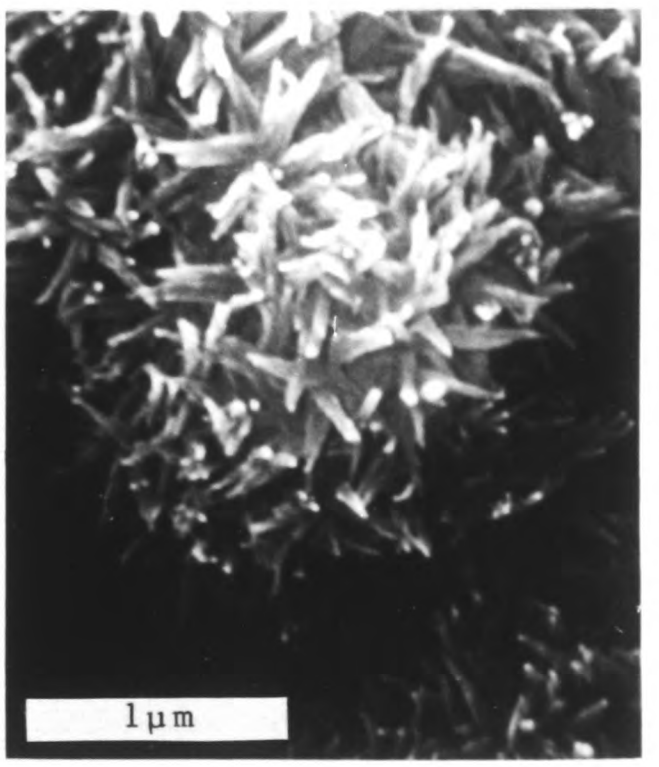

Fig 7.13 Control:
C_3S hydrated 9 hours

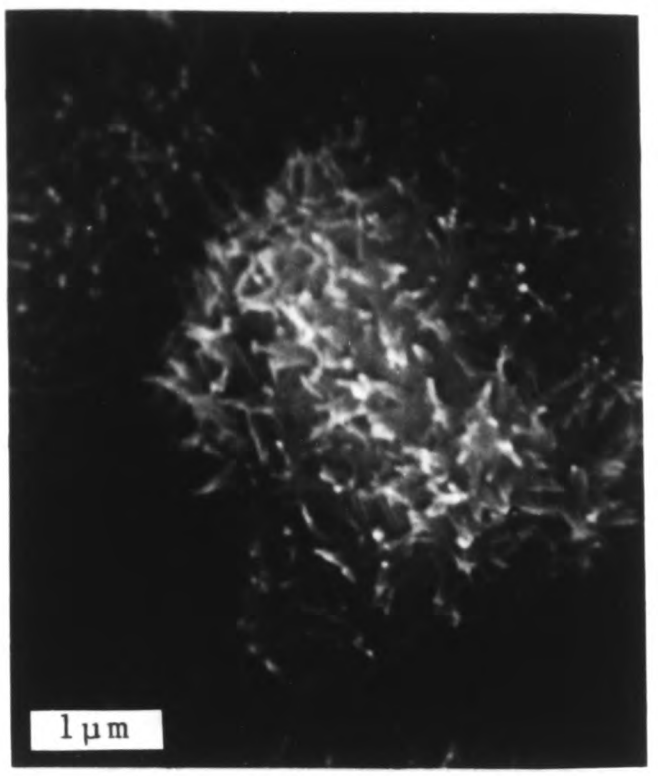

Fig 7.14 Control:
C_3S hydrated 10 hours

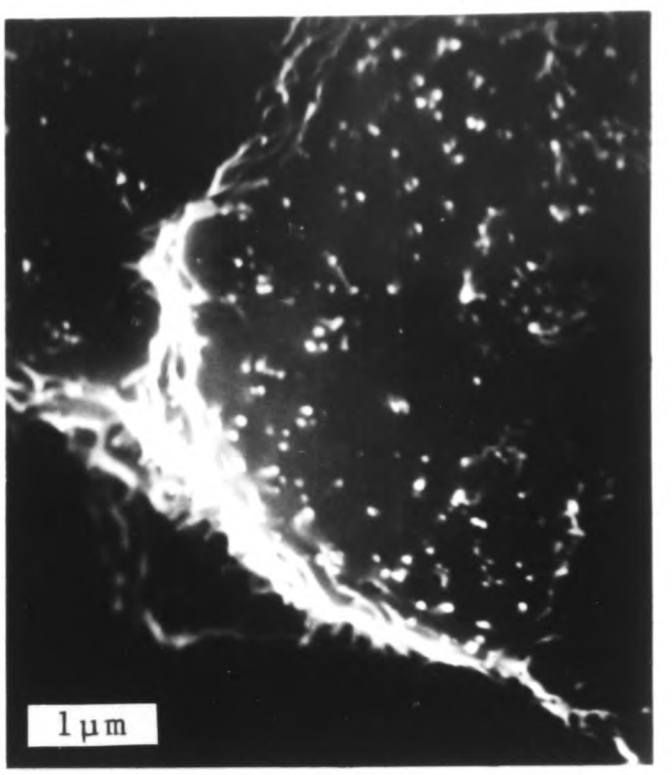

Fig 7.15 Control:
C_3S hydrated 10 hours

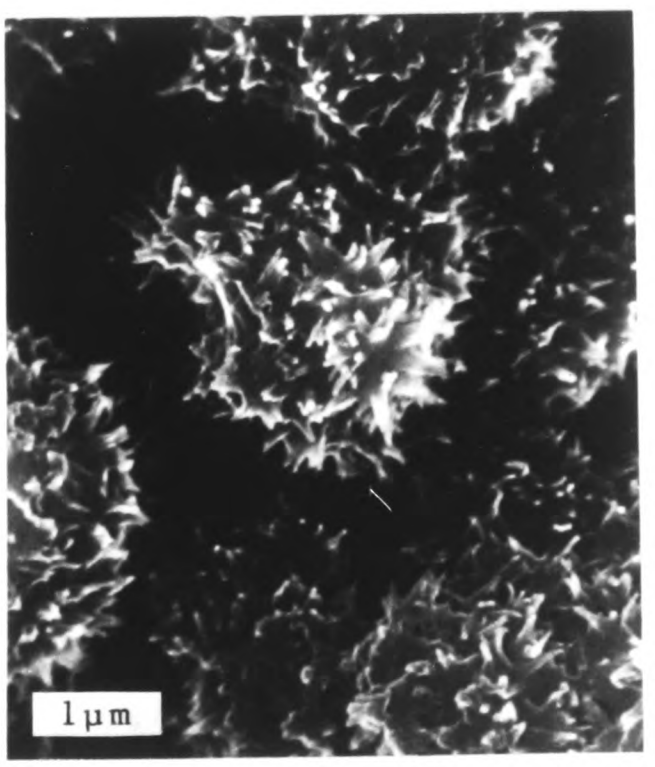

Fig 7.16 Control:
C_3S hydrated 24 hours

Further hydration results in infilling between the grains making the detailed morphology difficult to discern except where there are still open spaces between grains through which the line of fracture passes. In such areas the morphology remains similar to that developed during the deceleratory period (fig 7.16 at 24 hours).

In some cases there is a marked difference between grains in a given specimen. Figs 7.14 and 7.15 are both micrographs of grains hydrated for ten hours, but they have surprisingly different morphologies. Fig 7.14 shows a grain covered in layers of tapered growths similar to those observed in the other late samples (figs 7.12 & 7.13) while fig 7.15 shows a very smooth surface with only small needle like protrusions growing out from it.

7.3.c $CaCl_2$ accelerated

Figs 7.18 to 7.29 illustrate the morphological development of the $CaCl_2$ accelerated sample during its first four and a half hours of hydration. The degree of hydration of each sample and its position along the calorimetric heat output curve is given in fig 7.17.

During the induction period the morphological development of C_3S accelerated with $CaCl_2$ is very similar to that of the control. The surface of the grains remains relatively smooth, broken only by a few small outgrowths (fig 7.18).

After the end of the induction period these growths develop rapidly in size and number so that by the time two and a half hours have elapsed (figs 7.19 & 7.20) the surface is more or less covered and the original outlines have, to a large extent, been lost. At this time two distinct morphologies can be seen to be developing, both different from that of the control. Fig 7.19 shows a grain with a partial covering of lumpy

growths while fig 7.20 shows several grains more sparsely covered in smaller pointed growths.

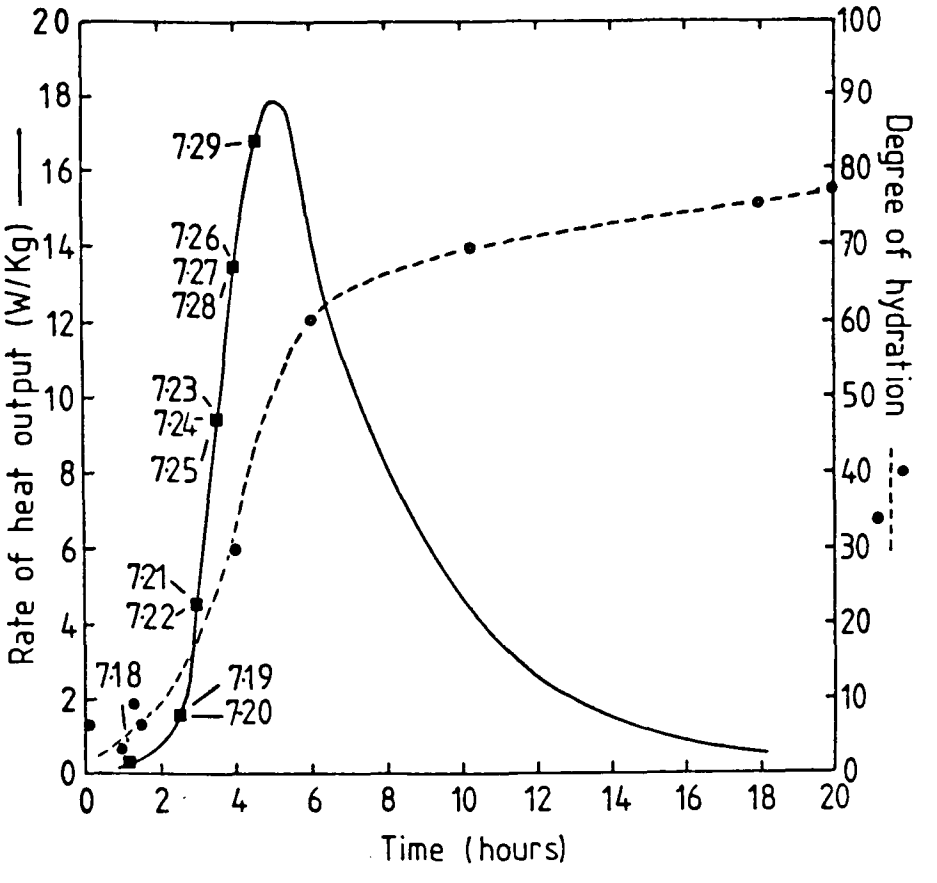

Fig 7.17: The degree of hydration and position along the calorimetric curve of the $CaCl_2$ accelerated C_3S samples used for SEM.

These two distinct morphologies seem to develop separately. Fig 7.21 and fig 7.22 are both micrographs of specimens hydrated for two and three quarter hours. The former exhibits a grain with a covering of broken sheet-like material in several layers which gives the impression of having originated from the lumpy growths while the latter exhibits a grain covered with an open fibrillar lattice work the fibres of which are highly branched and full of holes rather like a decayed leaf. Also evident at this time is a change in the mode of fracture in which the CSH gel coating fractures through to the underlying grain and often pulls completely away leaving a bare C_3S surface and a CSH gel case (fig 7.21). The thickness of this gel case has been estimated as 0.5 microns.

These features are repeated on the specimen hydrated for three and a half hours which is in the middle of the acceleratory period. Fig 7.23 illustrates the broken sheet morphology and the micrograph of a similar

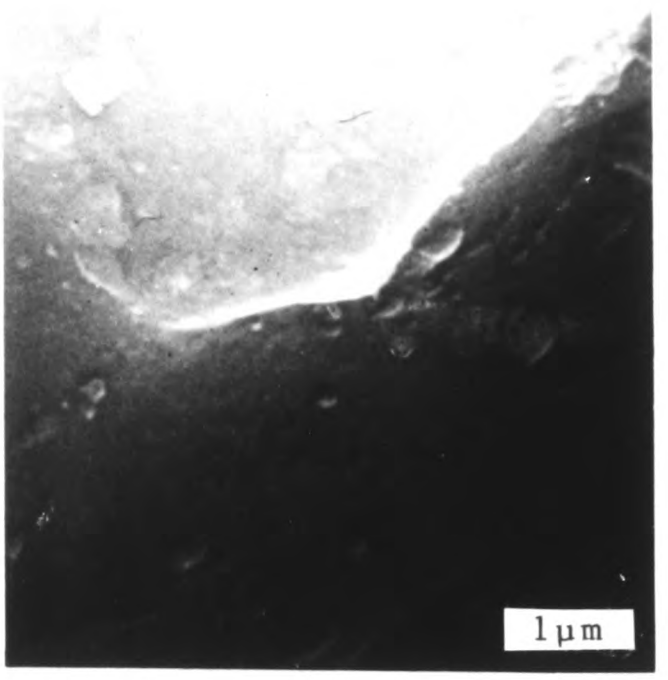

Fig 7.18 $CaCl_2$ accelerated:
C_3S hydrated 1.25 hours

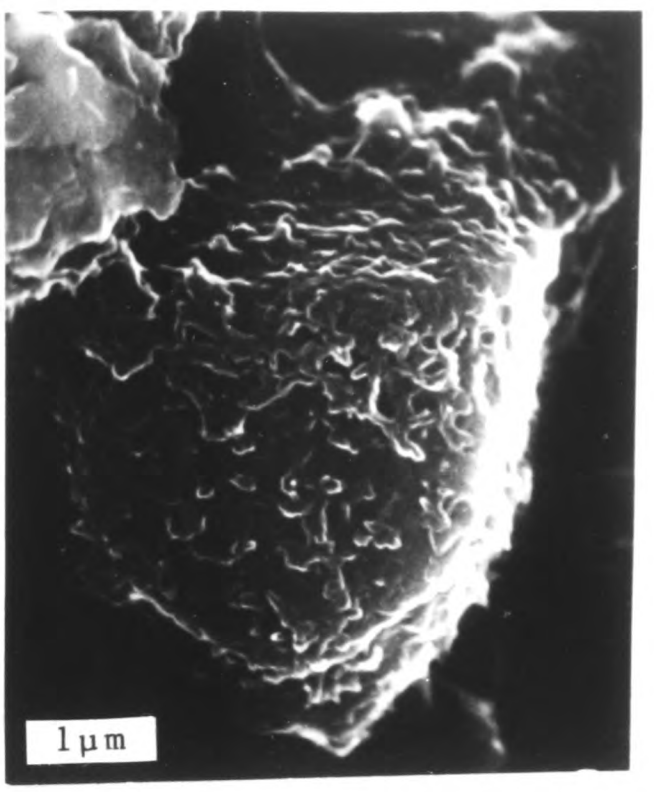

Fig 7.19 $CaCl_2$ accelerated:
C_3S hydrated 2.5 hours

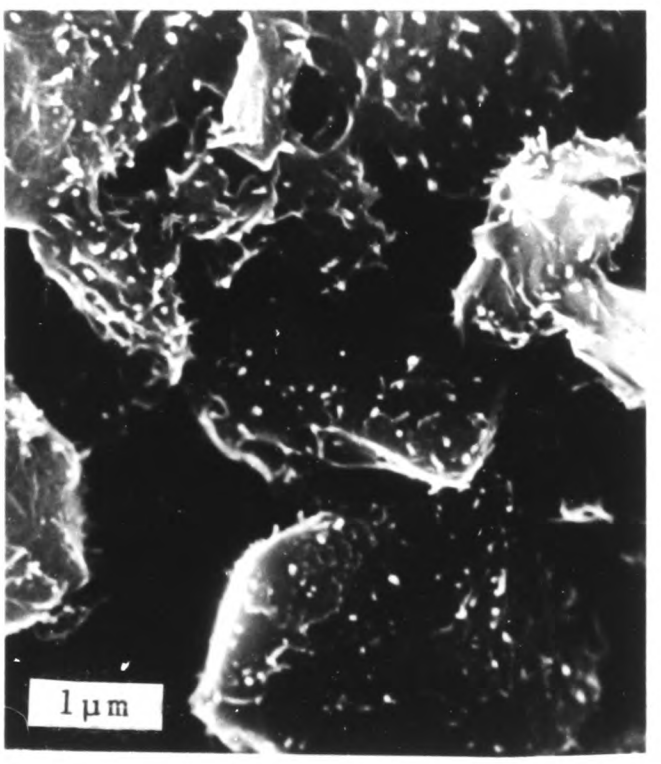

Fig 7.20 $CaCl_2$ accelerated:
C_3S hydrated 2.5 hours

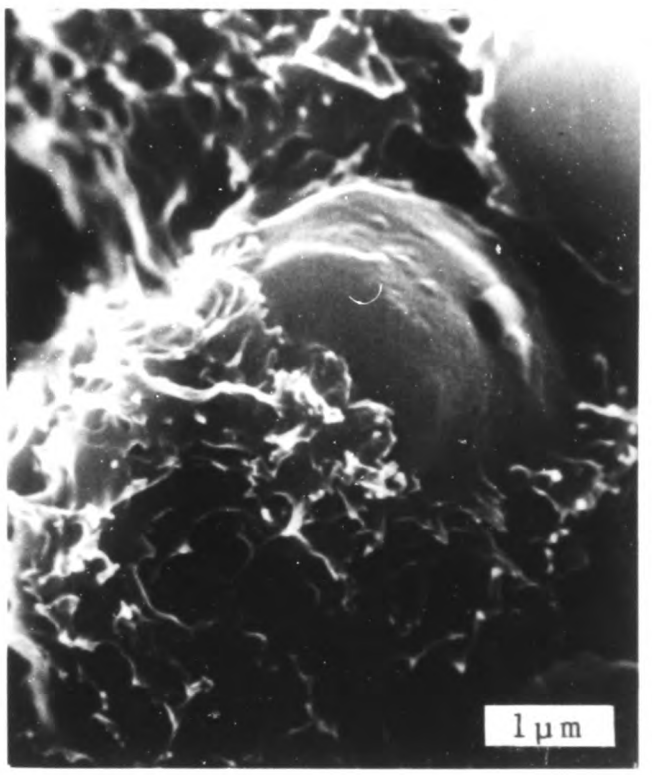

Fig 7.21 $CaCl_2$ accelerated:
C_3S hydrated 3 hours

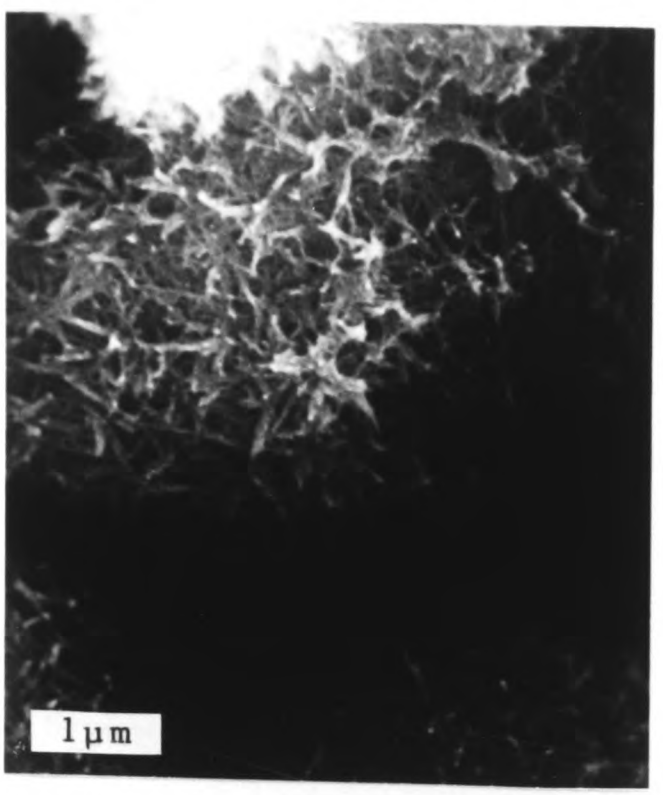

Fig 7.22 $CaCl_2$ accelerated:
C_3S hydrated 3 hours

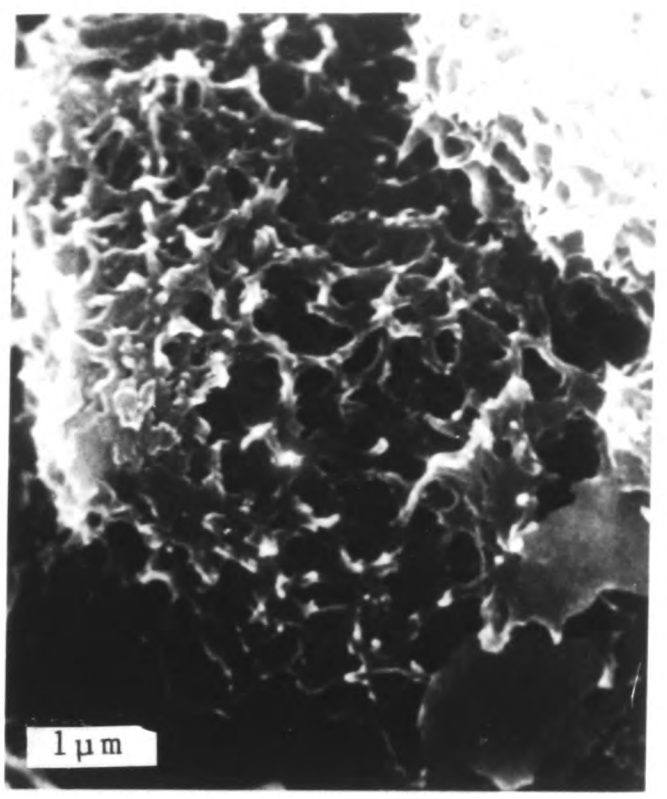

Fig 7.23 $CaCl_2$ accelerated:
C_3S hydrated 3.5 hours

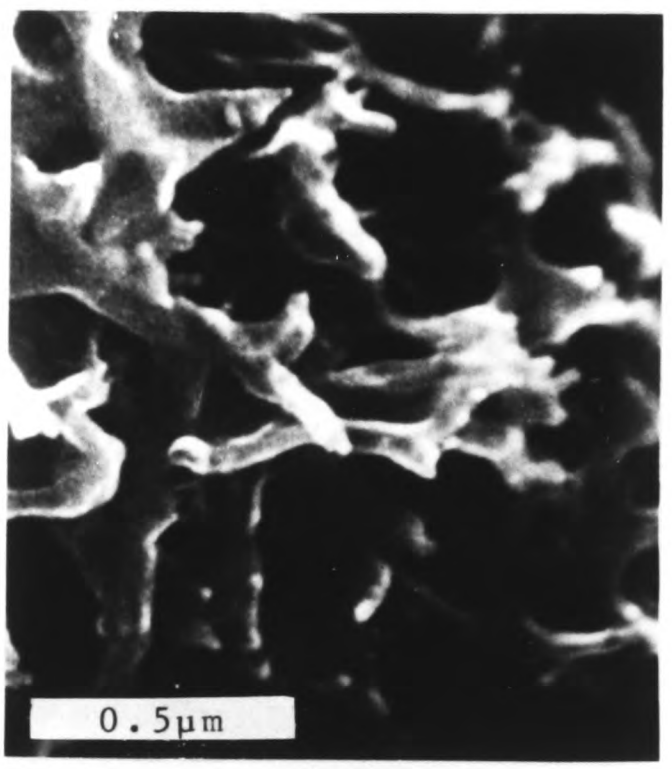

Fig 7.24 $CaCl_2$ accelerated:
C_3S hydrated 3.5 hours

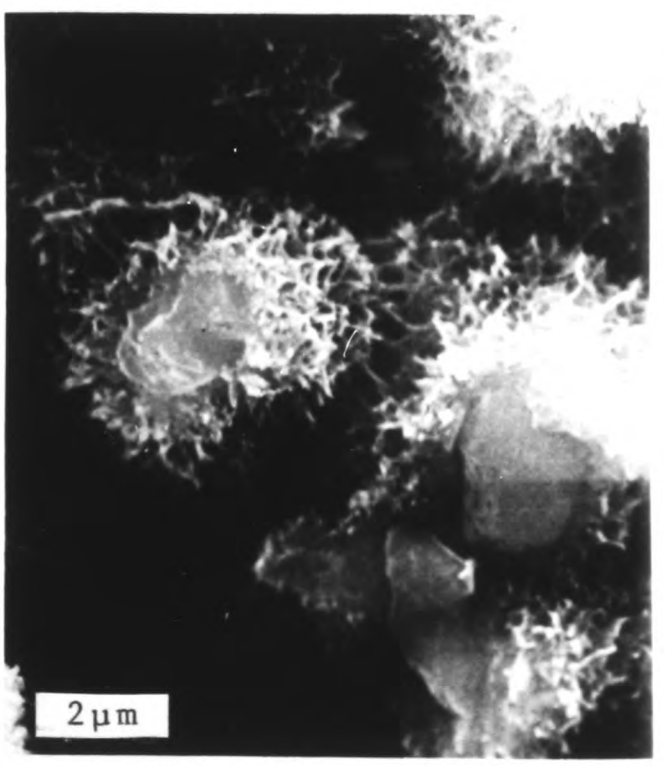

Fig 7.25 $CaCl_2$ accelerated:
C_3S hydrated 3.5 hours

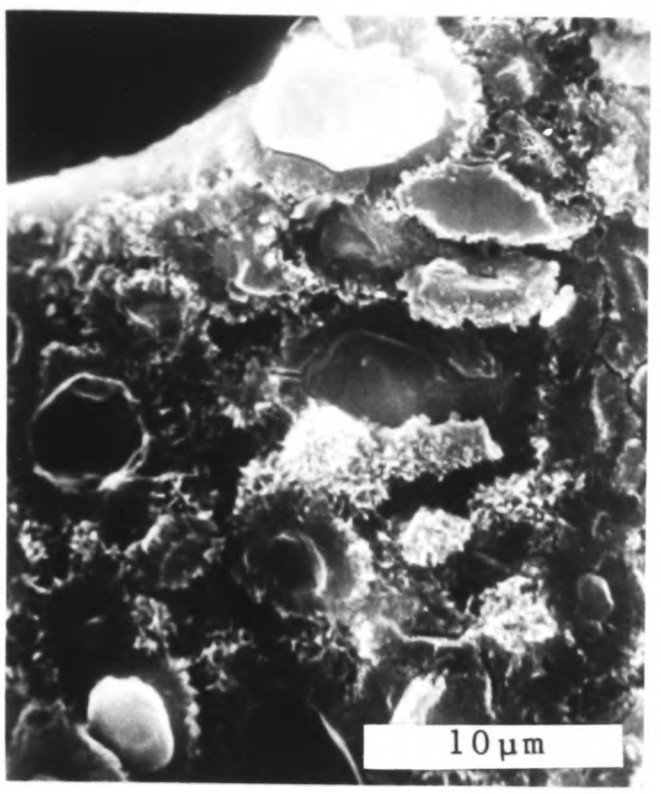

Fig 7.26 $CaCl_2$ accelerated:
C_3S hydrated 4 hours

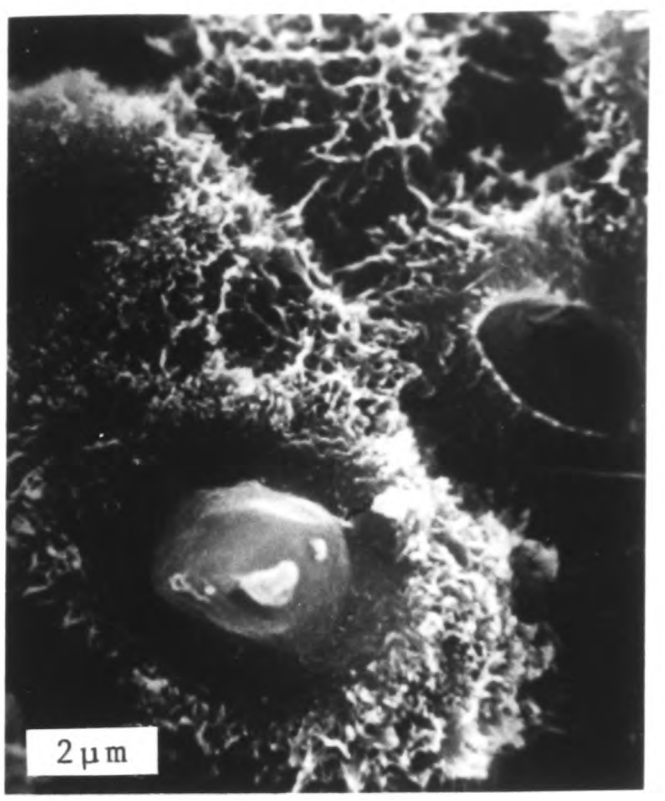

Fig 7.27 $CaCl_2$ accelerated:
C_3S hydrated 4 hours

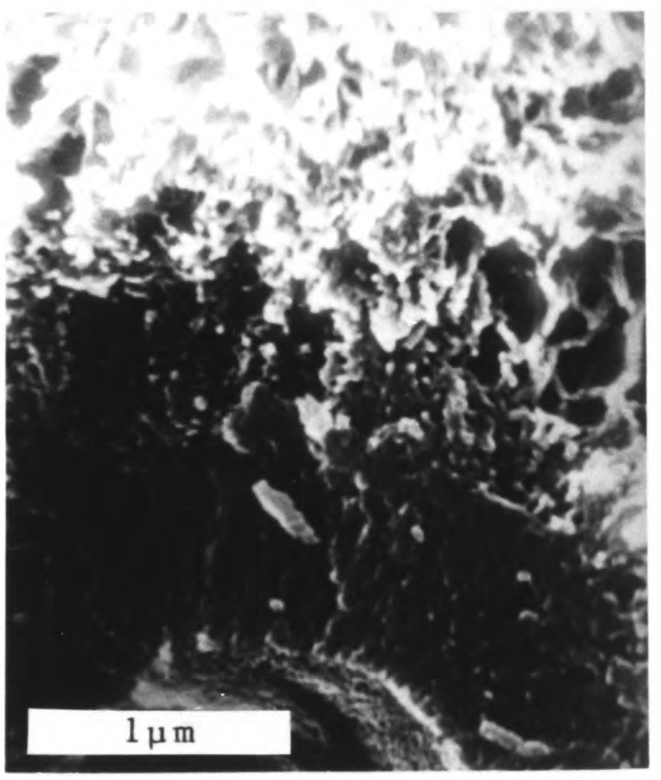

Fig 7.28 $CaCl_2$ accelerated:
C_3S hydrated 4 hours

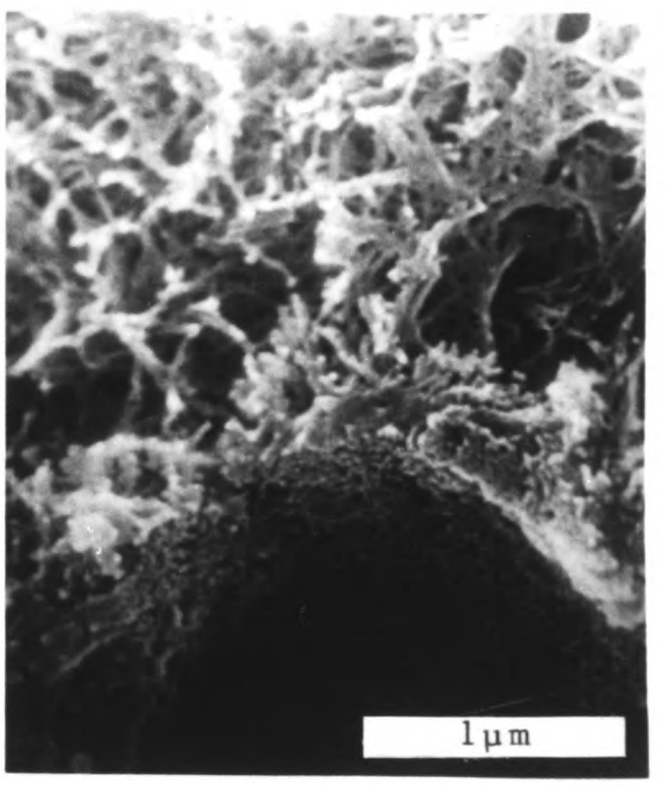

Fig 7.29 $CaCl_2$ accelerated:
C_3S hydrated 4.5 hours

area at higher magnification (fig 7.24) shows the sheets to consist of fairly thick layers of CSH about 0.1 microns in depth with no obvious porosity in the CSH gel itself. Fig 7.25 illustrates the other type of morphology together with a number of grains whose CSH gel case has been partially removed. The gel layer is considerably thicker than that in fig 7.21 (~0.9 microns).

Half an hour later and approaching the maximum in the rate of heat evolution, the gel layers coating the grains are even thicker (figs 7.26 to 7.28) ranging from 1.5 to 2.0 microns. Enlargement of areas of this gel which have been fractured through (figs 7.27 & 7.28) reveal a densely packed fine grained material close in to the grain giving way to the more open morphologies observed in previous specimens further away from the grain. The surface of the gel case which had been in contact with the grain and has subsequently pulled away (centre of extreme bottom of fig 7.28) reveals an interesting dimpled structure somewhat like orange peel. This dimpled appearance of the inner surface of the gel casing shows up more clearly in fig 7.29 which is a micrograph of a specimen after four and a half hours hydration (at about the maximum in the rate of heat evolution). It shows that there are a large number of holes in the gel in contact with the hydrating grain.

7.3.d Sucrose retarded

Figs 7.31 to 7.42 illustrate the morphological development of the sucrose retarded sample during its first three weeks of hydration. The degree of hydration of each sample and its position along the calorimetric heat output curve is given in fig 7.30. In this experiment the end of the induction period determined by calorimetry did not coincide with that determined by TGA and QXDA. It is thought that this may have been due to

slight variations in the concentrations of the sucrose solution used in the experiments as only very slight changes in concentration affect the rate of hydration markedly. As the specimens used in these microscopy studies were the same as those used for the TGA and QXDA studies the positions of the induction period etc. used in the description below have been taken from the TGA and QXDA studies rather than from the calorimetry results.

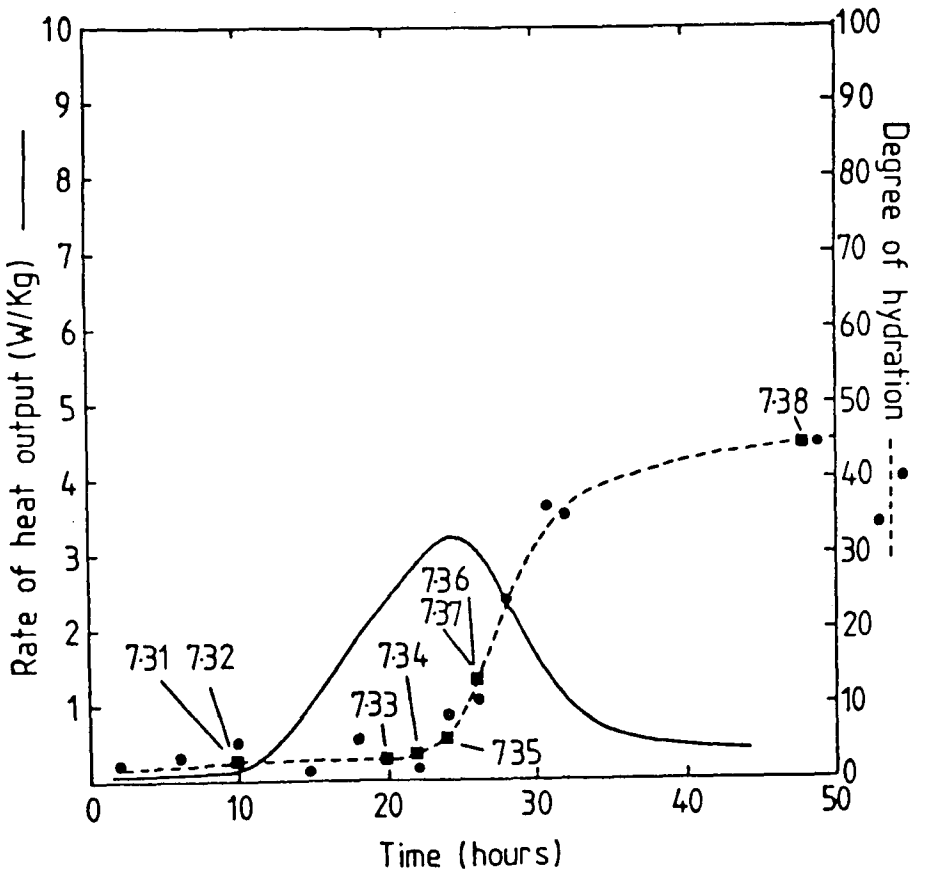

Fig 7.30: The degree of hydration and position along the calorimetric curve of the sucrose retarded samples of C_3S used for SEM.

During the induction period, which both the QXDA and TGA data indicates continues for at least 22 hours, there are only a few signs of hydration. Scattered small growths are evident on the originally smooth surface after six hours. These grow slowly in numbers during the rest of the induction period. Figs 7.31 & 7.33 show these growths after ten and twenty hours respectively and fig 7.32 shows an enlarged view of the growths, which are about 0.2 microns long, from the ten hour specimen. The surface of this specimen appears slightly eaten away in places.

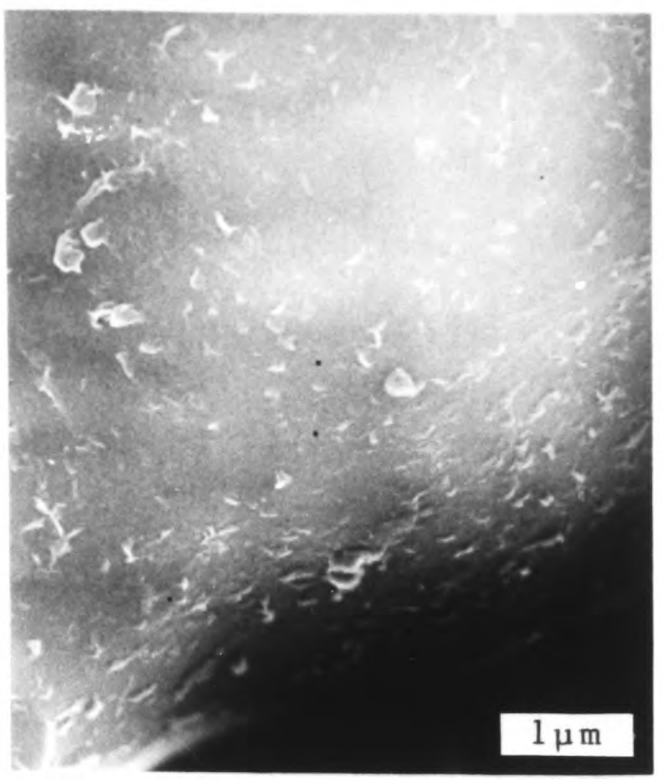

Fig 7.31 Sucrose retarded:
C_3S hydrated 10 hours

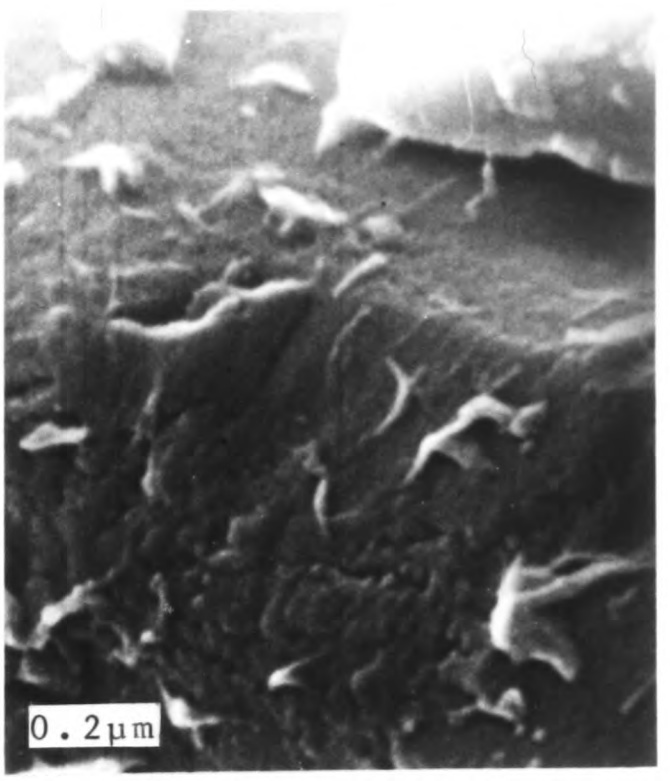

Fig 7.32 Sucrose retarded:
C_3S hydrated 10 hours

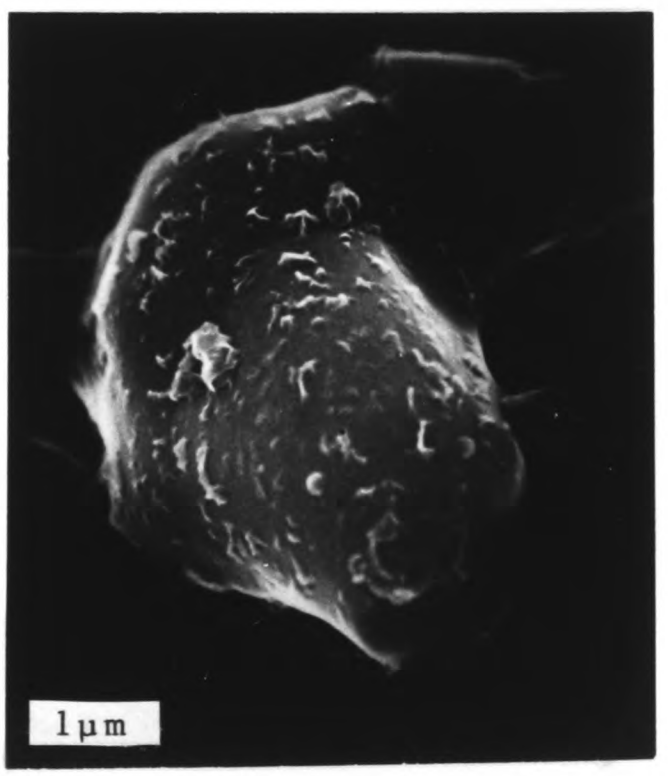

Fig 7.33 Sucrose retarded:
C_3S hydrated 20 hours

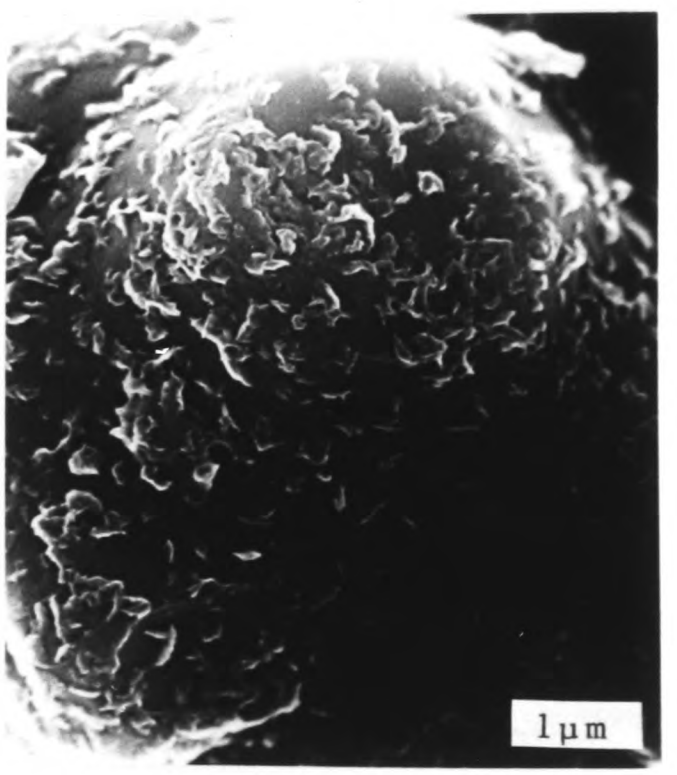

Fig 7.34 Sucrose retarded:
C_3S hydrated 22 hours

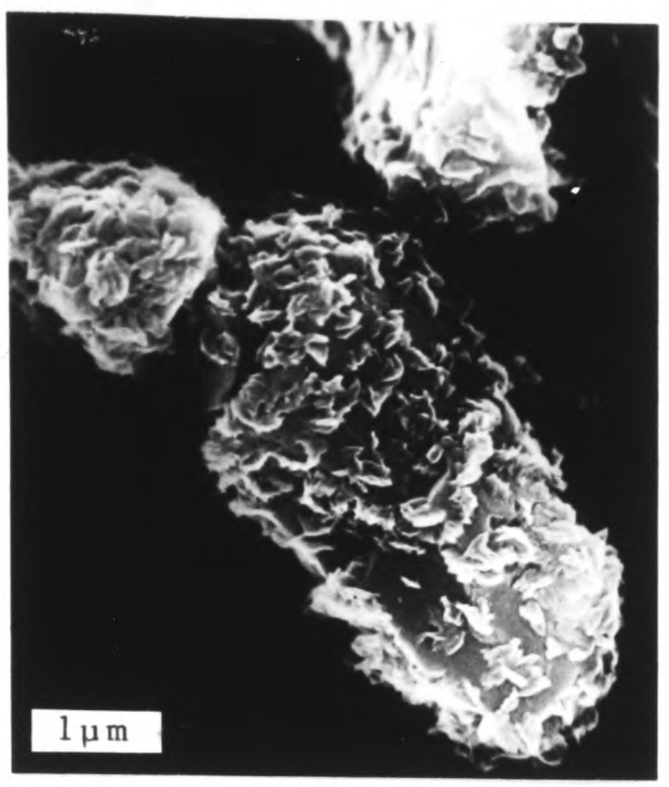

Fig 7.35 Sucrose retarded:
C_3S hydrated 24 hours

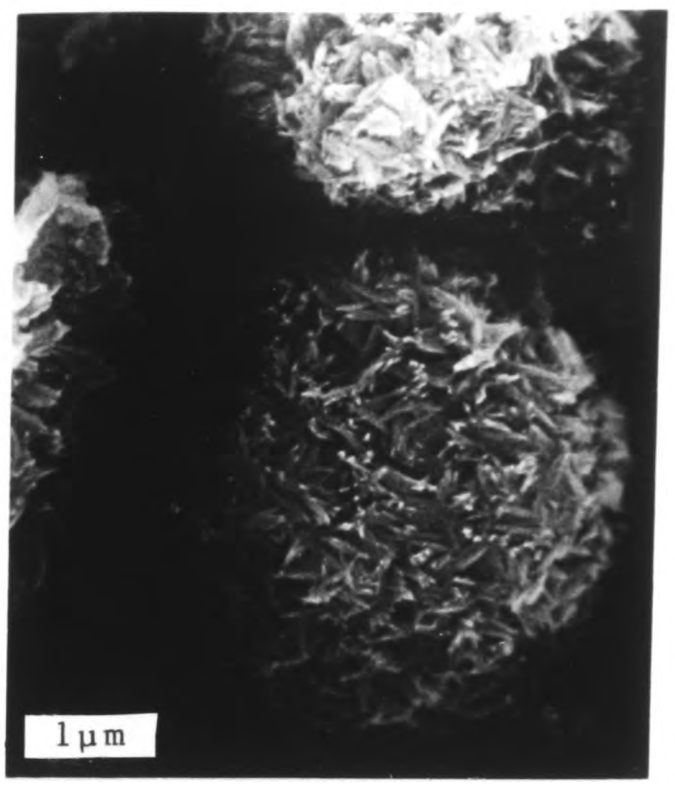

Fig 7.36 Sucrose retarded:
C_3S hydrated 26 hours

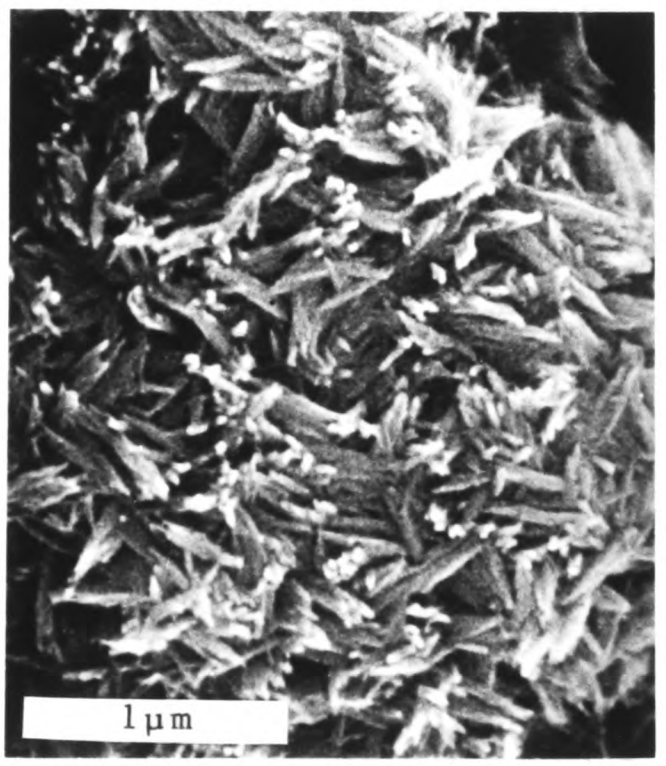

Fig 7.37 Sucrose retarded:
C_3S hydrated 26 hours

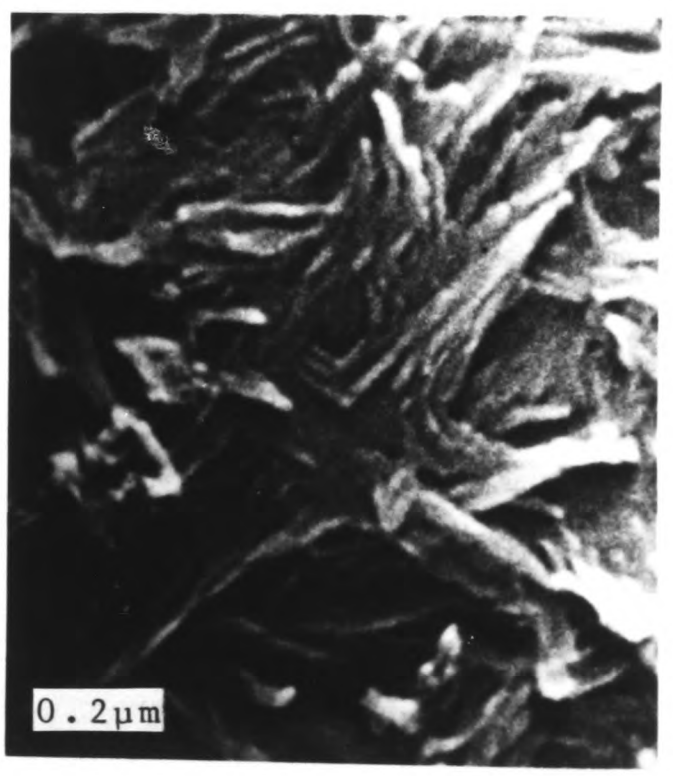

Fig 7.38 Sucrose retarded:
C_3S hydrated 49 hours



Fig 7.39 Sucrose retarded:
C_3S hydrated 3 weeks



Fig 7.40 Sucrose retarded:
C_3S hydrated 3 weeks

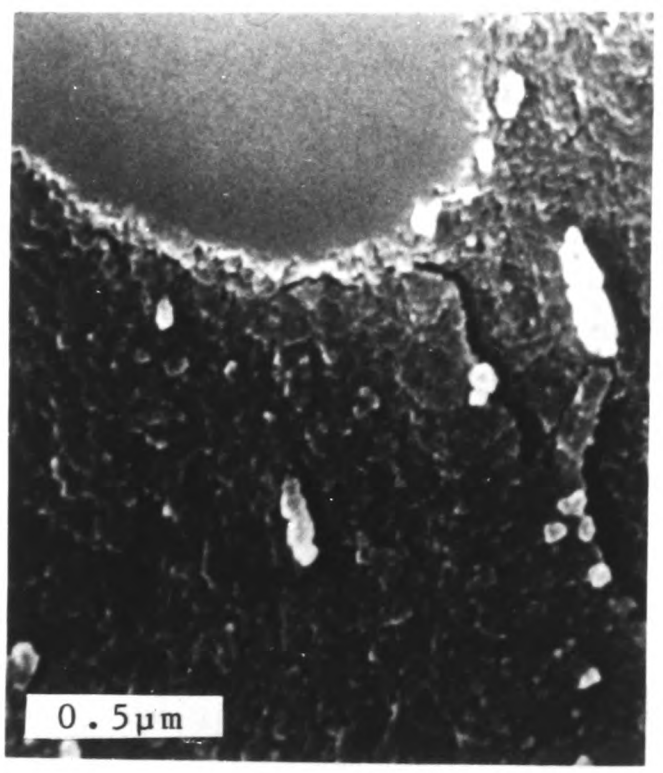

Fig 7.41 Sucrose retarded:
C_3S hydrated 3 weeks

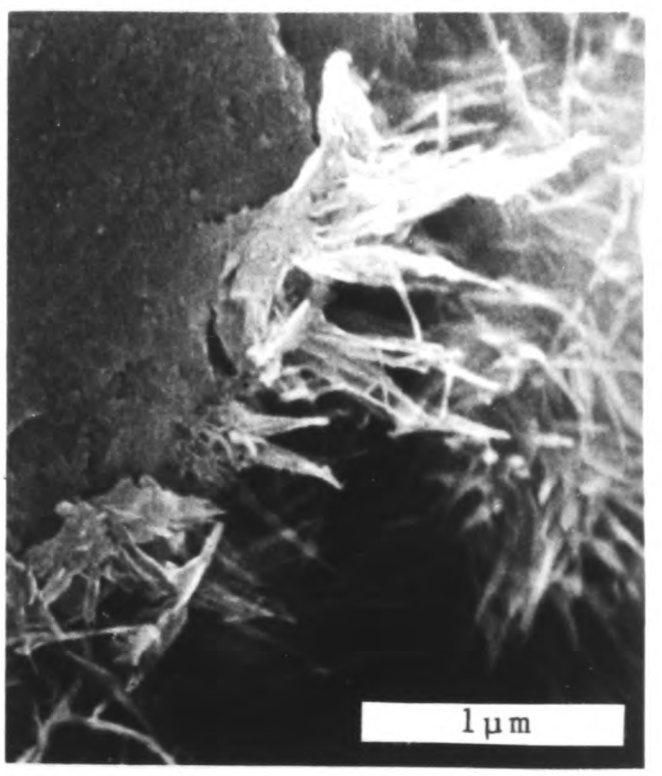

Fig 7.42 Sucrose retarded:
C_3S hydrated 3 weeks

At the end of the induction period these growths rapidly increase in size. Figs 7.34 & 7.35 after 22 and 24 hours respectively show that soon after the end of the induction period the entire surface of the grains is covered by small clumps of gel about 0.4 microns long. By the time 24 hours have elapsed, the clumps seem to have developed a slightly fibrous texture.

Two hours later, at the maximum in the acceleratory period, a distinct change has occurred. The grains are now covered in long, often tapered, growths similar to those seen on the control specimens during the deceleratory period (fig 7.36). The fibrils again often seem to form star shapes. Higher magnification (fig 7.37) shows that, in contrast to those of the control, these growths have a much more fibrous texture similar to coarse rope and have ragged ends rather than simple single points. An intermediate stage between the small clumps and the fibrillar growths was not observed.

The long fibrous growths remain over the rest of the hydration period. Fig 7.38 shows an even higher magnification micrograph of the growths after 49 hours clearly illustrating the texture of the fibres.

After 3 weeks the hydration has proceeded to such an extent that trans-particular fracture, rather than inter-particular fracture, occurs. Fig 7.39 and fig 7.40 are micrographs of such fracture surfaces. Areas of fibrillar growth can be seen between grains. Large areas of lamellar growth are visible. In some cases the gel and grain have cleaved through revealing the densely packed fine grained gel under the fibrillar growth and surrounding the residual C_3S grains. Fig 7.41 and fig 7.42 are details of the grain/inner product and inner/outer product boundaries respectively. In the former the densely packed gel is in close contact with the grain. No evidence for space between the gel product and the

residual grain can be seen. The boundary between the two is clearly visible. In the latter no such clear distinction between the two types of material can be detected, though the transition from dense to fibrous gel does seems to proceed through a finer fibrous product.

7.4 Results of the transmission studies

Note: Areas of figs 7.43, 7.45 & 7.46 exhibit large numbers of small roughly circular areas of lighter contrast which look like holes. These arise from heat damage of the specimen resulting either from the ion-beam thinning or the electron beam and are not a part of the microstructure.

Transmission micrographs of the thinned sections of C_3S reveal four main types of material:

1) Amorphous gel of an even contrast with a fine-grained texture. Occurs in roughly circular areas which are bordered by gel of type 2 such as the left hand side of fig 7.43.

2) Amorphous gel of a much less even contrast with a fibrous texture. Occurs on the boundary of areas of gel of type 1 such as the right hand side of fig 7.43. The texture of the fibrous material usually runs perpendicular to the line of contact of the two types of gel.

3) Crystalline material, often with a lamellar structure as in the area at the extreme right of fig 7.44. Occurs in massive lumps, often too thick for the beam to penetrate.

4) Very fine grained crystalline material intimately mixed with the gel of type 2. Can sometimes be seen in the microscope as dark spots. Difficult to differentiate from the gel.

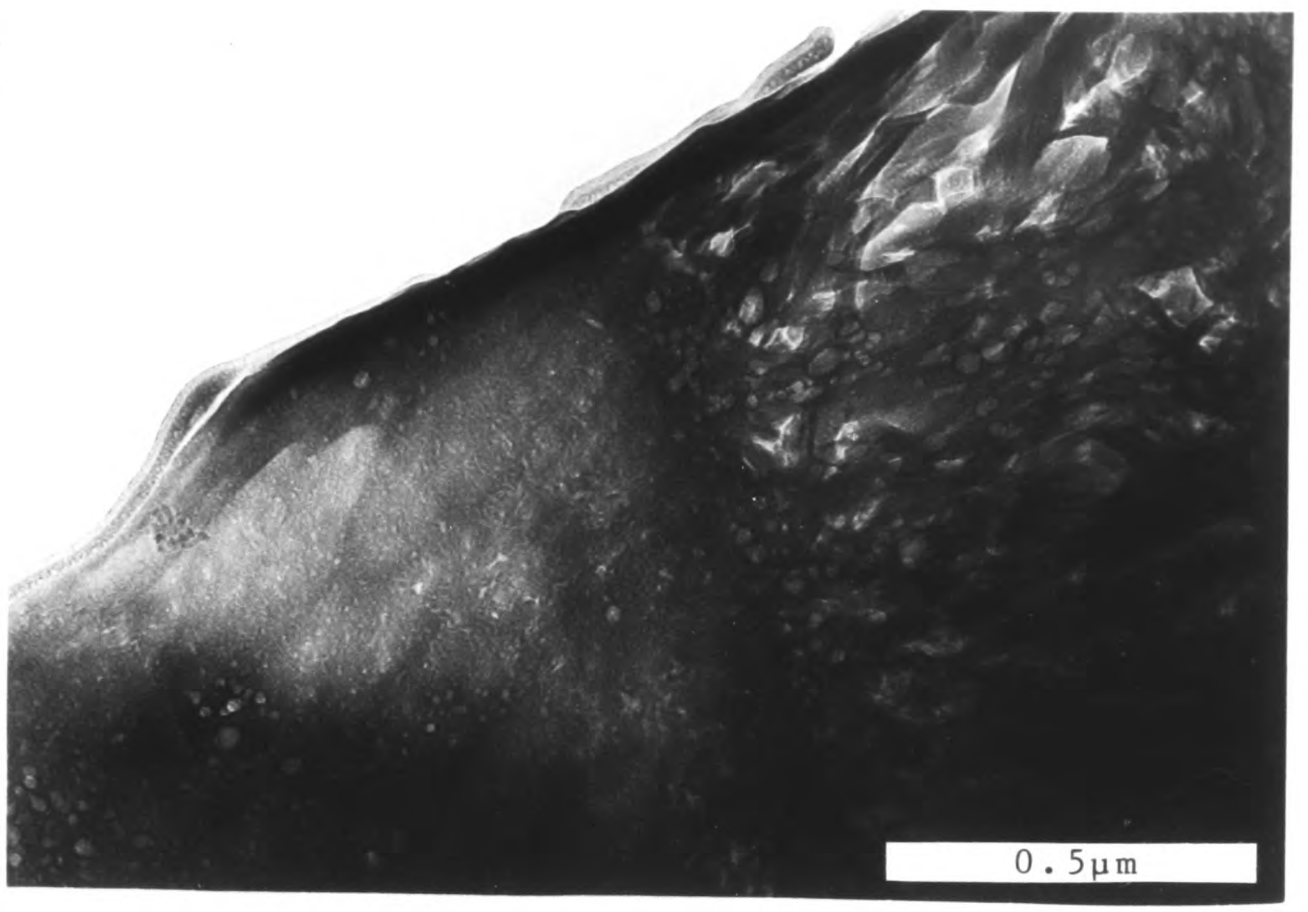

Fig 7.43 Transmission electron micrograph of a thinned section of C_3S (control) hydrated for 1 year showing two distinct types of gel material.

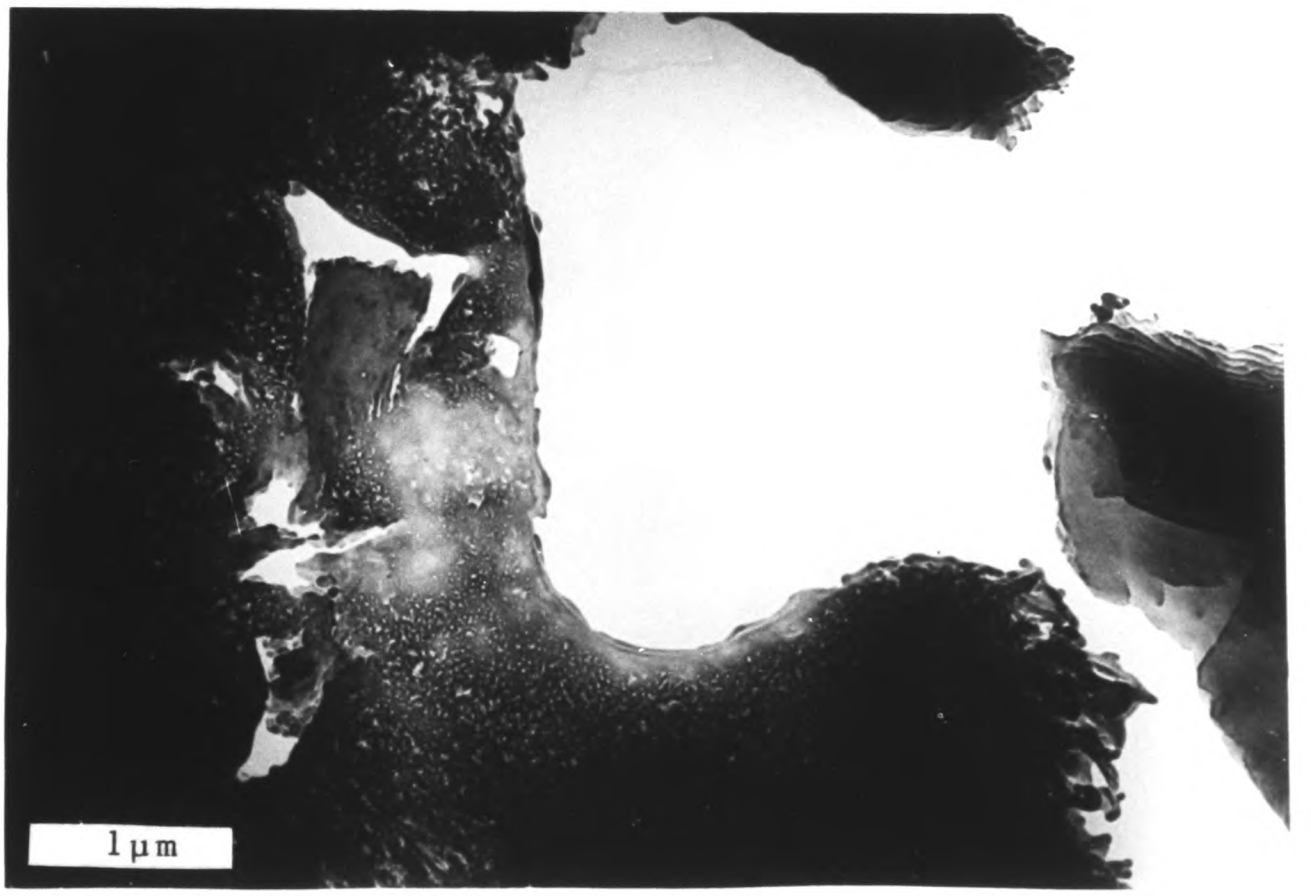

Fig 7.44 Transmission electron micrograph of a thinned section of C_3S ($CaCl_2$ accelerated) hydrated for $1\frac{1}{2}$ years showing similar features to fig 7.43.

Selected area diffraction patterns of materials 3 and 4 indicated them to be calcium hydroxide and calcium carbonate respectively. It is presumed that the calcium carbonate was originally calcium hydroxide which has since become carbonated. The inclusion of calcium carbonate or hydroxide in the areas used for analysis would lead to spuriously high C/S ratios. It was therefore necessary to ensure that any areas analysed were carbonate and hydroxide free. This was achieved by tilting the specimen to and fro, which shows up crystalline material by causing it to undergo rapid changes in diffraction contrast, and by ensuring the absence of diffraction spots in selected area diffraction patterns prior to analysis of those areas.

The same four types of material can be seen in the samples obtained from the pastes accelerated with $CaCl_2$ (fig 7.44). However, the gel of the $CaCl_2$ accelerated samples was much more easily beam-damaged then those of the control (fig 7.46), and this often made it difficult to differentiate the fine-grained textured gel from the fibrous textured gel.

X-ray analyses were carried out separately on the fine-grained and fibrous gel in the control sample. No such distinction was attempted for the $CaCl_2$ accelerated sample because of the scatter in the results from the control sample and because of the necessity to analyse beam damaged areas in which the two types of material could not be distinguished. The results of these analyses and those from the wollastonite standard are given in table 7.2.

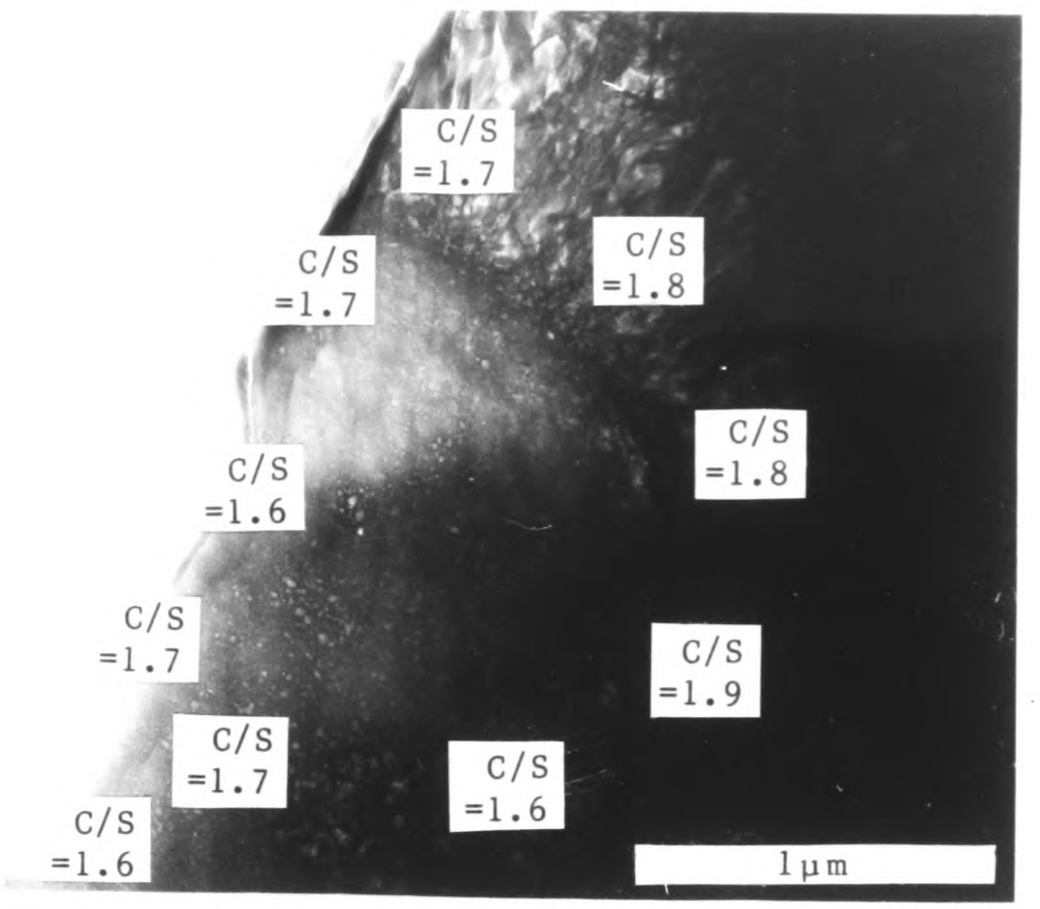

Fig 7.45 Thinned section of C_3S (control) used for chemical analysis. Areas used and values obtained are indicated.

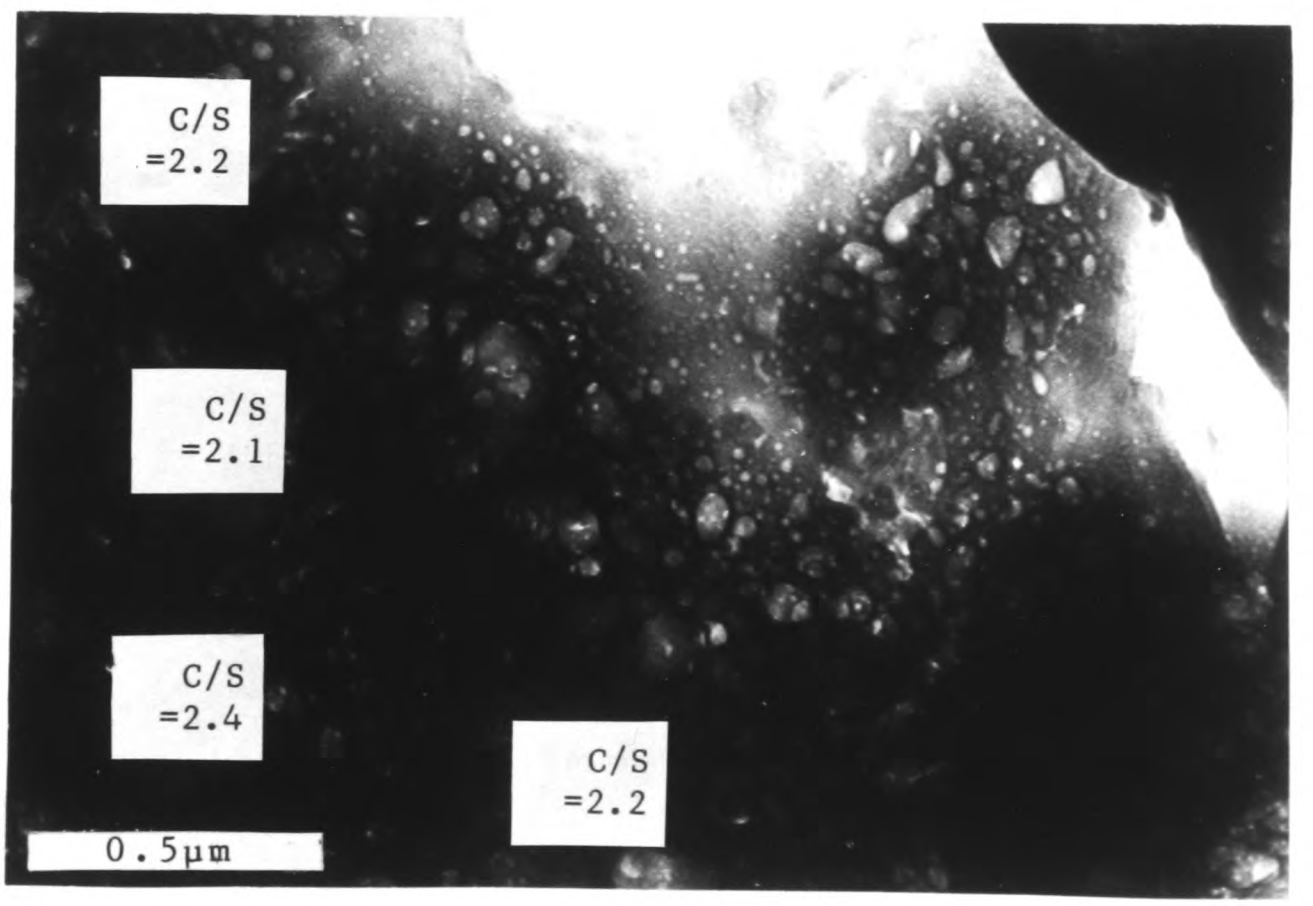

Fig 7.46 Thinned section of C_3S ($CaCl_2$ accelerated) used for chemical analysis. Areas used and values obtained are indicated.

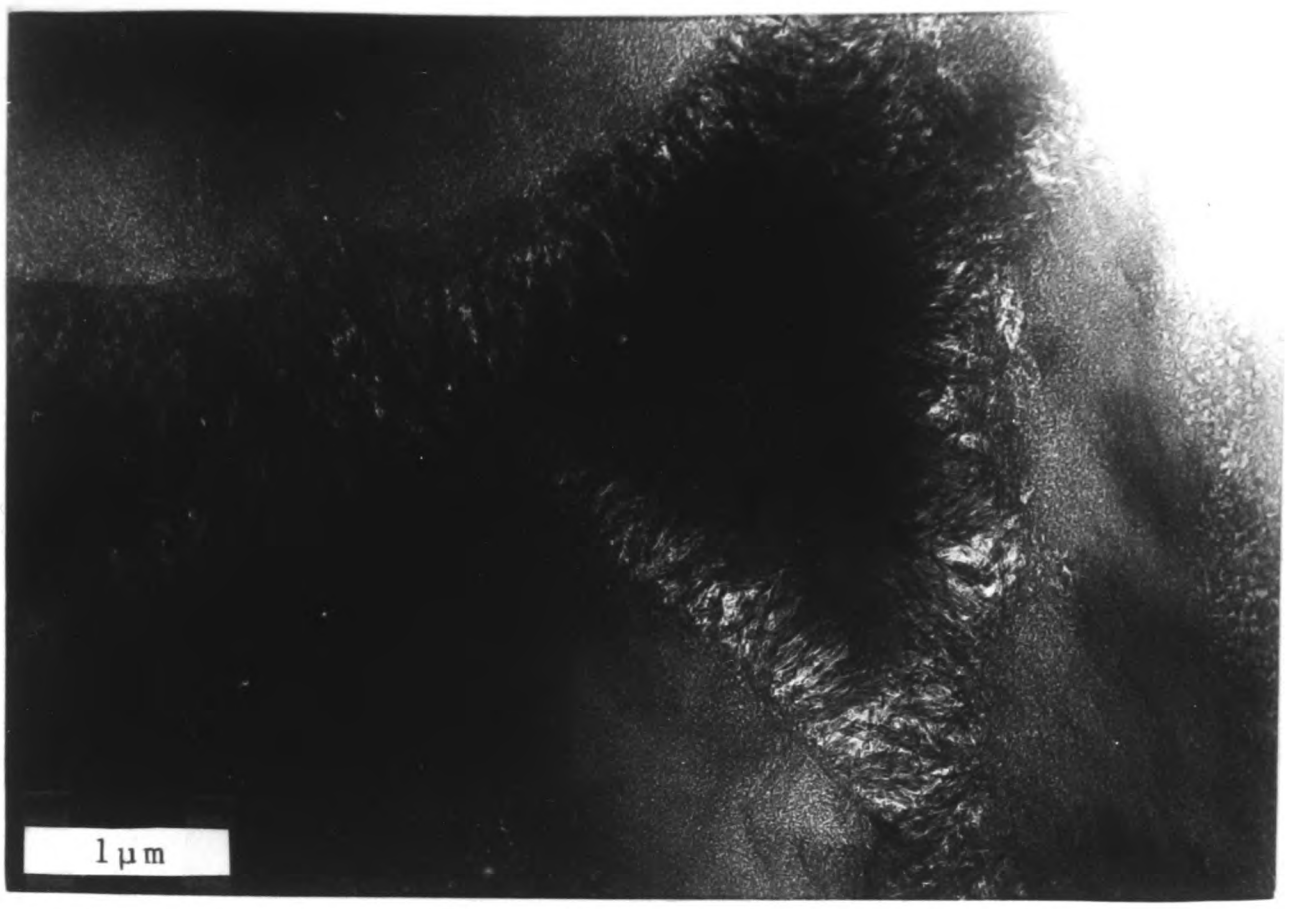

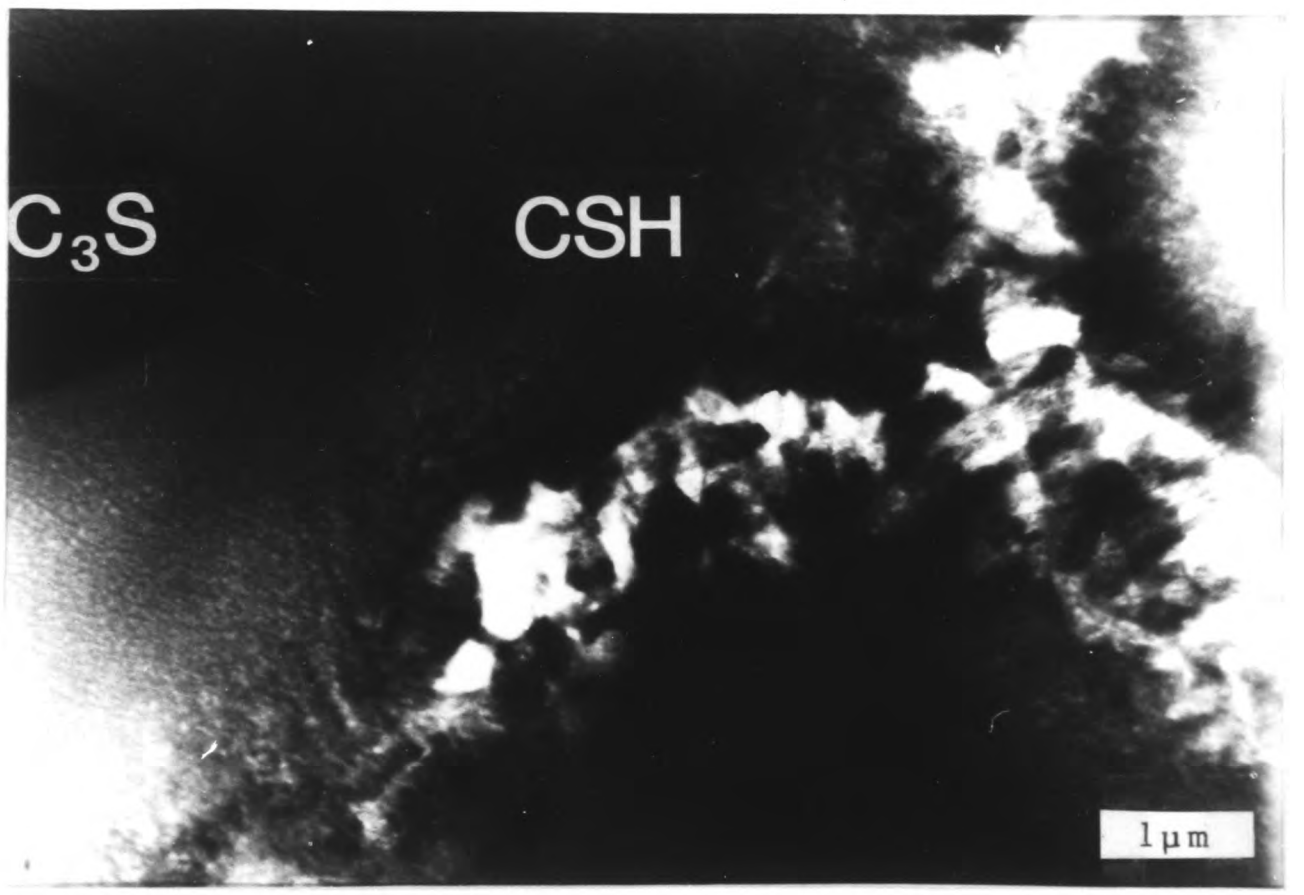

Fig 7.47 Transmission electron micrographs of thinned sections of C_3S (control) taken using the HVEM. The greater penetrating power of the higher energy electrons reveals cores of unreacted C_3S within the fine grained gel material.

Material type	Average Ca to Si peak ratio	Number of points	Standard deviation	C/S ratio
Wollastonite (C/S ratio = 1)	1.3	23	0.1	-
Control fine grained gel	2.4	16	0.3	1.8
Control fibrous gel	2.4	30	0.3	1.8
$CaCl_2$ fine and fibrous gel	2.7	14	0.3	2.1

Table 7.2: X-ray analysis results from the wollastonite standard and the control and $CaCl_2$ accelerated C_3S samples.

Figs 7.45 & 7.46 show areas from the control and $CaCl_2$ accelerated samples respectively from which some of the results were obtained. The areas analysed and the results obtained from those analyses are indicated.

7.5 Discussion and conclusions

7.5.a Morphological development

The slight blurring of the outlines of the grains during the first half hour of hydration of the control sample is taken to indicate the presence of a very thin gel coating covering the grain and debris particles alike. In contrast with previous observations (Fujii & Kondo 1974; Menetrier et al 1979; Jawed et al 1980; Jennings et al 1981) no product with a flakey or foil type of morphology was seen until later into the induction period. Groves (1983) has observed a similar thin continuous gel coating to completely cover the surface of thin sections of C_3S which had been hydrated for short lengths of time in the supernatant liquor of hydrating C_3S paste. These observations lend support to the theory that the very rapid fall off in rate of reaction after the initial heat peak and at the

start of stage 2 (see section 6.1.a) is due to the formation of some form of protective membrane which prevents further fast reaction from occurring. The nature of such a membrane and the manner in which it is protective can not be determined from the results obtained in this study.

QXDA, TGA and calorimetry indicate that while the reaction does continue during the induction period, it is very slow. The very gradual formation of small growths on the surface of the grains during the induction period supports this evidence. As the increase in the degree of hydration is so low during this stage it is likely that these growths account for most of the gel being formed; increases in the thickness of the layer of gel on the surface being minimal. Calculations by Stewart & Bailey (1983) have indicated that the growths can account for at least 3/4 of the reaction product up to the end of the acceleration stage.

Various suggestions have been made as to the manner in which these growths may be formed:

1) An osmotic pressure build up rupturing the gel layer and releasing supersaturated CSH solution into the surrounding solution where it immediately precipitates.

2) Formation of a compressed layer of CSH under the initial layer which forces the surface layer to crack and spall.

3) Reaction at active surface sites such as dislocations or other defects.

4) Rolling up of thin sheets of type E CSH as a result of drying.

The exact manner in which the growths are formed is still not clear. An interesting feature is that the growths increase both in numbers and in size during the induction period. This would appear to rule out a simple

'delayed nucleation of CSH' mechanism as being the cause of the induction period (see section 6.1.b.ii) because CSH has obviously nucleated and is growing. One further possible explaination which has not been mentioned before and which invokes the presence of a protective membrane as described above, is that this membrane surrounding the C_3S allows the ingress of water which reacts at the gel/grain interface to produce more CSH. Certain areas react faster than others, perhaps because they are associated with defects in the C_3S lattice, and at these the CSH builds up fastest, forming small mounds underneath the membrane. After a time the strain caused by the increase in size of the growths can not be accommodated by the membrane which then bursts. The CSH which is being formed under the membrane is formed under totally different conditions from that formed in the initial stages of the reaction and previous work and the results obtained in this work and mentioned in chapter 6 indicate that the CSH formed later on in the reaction has a different composition from the initially formed CSH. If, then, this different CSH is no longer protective then that would be reason enough for the end of the induction period and the start of the acceleration period.

During the acceleratory period the degree of hydration increases rapidly indicating that CSH is being formed in relatively large quantities. The increase in the size of the growths on the surface of the C_3S grains cannot account for all the CSH which is being formed and the generally accepted opinion is that during this stage the excess CSH is forming in the space left by the diminishing C_3S grain. Although not usually observed in immature pastes its formation can be inferred from the observation, in older fracture surfaces, of thick dense compact coatings of gel around the C_3S grains and underneath the outer more fibrous gel (e.g. figs 7.12, 7.27 & 7.39). Additional evidence for the presence of a thickening layer of CSH between the grain and the fibrous outer coating

is seen in the enlarged micrograph of the fracture surface of the specimen hydrated for six and a half hours (fig 7.11). On this specimen, in the regions without the tapered growths, the otherwise smooth surface gives the impression of being a substantial layer of gel material, rather than a thin surface coating on top of the C_3S grain, by virtue of the holes which penetrate into it and which are uncharacteristic of the surface of anhydrous C_3S.

As hydration progresses further the growths on the surface of the grains get larger and more numerous. It is envisaged that this could occur by one of three mechanisms. (a) Straight precipitation of new CSH on top of the old from the bulk solution, (b) precipitation of new CSH via an osmotic pump mechanism and (c) a change in the morphology of the outermost CSH. However, the low silicate ion level in solution at this stage suggests that straight precipitation is unlikely while the increasing thickness of the underlying gel would make the operation of an osmotic pump mechanism more and more difficult. The observations made in this study are, therefore, most easily rationalised by a mechanism in which at least some of the growths are formed by a splitting, peeling and rolling up of the top surface of the CSH. It is known that formation of CSH from C_3S involves a slight increase in volume and it has been suggested that the compression built up within the gel as a result of this volume increase could be relieved by a splitting/spalling process (Ball 1983). If such a mechansim were operating, then in order that the splits so formed did not continue down into the gel it is necessary to postulate a layer-like structure for at least the surface of the gel. Observations which support this postulation are (a) the formation of the growths in what looks like several interpenetrating layers, which it is thought arise from the splitting and rolling up of layers underneath the first, (b) what appears to be partially split and peeled growths on fig

7.11 - e.g. top left hand corner, directly below the roundish hole, (c) the formation of the star shaped groups of growths (figs 7.13 & 7.37) which are thought to arise by the the splitting of a single layer in a radial pattern with the eventual joining up of the splits and the rolling up of the fingers of CSH so formed, and (d) the high resolution micrograph of fig 7.38 which shows that, at least in the presence of sucrose, the growths are thin and wafer like and have a lamellar texture.

Interpretation of the TEM results is aided by similar work by Groves & Sinclair on identical material to that used in this work but examined in the HVEM. The greater penetrating capability of the higher energy electrons made it possible to observe thicker areas than those which could be viewed using the JEOL 100C electron microscope and has revealed the presence of residual C_3S grains (identified by their opaqueness - C_3S is much harder than CSH and so thins down at a much slower rate) inside some of the rounded areas of the fine-grained textured gel (fig 7.47 - courtesy Groves & Sinclair). It thus becomes clear that the fine-grained textured gel mentioned above is 'inner product' gel formed in the space left by the diminishing C_3S grain, while the fibrous textured gel is the 'outer product' or tapered growths, formed on the surfaces of the hydrating C_3S grains and seen on most of the fracture surfaces viewed in the scanning microscope. This implies that the tapered growths are a real phenomenon and not merely an artifact of drying.

The fibrous textured material observed in TEM, which corresponds to the outer fibrous product seen in SEM, has none of the porosity between the fibers which is observed in the SEM specimens. As the TEM specimens were much further hydrated than the SEM specimens it is clear that at some point CSH must be precipitated in the pore spaces between the grains so filling up the spaces between the fibers. This will be a slow process as

it involves diffusion of the calcium and silicate through an ever increasing CSH gel layer covering the C_3S grain. It is possible that areas such as those seen in fig 7.15 occur as a result of precipitation of CSH among the tapered growths leaving only the extremities of the growths protruding.

7.5.b Effect of admixtures

When C_3S is hydrated with either sucrose or $CaCl_2$ as admixtures the initial morphological development is similar to that of the control. A thin surface layer appears to form on the surface soon after mixing and small growths emerge from it during the induction period. After the end of the induction period marked differences between the various samples begin to be seen. Previous results (chapter 6) indicate that the C/S ratio of the gel product which is being formed at this time is the same in all cases. Any difference in morphology between the different samples must therefore arise by some other mechanism. One possibility is that the morphology may be affected by the rate at which the CSH is formed. Fast CSH formation may lead to a more disordered structure than slow CSH formation. If, as suggested above, the outer CSH has a layer structure which cracks and then peels, then the less ordered structure might be expected to crack and peel in a less ordered manner giving rise to large holes and branched fibres as seen on the $CaCl_2$ accelerated specimens. Conversely the more ordered structure might be expected to peel and crack in a more ordered fashion giving rise to the long needle like growths observed on the sucrose retarded specimens.

The effect of the admixtures on the physical properties of the gel is also seen in the difference in degree of hydration before a change in the mode of fracture (from inter-particlular to trans-particular) becomes apparent and in changes in the inner product gel revealed by such

fracture. Young et al (1973) report that a transition from inter-particular to trans-particular fracture usually occurs for C_3S pastes when the degree of hydration has reached ~50%. In this study the degree of hydration of the $CaCl_2$ accelerated sample was about 20% when such a changeover was first observed while for the sucrose retarded sample it was between 45 and 55%. Such a change in the mode of fracture must arise when the areas of contact between the gel surrounding neighbouring grains have developed to such a degree that they are as strong as the gel itself. An early changeover therefore points to a weakness in the gel. Close examination of the surfaces of the inner product gel revealed by such fracture shows that that produced in the presence of $CaCl_2$ has a rather coarser more porous structure than that formed in the presence of sucrose. Both of these observation suggest that the gel produced in the case of the $CaCl_2$ accelerated sample is weaker, more open and has a less ordered structure than that of the gel produced by the sucrose retarded samples. If this is true then it is likely that at least part of the accelerating action of $CaCl_2$ lies in the formation of a more open permeable gel network allowing increased rates of diffusion to and from the C_3S/gel interface and hence leading to an enhanced reactivity. Similarly it is likely that part of the retarding action of sucrose lies in the formation of a more densely packed, less permeable gel network through which diffusion can only occur with difficulty.

The temperature variation of the rate parameter (K) obtained by fitting the Avrami equation to calorimetric curves obtained from control and $CaCl_2$ accelerated samples (chapter 5) has led to the suggestion that acceleration by $CaCl_2$ arises from increases in the molecular transport terms rather than by decreases in the activation energy for the rate determining process. The tentative conclusion reached in this chapter,

that the gel produced in the case of $CaCl_2$ acceleration is more open and permeable than that of the control, implies acceleration by a consequent increase in molecular transport to and from the C_3S/CSH interface and hence is in accord with the suggestions made in chapter 5.

7.5.c X-ray analysis

X-ray analysis of thinned specimens potentially provides a very easy method of elemental analysis of very small areas. It overcomes many of the drawbacks found in X-ray analysis of thick specimens such as the spreading of the beam, and hence the analysed area, into the material below and to the side of the beam and the necessity for absorption corrections to be applied to the data before a correct analysis can be achieved. It does, however, have some limitiations. The most important of these is the smallness of the volume which is being analysed which limits the count rate and increases the liklihood of beam damage. Obtaining the best results is then a matter of balancing increases in the count rate, and hence reductions in the statistical variations between analyses, against the resultant increase in beam damage. In this study no attempt was made to analyse the smallest possible areas as the count rates from these would have been too low. Instead, areas of about 0.25 - 0.5 microns square were scanned in a rastor fashion and the analyses taken from these. Count rates could then be kept reasonably high without too much beam damage (note that the beam damage seen in figs 7.43, 7.45 & 7.46 is a result of the electron beam when viewing the specimen, not a result of the electron beam during analysis). In spite of this, the experimental scatter in the results was relatively high (see table 7.2). The scatter in the analyses from the wollastonite standard is lower than that for the CSH gel. This would seem to indicate that at least part of the scatter arises from small compositional variations in the gel itself.

The value obtained for the C/S ratio of the gel of the control sample of about 1.8 is in close agreement with the value obtained by the completely independent methods of TGA and QXDA (chapter 6). The value obtained for the $CaCl_2$ accelerated sample of 2.1 is slightly higher than expected on the basis of the results of chapter 6. Whether this is a real result or not remains in doubt as the experimental scatter in the analyses is large. It is also quite possible that the beam damage may have contributed to the high values.

CHAPTER 8

CONCLUSIONS AND SUGGESTIONS FOR FURTHER WORK

The following conclusions can be drawn from the results obtained in this study.

8.1 Calorimetry,

The conduction calorimeter, specially adapted so as to be sensitive enough to measure the heat output of small quantities of synthetic cement compounds, operated entirely satisfactorily. As long as the standard operating technique was followed both reproducible and accurate measurements of the rate of heat output of the hydrating cement could be obtained.

8.2 Factors affecting the reactivity of C_3S

The overall reactivity of C_3S is not an inherent property of the C_3S itself but is affected, not only by the hydration conditions, such as temperature, admixture and water/cement ratio, but also by other, less well characterised, factors influenced by the synthesis and storage conditions. In previous studies the effect of many of these factors has either not been recognised or has been ignored.

It is often not possible to deduce the influence of a factor on the reactivity of C_3S because altering that one factor will alter others as well. Thus for example the incorporation of impurity ions influences the grindability of the raw material. Therefore, even if identical grinding conditions are employed, any changes in reactivity must arise both from the presence of the impurity ions and from changes in the particle size distribution. Until such time as it becomes possible to predict the nature and extent of the influence of all of these factors it is not

strictly valid to draw conclusions from differences (or similarities) in reactivity of different preparations. It is recommended that when comparisons of different preparations are necessary (as in the study of the effects of impurity ions on the reactivity of C_3S), in order to make such comparisons more valid, a standard method of preparation should be adopted ensuring that, as far as is possible, the heating and cooling conditions during synthesis, the particle size distribution of the ground samples and the storage conditions are kept identical. Where possible, however, all comparisons should be made on the same preparation of C_3S. For this purpose sufficient C_3S for all experiments should be synthesised, ground and stored in a dry inert atmosphere with provision for the withdrawal of samples without the necessity of exposing the remainder of the batch to the atmosphere. Further, frequent tests should be made to ensure that the reactivity of the batch is not changing as a result of the storage conditions.

Most, if not all, of the changes in reactivity as a result of altering the synthesis and storage conditions, can be explained on the basis of changes in the nature and composition of the surface of the C_3S (by atmospheric hydration/carbonation or by surface decomposition/ recombination) and by changes in the concentration of defects in the C_3S crystal lattice (by stabilisation/destabilisation of the lattice resulting from the presence of impurity ions or by annealing out/quenching in of defects resulting from storage or heat treatment). It must be noted, however, that as yet, the evidence for such changes in surface composition are slight and no attempts have been made to find a correlation between the amount of change in the composition of the surface (e.g. degree of atmospheric hydration or carbonation) and the reactivity change which may result from it. Similarly, the experimental evidence for changes in the concentration of defects as a result of

changing the synthesis or storage conditions is also small. In most cases where defects are cited as contributing to the reactivity of the C_3S, their presence and the processes which change the concentration of the defects, and hence the reactivity of the C_3S, are assumed. In the few cases where some measure of the concentration of defects has been attempted, it has not been possible to fully characterise the defects nor has it been possible to determine the manner in which their presence increases the reactivity of the C_3S. It is clear that a large amount of work remains to be done in this area before the true causes of the changes in reactivity of C_3S can be fully established.

8.3 Mathematical modelling of C_3S hydration

The Avrami equation can, if the origin is suitably shifted, be made to fit experimental calorimetric curves from the end of the induction period to well after the end of the acceleratory period. The variations in the rate parameter (K) derived from such a fitting procedure carried out on calorimetric curves obtained at different temperatures both with and without $CaCl_2$, are consistent with the $CaCl_2$ causing the acceleration by increases in the transport frequencies rather than by a decrease in the activation energy of the rate determining process.

The apparent activation energies, derived by fitting the temperature variation of the rate parameter to an Arrhenius type expression, are not true chemical activation energies and can not be compared with them, though they can be compared amongst themselves.

The indeterminacy of the power exponent (n) of the Avrami equation and the necessity of offsetting its origin to obtain a good fit to calorimetric rate data, means that, even if it could be shown that nucleation and growth processes, as described by the Avrami equation, are

responsible for the reaction during the early acceleratory period, the mechanistic information which can be derived by fitting it to calorimetric heat output curves is small.

The Avrami equation can allow for variations in reactivity with changes in the specific surface of the C_3S by variations in the rate parameter (K). It cannot, however, allow for the changes in reactivity observed in this study which resulted from modifications in the particle size distribution. It is doubtful, therefore, that nucleation and growth processes, as described by the Avrami equation, are the sole contributers to the acceleratory stages of hydration.

8.4 Chemical and morphological studies

The chemical studies indicate the formation of two types of CSH gel during the hydration reaction. The first is formed during stages 1 & 2 (i.e. before the end of the induction period) and has a C/S ratio close to 3. The precise value of the C/S ratio could not be determined because of the inaccuracy of the analysis methods at these early stages. The second is formed after the end of the induction period, during stages 3, 4 & 5 and has a C/S ratio of 1.7 which is in close agreement with values obtained by other workers and with the values obtained by X-ray analysis of thinned sections of CSH in the transmission microscope. Although the water contents of the gel was also determined it was found to be dependent on the method of preparation and hence is not comparable with results obtained by other methods. Acceleration by $CaCl_2$ and retardation by sucrose was found not to alter the C/S ratio of the gel produced during the latter part of the reaction. Comparison of the C/S ratios of the gel produced during the early part of the reaction could not be made because of the reasons mentioned above.

The cause of the change in the length of the induction period and the difference in the speed of growth of the gel as a result of the presence of the admixtures is still not clear, though the morphological studies and the kinetic modelling using the Avrami equation suggest that changes in the physical characteristics of the gel which would alter the rate of transport of reactants and products to and from the C_3S/CSH interface (porosity, permeability etc.) play a part in determining the rate at which the gel is produced.

8.5 Suggestions for further work

a) Development of methods to measure the nature and concentration of defects in the C_3S crystal lattice, to determine their influence, if any, on the reactivity of C_3S and to find how the various factors discussed in this work influence the concentration of those defects.

b) Development of methods to measure changes in the surface composition of the C_3S to determine whether it influences the reactivity of C_3S. Determination of exactly how the surface is influenced by the various factors discussed in this work.

c) A more detailed study of the effect of particle size on the early hydration reaction of C_3S and the development of mathematical models to explain it.

d) Characterisation of the gel produced in the presence of different admixtures (permeability, pore size distribution etc.) to ascertain the changes resulting from the presence of the admixtures. Correlation of the changes with accelerating or retarding ability.

e) A more detailed study of the reaction during the induction and very early acceleratory periods involving calorimetry, QXDA, TGA or DTGA,

electron microscopy (SEM and if possible wet cell hydration of thinned specimens of C_3S) and analysis of the solution phase using normal water/cement ratios in an attempt to completely characterise the composition and the amount of the CSH gel being produced.

f) Similar work to that described in this work and above on the remainder of the cement compounds.

APPENDIX I

PROGRAM TO FILE RAW DATA AND PERFORM CALCULATIONS

```
100  HOME
110  CLEAR
120  GOSUB 8000
130  FOR N = 1 TO 5 STEP 4
140  VTAB (N): PRINT "********************
     ********************"
150  NEXT
160  FOR N = 2 TO 4
170  VTAB (N): PRINT "*";: HTAB (40): PRINT
     "*"
180  NEXT
190  NORMAL : VTAB (3): HTAB (11): PRINT "C
     ALOX DATA PROCESSING"
200  VTAB (8): PRINT "ENTER OPTION REQUIRED
     ;"
210  VTAB (10): PRINT "'1' - CREATE FILE"
220  PRINT "'2' - AMEND FILE"
230  PRINT "'3' - DELETE FILE"
240  PRINT "'4' - FILE INDEX"
250  PRINT "'5' - CALCULATIONS ON FILED DAT
     A"
260  PRINT "'6' - AVRAMI FITTING"
270  PRINT "'7' - GRAPH PLOTTING"
280  PRINT "'8' - START NEW DISK"
285  PRINT "'9' - QUIT"
290  VTAB (21)
300  POKE 34,20: POKE 35,21
310  INPUT "OPTION REQUIRED = ";A
320  POKE 34,0: POKE 35,24
325  IF A = 9 THEN  TEXT : HOME : END
330  ON A GOTO 1000,2000,3000,4000,5000,600
     0,6500,6700
340  VTAB (21): CALL  - 958
350  GOTO 300
1000  HOME
1010  VTAB 4: PRINT "'1'...38 POINTS TO 100
     0 MINS."
1020  PRINT "'2'...38 POINTS TO 1400 MINS."

1030  PRINT "'3'...FIXED TIME INTERVAL"
1040  PRINT "'4'...VARIABLE TIME AND HEAT"
1050  POKE 35,1
1060  VTAB 1: INPUT "ENTER DATA FILE TYPE R
     EQUIRED:";A%
1070  IF A% < 1 OR A% > 4 GOTO 1060
1080  POKE 35,24
1090 F = 0
1100  IF A% = 1 THEN F = 1000
1110  IF A% = 2 THEN F = 1400
1120  IF A% = 3 THEN  POKE 34,9: POKE 35,10
     : VTAB 10: INPUT "ENTER TIME INTERVAL (
     MINS):";F: POKE 34,0: POKE 35,24
1122  VTAB 12: INPUT "MULTIPLICATION FACTOR
     (Y/N) ";A$
1123  IF A$ = "N" THEN MF = 1: GOTO 1130
1124  IF A$ <  > "Y" THEN  PRINT  CHR$ (7);
     : GOTO 1122
1125  VTAB 14: INPUT "FACTOR=";MF
1130 A$ = "":ER% = 0:CN% = 0:BL = 0:TM = 0:
     TP = 298:W = 0: GOSUB 7000
1140  HOME
1150  VTAB 10: PRINT "DATA POINT ENTRY:": PRINT
     : HTAB 5: PRINT "ENTER HEAT=-1 TO CORRE
     CT LAST ENTRY. ": PRINT
1160  IF A% = 3 OR A% = 4 THEN  HTAB 5: PRINT
     "ENTER HEAT=9999 TO END DATA INPUT": GOTO
     1260
1170  ONERR  GOTO 9000
1180 FL = 1:F1 =  - 1
1190  PRINT UN$;CT$;F;",D1"
1200  PRINT OP$;CT$;F
1210  PRINT RD$;CT$;F
1220  FOR N = 0 TO 37: INPUT TI(N): NEXT
1230  PRINT CL$
1240  POKE 216,0
1250 TI(N) = 9999
1260  POKE 35,0
1270  VTAB 24
1280 N% = 0:CL% = 0:V% = 22
1290  VTAB 20: PRINT "PT. TIME HEAT   TIME
     HEAT   TIME HEAT"
1300  INVERSE : VTAB 22: HTAB 1: PRINT 1: NORMAL

1310  VTAB 24: HTAB 1: PRINT "PT.";: INVERSE
     : PRINT N% + 1;: NORMAL : PRINT " "; TAB(
     15);"     "; TAB( 25);"      "
1320  IF A% = 4 THEN  VTAB 24: HTAB 10: INPUT
     "TIME=";TI(N%): GOTO 1350
1330  IF A% = 3 THEN TI(N%) = F * N%
1340  IF TI(N%) = 9999 THEN 1450
1350  VTAB 24: HTAB 10: PRINT "TIME=";TI(N%
     );: HTAB 20: INPUT "HEAT=";HT(N%)
1360  IF HT(N%) =  - 1 THEN 1420
1370  IF A% = 3 OR A% = 4 THEN  IF HT(N%) =
     9999 THEN  GOTO 1450
1375 HT(N%) = HT(N%) * MF
1380  VTAB V%: HTAB (CL% * 12 + 5)
1390  PRINT TI(N%);" "; TAB( CL% * 12 + 10)
     ;( INT (HT(N%) * 100 + .5)) / 100;"  ";

1400 N% = N% + 1:CL% = CL% + 1: IF CL% = 3 THEN
     CL% = 0: POKE 35,22: PRINT : INVERSE : PRINT
     N% + 1;: NORMAL : POKE 35,0:V% = V% + 1
     : IF V% = 23 THEN V% = 22
1410  GOTO 1310
1420 N% = N% - 1: IF N% < 0 THEN N% = 0: GOTO
     1310
```

```
1430 CL% = CL% - 1: IF CL% =  - 1 THEN CL% =
    2:V% = V% - 1: IF V% = 0 THEN V% = 1
1440  GOTO 1310
1450 N% = N% - 1
1460  POKE 35,24
1470  HOME : VTAB 12: HTAB 9: PRINT "FILING
     DATA-PLEASE WAIT"
1480  ONERR  GOTO 9000
1490 ER$ = "     "
1500 AA$ =  STR$ (ER%):ER$ = AA$ +  RIGHT$
    (ER$,5 -  LEN (AA$))
1510 FL = 2:F1 =  - 2
1520  PRINT UN$;IM$;",D2"
1530  PRINT OP$;IM$
1540  PRINT RD$;IM$
1550  INPUT LN$
1560  INPUT TN
1570  PRINT OP$;CD$;ER$
1580  PRINT WR$;CD$;ER$
1590  PRINT "00000"
1600  PRINT LN$
1610  PRINT N%: PRINT A$: PRINT CN%: PRINT
    BL: PRINT TM: PRINT TP: FOR N = 0 TO N%
    : PRINT TI(N): PRINT HT(N): NEXT N: PRINT
    W
1620  PRINT CL$;CD$;ER$
1630  PRINT LK$;CD$;ER$
1640  IF TN = 0 GOTO 1720
1650 FL = 3:F1 =  VAL (LN$)
1660  PRINT UN$;CD$;LN$
1670  PRINT OP$;CD$;LN$
1680  PRINT WR$;CD$;LN$
1690  PRINT ER$
1700  PRINT CL$;CD$;LN$
1710  PRINT LK$;CD$;LN$
1720  PRINT OP$;IM$
1730  PRINT WR$;IM$
1740  PRINT ER$
1750  PRINT TN + 1
1760  PRINT CL$
1770  POKE 216,0
1780  GOTO 100
2000  HOME : PRINT "***          AMEND  FIL
    E            ***": POKE 34,2
2010  VTAB 3: INPUT "ENTER NO. OF FILE TO B
    E AMENDED:";ER$
2021  IF  LEFT$ (ER$,1) = "/" THEN ER% =  VAL
    ( RIGHT$ (ER$, LEN (ER$) - 1))
2022  IF  LEFT$ (ER$,1) <  > "/" THEN ER% =
     VAL (ER$)
2023  ONERR  GOTO 9000
2024 FL = 10:F1 = ER%
2025  IF  LEFT$ (ER$,1) = "/" THEN 2100
2040  POKE 35,24: PRINT UN$;CD$;ER%",D2": PRINT
    OP$;CD$;ER%: PRINT RD$;CD$;ER%: INPUT N
    N$: INPUT LN$: INPUT X: INPUT A$: PRINT
     CHR$ (4)
2050  VTAB 7: PRINT "DATA FILE NO.";ER%
2060  PRINT : PRINT "ADMIXTURE:";A$
2070  VTAB 11: INPUT "IS THIS IT? (Y/N) ";A
    A$
2080  IF AA$ = "N" THEN  TEXT : GOTO 2000
2090  IF AA$ <  > "Y" THEN 2070
2100  PRINT UN$;CD$;ER%;",D2": PRINT RD$;CD
    $;ER%: INPUT NN$: INPUT LN$: INPUT N%: INPUT
    A$: INPUT CN%: INPUT BL: INPUT TM: INPUT
    TP: FOR N = 0 TO N%: INPUT TI(N): INPUT
    HT(N): NEXT N: INPUT W: PRINT CL$
2110  POKE 216,0
2120 E% = ER%
2130  GOSUB 7000
2140 ER% = E%
2150  VTAB 20: PRINT "DO YOU WANT TO CHANGE
     ANY DATA POINTS?",,,"(Y/N) ";: INPUT "
    ";AA$
2160  IF AA$ = "N" THEN 2270
2170  IF AA$ <  > "Y" THEN 2150
2180  HOME : VTAB 22: PRINT "PT. TIME HEAT
      TIME HEAT   TIME HEAT"
2190  PRINT : FOR N = 0 TO N% STEP 3
2200  INVERSE : PRINT N + 1;: NORMAL
2210  FOR N1 = 0 TO 2: HTAB (N1 * 12 + 5): PRINT
    TI(N + N1); TAB( N1 * 12 + 10);( INT (H
    T(N + N1) * 100 + .5) / 100);: NEXT : PRINT

2220  NEXT : PRINT : PRINT : PRINT : PRINT
    : PRINT : PRINT
2230  VTAB 20: INPUT "WHICH PT. NO. (-1 TO
    END);";N
2240  IF N =  - 1 THEN 2270
2250 N = N - 1: IF N < 0 OR N > N% THEN 223
    0
2260  VTAB 20: CALL  - 958: PRINT "OLD TIME
    :";TI(N): VTAB 22: PRINT "OLD HEAT:";HT
    (N): VTAB 20: HTAB 20: INPUT "NEW TIME=
    ";TI(N): VTAB 22: HTAB 20: INPUT "NEW H
    EAT=";HT(N): VTAB 20: CALL  - 958: GOTO
    2230
2270  ONERR  GOTO 9000
2280 F1 = ER%:FL = 11
2290  PRINT OP$;CD$;ER%
2300  PRINT WR$;CD$;ER%
2310  PRINT NN$: PRINT LN$: PRINT N%: PRINT
    A$: PRINT CN%: PRINT BL: PRINT TM: PRINT
    TP: FOR N = 0 TO N%: PRINT TI(N): PRINT
    HT(N): NEXT N: PRINT W
2320  PRINT CL$
2330  PRINT LK$;CD$;ER%
2340  POKE 216,0
2350  TEXT : GOTO 100
3000  HOME : PRINT "***          DELETE FIL
    ES           ***": POKE 34,2: POKE 35,
    3
```

```
3010  VTAB 3: INPUT "ENTER NO. OF FILE TO B
    E DELETED:";ER%
3020  ONERR  GOTO 9000
3030 FL = 4:F1 = ER%
3040  POKE 35,24: PRINT UN$;CD$;ER%",D2": PRINT
    OP$;CD$;ER%: PRINT RD$;CD$;ER%: INPUT N
    N$: INPUT LN$: INPUT X: INPUT A$: PRINT
     CHR$ (4)
3045  PRINT LK$;CD$;ER%
3050  VTAB 7: PRINT "DATA FILE NO.";ER%
3060  PRINT : PRINT "ADMIXTURE:";A$
3070  VTAB 11: INPUT "IS THIS IT? (Y/N) ";A
    A$
3080  IF AA$ = "N" THEN  TEXT : GOTO 3000
3090  IF AA$ <  > "Y" GOTO 3070
3100  PRINT UN$;CD$;ER%
3110  PRINT DE$;CD$;ER%
3120  IF LN$ = "00000" GOTO 3190
3130 FL = 5:F1 =  VAL (LN$)
3140  PRINT UN$;CD$;LN$
3150  PRINT OP$;CD$;LN$
3160  PRINT WR$;CD$;LN$
3170  PRINT NN$: PRINT CL$
3180  PRINT LK$;CD$;LN$
3190  IF NN$ = "00000" GOTO 3300
3200 FL = 6:F1 =  VAL (NN$)
3210  PRINT UN$;CD$;F1
3220  PRINT OP$;CD$;F1
3230  PRINT RD$;CD$;F1
3240  INPUT NM$
3250  PRINT CL$
3260  PRINT OP$;CD$;F1
3270  PRINT WR$;CD$;F1
3280  PRINT NM$: PRINT LN$
3290  PRINT CL$: PRINT LK$;CD$;NN$
3300 FL = 7:F1 =  - 2
3310  PRINT UN$;IM$
3320  PRINT OP$;IM$
3330  PRINT RD$;IM$
3340  INPUT A$: INPUT NT
3350  PRINT CL$
3360  IF ER% =  VAL (A$) THEN A$ = LN$
3370  PRINT OP$;IM$
3380  PRINT WR$;IM$
3390  PRINT A$: PRINT NT - 1
3400  PRINT CL$: PRINT LK$;IM$
3410  POKE 216,0
3420  GOTO 100
```

```
4000  HOME : PRINT "***        DATA FILE IN
    DEX           ***": POKE 34,2
4010  VTAB 4: INPUT "ENTER THE START FILE N
    O.";SF
4020  VTAB 6: INPUT "ENTER THE END FILE NO.
     ";EF
4030  IF SF >  = EF THEN  GOTO 4010
4040  HOME : VTAB 10: PRINT "    SEARCHING
    FILES-PLEASE WAIT": POKE 34,12
4050  ONERR  GOTO 9000
4060 F1 =  - 2:FL = 8
4070  PRINT UN$;IM$;",D2"
4080  PRINT OP$;IM$
4090  PRINT RD$;IM$
4100  INPUT LN$: INPUT NT
4110  PRINT CL$: PRINT LK$;IM$
4120  DIM A$(NT,1)
4130 I = NT - 1
4140 A$(I,0) = LN$
4150 F1 =  VAL (LN$):FL = 9
4160  PRINT OP$;CD$;LN$
4170  PRINT RD$;CD$;LN$
4180  INPUT LN$: INPUT LN$: INPUT X: INPUT
    A$
4190  PRINT CL$
4210 A$(I,1) = A$
4220 I = I - 1: IF I >  = 0 GOTO 4140
4230  GOSUB 10000
4240  POKE 34,2: HOME
4245 MIN =  - 1
4250  FOR I = 0 TO NT - 1: IF  VAL (A$(I,0)
    ) < SF THEN MIN = I: GOTO 4290
4260  IF  VAL (A$(I,0)) > EF THEN 4290
4270 MAX = I
4280  PRINT A$(I,0);: HTAB 7: PRINT A$(I,1)

4290  NEXT : PRINT : PRINT
4300  VTAB 23: INPUT "DO YOU WANT A HARD CO
    PY (Y/N):";AA$: IF AA$ = "N" THEN 100
4310  IF AA$ <  > "Y" THEN 4300
4320  PRINT D$;"PR£1"
4330  POKE 1657,131: PRINT : PRINT D$;"PR£0
    ": PRINT D$;"PR£1"
4340  PRINT : PRINT : PRINT : PRINT  CHR$ (
    14);"CALOX DATA FILE INDEX": PRINT
4345  PRINT  CHR$ (15)
4350 I =  INT ((MA - MI + 1) / 2): FOR N =
    MI + 1 TO MI + I
4360  PRINT A$(N,0);"  ";A$(N,1);
```

```
4370  IF N + I > MAX THEN 4390
4380  HTAB (39): PRINT  SPC( 41);A$(N + I,0
   );"  ";A$(N + I,1)
4390  NEXT
4400  PRINT  CHR$ (18)
4410  PRINT D$;"PR#0"
4420  TEXT : GOTO 100
5000  HOME : PRINT "***    CALCULATIONS ON
   FILED DATA    ***": POKE 34,2
5005  HOME : VTAB 3: INPUT "ENTER FILE NO.
   ";ER$
5010  IF  LEFT$ (ER$,1) = "/" THEN ER% =  VAL
    ( RIGHT$ (ER$, LEN (ER$) - 1))
5012  IF  LEFT$ (ER$,1) <  > "/" THEN ER% =
     VAL (ER$)
5020 FL = 12:F1 = ER%
5025  IF  LEFT$ (ER$,1) = "/" THEN 5090
5030  PRINT UN$;CD$;ER%",D2": PRINT OP$;CD$
   ;ER%: PRINT RD$;CD$;ER%: INPUT NN$: INPUT
   LN$: INPUT X: INPUT A$: PRINT  CHR$ (4)

5035  PRINT LK$;CD$;ER%
5040  VTAB 7: PRINT "DATA FILE NO.";ER%
5050  PRINT : PRINT "ADMIXTURE:";A$
5060  VTAB 11: INPUT "IS THIS IT (Y/N) ";AA
   $
5070  IF AA$ = "N" THEN 5000
5080  IF AA$ <  > "Y" THEN 5060
5090  PRINT OP$;CD$;ER%;",D2": PRINT RD$;CD
   $;ER%: INPUT NN$: INPUT LN$: INPUT N%: DIM
   HH(N%),Q(N%),TT(N%): INPUT A$: INPUT CN
   %: INPUT BL: INPUT TM: INPUT TP
5091  FOR N = 0 TO N%: INPUT TI(N): INPUT H
   H(N):HT(N) = HH(N) - BL: NEXT : INPUT W
   : PRINT CL$
5096  IF CN% = 11 THEN K1 = .0132:K2 = 1.03
   95
5097  IF CN% = 12 THEN K1 = 0.015:K2 = 0.6
5100  IF CN% = 10 THEN K1 = .0149:K2 = 1.07
   9
5110  IF CN% = 3 THEN K1 = .01971:K2 = 12.5
   37
5120  IF CN% = 4 THEN K1 = .02125:K2 = 13.5
   97
5130  IF CN% = 7 THEN K1 = .0195:K2 = 15.45

5140 Q(0) = (K2 * (HT(1) - HT(0)) / ((TI(1)
    - TI(0)) * 60) + K1 * HT(0)) * 1000 /
   W
5150 Q(N%) = (K2 * (HT(N%) - HT(N% - 1)) /
    ((TI(N%) - TI(N% - 1)) * 60) + K1 * HT(
   N%)) * 1000 / W
5160  FOR N = 1 TO N% - 1:Q(N) = (K2 * (HT(
   N + 1) - HT(N - 1)) / ((TI(N + 1) - TI(
   N - 1)) * 60) + K1 * HT(N)) * 1000 / W
5170  NEXT N
5180 TT = 0: FOR N = 1 TO N%
5190 TT = TT + 0.5 * (Q(N - 1) + Q(N)) * (T
   I(N) - TI(N - 1)) * 60
5200 TT(N) = TT: NEXT
5210  PRINT D$;"PR#1": PRINT : POKE 1657,80
   : PRINT : PRINT
5212  PRINT  CHR$ (14);"*******************
   ***********************"
5213  PRINT  CHR$ (14);"*
                        *"
5214  PRINT  CHR$ (14);"*        CALOX DATA
    PROCESSING          *"
5215  PRINT  CHR$ (14);"*
                        *"
5216  PRINT  CHR$ (14);"*******************
   ***********************"
5240  PRINT : PRINT : PRINT  CHR$ (14);A$
5250  PRINT : PRINT "CALOX NO.";CN%;"  EXPE
   RIMENTAL RUN NO.";ER%
5260  PRINT "TEMPERATURE = ";TP;"K   WATER/
   CEMENT RATIO = 0.5"
5270  PRINT "K1=";K1;"(J/S/MV),  K2=";K2;"(
   J/MV)"
5280  PRINT "BASE LINE VOLTAGE CORRECTION:
   ";BL;" MV"
5290  PRINT "TIME  TO MINIMUM IN HEAT CURVE
   : ";TM;" MINUTES"
5300  PRINT "INTEGRATED AREA UNDER SECOND H
   EAT PEAK: "; INT (TT(N%) / 10 + .5) / 1
   00;" (J/G)"
5310  PRINT
5320  PRINT " TIME   RAW   CORRECTED  RATE
   OF HEAT  INTEGRATED"
5330  PRINT "        DATA    DATA      EVOL
   UTION    HEAT OUTPUT"
5340  PRINT "(MINS)  (MV)    (MV)     (J/S/
   KG)         (J/G)"
5350  PRINT
5360  FOR N = 0 TO N%
```

```
5370  PRINT  SPC( 1);TI(N) + TM;: HTAB 10: PRINT
     INT (HH(N) * 100 + .5) / 100;: HTAB 18
    : PRINT  INT (HT(N) * 100 + .5) / 100;:
     HTAB 30: PRINT  INT (Q(N) * 1000 + .5)
     / 1000;: HTAB 40: PRINT  SPC( 3); INT
    (TT(N) / 10 + .5) / 100
5380  NEXT
5390  PRINT : PRINT "CEMENT GROUP - 21,BANB
    URY ROAD, OXFORD"
5400  PRINT  CHR$ (12): PRINT D$;"PREO": GOTO
    100
6000  TEXT : HOME : PRINT D$;"RUNCAL-2,D1"
6500  TEXT : HOME : PRINT D$;"RUNCAL-3,D1"
6700  TEXT : HOME
6710  PRINT "***          START NEW DISC
          ***"
6720  VTAB 5: PRINT "PLEASE INSERT A NEW IN
    ITIALISED DISK    INTO DRIVE 2 THEN PRE
    SS RETURN.";
6730  GET AA$: IF AA$ <  > CHR$ (13) THEN
     GOTO 6730
6740  PRINT
6750  PRINT D$;"OPENINDEX MARKER,D2"
6760  PRINT D$;"WRITE INDEX MARKER"
6770  PRINT "00000"
6780  PRINT 0
6790  PRINT D$;"CLOSE"
6800  VTAB 10: FLASH : HTAB 17: PRINT "DONE
    ";: FOR N = 0 TO 1000: NEXT N
6810  NORMAL
6820  IF AA$ <  > "" THEN  GOTO 1460
6830  TEXT : GOTO 100
7000  HOME : VTAB 4: PRINT "ADMIXTURE
         :"A$
7010  VTAB 6: PRINT "EXPERIMENTAL RUN NO.:"
    ;ER%
7020  VTAB 8: PRINT "CALOX NO.           :"
    ;CN%
7030  VTAB 10: PRINT "WEIGHT OF CEMENT    :
    ";W
7040  VTAB 12: PRINT "BASE LINE VOLTAGE   :
    ";BL
7050  VTAB 14: PRINT "TIME TO MINIMUM     :
    ";TM
7060  VTAB 16: PRINT "TEMPERATURE (K)     :
    ";TP
7070  VTAB 20: PRINT "IF ENTRY IS CORRECT P
    RESS RETURN.",,,,"OTHERWISE ENTER CORRE
    CT VALUE."
7080  VTAB 4: HTAB 22: INPUT "";AA$: IF AA$
     <  > "" THEN A$ = AA$
7090  VTAB 4: HTAB 22: PRINT A$
7100  VTAB 6: HTAB 22: INPUT "";AA$: IF AA$
     <  > "" THEN ER% =  VAL (AA$)
7110  VTAB 6: HTAB 22: PRINT ER%
7120  VTAB 8: HTAB 22: INPUT "";AA$: IF AA$
     <  > "" THEN CN% =  VAL (AA$)
7130  VTAB 8: HTAB 22: PRINT CN%
7140  VTAB 10: HTAB 22: INPUT "";AA$: IF AA
    $ <  > "" THEN W =  VAL (AA$)
7150  VTAB 10: HTAB 22: PRINT W
7160  VTAB 12: HTAB 22: INPUT "";AA$: IF AA
    $ <  > "" THEN BL =  VAL (AA$)
7170  VTAB 12: HTAB 22: PRINT BL
7180  VTAB 14: HTAB 22: INPUT "";AA$: IF AA
    $ <  > "" THEN TM =  VAL (AA$)
7190  VTAB 14: HTAB 22: PRINT TM
7200  VTAB 16: HTAB 22: INPUT "";AA$: IF AA
    $ <  > "" THEN TP =  VAL (AA$)
7210  VTAB 16: HTAB 22: PRINT TP
7220  CALL  - 958
7230  VTAB 20: INPUT "ANY CORRECTIONS? (Y/N
    );";AA$: IF AA$ = "Y" GOTO 7000
7240  IF AA$ = "N" THEN  RETURN
7250  GOTO 7230
8000  DIM TI(200),HT(200)
8010 D$ =  CHR$ (4):IM$ = "INDEX MARKER":CD
    $ = "CALOX DATA FILE NO.":CI$ = "CALOX
    DATA FILE INDEX"
8020 RD$ = D$ + "READ":WR$ = D$ + "WRITE":O
    P$ = D$ + "OPEN":CL$ = D$ + "CLOSE":AP$
     = D$ + "APPEND"
8030 UN$ = D$ + "UNLOCK":LK$ = D$ + "LOCK":
    DE$ = D$ + "DELETE"
8040 CT$ = "CALOX TIMES "
8050  RETURN
9000  POKE 216,0: IF  PEEK (222) <  > 9 AND
     PEEK (222) <  > 10 AND  PEEK (222) <  >
    6 THEN  STOP
9010  ONERR  GOTO 9000
9020  IF  PEEK (222) = 10 THEN  VTAB 22: PRINT
    "DATA FILE ";ER%;" IS ALREADY IN USE.":
     INPUT "PLEASE ENTER A NEW NO.";ER%: GOTO
    1470
9025  IF  PEEK (222) <  > 9 GOTO 9040
```

```
9030  VTAB 20: PRINT "DISC FULL-PRESS 'R' T
    O RETURN TO MENU
    (LOSING DATA)                         'N'
     TO USE THE START NEW
      DISC OPTION."
9032  GET AA$: IF AA$ = "R" THEN  TEXT : GOTO
    100
9034  IF AA$ = "N" GOTO 6700
9036  GOTO 9032
9040  IF  PEEK (222) = 6 AND F1 <  > - 1 AND
    F1 <  > - 2 THEN  VTAB 22: PRINT "PLEA
    SE PLACE THE CORRECT DISK FOR FILE  NO.
    ";F1;" IN DRIVE 2, THEN PRESS RETURN.":
     GET AA$: GOTO 9070
9042  IF  PEEK (222) = 6 AND F1 =  - 2 THEN
     VTAB 22: PRINT "PLEASE PLACE A CORRECT
    LY INITIALISED    DATA DISC IN DRIVE 2
    THEN PRESS RETURN";: GET AA$: GOTO 9070

9050  VTAB 22: PRINT "PLEASE CHECK THE DISK
     IN DRIVE 1, THEN PRESS RETURN.": GET A
    A$
9070  VTAB 20: CALL  - 958: PRINT : ON FL GOTO
    1190,1530,1660,3040,3140,3210,3310,4070
    ,4160,2040,2290
9080  POKE 216,0: STOP
10000 M = 12: DIM L(M): DIM R(M):S = 0:L(0)
     = 0:R(0) = NT - 1
10010 R1 = R(S):L1 = L(S):S = S - 1
10020 I = L1:J = R1:X =  VAL (A$( INT ((L1 +
    R1) / 2),0))
10030  IF  NOT ( VAL (A$(I,0)) < X) THEN 10
    050
10040 I = I + 1: GOTO 10030
10050  IF  NOT (X <  VAL (A$(J,0))) THEN 10
    070
10060 J = J - 1: GOTO 10050
10070  IF I > J THEN  GOTO 10090
10080 W$ = A$(I,0):Y$ = A$(I,1):A$(I,0) = A
    $(J,0):A$(I,1) = A$(J,1):A$(J,0) = W$:A
    $(J,1) = Y$:I = I + 1:J = J - 1
10090  IF I <  = J THEN 10030
10100  IF I >  = R1 THEN 10120
10110 S = S + 1:L(S) = I:R(S) = R1
10120 R1 = J
10130  IF L1 < R1 THEN 10020
10140  IF S <  > - 1 THEN 10010
10150  RETURN
```

PROGRAM TO DRAW RATE OF HEAT OUTPUT GRAPHS

```
1  ONERR  GOTO 800
100  GOTO 280
110  HGR
120  HPLOT 24,0 TO 24,147
130  HPLOT 20,143 TO 279,143
140  FOR I = 0 TO MI
150  HPLOT 20,143 - 143 * I / MI TO 24,143 - 143 * I / MI
160  NEXT I
170  FOR I = 0 TO MT
180  HPLOT 24 + 255 * I / MT,143 TO 24 + 255 * I / MT,147
190  NEXT I
200  FOR M = 0 TO N%
210  IF (H(M) + 2) > 280 OR (V(M) - 2) < 0 THEN 260
220  IF (H(M) - 2) < 0 THEN 260
230 HH = H(M):VV = V(M)
240  HPLOT HH - 1,VV TO HH + 1,VV
250  HPLOT HH,VV - 1 TO HH,VV + 1
260  NEXT M
270  RETURN
280 D$ =  CHR$ (4):OP$ = D$ + "OPEN":CO$ = D$ + "CLOSE":RD$ = D$ + "READ":CL$ = "CALOX DATA FILE NO.":U
    N$ = D$ + "UNLOCK":LK$ = D$ + "LOCK"
290  DIM H(100),V(100),Q(100),T(100),R(100)
291  DIM AD$(10),NO(10):NO = 0
295  HCOLOR= 7
300  HOME : PRINT "***          GRAPH PLOTTING          ***":D = 2
310  POKE 34,2: POKE  - 16303,0: HOME : PRINT : PRINT
320  PRINT "ENTER DATA FILE NO.";: INPUT "";ER$
321  IF  LEFT$ (ER$,1) = "/" THEN ER% =  VAL ( RIGHT$ (ER$, LEN (ER$) - 1)): GOTO 420
322 ER% =  VAL (ER$)
330  PRINT UN$;CL$;ER%;",D2"
340  PRINT OP$;CL$;ER%
350  PRINT RD$;CL$;ER%
360  INPUT LN$: INPUT LN$: INPUT N%: INPUT A$: PRINT CO$
370  HOME : PRINT : PRINT "DATA FILE-";ER%
380  PRINT : PRINT "ADMIXTURE-";A$
390  PRINT : INPUT "IS THIS IT? (Y/N)";YN$
400  IF YN$ <  > "Y" AND YN$ <  > "N" THEN 370
410  IF YN$ = "N" THEN  HOME : GOTO 310
420  PRINT UN$;CL$;ER%;",D2": PRINT OP$;CL$;ER%: PRINT RD$;CL$;ER%
430  INPUT LN$: INPUT LN$: INPUT N%: INPUT A$: INPUT CN%: INPUT BL: INPUT TE: INPUT TP: FOR N = 0 TO N%
   : INPUT T(N): INPUT Q(N):Q(N) = Q(N) - BL: NEXT : INPUT W
440  PRINT CO$: PRINT LK$;CL$;ER%
445  IF  LEFT$ (ER$,1) = "/" THEN  PRINT : PRINT "ADMIXTURE - ";A$
446 AD$(NO) = A$:NO(NO) = ER%:NO = NO + 1
447  IF CN% = 11 THEN K1 = .0132:K2 = 1.0395
450  IF CN% = 10 THEN K1 = .0149:K2 = 1.2
460  IF CN% = 3 THEN K1 = 1.9706802E - 2:K2 = 12.537181
470  IF CN% = 4 THEN K1 = 2.1245013E - 2:K2 = 13.597284
475  IF CN% = 7 THEN K1 = .0195:K2 = 15.45
476  IF CN% = 12 THEN K1 = .015:K2 = .6
480 R(0) = (K2 * (Q(1) - Q(0)) / ((T(1) - T(0)) * 60) + K1 * Q(0)) / W
490 R(N%) = (K2 * (Q(N%) - Q(N% - 1)) / (T(N%) - T(N% - 1)) / 60 + K1 * Q(N%)) / W
```

```
500  FOR I = 1 TO N% - 1
510 R(I) = (K2 * (Q(I + 1) - Q(I - 1)) / (T(I + 1) - T(I - 1)) / 60 + K1 * Q(I)) / W
520  NEXT
530  IF O = 3 THEN 680
540  PRINT : PRINT "SET OWN SCALES? (Y/N) ";: INPUT "";YN$
550  IF YN$ <  > "Y" AND YN$ <  > "N" THEN  PRINT  CHR$ (7): GOTO 540
560  IF YN$ = "N" THEN 620
570  PRINT : INPUT "ENTER MAX TIME:";MT
580 MT =  INT (MT / 100) + 1
590  PRINT : INPUT "MAX HEAT:";MI
600 FL = 1
610  GOTO 680
620 MR = 0
630  FOR M = 0 TO N%
640  IF MR < R(M) THEN TM = T(M):MR = R(M)
650  NEXT M
660 MT = (T(N%) + TE) / 100: IF MT <  >  INT (MT) THEN MT =  INT (MT) + 1
670 MI =  INT (MR * 1000 + 2)
680  FOR M = 0 TO N%
690 V(M) = 143 - R(M) * 143000 / MI
700 H(M) = 24 + 255 * (T(M) + TE) / MT / 100
710  NEXT
720  POKE  - 16304,0: POKE  - 16297,0
730  ON O - 1 GOSUB 110,200
740  POKE 34,20: HOME : PRINT
750  VTAB 21: HTAB 17: PRINT "1--PRINT GRAPH": PRINT "ENTER OPTION:"; TAB( 17);"2--NEW GRAPH": HTAB 17:
     PRINT "3--OVERLAY NEW FILE": HTAB 17: PRINT "4--RETURN";
760  VTAB 22: HTAB 14: INPUT "";O: IF O < 1 OR O > 4 THEN  END
770  ON O GOTO 840,780,310,790
780  TEXT : RUN
790  POKE 34,0: HOME : TEXT : PRINT D$;"RUNCAL-1,D1"
800  IF  PEEK (222) <  > 6 AND  PEEK (222) <  > 9 THEN  POKE 216,0: STOP
610  VTAB 22
815  PRINT  CHR$ (7); CHR$ (7): INVERSE : PRINT "DATA FILE NO.";ER%;" IS NOT ON CURRENT DISC": NORMAL :
     PRINT : PRINT "PRESS ";: INVERSE : PRINT "ESC";: NORMAL : PRINT " TO ENTER A NEW NUMBER ";: INVERSE
    : PRINT " OR ": NORMAL
816  PRINT "PLACE CORRECT DISC IN DRIVE 2 THEN PRESS";: INVERSE : PRINT "RETURN": NORMAL
830  GET AA$: IF AA$ =  CHR$ (13) THEN  HOME : PRINT : GOTO 321
832  IF AA$ =  CHR$ (27) THEN  GOTO 310
833  GOTO 830
840  PRINT  CHR$ (13);D$;"PR£1"
850  POKE 1657,80
860  PRINT  CHR$ (18)
880  PRINT "FILE NO.";: HTAB (15): PRINT "ADMIXTURE": PRINT
890  FOR N = 0 TO NO - 1: PRINT NO(N);: HTAB (15): PRINT AD$(N): NEXT
900  PRINT  CHR$ (17)
910  PRINT  CHR$ (13);D$;"PR£0"
920  GOTO 740
```

PROGRAM TO DRAW INTEGRATED HEAT OUTPUT GRAPHS

```
100  GOTO 280
110  HGR
120  HPLOT 24,0 TO 24,147
130  HPLOT 20,143 TO 279,143
140  FOR I = 0 TO MI
150  HPLOT 20,143 - 143 * I / MI TO 24,143 - 143 * I / MI
160  NEXT I
170  FOR I = 0 TO MT
180  HPLOT 24 + 255 * I / MT,143 TO 24 + 255 * I / MT,147
190  NEXT I
200  FOR M = 0 TO N%
210  IF (H(M) + 2) > 280 OR (V(M) - 2) < 0 THEN 260
220  IF (H(M) - 2) < 0 THEN 260
230 HH = H(M):VV = V(M)
240  HPLOT HH - 1,VV TO HH + 1,VV
250  HPLOT HH,VV - 1 TO HH,VV + 1
260  NEXT M
270  RETURN
280 D$ =  CHR$ (4):OP$ = D$ + "OPEN":CO$ = D$ + "CLOSE":RD$ = D$ + "READ":CL$ = "CALOX DATA FILE NO.":U
    N$ = D$ + "UNLOCK":LK$ = D$ + "LOCK"
290  DIM H(100),V(100),Q(100),T(100),R(100)
295  DIM AR(100)
300  HOME : PRINT "***         GRAPH PLOTTING          ***":Q = 2
310  POKE 34,2: POKE  - 16303,0: HOME : PRINT : PRINT
320  PRINT "ENTER DATA FILE NO.:";: INPUT "";ER%
330  PRINT UN$;CL$;ER%;",D2"
340  PRINT OP$;CL$;ER%
350  PRINT RD$;CL$;ER%
360  INPUT LN$: INPUT LN$: INPUT N%: INPUT A$: PRINT CO$
370  HOME : PRINT : PRINT "DATA FILE-";ER%
380  PRINT : PRINT "ADMIXTURE-";A$
390  PRINT : INPUT "IS THIS IT? (Y/N)";YN$
400  IF YN$ <  > "Y" AND YN$ <  > "N" THEN 370
410  IF YN$ = "N" THEN  HOME : GOTO 310
420  PRINT UN$;CL$;ER%: PRINT OP$;CL$;ER%: PRINT RD$;CL$;ER%
430  INPUT LN$: INPUT LN$: INPUT N%: INPUT A$: INPUT CN%: INPUT BL: INPUT TE: INPUT TP: FOR N = 0 TO N%
    : INPUT T(N): INPUT Q(N): NEXT : INPUT W
440  PRINT CO$: PRINT LK$;CL$;ER%
445  IF CN% >  = 11 THEN K1 = .0132:K2 = 1.0395
446  IF CN% = 12 THEN K1 = 0.015:K2 = 0.6
450  IF CN% = 10 THEN K1 = .0149:K2 = 1.2
460  IF CN% = 3 THEN K1 = 1.9706802E - 2:K2 = 12.537181
470  IF CN% = 4 THEN K1 = 2.1245013E - 2:K2 = 13.597284
475  IF CN% = 7 THEN K1 = .0195:K2 = 15.45
480 R(0) = (K2 * (Q(1) - Q(0)) / ((T(1) - T(0)) * 60) + K1 * Q(0)) / W
490 R(N%) = (K2 * (Q(N%) - Q(N% - 1)) / (T(N%) - T(N% - 1)) / 60 + K1 * Q(N%)) / W
```

```
500  FOR I = 1 TO N% - 1
510 R(I) = (K2 * (Q(I + 1) - Q(I - 1)) / (T(I + 1) - T(I - 1)) / 60 + K1 * Q(I)) / W
520  NEXT
521 AA = 0
522  FOR I = 1 TO N%:AA = AA + 0.5 * (R(I - 1) + R(I)) * (T(I) - T(I - 1)) * 60:AR(I) = AA: NEXT
530  IF Q = 3 THEN 680
540  PRINT : PRINT "SET OWN SCALES? (Y/N) ";: INPUT "";YN$
550  IF YN$ <  > "Y" AND YN$ <  > "N" THEN 540
560  IF YN$ = "N" THEN 620
570  PRINT : INPUT "ENTER MAX TIME:";MT
580 MT =  INT (MT / 100) + 1
590  PRINT : INPUT "MAX HEAT:";MI
600 FL = 1
610  GOTO 680
620 MR = 0
630  FOR M = 0 TO N%
640  IF MR < R(M) THEN TM = T(M):MR = R(M)
650  NEXT M
660 MT = (T(N%) + TE) / 100: IF MT <  >  INT (MT) THEN MT =  INT (MT) + 1
670 MI = 3
680  FOR M = 0 TO N%
690 V(M) = 143 - AR(M) * 1.43 / MI
700 H(M) = 24 + 255 * (T(M) + TE) / MT / 100
710  NEXT
720  POKE  - 16304,0: POKE  - 16297,0
730  ON Q - 1 GOSUB 110,200
740  POKE 34,20: HOME : PRINT
750  VTAB 21: HTAB 17: PRINT "1--PRINT GRAPH": PRINT "ENTER OPTION:"; TAB( 17);"2--NEW GRAPH": HTAB 17:
     PRINT "3--OVERLAY NEW FILE": HTAB 17: PRINT "4--RETURN";
760  VTAB 22: HTAB 14: INPUT "";Q: IF Q < 1 OR Q > 4 THEN  END
770  ON Q GOTO 840,780,310,790
780  TEXT : RUN
790  POKE 34,0: HOME : TEXT : PRINT D$;"RUNCAL-1,D1"
800  IF  PEEK (222) <  > 6 THEN  POKE 216,0: STOP
810  VTAB 22
820  PRINT "PLEASE PLACE THE CORRECT DISC FOR DATA  FILE NO.";ER%;" IN DRIVE 2",,"THEN PRESS RETURN."
830  INPUT "";AA$: POKE 216,0: GOTO 310
840  PRINT  CHR$ (13);D$;"PR£1"
850  POKE 1657,80
860  PRINT  CHR$ (18)
870  IF Q = 3 THEN 900
880  PRINT "ADMIXTURE--";A$
890  PRINT "DATA FILE NO.";ER%
900  PRINT : PRINT : PRINT  CHR$ (17)
910  PRINT  CHR$ (13);D$;"PR£0"
920  GOTO 740
```

APPENDIX II.i

FRANKE DETERMINATION OF FREE LIME

Reagents:

Thymol blue indicator (0.1g per 100 ml isobutyl alcohol)
Standard perchloric acid solution (0.2N in isobutyl alcohol).
Organic solvent solution (150 ml ethyl acetoacetate mixed with 1 litre isobutyl alcohol).

Procedure:

Accurately weigh about 1 g of finely ground sample into a clean oven dried 250 ml conical flask. Add 70 ml organic solvent solution, swirl to mix and reflux for 2 hours. Stopper the flask and allow to cool.

Filter through a Whatman no. 40 filter into a second dry conical flask. Wash the original flask and residue with 50 ml organic solvent solution.

Add 10-12 drops of indicator solution to the filtrate and titrate against standard perchloric acid (0.2N) to a distinct reddish tinge.

Calculation:

For 0.2N perchloric acid

1 ml acid = 5.6mg CaO

APPENDIX II.ii

CHEMICAL ANALYSIS OF C_3S TO DETERMINE THE C/S RATIO AND THE LEVELS OF IMPURITIES

(a) Dissolution of C_3S and determination of insoluble silica

Procedure:

Accurately weigh 1.0000 g of finely ground C_3S into a 100 ml beaker and thoroughly mix with 1.0 g of ammonium chloride. Cover the beaker with a watch glass and carefully add 10 ml of hydrochloric acid (conc.), allowing the acid to run down the side of the beaker. After the reaction has subsided, lift the cover, add one or two drops of nitric acid, stir the mixture with a glass rod, replace the cover and set the beaker on a boiling water bath for 30 mins. Filter through a 90 mm ashless, rapid filter paper (e.g. Whatman no. 41), transferring the jelly-like mass of silicic acid to the filter as completely as possible without dilution and allowing the solution to drain through. Scrub the beaker with a rubber policeman, rinse the beaker and policeman and wash the filter two or three times with hot hydrochloric acid (1+99). Then wash the filter with ten or twelve small portions of hot water, allowing each portion to drain through completely. Reserve the filtrate and washings.

Transfer the filter paper and residue to a weighed platinum crucible. Dry and ignite until the carbon of the paper is completely consumed without inflaming by placing the crucible and contents in an oven and slowly raising the temperature to 600 degrees (about 45 mins). Finally fire the crucible and contents at 1200 degrees for 30 minutes. Cool in a dessicator to room temperature (about 15 mins) and weigh. Record the weight of the residue (W_{iis}) as the weight of impure insoluble silica.

Treat the silica thus obtained, which will contain small amounts of impurities, in the crucible with 0.5 ml of water, 2 drops of sulphuric acid (conc.) and about 10 ml of hydrofluoric acid and evaporate cautiously to dryness in a fume cupboard, Heat the small residue finally at 1200 degrees for a minute or two, cool and weigh. Record the weight of the residue (W_r). The difference between the weight of the residue (W_r) and the weight of impure insoluble silica previously obtained (W_{iis}) represents the amount of insoluble silica (W_{is}).

Fuse the residue with 0.5 g potassium hydrogen sulphate. Dissolve the cold melt in 5 ml of hydrochloric acid (1+4) and add the solution to the reserved filtrate. Dilute the solution in a volumetric flask to 500 ml. Mix and reserve.

(b) Determination of silica remaining in solution

Reagents:

Ammonium molybdate (10 g ammonium molybdate dissolved in 100 ml water).

Citric acid (10 g of citric acid monohydrate dissolved in water and made up to 100 ml).

Reducing solution (0.15 g of 1-amino-2-napthol-4-sulphonic acid, 1.4 g sodium sulphite and 9.0 g sodium metabisulphite dissolved in water, made up to 100 ml). Store in a fridge.

Standard silica solution (1ml containing 1mg silica).

Compensating solution (0.8 g ammonium chloride and 8 ml hydrochloric acid dissolved in water and diluted to 100 ml).

Procedure:

Prepare two standard solutions, one containing 0.1 mg silica and one blank. To each, in a 100 ml flask, add 5.0 ml of compensating solution and dilute to about 20 ml. Add 5.0 ml ammonium molybdate solution, rinse the necks of the flasks, swirl to mix and allow to stand for 5 - 10 mins. Add 5 ml citric acid to each flask, rinse, mix and wait 5 mins. Add 2 ml of reducing solution, make up to 100 ml with water and mix. Allow to stand for at least 30 mins before measuring the colour.

Pipette 20 ml of the C_3S filtrate solution into a 100 ml volumetric flask. Add 5 ml of ammonium molybdate and 20 ml water and continue as in the preceding paragraph.

Measure the colour at a wavelength of 650 nm on a spectrophotometer.

By comparison with the standards, determine the amount of soluble silica in the 20 ml of C_3S filtrate. Multiply this by 25 to give the weight of soluble silica in the 500 ml of filtrate (W_{ss}). The total amount of silica in the original sample of C_3S is then the sum of the insoluble and the soluble silica ($W_{is} + W_{ss}$).

(c) Determination of total calcium oxide

Reagents:

Potassium hydroxide solution (200 g of potassium hydroxide dissolved in one litre of water).

Triethanolamine solution (200 ml of pure triethanolamine diluted to one litre with water).

Murexide indicator (0.5 g of murexide (ammonium purpurate - colour index 56085) and 100 g sodium chloride ground together to form a homogeneous mixture).

EDTA solution (6.67 g of EDTA disodium salt dissolved in distilled water, with the pH adjusted to 10 with potassium hydroxide solution and diluted to one litre). Store in a polythene bottle.

Standardisation:

Accurately weigh about 0.1 g pure calcium carbonate and dissolve in dilute hydrochloric acid, taking care that no loss of liquid occurs. Warm to remove carbon dioxide, cool and dilute to about 200 ml with water. Adjust the pH to 12.2 to 12.5 with potassium hydroxide solution. Add approximately 0.06 g of murexide indicator and titrate with EDTA solution in a photometric end-point detector (e.g. Quantitrator - suppliers: Evans Electroselenium Ltd.). An increase in optical density occurs as the end-point is approached. As the end-point is approached add successive, small, equal increments of the EDTA and note the steady galvanometer reading after each increment. Continue until the galvanometer is not, or is only slightly, affected by the addition of EDTA.

Plot the galvonometer readings against the volume of EDTA and find the end-point by the intersection of the line of steepest slope and the line of constant optical density. Use only those points in the immediate vicinity of the end-point.

Calculation:

If W = weight of $CaCO_3$

and t = ml of EDTA for equivalence

$$1 \text{ ml EDTA} = \frac{56.08 * 1000 * W}{100.09 * t} \text{ mg CaO}$$

Procedure:

Take 25 ml aliquots, add 10 ml triethanolamine and adjust to pH 12.2 to 12.5 with potassium hydroxide, using a pH meter. Add approximately 0.06 g of murexide indicator. Titrate with EDTA in the photo-electric end-point detector. Record the volume of EDTA added and the galvanometer readings, using only those results in the immediate vicinity of the end-point, and find the exact end-point as in the previous case.

Calculation:

if V ml = vol EDTA required for equivalence with the 25 ml aliquot

and E = standardisation factor of the EDTA solution

then CaO (wt%) = V * E * 20

(c) Determination of chromium

Reagents:

Potassium dichromate (10 ml of a solution of 0.1471 g potassium dichromate dissolved in 1 litre of distilled water made up to 100 ml).

Dephenyl indicator (4 g phthallic anhydride and 0.25 g diphenyl carbazide dissolved in 100 ml of 95% ethanol and 5% water).

Procedure:

Take a 25 ml aliquot of C_3S filtrate, add 50 ml water and neutralise with 8% sodium hydroxide solution and methyl red indicator. Note the volume of the titre. Discard the solution. Neutralise another 25 ml aliquot of the filtrate solution using no indicator. Add 3.3 ml sulphuric acid (1+5) and heat to just below boiling. Cool and transfer to a 100 ml flask. Add 1 ml of diphenyl indicator and make up to the mark with distilled water.

Prepare a set of standard potassium dichromate solutions such that they contain 0, 0.01, 0.02 and 0.05 mg Cr_2O_3 in 100 ml, add 1ml diphenyl indicator and 3.3 ml sulphuric acid to each and make up the the mark in a 100 ml flask with distilled water.

Compare the colour intensities at a wavelength of 540 nm on a spectrophotometer.

(d) Determination of iron and aluminum

Reagents:

Copper complexonate (0.2250 g copper sulphate dissolved in 25 ml water with the required volume of standardised 0.02 M EDTA solution to react with all the copper added from a burette).

PAN indicator (0.1 g of PAN dissolved in 100 ml ethanol).

EDTA solution (0.02 M).

Procedure:

Add 5 ml of concentrated acetic acid to 100 ml of C_3S filtrate solution in a 500 ml beaker. Adjust the pH to 3.0 by adding ammonium acetate (25%) drop by drop. Heat the solution to boiling in a fume cupboard and add 3

colour first changes from violet-pink to yellow. Continue boiling the solution gently, and when the pink colour returns, add the 0.02 M EDTA solution drop by drop until yellow again. Repeat this titration procedure several times until the solution remains a yellow colour after boiling for at least 1 minute. Record the volume of EDTA solution used and from this calculate the Al_2O_3 and Fe_2O_3 content of the C_3S.

Note:

In the determination carried out in this work the colour change occurred with the addition of one drop of the EDTA solution. The C_3S therefore contained insufficient iron and alumina (combined) for determination by this method and it was considered unnecessary to attempt to determine the iron and alumina contents of the C_3S separately.

APPENDIX II.iii

DETERMINATION OF THE SPECIFIC SURFACE OF A CEMENT BY THE LEA AND NURSE METHOD (B.S. 12:1958).

Method:

Determine the density of the cement by a suitable method.

Weigh out enough cement to form a bed 1 cm deep of known porosity (usually 0.475 but was 0.6 used in this work for C_3S) in the permeability cell (the bed is a cylinder of 2.54 cm diameter so the weight of cement can be calculated from a knowledge of the density of the cement and the volume of the bed).

Carefully transfer all the cement into the permeability cell, shake gently from side to side to level off the surface and tap four times from a height of ~1 cm onto a wooden bench. Insert the plunger slowly until the collar is in contact with the top of the permeability cell.

Without twisting the plunger while it is in contact with the surface of the cement, withdraw the plunger a short distance, then, slowly and with a twisting motion withdraw it completely.

Insert the upper bung of the flowmeter into the cell and slowly turn on the air. Next insert the lower bung. Adjust the flow of air until the flowmeter show a difference in level of 30 - 50cm. Record the difference in level h_1 of the manometer and of the difference in level h2 of the flowmeter at several different rates of flow of air.

Calculation:

The specific surface (S) is given by the formula:

$$S = K. \frac{h_1}{h_2}$$

$$\text{where } K = \frac{14}{d.(1-e)} \frac{e^3.A}{C.L}$$

e = porosity

A = area of cement bed (cm^2)

L = depth of cement bed (cm)

d = density of the cement (g/cm^3)

C = flowmeter constant

APPENDIX III

PROGRAM TO FIT AVRAMI EQUATION TO CALORIMETRIC HEAT OUTPUT DATA

```
100  GOTO 280
110  HGR
120  HPLOT 24,0 TO 24,147
130  HPLOT 20,143 TO 279,143
140  FOR I = 0 TO MI
150  HPLOT 20,143 - 143 * I / MI TO 24,143 -
    143 * I / MI
160  NEXT I
170  FOR I = 0 TO MT
180  HPLOT 24 + 255 * I / MT,143 TO 24 + 25
    5 * I / MT,147
190  NEXT I
200  FOR M = 0 TO N%
210  IF (H(M) + 2) > 280 OR (V(M) - 2) < 0 THEN
    260
220  IF (H(M) - 2) < 0 THEN 260
230 HH = H(M):VV = V(M)
240  HPLOT HH - 1,VV TO HH + 1,VV
250  HPLOT HH,VV - 1 TO HH,VV + 1
260  NEXT M
270  RETURN
280 D$ =  CHR$ (4):OP$ = D$ + "OPEN":CO$ =
    D$ + "CLOSE":RD$ = D$ + "READ":CL$ = "C
    ALOX DATA FILE NO.":UN$ = D$ + "UNLOCK"
    :LK$ = D$ + "LOCK"
290  HOME : PRINT "***          AVRAMI FITTI
    NG          ***"
300  POKE 34,2: HOME : PRINT : PRINT : PRINT
    "ENTER DATA FILE NO.:";: INPUT "";ER$
310  ONERR  GOTO 1060
315  IF  LEFT$ (ER$,1) = "/" THEN ER% =  VAL
    ( RIGHT$ (ER$, LEN (ER$) - 1)): GOTO 41
    0
316 ER% =  VAL (ER$)
320  PRINT UN$;CL$;ER%;",D2"
330  PRINT OP$;CL$;ER%
340  PRINT RD$;CL$;ER%
350  INPUT LN$: INPUT LN$: INPUT N%: INPUT
    A$: PRINT CO$
360  HOME : PRINT : PRINT "DATA FILE-";ER%
370  PRINT : PRINT "ADMIXTURE-";A$
380  PRINT : INPUT "IS THIS IT? (Y/N)";YN$
390  IF YN$ <  > "Y" AND YN$ <  > "N" THEN
    360
400  IF YN$ = "N" THEN  HOME : GOTO 300
410  PRINT UN$;CL$;ER%;",D2": PRINT OP$;CL$
    ;ER%: PRINT RD$;CL$;ER%
430  INPUT LN$: INPUT LN$: INPUT N%: DIM A(
    9),B(9),C(9),D(9),W(9),X(9),H(N%),V(N%)
    ,Q(N%),T(N%),R(N%): INPUT A$: INPUT CN%
    : INPUT BL: INPUT TE: INPUT TP: FOR N =
    0 TO N%: INPUT T(N): INPUT Q(N): NEXT :
     INPUT W
440  PRINT CO$: PRINT LK$;CL$;ER%
442  IF  LEFT$ (ER$,1) = "/" THEN  PRINT : PRINT
    "ADMIXTURE - ";A$
445  IF CN% >  = 11 THEN K1 = .0132:K2 = 1.
    0394
450  IF CN% = 10 THEN K1 = .0149:K2 = 1.2
460  IF CN% = 3 THEN K1 = 1.9706802E - 2:K2
     = 12.537181
470  IF CN% = 4 THEN K1 = 2.1245013E - 2:K2
     = 13.597284
480 R(0) = (K2 * (Q(1) - Q(0)) / ((T(1) - T
    (0)) * 60) + K1 * Q(0)) / W
490 R(N%) = (K2 * (Q(N%) - Q(N% - 1)) / (T(
    N%) - T(N% - 1)) / 60 + K1 * Q(N%)) / W

500  FOR I = 1 TO N% - 1
510 R(I) = (K2 * (Q(I + 1) - Q(I - 1)) / (T
    (I + 1) - T(I - 1)) / 60 + K1 * Q(I)) /
    W
520  NEXT
530 MR = 0
540  FOR M = 0 TO N%
550  IF MR < R(M) THEN TM = T(M):MR = R(M):
    MM = M - 6
560  NEXT M
570 MT = (T(N%) + TE) / 100: IF MT <  > INT
    (MT) THEN MT =  INT (MT) + 1
580 MI =  INT (MR * 1000 + 2)
590  FOR M = 0 TO N%
600 V(M) = 143 - R(M) * 143000 / MI
610 H(M) = 24 + 255 * (T(M) + TE) / MT / 10
    0
620  NEXT
630  REM  CUBIC SPLINE FITTER
640 N = 8: FOR I = 0 TO N:A(I) = R(I + MM):
     NEXT
650  FOR I = 0 TO N - 1:D(I) = (T(I + MM +
    1) - T(I + MM)): NEXT
660 D(N) = D(N - 1):D(N + 1) = D(0)
670 B(0) = 2 * D(0): FOR I = 1 TO N - 1:B(I
    ) = 2 * (D(I) + D(I - 1)): NEXT
680 B(N) = 2 * D(N - 1)
690 C(0) = 3 * (A(1) - A(0)): FOR I = 1 TO
    N - 1:C(I) = (D(I - 1) * (A(I + 1) - A(
    I))) / D(I)
700 C(I) = C(I) + ((D(I) / D(I - 1)) * (A(I
    ) - A(I - 1)))
710 C(I) = 3 * C(I): NEXT :C(N) = 3 * (A(N)
     - A(N - 1))
720 X(0) = B(0):X(1) = B(1) - (D(1) * D(N +
    1) / X(0))
730  FOR I = 2 TO N:X(I) = B(I) - ((D(I) *
    D(I - 2)) / X(I - 1)): NEXT
```

```
740 W(0) = C(0): FOR I = 1 TO N:W(I) = C(I)
    - (D(I) * W(I - 1) / X(I - 1)): NEXT
750 B(N) = W(N) / X(N): FOR I = (N - 1) TO
    1 STEP  - 1:B(I) = (W(I) - (D(I - 1) *
    B(I + 1))) / X(I): NEXT
760 B(0) = (W(0) - (D(N + 1) * B(1))) / X(0
    )
770 C(0) = 0:C(N) = 0: FOR I = 1 TO N - 1:C
    (I) = (A(I + 1) - A(I)) / (D(I) ^ 2):C(
    I) = C(I) * 3 - (((2 * B(I)) + B(I + 1)
    ) / D(I)): NEXT
780  FOR I = 0 TO N - 1:D(I) = (C(I + 1) -
    C(I)) / (3 * D(I)): NEXT
790  FOR I = 2 TO 7:ROOT = 4 * C(I) * C(I) -
    12 * D(I) * B(I): IF  SGN (ROOT) <  > -
    1 THEN F1 = ( SQR (ROOT) - 2 * C(I)) /
    6 / D(I):F2 = ( -  SQR (ROOT) - 2 * C(I
    )) / 6 / D(I)
800  IF  SGN (ROOT) =  - 1 THEN 830
810 XX = (T(I + MM + 1) - T(I + MM)): IF F1
     < XX AND F1 >  = 0 THEN TU = F1: GOSUB
    840
820  IF F2 < XX AND F2 >  = 0 THEN TU = F2:
     GOSUB 840
830  NEXT : GOTO 870
840 YT = A(I) + B(I) * TU + C(I) * TU * TU +
    D(I) * TU ^ 3
850 TU = T(I + MM) + TU
860  IF YY < YT THEN YY = YT:MN = I + MM:TM
     = TU: RETURN
870  POKE 34,20
880  GOSUB 110
890  HOME : PRINT : PRINT "ENTER TIME OFFSE
    T (MINS)";: INPUT "";T1
900  IF T1 < 0 THEN 1210
910 TA = TE - T1
920  PRINT : PRINT "ENTER HEAT OFFSET";: INPUT
    " ";HO:HO = YY - HO / 1000
930  GOSUB 110
940 K = 1.5 / (2.5 * (((TM + TA) * 60) ^ 2.
    5))
950 HH = (HO * ((TM + TA)) * 60) / (1.5 *  EXP
    ( - 0.6))
960  FOR M = 0 TO N%
970  IF TA + T(M) <  = 0 THEN 1040
980 S = 2.5 * K * HH * ((TA + T(M)) * 60) ^
    1.5 *  EXP ( - K * ((TA + T(M)) * 60) ^
    2.5)
990 S = S + YY - HO
1000 V = 143 - S * 143000 / MI
1010 H = H(M)
1020  IF (H + 2) > 280 OR (V - 2) < 0 THEN
    1040
1030  HPLOT H - 1,V - 1 TO H - 1,V + 1 TO H
     + 1,V + 1 TO H + 1,V - 1 TO H - 1,V -
    1
1040  NEXT M
1050  GOTO 890
1060  IF  PEEK (222) <  > 6 THEN  POKE 216,
    0: STOP
1070  VTAB 22
1080  PRINT "PLEASE PLACE THE CORRECT DISC
    FOR DATA  FILE NO.";ER%;" IN DRIVE 2",,
    "THEN PRESS RETURN."
1090  INPUT "";AA$: POKE 216,0: GOTO 300
1100  PRINT  CHR$ (13);D$;"PR#1"
1110  POKE 1657,80
1120  PRINT  CHR$ (18)
1130  PRINT "ADMIXTURE--";A$
1140  PRINT "DATA FILE NO.";ER%
1150  PRINT "TIME OFFSET="; INT ((TE - TA) +
    .5)
1160  PRINT "HEAT OFFSET=";(YY - HO) * 1000
1170  PRINT "MAX HEAT=";YY * 1000;" WATTS/K
    G"
1180  PRINT "TIME TO MAX=";(TM + TE);" MINS
    "
1190  PRINT : PRINT : PRINT  CHR$ (17)
1200  PRINT  CHR$ (13);D$;"PR#0"
1210  HOME : PRINT
1220  HTAB 17: PRINT "1--PRINT GRAPH": PRINT
    "ENTER OPTION:"; TAB( 17);"2--NEW FILE"
    : HTAB 17: PRINT "3--OLD FILE": HTAB 17
    : PRINT "4--RETURN";
1230  VTAB 22: HTAB 14: INPUT "";O: IF O <
    1 OR O > 4 THEN  END
1240  ON O GOTO 1100,1250,890,1260
1250  TEXT : RUN
1260  POKE 34,0: HOME : TEXT : PRINT D$;"RU
    NCAL-1,D1"
```

REFERENCES

Aldous, R.T.H. 1983 'The Hydraulic Behaviour of Rhombohedral Alite', Cem. Conc. Res. 13, 89.

Alexander, K.M., Taplin, J.H. & Wardlaw, J. 1968 'Correlation of Strength and Hydration with Composition of Portland Cements', Proc. 5th Int. Cong. Chem. Cem., Tokyo, suppl. paper III-72, p.152.

Assarsson, G. & Sundius, N. 1929 'Compositions of Hydrated Portland Cement', Swedish Geol. Survey, Ser.C, No 357, 9 (ref 1, p.101 in Lea 1970).

Avrami, M., 1939 'Kinetics of Phase Change I', J. Chem. Phys. 7, 1103.

Avrami, M., 1940 'Kinetics of Phase Change II', J. Chem. Phys. 8, 212.

Avrami, M., 1941 'Kinetics of Phase Change III', J. Chem. Phys. 9, 177.

Bailey, J.E. & Stewart, H.R., 1984 'C_3S Hydration Products Viewed Using a Cryo Stage in SEM', J. Mater. Sci. Letters 3, 411.

Ball, M.C. 1983 'Stress as a Factor in the Hydration of C_3S', Cem. Conc. Res. 13, 744

Ball, M.C., Simmons, R.E. & Sutherland, I. 1984 'Surface Composition of Anhydrous Calcium Silicates' Proc. Brit. Ceram. Soc., 35 (in press).

Barnes, P., Ghose, A. & Makay, A.L. 1980 'Cement Tubules - Another Look', Cem. Conc. Res. 10, 639.

Barnes, P. (Ed.) 1983 'Structure and Performance of Cements', Applied Science Publishers Ltd., Barking, Essex.

Barret, P. & Menetrier, D. 1980 'Filter Dissolution of C_3S as a Function of the Lime Concentration in a Limited Amount of Water', Cem. Conc. Res. 10, 521.

Barret, P., Menetrier, D., Bertrandie, D. & Regourd, M. 1980 Proc. 7th Int. Cong. Chem. Cem., Paris, II, II-279.

Barret, P., Menetrier, D. & Bertrandie, D. 1983 'Mechanism of C_3S Dissolution and Problem of Congruency in the Very Initial Period and Later On', Cem. Conc. Res. 13, 728.

Bensted, J. 1982 'Hydration of Portland Cement', In 'Advances in Cement Technology' (Ed. S.N. Ghosh), p.307

Berger, R.L., Lawrence, F.V.(Jr) & Young, J.F. 1973 'Studies on the Hydration of Tricalcium Silicate Pastes: (II) Strength Development and Fracture Characteristics', Cem. Conc. Res. 3, 497.

Bezjak, A. & Jelenic, I. 1980 a 'On the Determination of Rate Constants for Hydration Processes in Cement Pastes', Cem. Conc. Res. 10, 553.

Bezjak, A., Jelenic, I., Mlakar, V. & Panovic, A. 1980 b 'A Kinetic Study of Alite Hydration', Proc. 7th Int. Cong. Chem. Cem., Paris, II, II-111.

Bezjak, A. & Alujavic, V. 1981 'A Kinetic Study of Hydrothermal Reaction in Gamma-C_2S-Quartz: (I) Determination of Rate Constants for Processes with Two Acceleration Periods', Cem. Conc. Res. 11, 19.

Bigare, M. 1965 'Improvement of a Camera for X-ray Diffraction at High Temperatures in a Controlled Atmosphere. A Series of Solid Solutions of Alumina in Tricalcium Silicate', Rev. Mater. Construct. Trav. Publ. 598-99, 325 & 600, 394.

Bigare, M., Guiner, A., Mazieres, C., Regourd, M., Yannaquis, N., Eysel, W., Hahn, Th. & Woermann, E. 1967 'Polymorphism of Tricalcium Silicate and its Solid Solutions', J. Am. ceram. Soc. 50, 609.

Birchall, J.D., Howard, A.J. & Bailey, J.E. 1978 'On the Hydration of Portland Cement', Proc. Roy. Soc. Lond. A360, 445.

Birchall, J.D., Howard, A.J. & Double, D.D. 1980 'Some General Considerations of a Membrane/Osmosis Model for Portland Cement Hydration', Cem. Conc. Res. 10, 145.

Bogue, R.H. 1955 'The Chemistry of Portland Cements' (2nd Edn.), Reinhold, New York.

Boikova, A.I. 1968 'Ordered and Disordered Structures of Tricalcium Silicate Solid Solutions', Proc. 9th Conf. Silicate Ind., Budapest, p.41.

Brown, P.W., Franz, E., Frohnsdorff, G. & Taylor, H.F.W. 1984 'Analyses of the Aqueous Phase During Early C_3S Hydration', Cem. Conc. Res. 14, 259.

Brunauer, S. & Kantro, D.L. 1964 'The Hydration of Tricalcium Silicate and beta-Dicalcium Silicate from 5 to 50 degrees', Chapter 7 in 'Chemistry of Cements', Ed. H.F.W. Taylor, Vol I, p.287.

Brunauer, S., Yudenfreund, M., Odler, I. & Skalny, J. 1973 'Hardened Cement Pastes of Low Porosity: (VI) Mechanism of the Hydration Process', Cem. Conc. Res. 3, 129.

Butt, Yu.M., Timashev, V.V. & Kaushanski, V.E. 1968 'Properties of Tricalcium Silicate and its Solid Solutions', Proc. 9th Conf. Silicate Ind., Budapest, p.59.

Butt, Yu.M., Timasev, V.V., Buksutov, V.S., Iljuchin, V.V. & Golobacev, V.P. 1969 'The Structure of Hardened Cement Paste After Storage for Several Years' (in Russian), Cement 35, 10, 14.

Bye, G. 1983 'Portland Cement: Composition, Production and Properties', Pergamon Press.

Calvet, E. & Prat, H. 1963 'Recent Progress in Microcalorimetry', Macmillan Co., New York.

Carlson, R.W. 1934 'The Vane Calorimeter', Proc. Am. Soc. Testing Materials, 34, 322.

Celani, A., Moggi, P.A. & Rio, A. 1968 'The Effect of Tricalcium Aluminate on the Hydration of Tricalcium Silicate and Portland Cement', Proc. 5th Int. Cong. Chem. Cem., Tokyo, suppl. paper II-134, p.492.

Christian, J.W. 1975 'The Theory of Transformations in Metals and Alloys', 2nd. edition., Pergamon Press, London.

Ciach, T.D., Gillott, J.E., Swenson, E.G. & Sereda, P.J. 1971 'Microstructure of Calcium Silicate Hydrates', Cem. Conc. Res. 1, 13.

Clayden, N.J., Dobson, C.M., Groves, G.W., Hayes, C.J. & Rodger, S.A. 1984 'Solid State NMR Studies of Cement Hydration', Proc. Brit. Ceram. Soc., 35 (in press).

Cliff, G. & Lorimer, G.W. 1975 'The Quantitative Analysis of Thin Specimens', J. Microsc. 103, 203.

Coatman, R.D., Thomas, N.L. & Double, D.D. 1980 'Studies of the Growth of "Silicate Gardens" and Related Phenomena', J. Mater. Sci. 15, 2017.

Copeland, L.E. & Kantro, D.L. 1968 'Hydration of Portland Cement', Proc. 5th Int. Cong. Chem. Cem., Tokyo, princ. paper II-5, p.387.

Daimon, M., Ueda, S. & Kondo, R. 1971 'Morphological Study on Hydration of Tricalcium Silicate', Cem. Conc. Res. 1, 391.

Dalgleish, B.J. & Ibe, K. 1981 'Thin-Foil Studies of Hydrated Portland Cement', Cem. Conc. Res. 11, 729.

Dent Glasser, L.S., Lachowski, E.E., Mohan, K. & Taylor, H.F.W. 1978 'A Multi-Method Study of C_3S Hydration', Cem. Conc. Res. 8, 733.

Diamond, S. 1976 C/S Mole Ratio of CSH gel in a Mature C_3S Paste as Determined by EDXA', Cem. Conc. Res. 6, 413

Double, D.D. 1973 'Some Studies of the Hydration of Portland Cement Using High Voltage (1 MV) Electron Microscopy', Mater. Sci. Eng. 12, 29.

Double, D.D., Hellawell, A. & Perry, S.J. 1978 'The Hydration of Portland Cement', Proc. R. Soc. Lond. A359, 435.

Double, D.D., Thomas, N.L. & Jameson, D.A. 1980 Proc. 7th Int. Cong. Chem. Cem., Paris, II, II-256.

Double, D.D. 1981 'A Discussion of the Paper "Cement Tubules - Another Look" by P. Barnes, A. Ghose and A.L. Makay', Cem. Conc. Res. 11, 303.

Double, D.D. 1983 'New Developments in Understanding the Chemistry of Cement Hydration', Phil. Trans. R. Soc. Lond. A310, 53.

Edwards, G.C. & Angstadt, R.L. 1966 'The Effects of some Soluble Inorganic Admixtures on the Early Hydration of Portland Cement', J. Appl. Chem. 16, 166.

Eroveef, B.V. 1946 Dokl. Akad. Nauk. Sssr, 52, 515 (ref 3 in Urzhenko 1974)

Fierens, P. & Verhaegen, J.P. 1972 'Structure and Reactivity of Chromium Doped Tricalcium Silicate', J. Am. ceram. Soc. 55, 309.

Fierens, P. & Verhaegen, J.P. 1974 'Thermoluminescence Applied to the Kinetic Study of the Chemisorption of Water by Tricalcium Silicate', Silicate Ind. 39, 125.

Fierens, P. 1976 'Microcathodoluminescence of C_3S', Il Cemento 73, 39.

Fierens, P. & Verhaegen, J.P. 1976 a 'Proprietes Nucleophiles de Surfaces de Silicate Tricalcique', Cem. Conc. Res. 6, 103.

Fierens, P. & Verhaegen, J.P. 1976 b 'Hydration of Tricalcium Silicate in Paste - Kinetics of Calcium Ions Dissolution in the Aqueous Phase', Cem. Conc. Res. 6, 337.

Fierens, P., Kabuema, Y. & Tirlocq, J. 1982 a 'Influence du Milieu de Trempe sur la Cinetique d'Hydration du Silicate Tricalcique', Cem. Conc. Res. 12, 191.

Fierens, P. Kabuema, Y. & Tirlocq, J. 1982b 'Influence de la Temperature de Recuit sur la Cinetique de l'Hydration du Silicate Tricalcique', Cem. Conc. Res. 12, 455.

Fletcher, K.E. 1965 'The Polymorphism of Tricalcium Silicate: A Comparison of the Effect of the Fe^{3+} and Al^{3+} Ions', Trans. Brit. Ceram Soc. 64, 377.

Flint, E.P. & Wells, L.S. 1934 J. Res. natn. Bur. Stand. 12, 751.

Forrester, J.A. 1970 'A Conduction Calorimeter for the Study of Cement Hydration', Cement Technology, May/June.

Forsen, L. 1938 'The Chemistry of Retarders and Accelerators', Proc. 1st Int. Cong. Chem. Cem., Stockholm, 298 & 364.

Frohnsdorff, G., Fryer, W. & Johnson, P. 1969 'The Mathematical Simulation of Chemical, Physical and Mechanical Changes Accompanying the Hydration of Cement', Proc. 5th Int. Cong. Chem. Cem., Tokyo, suppl. paper II-33, p.321.

Fujii, K. & Kondo, W. 1974 'Kinetics of the Hydration of Tricalcium Silicate', J. Am. ceram. Soc. 57, 492.

Fujii, K. & Kondo, W. 1975 'Hydration of Tricalcium Silicate in a Very Early Stage', Proc. 5th Int. Cong. Chem. Cem., Tokyo, suppl. paper 11-93, p.362.

Ghosh, S.N. 1980 'Synthesis of Dicalcium Silicate and Tricalcium Silicate Phases', Proc. 7th Int. Cong. Chem. Cem., Paris, II, I-12.

Ghosh, S.N. (Ed.) 1982 'Advances in Cement Technology', Pergamon Press, London.

Golovastikov, N.I. 1975 'Crystal Structure of Tricalcium Silicate', Kristallografiya 20, 721.

Goto, S., Daimon, M., Hosaka, G. & Kondo, R. 1976 'Composition and Morphology of Hydrated Tricalcium Silicate', J. Am. ceram. Soc. 59, 281.

Groves, G.W. 1983 'T.E.M. Studies of Cement Clinker Compounds, their Hydration and Strong Cement Pastes', Phil. Trans. R. Soc. Lond. A310, 79

Gutteridge, W. 1984 'Quantitative X-Ray Powder Diffraction in the Study of some Cementive Materials', Proc. Brit. Ceram. Soc. 35 (in press)

Gylling, N. 1982 'Mathematical Models of Cement Hydration', M.Sc Thesis, Institute of Mineral Industry, Technical University of Denmark.

Hahn, Th., Eysel, W. & Woermann, E. 1968 'Crystal Chemistry of Tricalcium Silicate Solid Solutions', Proc. 5th Int. Cong. Chem. Cem., Tokyo, suppl paper I-55, p.61.

Hansen, W. 1928 J. Am. ceram. Soc. 11, 68.

Higgins, D.D. & Bailey, J.E. 1976 'Fracture Measurement on Cement Paste', J. Mater. Sci. 11, 1995.

Hirljac, J., Wu, Z.Q. & Young, J.F. 1983 'Silicate Polymerisation During the Hydration of Alite', Cem. Conc. Res. 13, 877.

Jawed, I., Menetrier, D. & Skalny, J. 1980 'Early Hydration of Calcium Silicates: Surface Phenomena', Proc. 7th Int. Cong. Chem. Cem., Paris, II, II-182.

Jeffery, J.W. 1952 'The Crystal Structure of Tricalcium Silicate', Acta. Cryst. 51, 26.

Jelenic, I. & Bezjak, A. 1981 'On the Hydration Kinetics of alpha prime and beta Modifications of Dicalcium Silicate', Cem. Conc. Res. 11, 467.

Jelenic, I. & Bezjak, A. 1982 'Kinetics of Hydration of Cement Phases', In 'Advances in Cement Technology' (Ed. S.N. Ghosh), p.397.

Jennings, H.M. & Pratt, P.L. 1979 'An Experimental Argument for the Existence of a Protective Membrane Surrounding Portland Cement During the Induction Period', Cem. Conc. Res. 9, 501.

Jennings, H.M. & Pratt, P.L. 1980 'The Use of a High Voltage Electron Microscope and Gas Reaction Cell for the Microstructural Investigation of Wet Portland Cement', J. Mater. Sci. 15, 250.

Jennings, H.M. Dalgleish, B.J. & Pratt, P.L. 1981 'Morphological Development of Hydrating Tricalcium Silicate as Examined by Electron Microscopy Techniques', J. Am. ceram. Soc. 64, 567.

Jennings, H.M. 1982 'The Developing Microstructure in Portland Cement', In Advances in Cement Technology' (Ed. S.N. Ghosh), p. 349

Kantro, D.L., Brunauer, S. & Weise, C.H. 1962 'Development of Surface in the Hydration of Calcium Silicates: (II) Extension of Investigations to Earlier and Later Stages of Hydration', J. Phys. Chem. 66, 1804

Kantro, D.L., Weise, C.H. & Brunauer, S. 1966 'Paste Hydration of beta-Dicalcium Silicate, Tricalcium Silicate and Alite', Highw. Res. Board, Sp. Rept. 90, Washington, p.309.

Kantro, D.L. 1975 'Tricalcium Silicate Hydration in the Presence of Various Salts', J. Test. Eval. 3, 312.

Knudsen, T. 1980 'On Particle Size Distribution in Cement Hydration', Proc. 7th Int. Cong. Chem. Cem., Paris, II, I-170.

Kondo, R., Ueda, S. & Kodama, M. 1967 'Reaction Process of the Hydration of $3CaO.SiO_2$' (in Japanese), Semento Gijutsu Nenpo 21, 83.

Kondo, R., Daimon, M. & Akiba, T. 1968 'Study on the Hydration of Cement by Calorimetry' (in Japanese), Semento Gijutsu Nenpo 22, 73.

Kondo, R. & Ueda, S. 1969 'Kinetics and Mechanisms of the Hydration of Cements', Proc. 5th Int. Cong. Chem. Cem., Tokyo, princ. paper II-4, p.203.

Kondo, R. Daimon, M. & Okabayashi, S. 1971 'Effects of Grain Size Distribution in Cement on Pore Size Distribution and Strength of Hardened Mortar', Cem. Assoc. Japan Rev. 25, Gen. Meeting, 56 (ref 68 in Locher & Richartz 1974).

Kurdowski, W. 1974 'Influence of Minor Components on Hydraulic Activity of Portland Cement Clinker', Proc. 6th Int. Cong. Chem. Cem., Moscow.

Le Chatelier, H. 1887 'Comptes Rendus Hebdomadaires des Seances de L'academie des Science', Paris 94, 13. (ref 18 in Bensted 1982)

Lea, F.M. 1970 'The Chemistry of Cement and Concrete' (3rd edn.), Edward Arnold Publishers Ltd., London 1976.

Lentz, C.W. 1966 'The Silicate Structure Analysis of Hydrated Portland Cement Paste', Highw. Res. Board, Sp. Rept. 90, Washington, p.269.

Lerch, W. & Bogue, R.H. 1927 'Studies on the Hydrolysis of Compounds which may occur in Portland Cement', J. Phys. Chem. 31, 1627.

Lerch, W. 1946 'Influence of gypsum on the Hydration and Properties of Portland Cement Pastes', Proc. Am. Soc.Testing Materials, 46, 1252.

Lippma, E., Magi, M., Tarmak, M.,Wieker, W. & Grimmer, A.R. 1982 'A High Resolution ^{29}Si NMR Study of the Hydration of Tricalcium Silicate', Cem. Conc. Res. 12, 597.

Locher, F.W. 1960 'Solid Solution of Alumina and Magnesia in Tricalcium Silicate', Proc. 4th Int. Cong. Chem. Cem., Washington, II-S5, p.98.

Locher, F.W. 1966 'Stoichiometry of Tricalcium Silicate Hydration', Highw. Res. Board, Sp. Rept. 90, Washington, p.300.

Locher, F.W. & Richartz, W. 1974 'Study on the Hydration Mechanism of Cement', Proc. 6th Int. Cong. Chem. Cem., Moscow.

Ludwig, U. & Wolter, A. 1980 'Formation and Stability of C_3S and Alites', Proc. 7th Int. Cong. Chem. Cem., Paris, II, I-99.

Mack. J.L. 1905 'Experimental Researches on the Constitution of Hydraulic Mortars' New York. (ref 6, p.99 in Lea 1970).

Magnan, R., Cottin, B. & Garden, J. 1974 'Initial Stages in the Hydration Activity of Sulphate, Aluminate and Silicate compounds of Calcium', Proc. 6th Int. Cong. Chem. Cem., Moscow.

Maki, I. & Chromy, S. 1978 'Microscopic Study on the Polymorphism of Ca_3SiO_5', Cem. Conc. Res. 8, 407.

Mascolo, G., Eysel, W., Hahn, Th. & Woermann, E. 1974 'Thermal Behaviour of Synthetic Alites', Proc. 6th Int. Cong. Chem. Cem., Moscow.

Mascolo, G. & Ramachandran, V.S. 1978 'Hydration and Strength Characteristics of Synthetic Al-, Mg- and Fe Alites', Mater. Constr. (Paris) 8, 373.

Maultzsch, M., Gierloff, M. & Schimmelwitz, P. 1980 'Aging of Cement Through Long Term Storage', Proc. 7th Int. Cong. Chem. Cem., Paris, II, I-128.

Maycock, J.N., Skalny, J. & Kalyoncu, R. 1974 'Crystal Defects and Hydration: (I) Influence of Lattice Defects', Cem. Conc. Res. 4, 835.

Mehta, P.K. & Williamson, R.B. 1973 'Hydration Characteristics and Properties of Alite Pastes Containing C_3A, C_4AF and Gypsum', Proc. 11th Conf. Silicate Ind., Budapest, p.401.

Menetrier, D., Jawed, I., Sun, T.S. & Skalny, J. 1979 'ESCA and SEM Studies on Early C_3S Hydration', Cem. Conc. Res. 9, 473.

Menetrier, D., Jawed, I. & Skalny, J. 1980 'Hydration of Tricalcium Silicate - A Study by High Resolution Scanning Electron Microscopy', Silicates Ind. 45, 243.

Michaelis, W. 1893 Chem. Zeit. 17, 982. (ref 19 in Bensted 1982)

Mohan, K. & Taylor, H.F.W. 1982 'A Trimethylsylylation Study of Tricalcium Silicate Pastes', Cem. Conc. Res. 12, 25.

Mondal, P. & Jeffery, J.W. 1975 'Crystal Structure of C_3A', Acta. Cryst. 31B, 686.

Nurse, R.W., Midgley, H.G., Gutt, W. & Fletcher, K. 1966 'Effect of Polymorphism of Tricalcium Silicate on its Reactivity', Highw. Res. Board, Sp. Rept. 90, Washington, p.258.

Odler, I. & Skalny, J. 1971 'Influence of Calcium Chloride on Paste Hydration of Tricalcium Silicate', J. Am. ceram. Soc. 54, 362.

Odler, I. & Skalny, J. 1973 'Hydration of Tricalcium Silicate at Elevated Temperatures', J. Appl. Chem. Biotechnol. 23, 661.

Odler, I. & Dorr, H. 1977 'Tricalcium Silicate Formation by Solid State Reactions', Am. ceram. Soc. Bull. 56, 1086.

Odler, I. & Dorr, H. 1979 b 'Early Hydration of Tricalcium Silicate: (I) Kinetics of the Hydration Process and the Stoichiometry of the Hydration Products', Cem. Conc. Res. 9, 239

Odler, I. & Dorr, H. 1979 a 'Early Hydration of Tricalcium Silicate: (II) The Induction Period', Cem. Conc. Res. 9, 277

Odler, I. & Schuppstuhl, J. 1981 'Early Hydration of Tricalcium Silicate: (III) Control of the Induction Period', Cem. Conc. Res. 11, 765.

Odler, I. & Abdul-Maula, S. 1983 'Polymorphism and Hydration of Tricalcium Silicate Doped With ZnO', J. Am. ceram. Soc. 66, 1.

Pratt, P.L. & Jennings, H.M. 1981 'The Microchemistry and Microstructure of Portland Cement', Ann. Rev. Mater. Sci. 11, 123.

Previte, R.W. 1971 'Some Insights on the Mechanism of Saccharide Set Retardation of Portland Cement', Cem. Conc. Res. 1, 301.

Perry, S.J. 1974 'Calorimetric Studies of the Hydration of Cement', Part II thesis, Dept. of Metallurgy and Science of Materials, University of Oxford.

Polivka, M., Klein, A. & Best, C.H. 1961 'Laboratory Preparation of High-Purity Tricalcium Silicate', Materials Research and Standards, 1, 524.

Pommersheim, J.M. & Clifton, J.R. 1979 a 'Mathematical Modelling of Tricalcium Silicate Hydration', Cem. Conc. Res. 9, 765.

Pommersheim, J.M. & Clifton, J.R. 1979 b 'Special Review: Mathematical Models of Cement Hydration', Cem. Res. Prog., Am. Ceram. Soc., Ohio (1980), p.281.

Pommersheim, J.M. & Clifton, J.R. 1980 'Conceptual and Mathematical Models for Tricalcium Silicate Hydration', Proc. 7th Int. Cong. Chem. Cem., Paris, III, VI-195.

Powers, T.C. 1961 'Some Physical Aspects of the Hydration of Portland Cement', J. Portland Cem. Assn. Res. Dev. Labs. 3, 47.

Ramachandran, V.S. 1971 a 'Possible States of Chloride in the Hydration of Tricalcium Silicate in the Presence of Calcium Chloride', Materiaux et Constructions No.19, 4, 3.

Ramachandran, V.S. 1971 b 'Kinetics of Hydration of Tricalcium Silicate in Presence of Calcium Chloride by Thermal Means', Thermochimica Acta. 2, 41.

Regourd, M. & Guinier, A. 1974 'The Crystal Chemistry of the Constituents of Portland Cement Clinker', Proc. 6th Int. Cong. Chem. Cem., Moscow.

Regourd, M., Thomassin, J.H., Baillif, P. & Touray, J.C. 1980 'Study of the Early Hydration of Ca_3SiO_5 by X-Ray Photoelectron Spectroscopy', Cem. Conc. Res. 10, 223.

Regourd, M. 1983 'Crystal Chemistry of Portland Cement Minerals', Chapter 3 in 'Structure and Performance of Cements' (Ed. P. Barnes), Applied Science Publishers Ltd., Barking, Essex.

Ritzmann, H. 1968 'On the Relation Between Particle Size Distribution and the Strength of Portland Cement' (in German), Zement-Kalk-Gips, 21, 390.

Roed, G. 1974 'Tricalcium Silicate Solid Solutions in the System $CaO-Al_2O_3-SiO_2$', Proc. 6th Int. Cong. Chem. Cem., Moscow.

Sakurai, T., Sato, T. & Yoshinaga, A. 1968 'The Effect of Minor Components on the Early Hydraulic Activity of the Major Phases of Portland Cement Clinker', Proc. 5th Int. Cong. Chem. Cem., Tokyo, suppl. paper I-105, 300.

Sasaki, H. 1964 'Introduction of Particle-Size Distribution into Kinetics of Solid-State Reaction', J. Am. ceram. Soc. 47, 512.

Sersale, R. 1974 'Hydraulic Behaviour of Al, Fe, Mg-Bearing Alites', Proc. 6th Int. Cong. Chem. Cem., Moscow.

Sinclair, W. & Groves, G.W. 1984 'Transmission Electron Microscopy and X-ray Diffraction of Doped Tricalcium Silicate', J. Am. ceram. Soc. 67, 325.

Singh, N. B. & Ojha, P.N. 1981 'Effect of $CaCl_2$ on the Hydration of Tricalcium Silicate' J. Mater. Sci. 16, 2675.

Skalny, J., Odler, I. & Hagymassy, J. 1971 'Pore Structure of Hydrated Calcium Silicates: (I) Influence of Calcium Chloride on the Pore Structure of Hydrated C_3S', J. Colloid Interface Sci. 3, 434.

Skalny, J.P. & Young, J.F. 1980 'Mechanisms of Portland Cement Hydration', Proc. 7th Int. Cong. Chem. Cem., Paris, I, II-1/3.

Stein, H.N. 1961 'Influence of some Additives on the Hydration Reactions of Portland Cement: (I) Non-ionic Organics', J. Appl. Chem. 11, 474.

Stein, H.N. & Stevals. J. 1964 'Influence of Silica on the Hydration of $3CaO.SiO_2$', J. Appl. Chem. 14, 338.

Stein, H.N. 1977 'The Initial Stages of Hydration of C_3S', Il Cemento, 74, 3.

Stevula, L. & Petrovic, J. 1981 'Hydration of Polymorphic Modification C_3S', Cem. Conc. Res. 11, 183.

Stewart, H.R. & Bailey, J.E. 1983 'Microstructural Studies of the Hydration Products of Three Tricalcium Silicate Polymorphs', J. Mater. Sci. 18, 3686.

Suzuki, S. & Nishi, S. 1959 Semento Gijustu Nenpo, 13, 160. (ref from Thomas & Birchall 1983)

Sylla, H.M. 1972 'Cooling of Cement Clinker' (in German), Zement-Kalk-Gips, 25, 561.

Tadros, M.E., Skalny, J. & Kalyoncu, R.S. 1976 'Early Hydration of Tricalcium Silicate', J. Am. ceram. Soc. 59, 344.

Taplin, J.H. 1962 a 'Discussion of Paper of H.E. Vivian', Proc. 4th Int. Conf. Chem. Cem., Washington, II, p.924.

Taplin, J.H. 1962 b 'The Temperature Coefficient of the Rate of Hydration of beta-Dicalcium Silicate', Proc. 4th Int. Cong. Chem. Cem., Washington III-S3, 263.

Taplin, J. 1969 a Written discussion of "Kondo & Ueda 1969", Proc. 5th Int. Cong. Chem. Cem., Tokyo, p.249.

Taplin, J. 1969 b 'On the Hydration Kinetics of Hydraulic Cements', Proc. 5th Int. Cong. Chem. Cem., Tokyo, suppl. paper II-70, p.337.

Taplin, J. 1980 'Tarnishing Kinetics of Powders With Lognormal Particle Size Distributions', J. Chem. Soc. Faraday I. 76, 2229.

Tashiro, C. 1980 'The Effects of Several Heavy Metal Oxides on the Hydration and the Microstructure of Hardened Mortar of C_3S', Proc. 7th Int. Cong. Chem. Cem., Paris, II, II-37.

Taylor, H.F.W. (Ed.) 1964 'The Chemistry of Cements' 1964, Academic Press, London.

Taylor, H.F.W. 1979 'Cement Hydration Reactions: The Silicate Phases', Proc. Eng. Found Conf., New Hampshire' (Ed. J. Skalny) p.107.

Taylor, H.F.W. & Newbury, D.E. 1984 'Calcium Hydroxide Distribution and Calcium Silicate Hydrate Composition in Tricalcium Silicate and beta-Dicalcium Silicate Pastes', Cem. Conc. Res. 14, 93.

Tenoutasse, N. & De Donder, A. 1970 'La Cinetique et le Mecanisme de l'Hydration du Silicate Tricalcique', Silicates Ind. 35, 301.

Thomas, N.L. & Double, D.D. 1983 'Calcium and Silicon Concentrations in Solution During the Early Hydration of Portland Cement and Tricalcium Silicate', Cem. Conc. Res. 13, 391.

Thomas, N.L. & Birchall, J.D. 1983 'The Retarding Action of Sugars on Cement Hydration', Cem. Conc. Res. 13, 830.

Thompson, R.A., Killoh, D.C. & Forrester, J.A. 1975 'Crystal Chemistry and Reactivity of the MgO-Stabilized Alites', J. Am. ceram. Soc. 58, 54.

Tian, A. 1923 a Bull. Soc. Chim. de Fran. 33, 427.

Tian, A. 1923 b 'Util de la Methode Cal. Dyn. Chem.', Soc. Chim. de Fran. 33, 4.

Tomita, K., Ogawa, T., Abe, s. & Sagiya, I. 1969 'The Effect of Cooling Rate of Cement Clinker on the Strength of Cement', Cem. Assoc. Japan Rev. 23, Gen. Meeting (1969), 81.

Tornebohm 1897 Tonind. Zeit. 1148. (ref 8, p.99 in Lea 1970)

Traetteberg, A., Ramachandran, V.S. & Grattan-Bellew, P.E. 1974 'A Study of the Microstructure and Hydration Characteristics of Tricalcium Silicate in the Presence of Calcium Chloride', Cem. Conc. Res. 4, 203.

Ueda, S., Hashimoto, M. & Kondo, R. 1968 Semento Gijutsu Nenpo, 22, 67.

Urzhenko, A.A. & Usherov-Marshak, A.V. 1974 'Hydration Kinetics of $3CaO.SiO_2$ Between 20 and 80 degrees C', Inorganic Materials, 10, 761.

Valenti, G.L., Sabatelli, V. & Marchese, B. 1978 'Hydration Kinetics of Tricalcium Silicate Solid Solutions at Early Ages', Cem. Conc. Res. 8, 61.

Vivian, H.E. 1966 'Effect of Particle Size on the Properties of Cement Paste', Highw. Res. Board, Sp. Rept. 90, Washington, p.18.

Wilding, C.R., Walter, A. & Double, D.D. 1984 'A Classification of Inorganic and Organic Admixtures by Conduction Calorimetry', Cem. Conc. Res. 14, 185.

Woermann, E., Hahn, Th. & Eysel, W. 1963 'Chemical and Structural Investigations on the Solid Solutions of Tricalcium Silicate', Zement-Kalk-Gips 16, 370.

Woermann, E., Eysel, W. & Hahn, Th. 1967 'Chemical and Structural Investigations into the Formation of Solid Solutions of Tricalcium Silicate', Zement-Kalk-Gips 56, 385.

Yamaguchi, G., Shirasuka, K. & Ota, T. 1966 'Comparison of Hydrated Properties Between Monoclinic and Inverted Triclinic Alite', Highw. Res. Board Sp. Rept. 90, Washington, p.263.

Young, J.F. 1972 'A Review of the Mechanisms of Set-Retardation in Portland Cement Pastes Containing Organic Admixtures', Cem. Conc. Res. 2, 415.

Young, J.F., Berger, R.L. & Lawrence, F.V.(Jr) 1973 'Studies on the Hydration of Tricalcium Silicate Pastes: (III) Influence of Admixtures on Hydration and Strength Development', Cem. Conc. Res. 3, 689.

Young, J.F., Tong, H.S. & Berger, R.L. 1977 'Compositions of Solutions in Contact with Hydrating Tricalcium Silicate Pastes', J. Am. ceram. Soc. 60, 193.